THE IDENTIFICATION OF VISUAL FIELD PROGRESSION.

NATALIE HUTCHINGS

Doctor of Philosophy

THE UNIVERSITY OF ASTON IN BIRMINGHAM

October 1996

The University of Aston in Birmingham

The identification of visual field progression

Natalie Hutchings

Doctor of Philosophy

1996

The study developed statistical techniques to evaluate visual field progression for use with the Humphrey Field Analyzer (HFA).

The long-term fluctuation (LF) was evaluated in stable glaucoma. The magnitude of both LF components showed little relationship with MD, CPSD and SF. An algorithm was proposed for determining the clinical necessity for a confirmatory follow-up examination.

The between-examination variability was determined for the HFA Standard and FASTPAC algorithms in glaucoma. FASTPAC exhibited greater between-examination variability than the Standard algorithm across the range of sensitivities and with increasing eccentricity. The difference in variability between the algorithms had minimal clinical significance.

The effect of repositioning the baseline in the Glaucoma Change Probability Analysis (GCPA) was evaluated. The global baseline of the GCPA limited the detection of progressive change at a single stimulus location.

A new technique, pointwise univariate linear regressions (ULR), of absolute sensitivity and, of pattern deviation, against time to follow-up was developed. In each case, pointwise ULR was more sensitive to localised progressive changes in sensitivity than ULR of MD, alone. Small changes in sensitivity were more readily determined by the pointwise ULR than by the GCPA. A comparison between the outcome of pointwise ULR for all fields and for the last six fields manifested linear and curvilinear declines in the absolute sensitivity and the pattern deviation.

A method for delineating progressive loss in glaucoma, based upon the error in the forecasted sensitivity of a multivariate model, was developed. Multivariate forecasting exhibited little agreement with GCPA in glaucoma but showed promise for monitoring visual field progression in OHT patients.

The recovery of sensitivity in optic neuritis over time was modelled with a Cumulative Gaussian function. The rate and level of recovery was greater in the peripheral than the central field. Probability models to forecast the field of recovery were proposed.

Long-term fluctuation, variability, Glaucoma Change Probability Analysis, regression, optic neuritis.

To

Peter & Megan

ACKNOWLEDGEMENTS

I would like to thank my supervisor, Dr John Wild and my associate supervisor, Mr Michael Hussey, for their advice, encouragement and help.

I am also very grateful to: Professors John Flanagan and Graham Trope of the Department of Ophthalmology, University of Toronto, Canada for providing data from the Glaucoma Service of the Toronto General Hospital; Professor Chris Johnson for allowing access to the Optic Neuritis Treatment Trial database; Mr James Cassidy for his computer programming expertise; Mr Tony Bray for his help in establishing the electronic links necessary for the data transfer.

LIST OF CONTENTS

LIST OF FIGURES

LIST OF TABLES

1.1. Principles of perimetry.

The visual field describes that portion of space in which objects are simultaneously visible to the steadily fixating eye. The extent of the visual field and the texture, form, resolution and colour of objects within it are a spatial projection of the visual pathway. Monocularly, the normal visual field extends, maximally, 100° to the temporal limit, 75° to the inferior limit and 60° to the nasal and superior limits (Anderson 1992). The extent of the field varies between individuals due to restrictions of the field by the orbital bones and the nose. Historically, the first attempt to document the visual field dates from Ptolemy in 150 BC. Hippocrates described hemianopic visual field defects in his writings dated 5 BC (Atchison 1979).

The topography of the visual field has been likened to a hill, or island, of vision surrounded by a sea of blindness (Traquair 1938). The peak of the hill represents foveal fixation. The central area of the hill corresponds to the area at which dimmer or smaller stimuli and colour may be perceived. Towards the periphery of the visual field, resolution and colour discrimination reduce such that only brighter or larger stimuli are perceived.

Appraisal of the visual field is achieved by measurement of the differential light threshold, defined as the minimum stimulus luminance (ΔL) required to elicit a response against a background of constant luminance (L). The differential light threshold is expressed as $\Delta L/L$ and is the reciprocal function of sensitivity. Two methods are used to determine the differential light threshold, kinetic perimetry and static perimetry. A schematic representation of the kinetic and static perimetric techniques is shown in Figure 1.1. The stimulus presentation can be performed manually by the examiner or can be automated in which the presentation is partially or fully controlled by computer (Greve 1982).

The technique of kinetic perimetry involves the movement of a stimulus of constant luminance and size from non-seeing to seeing, perpendicular to the visual axis and toward the central point of fixation. The location at which the stimulus is just perceived along the stimulus path represents the sensitivity to the given stimulus. The stimulus path is repeated along different

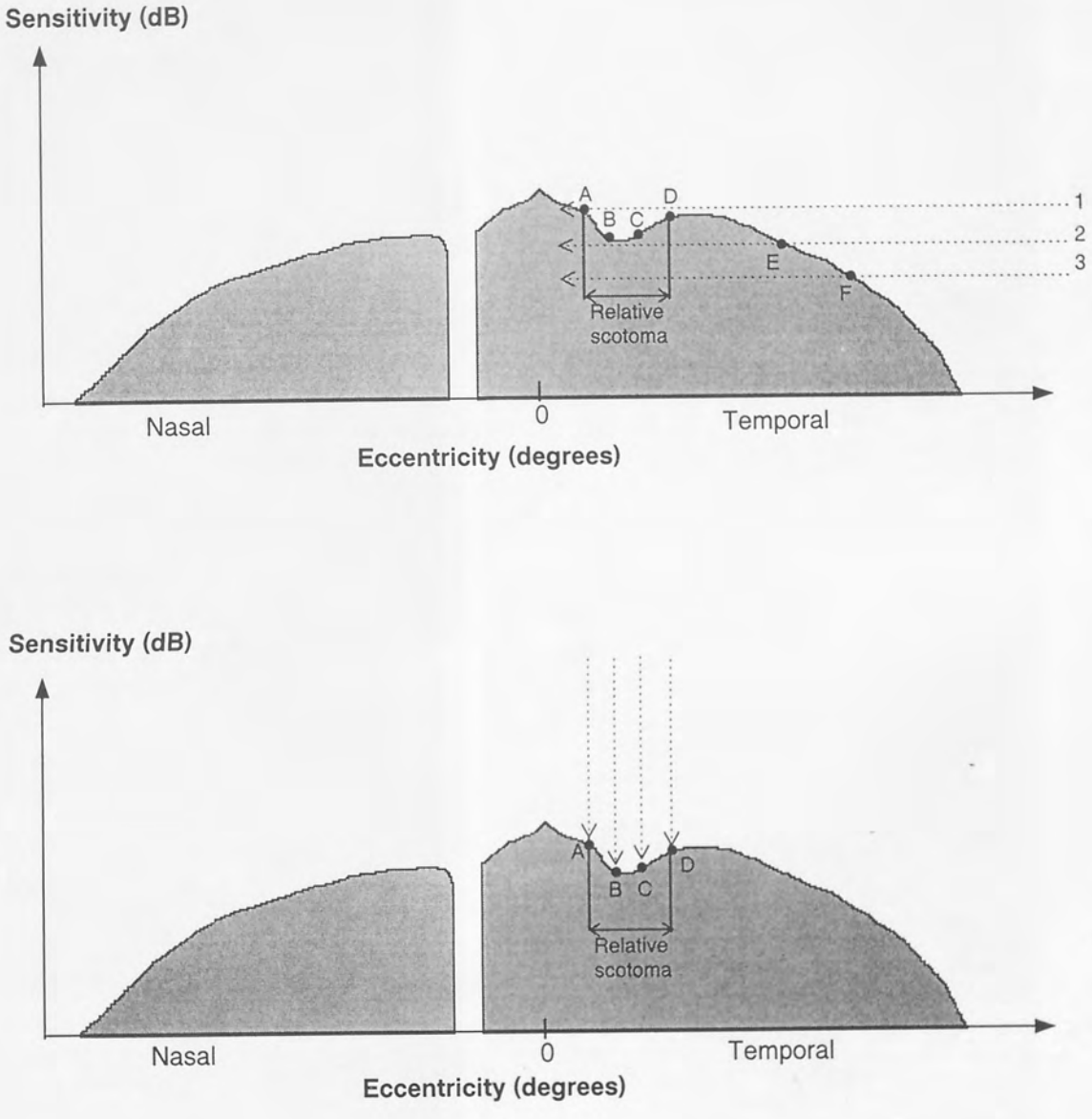

Figure 1.1. (Top) Schematic diagram of a visual field profile undergoing kinetic perimetry. The dotted lines represent the kinetic stimulus, of constant luminance, increasing in size from 1 to 3. The stimulus, when detected at A, E and F respectively, remains apparent as it is moved toward fixation. The nasal relative scotoma lies undetected between the isopters produced by stimuli 1 and 2. (Bottom) Schematic diagram of the same visual field profile undergoing static perimetry. The dotted lines each represent a stimulus of increasing luminance presented at the fixed stimulus locations of A, B, C and D. The reduction in sensitivity at locations B and C, due to the relative scotoma, are detected by the static technique.

meridia such that the entire visual field is investigated. A line joining locations of equal sensitivity is termed an isopter and describes the area within which a given stimulus is perceived by the steadily fixating observer. In the analogy of the 'hill' of vision, the isopter may be likened to contour lines on a two-dimensional map of the hill. The area of the isopter depends on the luminance, size and colour of the stimulus and, in order to fully describe the gradient of the hill of vision, the examination is repeated with stimuli of different size and/or colour. The visual angle subtended by the stimulus and the rate of stimulus movement influence the threshold. Goldmann stimuli 0 to V subtend visual angles of 0.054°-1.724° respectively and visual field sensitivity improves as the stimulus visual angle is increased with the trend becoming more marked towards the periphery (Fankhauser & Schmidt 1958). An increase in the stimulus velocity produces a relatively greater improvement in the peripheral field than nearer to the fovea (Tynan & Sekular 1982). The effect of the stimulus velocity is more pronounced in the presence of large and deep visual field defects (Aulhorn 1969; Fankhauser 1969; Greve 1973). The reaction time of the patient to the moving stimulus will also influence the outcome of the threshold (Fankhauser 1969), as will the reaction time of the examiner to the subjects response. An increase in the latency between perception of, and response to, the stimulus reduces the size of the isopter at a velocity of 4° sec^{-1} or greater (Johnson & Keltner 1987). The reaction time is slower in the peripheral field (Ball & Sekular 1980; Keele 1986; Rains 1963).

In static perimetry, the stimulus is presented at fixed locations and the stimulus luminance is varied. As a clinically viable alternative to kinetic perimetry, static perimetry was first described in 1939 by Sloan. The initial stimulus presentation is at a luminance which is either above or below threshold and the luminance is decreased or increased in various intervals of brightness level until threshold is crossed from seeing to non-seeing or vice versa. The static perimetric technique, unlike that of kinetic perimetry, is not influenced by the reaction time of the patient (Greve 1975; Trope & Britton 1987). Static perimetry has also been shown to detect small, isolated scotoma more efficiently than kinetic (Greve & Verduin 1976) and is generally more precise (Armaly 1971; Drance et al. 1967).

The various factors influencing static and kinetic perimetry result in a difference in the threshold between the two techniques. This difference is termed stato-kinetic dissociation (SKD) and manifests as a greater kinetic sensitivity in the periphery and a greater static sensitivity centrally (Fankhauser & Schmidt 1960). In normals the difference in the periphery between the two techniques, determined using automated perimetry, is approximately 4dB (Hudson & Wild 1992). The magnitude of SKD is largely independent of stimulus size, stimulus meridian and eccentricity (Hudson & Wild 1992). SKD is also correlated with spatial summation in the normal eye and the correlation substantially increases with an increase in age (Casson et al. 1995). However, the greater inherent variability of kinetic perimetry coupled with a need to minimise examination time (particularly in glaucoma patients) determine that static perimetry is the method of choice.

Visual field defects are regions where the sensitivity of the measured visual field is reduced with respect to that of a normal observer. The regions may be relative or absolute reductions in sensitivity; the shape of which is characteristic of the position at which the damage to the neural pathway has occurred. Localised areas of reduced sensitivity are termed scotomata, derived from the Greek meaning dark growth. Reductions in sensitivity extending across the greater part of the visual field are termed diffuse. The optic nerve head produces a vertically oval physiological blind spot; an absolute scotoma caused by the absence of photoreceptors. The blind spot subtends approximately 9° by 6° and is located 15° temporally.

The perimeters in current use owe much to the early work of Ferree & Rand (1922). These individuals provided the initial impetus for the standardisation of the stimulus parameters. The influence of retinal adaptation, stimulus visual angle, refractive error and age were then subsequently studied (Ferree & Rand 1924; Ferree & Rand 1927; Ferree et al. 1929).

The introduction of the Goldmann projection bowl perimeter was a further milestone in the development of perimetry as a science. The instrument was furnished with a standard series of targets, a fixation monitor and a calibration system. Thus, constant stimulus luminance was maintained and the bowl design allowed a constant level of retinal adaptation (Goldmann 1945; Goldmann 1946). Later Aulhorn and Harms (1959) developed the Tübinger perimeter,

which also permitted static perimetry under carefully controlled examination conditions (Harms & Aulhorn 1959).

The implementation of microcomputers in perimetry facilitated control of stimulus presentation, storage and information processing of the data and a reduction in the duration relative to the manual static perimetric examination (Lynn & Tate 1975). The Octopus automated perimeter was the first perimeter available of this type, developed initially as a research tool (Fankhauser et al. 1972; Koch et al. 1972; Spahr 1975). This instrument was followed by a number of other automated perimeters including the Competer (Heijl & Krakau 1975a; Heijl & Krakau 1975b), the Fieldmaster (Keltner et al. 1979), the Peritest (Greve 1980a) and the Humphrey Field Analyzer (Heijl 1985).

1.2. Sensitivity gradient and stimulus parameters.

The sensitivity profile describes the change in sensitivity across the 'hill' of vision. Factors related to the design of the perimeter and to the patient dictate the shape of the measured profile, although each profile will have common general characteristics. When the level of retinal adaptation (see 1.2.1) falls within the photopic range, the ability to detect visual stimuli declines as eccentricity increases. The gradient of threshold from centre to periphery is more gradual for larger targets and steeper for smaller targets and the difference between the gradients is not uniform across locations.

1.2.1. Background luminance.

The performance of the human visual system is limited by the number of quanta absorbed by the retina (Barlow 1972). This concept is more usually referred to as retinal adaptation. In perimetry, the degree of retinal adaptation is dependent upon the background luminance (L) adopted by the perimeter and is therefore a contributory factor to the sensitivity obtained for a given stimulus. The relationship between $\Delta L/L$ has been assumed to follow a linear relationship according to the Weber-Fechner law, however this only holds when the stimulus is presented at greater than $31.8cdm^{-2}$ (100asb) i.e. within the photopic range. At light levels corresponding to the low photopic and mesopic range, the Rose-de Vries Law is a more appropriate expression:

$$\frac{\Delta L}{L^{0.5}} = K \qquad \text{Eq. (1.1)}$$

A further reduction of light levels to less than 0.3cdm^{-2} (1asb), i.e. within the scotopic range, results in a linear relationship dependent on ΔL, alone:

$$\Delta L = K \qquad \text{Eq. (1.2)}$$

The application of the Rose-de Vries Law to best describe the relationship between ΔL and L in automated perimetry has been advocated by Fankhauser (1979; 1986) and Flanagan et al. (1991). However, other investigators postulate that the Weber-Fechner Law is more appropriate at the background luminance used by most perimeters (10.0cdm^{-2}) (Aulhorn & Harms 1972; Greve 1973; Klewin & Radius 1986; Wood et al. 1988) but not at the background luminance of 1.3cdm^{-2} employed by the Octopus automated perimeter (Klewin & Radius 1986). The uncertainty of the Weber-Fechner assumption results from the considerable overlap between the luminance ranges at which each law may be considered effective. Alterations in the stimulus luminance and the background luminance modulate, in part, the pupil diameter. Principally, the degree of retinal adaptation is influenced by pupil diameter only in the mesopic range and produces a change in retinal sensitivity.

1.2.2. Stimulus generation.

The stimulus may be generated by a variety of means: projection, LED light sources and fibreoptic light bundles. Projection systems using an integrating hemisphere are considered to be the most favourable.

In a projection perimeter, the stimulus is produced by an incandescent light source, projected to a stipulated location by a mirror optical system. The orientation of the mirror is controlled by small stepper motors, the positioning accuracy of which are checked at the beginning of each test and at each subsequent crossing of the vertical and horizontal meridia. The variations in luminances and colours of the stimulus target are achieved by a wheel of neutral density and colour filters situated adjacent to the incandescent source. An aperture wheel, generally corresponding to Goldmann stimuli I to V, is also located at the illumination source. Incandescent light sources are prone to ageing and are monitored by photoelectric cells that

initiate calibration of the instrument. The stimulus is then projected on an evenly illuminated background and thus enables a true incremental threshold to be determined. The chief advantage of the projection system is the flexibility that it offers. The ability to direct the stimulus target to a chosen position, with a resolution of 0.2° or less (Fankhauser 1979), allows custom examinations to be created at which only selected locations are thresholded. In addition, the projection system facilitates manipulation of both the stimulus luminance and size. Although the intricacies in design increase the accuracy of the projection system, they are relatively expensive to produce and mechanically frail. Furthermore, the motor rotating the mirror may act either as an audible cue to the stimulus presentation and/or a distraction to the patient.

In contrast, LED stimuli offer a rapid, silent and relatively inexpensive method of stimulus generation. They are mechanically robust and their simple design permits easy maintenance. The diodes are selected such that the peak of their spectral sensitivity approximates, within 15nm, to that of the retina at 555nm (Davson 1980a; Taylor et al. 1984). The LED light emission is narrow and variable and, as each diode acts as a separate light source, must be individually calibrated at each stimulus location. LED stimuli are of fixed position and size, in that individual diodes are mounted in apertures at pre-determined locations. The finite number of stimulus positions and invariability of stimulus size thus limits the application of custom examinations. Early designs of LED perimeter mounted the diode slightly behind the perimeter surface creating a visible "black-hole". The presence of "black holes" effected changes in local retinal adaptation (Heijl 1985; Mills 1985) and an increased threshold variability, particularly in areas of high sensitivity (Desjardins & Anderson 1988). In addition, perimeters employing recessed diode stimuli produce a steeper gradient of the sensitivity profile with eccentricity (Flanagan et al. 1988). Covering the recessed diodes with a diffusing surface minimises the "black hole" effect.

Fibre-optic stimuli employ a single source from which fibre-optic bundles emanate to fixed stimulus locations. The spectral response to fibre-optic stimuli is less linear than that of LEDs, particularly when the luminance of the source is controlled by a rheostat (Taylor et al. 1984). However, since the system uses a single source, luminance and colour may be varied by the

use of neutral density and colour filters positioned in front of the source. Furthermore, the single source, alone, need only be calibrated. The fixed pattern and stimulus size limit the manipulation of the system in a similar manner to that of LEDs. Moreover, the additional costs in production of a fibre-optic stimulus are not outweighed by any significant benefits.

1.2.3. Stimulus size and dynamic range.

The dynamic range has been defined as the measurement range over which the neurovisual system can be tested, using specific equipment with a given set of variables (Fankhauser 1979). The dynamic range can be maximised by increasing the maximum stimulus luminance or by reducing the background luminance and by increasing the stimulus size. At an eccentricity of 50° and a background luminance of 1.3cdm^{-2}, a change in the stimulus size from Goldmann I to III increases the dynamic range by 12dB. Alteration of both factors, that is increasing the stimulus size and decreasing the background luminance from 12.7cdm^{-2} to 1.3cdm^{-2}, will produce a 50 fold (17dB) increase in the dynamic range (Fankhauser 1979). The increase in dynamic range is a result of spatial summation, described mathematically as:

$$\Delta L . A^{k} = \text{Constant} \qquad \text{Eq. (1.3)}$$

Where ΔL is the stimulus luminance, A the stimulus area and k the summation coefficient. When k=1, complete spatial summation occurs in keeping with Ricco's Law. Complete spatial summation breaks down when the stimulus area is increased beyond the size of the critical area i.e. areas at which the relationship between luminance and area is no longer a reciprocal function. At stimulus sizes larger than the critical area partial spatial summation occurs and the summation coefficient (k) falls between 0 and 1. Pieron's law (k=0.3), Piper's law (k=0.5) and Goldmann's approximation (k=0.8) have been proposed as expressions to describe partial summation. When k=0, Weber's law applies and an increase in stimulus area has no effect on threshold.

The default stimulus size for automated static projection perimetry is Goldmann size III. However, selection of a different stimulus size on the basis of the magnitude of sensitivity has been advocated. Small shallow scotoma found using a Goldmann size I stimulus may remain undetected using stimulus size III (Gramer et al. 1981) or appear smaller and less deep

(Gramer et al. 1981; Zalta & Burchfield 1990). The use of a smaller stimulus reduces the dynamic range, particularly in the peripheral field. Furthermore, those patients in whom a peripheral loss precedes the more common central loss may be overlooked. Examination with a stimulus size larger than the standard size has proved to be advantageous in patients with end-stage glaucoma. Regions of absolute visual field loss determined using stimulus size III can sometimes exhibit visual function with stimulus size V (Takashima et al. 1993; Wilensky et al. 1986), although relative scotoma are shallower and greatly underestimated centrally (Zulauf & Caprioli 1993). The gain in sensitivity obtained by increasing the stimulus size from III to V follows a linear function which is independent of eccentricity (Weber & Baltes 1995).

Threshold variability is also influenced by stimulus size. In general, variability within an examination increases as the stimulus size is reduced in normals (Gundersen et al. 1993) and in glaucoma (Wall et al. 1993) and this trend is more marked with deeper defects (Wall et al. 1993). However, with 30° eccentricity of the visual field the magnitude of the variability is similar between stimulus size III, IV and V (Gilpin et al. 1990).

1.2.4. Stimulus duration.

The duration of the stimulus presentation affects the magnitude of sensitivity. Temporal summation describes the aggregation of luminance signals by the visual system over time. For small stimuli of short duration the relationship between the detection of the stimulus and the duration is described by Bloch's law:

$$\Delta L . T^{k} = Constant \qquad \text{Eq. (1.4)}$$

where ΔL is the stimulus luminance, T is the stimulus duration and k is the summation coefficient. Complete temporal summation occurs when k=1 and the stimulus duration is less than the critical time, T_c. Partial temporal summation occurs when T_c is exceeded and, in these conditions the summation coefficient falls between 0 and 1. When k=0 and all other stimulus parameters remain constant, an increase in stimulus duration has no further effect on the threshold determination.

The critical time in normals ranges from 60ms to 100ms but is dependent on the interaction with eccentricity and retinal adaptation (Adler 1987; Barlow 1958; Greve 1973; Saunders 1975). Indeed, at background luminances of $0.03cdm^{-2}$ (0.1asb) and $3.2cdm^{-2}$ (10asb) the critical time can exceed 100ms (Dannheim & Drance 1971). Temporal summation increases with decreasing retinal adaptation and is greater for smaller stimuli (Barlow 1958; Saunders 1975). However, diseased areas of the visual field appear to exhibit heightened temporal summation and may be better detected with a shorter stimulus duration (Krakau 1989; Wood et al. 1986). A saccadic eye movement out to 30° eccentricity takes approximately 90ms (Bahill et al. 1981; Baloh et al. 1975; Robinson 1964), with a latency of approximately 75ms (Robinson 1964). A stimulus duration of 200ms represents a compromise between the duration required to eliminate temporal summation (Aulhorn & Harms 1972; Harms 1952) and the inhibition of fixation loss. In addition, stimulus durations between 65ms to 500ms have little influence on the degree of within- and between-test fluctuation in normal subjects (Pennebaker et al. 1992).

1.2.5. Spatial arrangement of stimuli.

The arrangement and density of the stimulus locations is of paramount importance. Theoretically, a spatial grid with a small angular separation between stimulus locations represents the optimal strategy for detecting areas of visual field loss. However, this approach introduces a concurrent increase in the duration of the examination (Fankhauser & Bebié 1979).

The size of the visual field defect determines the probability with which it will be detected. The 6° square grid represents the default spatial arrangement of stimuli in current use. A 6° square grid has the capability of detecting an 8.4° diameter scotoma with 100% probability, which reduces to 79% with a scotoma diameter of 6° (Fankhauser & Bebié 1979). Conversely, the resolution of the 6° inter-stimulus separation is not sufficient to detect the physiological blind spot at every examination (King et al. 1986; Wild et al. 1986). It has been postulated that as many as 452 stimulus locations are required to detect a 3° diameter scotoma situated within 30° eccentricity of the visual field (Greve 1975). However, it has been demonstrated that greater than 140-150 stimulus locations produce no material increase in detection rate of

clinically significant visual field loss (Johnson & Keltner 1981). The relationship between sensitivity and the number of stimulus locations used in an examination is logarithmic whilst the specificity is linear (Henson et al. 1988). Indeed, increasing the number of stimulus locations within a given extent of the field reduces the mean sensitivity and increases the within-examination fluctuation, thus confounding the measurement and, subsequently, its reproducibility (Fujimoto & Adachi-Usami 1992a; Fujimoto & Adachi-Usami 1992b). The use of interlocking complimentary 6° grids theoretically improves the resolution of the examination to a 4.2° inter-stimulus separation. However, it has been suggested that a localised visual field defect is unlikely to incorporate only one stimulus location within an inter-stimulus separation of 6° (Heijl 1993) and increasing the frequency of examination with a single grid is more desirable than examination with complimentary grids (Heijl 1993; Weber & Diestelhorst 1992). Nevertheless, examination with the combined grids has illustrated a ten times higher frequency of scotoma detection per stimulus location at the centre of the visual field in glaucoma compared to that of the periphery. Consequently, a grid incorporating an inter-stimulus separation of 3° within an eccentricity of 10° of the visual field, a 4.2° grid between 10° and 20° eccentricity and a 6° grid between 20° and 30° eccentricity has been proposed (Weber & Dobek 1986). A stimulus configuration of this type permits an increased stimulus density centrally, similar to that afforded by interlocking grids with a fixed inter-stimulus separation of 6°, and a reduced peripheral stimulus density where informational content is lower. As default, the Humphrey Field Analyzer uses a fixed 6° grid and the Octopus 1-2-3 perimeter uses a variable inter-stimulus separation, with a higher density of locations positioned centrally.

Examination of the visual field with fewer stimulus locations than the 50 to 80 locations incorporated in a standard program has been proposed to shorten the duration of an examination. One approach used linear and multiple regression to identify the four locations that most frequently show progression in glaucoma: a high correlation was found between the estimate of global sensitivity based on these four locations and that of all the locations (de la Rosa et al. 1990). An alternative approach, utilised in the standard Octopus G1 program which investigates fifty-nine locations in each of two phases. Reducing the stimulus locations in the

first phase from fifty-nine to twelve produced a lowering of the sensitivity and specificity is lowered from 97% and 99% to 80% and 80% respectively (Zeyen et al. 1993).

Spatially adaptive screening techniques can augment increased location density programs at areas where the visual field appears 'abnormal' after an initial screening examination. SAPRO (Spatially Adaptive Program) and the Automatic Diagnostic program were such examination strategies developed for the Octopus and Humphrey perimeters respectively (Haeberlin & Fankhauser 1980; Haeberlin et al. 1980). The stimulus density had three modes: coarse, medium and fine. A coarse grid was initially employed and areas of apparent loss were re-examined with the finer grids. Despite allowing the perimetrist to modify the stimulus density at the time of examination, the strategy increased the duration of the examination (Fankhauser et al. 1986a; Fankhauser et al. 1986b). Moreover, enhancement of a visual field screening with a spatially adaptive program does not produce an increased sensitivity or specificity over and above that of the coarse resolution alone (Åsman et al. 1988). Custom programs may also be created to specifically investigate regions of interest.

1.3. Units of measurement.

The differential light threshold is an expression of the Weber-Fechner law:

$$\frac{\Delta L}{L} = K \qquad \text{Eq. (1.5)}$$

where ΔL is the change in the stimulus luminance that is detected; L is the background luminance and K is a constant. In relation to perimetry, ΔL is the difference between the stimulus luminance (L_s) and the background luminance (L_b). i.e.:

$$L_s = L_b + \Delta L \qquad \text{Eq. (1.6)}$$

The units of measurement in perimetry are the candela per square metre (cdm^{-2}), the apostilb (asb) and the decibel (dB). The candela per square metre is proportionally related to π apostilbs. The candela per square metre is an absolute measure which is used to describe the background and stimulus luminances, whereas the decibel is a relative measure used to describe sensitivity. The decibel is logarithmically related to the candela per square metre. The maximum stimulus luminance corresponds to zero decibels and the decibel scale of

measurement is reversed with respect to the candela per square metre scale, thus allowing threshold to be directly interpreted as sensitivity. The maximum stimulus luminance and the background luminance vary between different makes of perimeter and, as decibels are a relative measurement referenced to the maximum stimulus luminance, it follows that a similar decibel measurement on each instrument does not indicate a similar sensitivity (Anderson et al. 1989).

1.4. Examination strategy.

The stimulus strategy employed by a perimeter may be either supra-threshold or threshold. Supra-threshold strategies, also known as screening strategies, elicit an approximate description of the visual field whilst detailed strategies are utilised for the precise determination of visual field loss.

1.4.1. Supra-threshold strategies.

Supra-threshold examination strategies offer a rapid method of determining whether the visual field is normal (Bebié 1985; Lewis et al. 1986). They are more generally used to confirm normality in a population expected to be predominantly normal. One-level strategies employ a stimulus of constant luminance which is presented at all locations. This type of strategy takes no account of the sensitivity gradient. Consequently, it has little application in clinical perimetry due to the limited specificity (Gramer et al. 1982). Modification of the one-level strategy to present an increasingly brighter stimulus with increasing eccentricity is termed gradient adapted and as such, demonstrates improved specificity (Keltner et al. 1979). It can be achieved by increasing the stimulus brightness or by increasing the stimulus size, causing an apparent increase in the stimulus brightness. The chosen stimulus brightness is unrelated to the actual threshold value, but is dependent upon a knowledge of the sensitivity gradient in a normal visual field.

Threshold-related gradient adapted methods determine threshold at one or more central locations and present the subsequent stimuli at a pre-determined level above threshold (usually 4-6dB) at the remaining stimulus locations. The stimulus luminance presented at the subsequent stimulus locations relies on accurate estimation of the threshold at the central

locations (Stewart et al. 1989). By estimating the threshold at more than one central location the selection of an inappropriate threshold level due to an erroneous subject response is minimised (Heijl 1985). The sensitivity and specificity of a threshold-related supra-threshold strategy is greater than a basic one-level strategy and a gradient adapted technique unrelated to threshold. However, the threshold-related technique remains unsatisfactory in detecting shallow relative scotoma (Stewart et al. 1989).

Gradient adapted supra-threshold screening for glaucoma with a minimum number of test locations (8 to 16) has been advocated. It is more sensitive than screening methods relying on optic-disc appearance and intraocular pressures alone (Henson 1989; Henson et al. 1988). A supra-threshold gradient adapted stimulus presentation that is not seen at a given location can be re-presented with a stimulus at the maximum luminance to determine the presence of a relative or absolute loss (Keltner et al. 1979). A similar approach, whereby a 'not seen' supra-threshold stimulus is re-thresholded with a more precise 4-2dB staircase has been termed "Quantity Defects".

1.4.2. Full threshold strategies.

Full threshold strategies attempt to quantify the extent and depth of visual field loss. Automated static perimeters utilise staircase procedures to measure the differential light threshold. The 'up-and-down' staircase procedure (Cornsweet 1962) is an efficient method of estimating threshold, but is abbreviated in clinical perimetry due to the time consuming nature of the full staircase. The size of staircase step, the starting position of the staircase and the endpoint of the staircase vary between perimeter programs. This type of strategy is more fully reviewed in Chapter 4.

1.5. Reliability parameters.

The co-operation of the patient in manual perimetry is assessed by the perimetrist. In automated perimetry an objective measure of patient reliability is provided (Fankhauser et al. 1977; Neuhann & Greite 1981). Reliability is most frequently defined in terms of the patient response to the routinely performed catch trials: fixation losses, false-positive responses and false-negative responses. The short-term fluctuation has been similarly proposed as an

indicator of patient reliability (Bebié et al. 1976; Mills et al. 1991) but, although it may influence the number of catch trials performed (Whalen 1985b), it is generally considered a poor gauge (Fankhauser 1993; Zulauf & Caprioli 1991).

1.5.1. Fixation.

Fixation can be monitored subjectively using a telescope or video monitor integral to the fixation target (Haley 1987). In addition, fixation can be monitored objectively using the Heijl-Krakau technique whereby a stimulus is presented within the boundaries of the plotted blind spot (Heijl & Krakau 1975a; Heijl & Krakau 1975b). A positive response to this stimulus is recorded as a fixation loss and a rate of response to the blind spot checks exceeding 20% is generally classed as unacceptable (Haley 1987). The accuracy of the Heijl-Krakau technique is limited by the precision with which the blind spot is initially located (Zulauf & Caprioli 1991) and by the intermittent nature of the monitoring. Straylight arising from the media or due to reflection from the blind spot itself (Fankhauser & Haeberlin 1980) may allow the stimulus to be detected by pericoecal receptors (Fankhauser 1993). Furthermore, the technique is limited in cases of an enlarged blind spot (Fankhauser 1993). For this reason poor fixation in a patient manifesting focal loss involving the blind spot may be considered a more significant finding than poor fixation in a normal patient (Katz & Sommer 1988). Paradoxical classification of poor fixators due to false-positive responses and, conversely, good fixators due to false-negative responses also confounds the results by this technique (Fankhauser 1993; Henson et al. 1995). False-positive responses are the causative factor in approximately 7% of subjects exhibiting a high rate of fixation losses (Sanabria et al. 1991) and a positive correlation exists between these parameters (Bennett et al. 1991).

Video based systems (Henson et al. 1995) may improve the accuracy in monitoring translational fixation loss and head movements, but are likely to be insensitive to rotational head movements (Fankhauser 1993). Gaze monitoring, incorporated into recent models of the Humphrey Field Analyzer, indicate the position of fixation at the time of stimulus presentation. The resulting Gaze Graph consists of a horizontal line of origin from which upward vertical lines indicate loss of fixation and downward vertical lines indicate that the direction of gaze was unable to be obtained or that the patient had blinked.

Fixation losses are the most common cause of poor reliability (Bickler-Bluth et al. 1989; Chauhan et al. 1993; Johnson & Nelson-Quigg 1993; Katz & Sommer 1988; Katz et al. 1991; Nelson-Quigg et al. 1989). An increase in the fixation loss criterion from 20% to 26% (Chauhan et al. 1993), 30% (Johnson & Nelson-Quigg 1993) or 33% of the total number of catch trials (Katz & Sommer 1988) have been proposed. The relationship between the number of fixation losses and age is equivocal: Reynolds et al (Reynolds et al. 1990) found a positive correlation, whilst most investigators found this not to be the case (Bickler-Bluth et al. 1989; Heijl et al. 1987c; Jenni & Flammer 1987; Katz & Sommer 1988; Nelson-Quigg et al. 1989). Over a series of examinations, the number of fixation losses remains relatively constant (Chauhan et al. 1993; Katz et al. 1991) or reduces slightly (Bickler-Bluth et al. 1989; Johnson & Nelson-Quigg 1993) but the variability due to fixation losses, particularly at the steep border of isolated scotomata, may hamper serial field analysis (Henson & Bryson 1991).

1.5.2. False-positive and false-negative responses.

False-positive responses are presented using the audible sound which is produced on each occasion that the stimulus is presented. The sound is due to the mirror stepper motor and the operation of the shutter mechanism. In any given examination approximately 5% (Jenni & Flammer 1987; Whalen 1985b; Zulauf et al. 1992) of the total number of stimulus presentations are false-positive stimuli. A high degree of false-positive responses in a single examination is usually associated with an over-eager and/or anxious patient. The criterion for poor reliability is generally taken as greater or equal to 33% false-positive responses.

False-negative stimuli are presented at any location at which the threshold has previously been determined. The instrument projects a brighter stimulus (usually at the maximum stimulus luminance) than the previously detected stimulus and a false-negative response is recorded when the patient fails to respond. False-negative responses are determined in approximately the same proportion of cases as false-positive responses. The criterion for poor reliability is generally taken as greater or equal to 33% and a high degree of false-negative responses usually indicates an inattentive patient.

Several investigators have reported that between 30% to 40% of patients fall outside the designated limits for reliable responses (Enger & Sommer 1987; Katz & Sommer 1988; Katz & Sommer 1990; Katz et al. 1991), whilst others report a lesser extent of poor reliability (Bennett et al. 1991; Hardage & Stamper 1989; Johnson & Nelson-Quigg 1993; Nelson-Quigg et al. 1989). Thorough patient instruction and interruption of an examination where an individual exhibits a propensity for poor fixation and/or false-positive responses reduces the frequency of unreliable visual field results (Nelson-Quigg et al. 1989; Sanabria et al. 1991).

False-positive responses significantly improve the mean deviation and the mean sensitivity in normals (Cascairo et al. 1991; Demirel & Vingrys 1995; Katz & Sommer 1990) and in glaucoma patients (Katz & Sommer 1990), particularly in the latter at a more negative mean deviation than -15dB (McMillan et al. 1992). In contrast, a high degree of false-negative responses culminate in a worse mean deviation and mean sensitivity (Cascairo et al. 1991; Katz & Sommer 1990; McMillan et al. 1992) and occur more frequently in glaucomatous subjects (Heijl et al. 1987c; Jenni & Flammer 1987; Johnson & Nelson-Quigg 1993; Katz & Sommer 1988; Katz et al. 1991). High false-negative and false-positive rates in normal subjects are associated with an increase in pattern standard deviation from baseline (Cascairo et al. 1991; Katz & Sommer 1990). The short-term fluctuation increases with a false-positive rate of greater than 33% and decreases for a false-negative rate of 20% in normal patients (Cascairo et al. 1991).

The use of alternative thresholding techniques to that of the traditional 4-2dB staircase algorithm of the HFA enable estimation of patient reliability without the presentation of additional catch trial stimuli. The heuristic strategies MOBS and RIOTS, determine reliability using a Boolean logic model based upon the number of locations requiring re-testing as a result of inconsistencies in the patient response course (Johnson & Shapiro 1989; Johnson & Shapiro 1991). Estimation of patient reliability has also been achieved by the use of a maximum likelihood technique which determines the frequency of false-positive and false-negative responses. By this method, additional catch trial stimuli were unnecessary in simulations of normal patients and were reduced by 50% in simulations of visual field loss (Olsson et al. 1989). In addition, the variance of false-positive and false-negative responses

between tests was also reduced (Olsson et al. 1995). The difference between the expected and the actual number of stimulus presentations, entitled stimulus discrepancy, has also been advocated as a measure of reliability (Whalen 1985b; Zulauf et al. 1992).

1.6. Data Presentation.

A variety of perimeters are currently available and each contain their own particular form of data display and visual field indices. However, in the research community the two most commonly used perimeters are the Octopus and the Humphrey Field Analyzer.

1.6.1. Numerical presentations.

The measured sensitivity in decibels at each stimulus location examined is the simplest form of display.

1.6.2. Graphical presentations.

Grey grid and grey scale.

The grey grid represents a qualitative description of the measured sensitivities and facilitate the ease with which the visual field may be assessed (Fankhauser & Bebié 1979; Whalen 1985a). The sensitivity scale is usually arranged in intervals of 5dB, each of which is assigned a grey tone. Each stimulus location is represented by a symbol of the appropriate grey tone representing the measured sensitivity. The grey tone becomes increasingly dark as the differential light sensitivity decreases.

The grey scale has a similar appearance to that of the grey grid. The sensitivity between stimulus locations is interpolated by a mathematical function to give a continuous two dimensional map of the visual field. The function utilised in the interpolation procedure influences the appearance of the greyscale. The original interpolated locations were based upon the sensitivity of the neighbouring four locations (Fankhauser & Bebié 1979). Linear (parallel to the x and y axes) and mixed (four point and linear combined) interpolations may also be performed. The appearance of a scotoma with four point and linear interpolation gives a rounded border consistent with the morphological appearance. Mixed interpolation is more mathematically exact and is recommended for research purposes (Weber & Geiger 1989).The

grey scale, in common with all types of graphical display, is a relatively poor representation of diffuse depression (Flammer 1986).

Meridian and three-dimensional plots.

Meridian plots depict the sensitivity of the locations along the chosen meridian and are similar to the profile plot produced by manual static perimetry. Along the chosen meridian the plot is interpolated between the direct measures of sensitivity (Whalen 1985a). Three-dimensional plots provide a quantitative illustration of the 'hill of vision'. The addition of colour allows a coarse qualitative assessment of defective areas (Lambrou et al. 1987). However, little standardisation of the display parameters (grid resolution, sensitivity scaling and plot orientation) generally prevents comparison between three-dimensional plots (Hart & Hartz 1982; Wild et al. 1987b).

1.6.3. Analytical representations.

Cumulative defect curve (Bebié Curve).

The cumulative defect curve is a graphical display of the cumulative distribution of the ranked deviations of the measured sensitivity from their corresponding age-matched normal value. The cumulative distribution of the 5th, 95th and 99th percentiles of the age-matched normal data serve as a comparison for the measured distribution (Bebié et al. 1989). A normal visual field yields a curve that is situated above or closely follows that of the 95th percentile. Diffuse loss depresses the curve to a level below either that of the 95th or 99th percentile. The degree of diffuse loss is illustrated by the magnitude of depression of the curve. In individuals with localised loss the curve representing the deviations deemed as normal will follow the normal 95th percentile curve. Those locations exhibiting focal loss present as those with the largest deviations in the distribution. The cumulative defect curve enables differentiation between diffuse and focal loss but, as the spatial relationships between the deviations are lost in the ranking procedure, the curve should be utilised in conjunction with spatial displays (Kaufmann & Flammer 1989).

Probability Maps.

Probability maps determine the difference (total deviation) between the measured sensitivity and the age-matched normal sensitivity and compare the deviation to an empirically derived distribution of deviations at each location. At any given stimulus location the pointwise deviations of the measured sensitivity from the age corrected normal value describes a distribution which is non-Gaussian. Early probability plots assumed a Gaussian distribution at each location (Schwartz & Nagin 1985). However, the suitability of a Gaussian distribution to describe the deviations decreases with increasing eccentricity (Brenton & Phelps 1981; Heijl et al. 1987a). A Gaussian model has recently been reported for short-wavelength-sensitive perimetry in normals out to 24° eccentricity (Wild et al. 1995). Total deviation maps formulated using empirical distributions show an improved sensitivity and specificity of approximately 10% in normal subjects compared to the Gaussian distribution, particularly in the periphery where variability is greatest (Heijl & Åsman 1989).

It has been postulated that diffuse visual field loss may be a present in glaucoma (Anctil & Anderson 1984; Drance 1991; Glowazki & Flammer 1987). The total deviation probability map is more sensitive to generalised depression of visual field sensitivity (Haley 1987; Heijl et al. 1987a; Heijl et al. 1987b; Heijl et al. 1989c) and as such, localised loss may be obscured. The pattern deviation map is a modification of the total deviation map and enables localised loss to be highlighted. The map is achieved by ranking the total deviations from most negative to most positive and estimating the 'general height' of the visual field as the 85th percentile of the ranked deviations. The highest ranked deviations (ie. the most positive) are assumed to be unaffected by localised loss. Stimulus locations situated outside 21° of eccentricity (except -27,±3 for a right eye) and immediately below the blind spot are excluded from the ranking as they exhibit high degrees of variability. Thus, the reference field is altered to the level of the general height by adding the 85th percentile to the total deviation at each location.

The Total and Pattern Deviations are determined for probability levels of 0.05, 0.02, 0.01 and 0.001. The symbol becomes darker with increasing statistical significance and indicate the statistical likelihood of the numerical values of Total or Pattern Deviation occurring in an age-matched normal population (Åsman 1992).

1.7. Summary visual field measures.

Threshold automated perimetry generates a large amount of data for each examination. Visual field indices reduce the numerical values of sensitivity values across the visual field into single summary statistics (Bebié 1985; Flammer 1986; Heijl et al. 1987b). The indices are therefore global measures and describe the height and shape of the visual field over time.

Normal sensitivity.

The effect of increasing age on the hill of vision was initially thought to be a uniform reduction in height (Bebié 1985). However, it was subsequently shown that although all stimulus locations exhibited a constant linear decline over time, the rate of decay with age was different between locations. The resultant effect on the profile of the visual field is a depression and a steepening with increasing age (Collin et al. 1988; Heijl et al. 1987a). The deviations from the mean at the individual stimulus locations did not show a Gaussian distribution, but showed significant skewness and kurtosis - the degree of which varied according to the spatial position of the stimulus location (Heijl et al. 1987a).

1.7.1. Mean Sensitivity (MS) index.

The Mean Sensitivity, in dB, expresses the arithmetic mean of the sensitivities of all the measured locations in the visual field.

$$MS = \frac{1}{n}\sum_{i=1}^{n} \bar{x}_i \qquad \text{Eq. (1.7)}$$

where n is the number of stimulus locations; $\bar{x}_i$ represents the result of a repeated threshold at location i and is determined by:

$$\bar{x}_i = \frac{1}{j}\sum_{k=1}^{j} x_{ik} \qquad \text{Eq. (1.8)}$$

where j is the total number of replications and k is each replication. MS is a numerical expression of visual field height and is advantageous in that it requires no normative values of sensitivity in its calculation. MS is more sensitive to diffuse loss and small areas of localised loss have little effect on its magnitude (Flammer 1986).

1.7.2. Mean Defect (MD) and Mean Deviation (MD_H) indices.

Mean Defect (MD) represents the arithmetic mean of the deviations between the normal value and the measured sensitivity at each location. The normal value is derived from a reference field obtained from a sample of normal individuals of the same age. The normal reference field acts as 'zero-point' and a depressed field elicits a positive value of MD (Augustiny & Flammer 1985; Flammer et al. 1985). Consequently, the MD is an expression of the relative decrease, or increase, in the height of the measured field with respect to the age matched normal reference field expressed in decibels (dB) (Flammer 1986). It may be expressed as:

$$MD = \frac{1}{n}\sum_{i=1}^{n}\left(N_i - \bar{x}_i\right) \qquad \text{Eq. (1.9)}$$

where N_i is the age-matched normal value at location i, $\bar{x}_i$ is the result of a repeated threshold (equation 1.8) and n is the number of locations. Mean Defect is analogous to the Mean Deviation (MD_H) index of the Humphrey Field Analyzer which is determined:

$$MD_H = \left\{\frac{1}{n}\sum_{i=1}^{n}\frac{(x_i - N_i)}{s_{1i}^2}\right\} / \left\{\frac{1}{n}\sum_{i=1}^{n}\frac{1}{s_{1i}^2}\right\} \qquad \text{Eq. (1.10)}$$

where x_i represents the measured sensitivity and N_i the normal sensitivity at stimulus location i, the number of which is denoted by n. There are, however, two fundamental differences. Firstly, in contrast to Mean Defect, the age-matched normal value is subtracted from the measured sensitivity. As a consequence Mean Deviation is always negative and becomes more negative with increasing loss of sensitivity. Secondly, the Mean Deviation is weighted at each location (i) for the variation of threshold concurrent with an increase in eccentricity (s_{1i}^2). The relative weighting function between stimulus locations depicts the increasing variation found at the more peripheral locations (Heijl et al. 1987b). Mean Defect and Mean Deviation are most sensitive to a uniform reduction in sensitivity which, if deteriorating consistently over time, has been attributed to cataract progression (Åsman & Heijl 1994).

1.7.3. Loss Variance (LV) and Pattern Standard Deviation (PSD) indices.

Loss Variance, expressed in dB^2, is the variance of the differences at each stimulus location between the measured sensitivity and the sensitivity of the normal age-matched reference

field. LV describes a departure from the shape of the normal visual field and, as the differences between the measured sensitivities and the age-matched normal values are squared, LV is always positive.

$$LV = \frac{1}{(n-1)} \sum_{i=1}^{n} (N_i - MD - \bar{x}_i)^2 \qquad \text{Eq. (1.11)}$$

where MD represents the Mean Defect, N_i represents the normal value of sensitivity, and $\bar{x}_i$ (equation 1.8) is the result of a repeated threshold measurement at location i. Loss Variance is analogous to the square of PSD, although the PSD is weighted in a similar manner to that of the Mean Deviation:

$$PSD = \sqrt{\left\{\frac{1}{n}\sum_{i=1}^{n} s_{1i}^2\right\} \times \left\{\frac{1}{n-1}\sum_{i=1}^{n} \frac{(x_i - N_i - MD)^2}{s_{1i}^2}\right\}} \qquad \text{Eq. (1.12)}$$

The weighting function of s_{1i}^2 minimises the magnitude of PSD in normal patients, but significantly increases the magnitude of the PSD in primary open angle glaucoma patients (Flanagan et al. 1993b). The magnitudes of LV and PSD are always positive and become increasingly so as the disparity in shape between the measured field and that of the normal reference field becomes greater. Hence, values of LV and PSD tending towards zero indicate that the shape of the measured field closely matches that of the reference field, with or without a uniform reduction in visual field height. Larger values of PSD are due to either the presence of localised loss or an increased measurement error. The difference between the weighted PSD and unweighted LV becomes more evident as the depth of loss increases. In addition, the difference between the appropriate weighted and unweighted may differ as a function of the characteristics of the subjects values of normal data (Heijl et al. 1992) and due to methodological differences in determining threshold (Fankhauser et al. 1988).

1.7.4. Short-term Fluctuation (SF) index.

The Short-term Fluctuation, in dB, is an expression of the measurement error. Local Short-term Fluctuation describes the standard deviation of two determinations of threshold at each stimulus location. Global Short-term Fluctuation is the root mean square of the difference between each determination of threshold at the stimulus locations where a double determination of threshold has occurred. The number of double determinations from which the

SF is calculated does, however, vary between perimeters. Mathematically, the unweighted SF is described as:

$$SF = \sqrt{\frac{1}{n}\sum_{j=1}^{n}\frac{(x_{j1} - x_{j2})^2}{2}} \qquad \text{Eq. (1.13)}$$

and the weighted SF as:

$$SF = \sqrt{\left\{\frac{1}{n}\sum_{j=1}^{n} s_{2j}^2\right\} x \left\{\frac{1}{n}\sum_{j=1}^{n}\frac{(x_{j1} - x_{j2})^2}{2s_{2j}^2}\right\}} \qquad \text{Eq. (1.14)}$$

where x_{j1} represents the first measurement of sensitivity and x_{j2} the second. The integer n represents the number of locations at which a double determination of threshold is undertaken. The normal measurement variation within an examination (s_{2j}^2) at each location i weights the outcome in a similar manner to that of the PSD, but is different in that it represents a difference between intra-individual sensitivity measurements rather than between the measured sensitivity and an age-matched normal reference field. Short-term Fluctuation is more comprehensively reviewed in Chapter 3.

1.7.5. Corrected Loss Variance (CLV) and Corrected Pattern Standard Deviation (CPSD) indices.

Corrected Loss Variance, expressed in dB^2, portrays the LV corrected for the measurement error (SF). In this way it describes any true defect in the shape of the hill of vision, distinct from that contaminated by the measurement error:

$$CLV = LV - \left(\frac{1}{n}SF^2\right) \qquad \text{Eq. (1.15)}$$

CLV has been found to correlate with mean defect in early and moderate glaucomatous loss (Flammer et al. 1985; Pearson et al. 1990). CLV has a weighted counterpart index, Corrected Pattern Standard Deviation (CPSD), in which the PSD is corrected for the Short-term Fluctuation:

$$CPSD = \sqrt{\left\{PSD^2 - \left(k.SF^2\right)\right\}} \qquad \text{Eq. (1.16)}$$

where k is a constant greater than 1, which corrects for the difference in spatial distributions of the 10 stimulus locations used in the calculation of the SF. A negative value of $(CPSD)^2$ may occur when the magnitude of the $(SF)^2$ is significantly larger than $(PSD)^2$. When this occurs the CPSD is assigned a value of zero due to the shape deviation being wholly attributable to the measurement error.

1.7.6. Global Compound Index (GCI) and Global Number (GN) index.

Peridata was designed as a stand alone analysis program, able to accept data transmission from both the Ocotpus and HFA automated perimeters. The program includes the database of normal values for each instrument.

Peridata (v. 6.3α) calculates the Global Compound Index (GCI), and the Global Number (GN). The Global Compound Index is calculated as:

$$GCI = MD^2 + PSD^2 \qquad \text{Eq. (1.17)}$$

To distinguish between normal and abnormal fields, GCI may be considered as a better parameter than the MD and/or PSD indices alone as it incorporates a description both of uniform deterioration and localised deterioration. The GN index indicates the number of locations included in the calculation of the indices.

Peridata offers several unique topographical indices in addition to standard greyscale, numerical and cumulative defect displays. The Graphical Analysis of Topographical Variation (GATV) produces a greyscale display of areas of stability (homogeneous shading) and areas of fluctuation (horizontal stripes). The contrast of the horizontal stripes indicate the extent of the local variation. The Graphical Analysis of Congruence (GAC) determines the similarity between the right and left fields, which is of particular importance in neurological cases. Areas of homogeneous appearance indicate equality between the left and right visual fields; areas with positive differences are depicted with horizontal stripes and those with negative differences, vertical stripes. An increase in contrast indicates a greater incongruity. This index may be also used between two fields of the same eye. In addition, homonymous and heteronymous congruence may be determined by the combined congruence index (Weber 1993). The conformity index compares the actual defect pattern with seven standard defect

patterns stored in a database. The seven patterns describe vertical and horizontal hemifields, quadrants, 30° sectors, 5° and 10° concentric rings and retinal nerve fibre bundles (Weber & Ulrich 1991). A value of the conformity index between 1.15 and ≤1.20 represents a 90th percentile match and a value of greater than 1.20 represents a 95th percentile match.

1.7.7. Third central moment (M3) and skewness (Q) indices.

The M3 index, expressed in dB^3, represents the third central moment of the distribution of deviations of the measured sensitivities from their age-matched normal values:

$$M3 = \frac{1}{n}\sum_{i=1}^{n}(N_i - MD - \bar{x}_i)^3 \qquad \text{Eq. (1.18)}$$

where N_i is the normal value of sensitivity at location i, MD is the Mean Defect and $\bar{x}_i$ is the outcome of a repeated threshold measure (equation 1.8). The M3 index describes those locations which deviate by the greatest degree from their age-matched normal values and a small number of aberrant deviations will greatly influence the magnitude of the M3 index. Principally, M3 is utilised in the calculation of the 'Q' statistic. Skewness (Q) (Brechner & Whalen 1984), also expressed in dB^3, essentially represents a standardised M3. Mathematically it may be presented as:

$$Q = \frac{\frac{1}{n}\sum_{i=1}^{n}(N_i - \bar{x}_i)^3}{\sqrt[3]{\left(\frac{1}{n}\sum_{i=1}^{n}(N_i - \bar{x}_i)^2\right)^2}} \qquad \text{Eq. (1.19)}$$

The Q statistic was developed to identify those locations that most deviate from their expected threshold, due to the hypothesis that early visual field defects follow an increase in variability of threshold (Werner & Drance 1977). The Q statistic underwent a Box-Cox transformation to obtain a normal probability distribution and the resulting transformed statistic (Q_T) is tested at probability levels of 1%, 5% and 10%. Q_T is sensitive to a small subset of abnormal locations. The impact of these locations is magnified by raising their difference from normal to the third power. Furthermore, the cubic function maintains a vector quality. The Q statistic is most effective in a normal sample which exhibits low variability. However, in normals, ocular hypertensive and glaucoma patients the degree of typical variability is sufficient to reduce the

sensitivity of Q. In consequence, a large degree of variability masks any visual field defect and as such denigrates the usefulness of the Q statistic in glaucoma (Pearson et al. 1990).

1.7.8. Spatial Correlation (SC) and Glaucoma Pattern (GPI) indices.

In static perimetry, a cluster is defined as two or more adjacent stimulus locations that exhibit reduced sensitivities (Chauhan et al. 1989b). This definition may be further refined in glaucoma by only considering deviant stimulus locations which are positioned along the route of the retinal nerve fibre layer (Åsman et al. 1992). The Spatial Correlation index describes the extent of clustering of abnormal stimulus locations across the visual field. The sensitivity at each stimulus location is corrected for its corresponding age-matched normal value and the overall depression of sensitivity. It is then multiplied by the corrected sensitivity of the adjacent stimulus location. Mathematically it may be expressed as:

$$SC = \frac{1}{p} \sum_{(ij)} (N_i - MD - \bar{x}_i)(N_i - MD - \bar{x}_j) \qquad \text{Eq. (1.20)}$$

where N_i is the normal value of sensitivity, MD is the Mean Defect and $\bar{x}_i$ and $\bar{x}_j$ are the results of the repeated threshold measurements at the adjacent locations i and j. The pairs of adjacent stimulus locations are indicated by ij and the number of pairs summated by p. When defects are randomly distributed, SC tends toward zero (Bebié 1985). A development of the SC index, the glaucoma pattern index (GPI), has been proposed whereby the most common pairs of abnormal adjacent locations in glaucoma are only considered. ie.:

$$GPI = \frac{1}{p} \sum_{(ij)'} (N_i - \bar{x}_i)(N_i - \bar{x}_j) \qquad \text{Eq. (1.21)}$$

where $(ij)'$ are correlated adjacent abnormal locations (Mandava et al. 1992; Mandava et al. 1993). The GPI has a higher diagnostic precision, with respect to glaucoma, than the standard visual field indices (Mandava et al. 1993) but it is not known whether it is more efficient than SC.

1.7.9. Cluster analysis indices.

Cluster analysis is based on the low probability that a normal visual field will display two or more clusters of locations with reduced sensitivities. Clustered deteriorating locations occur

more frequently in the superior hemifield than in the inferior hemifield in glaucoma (Chauhan et al. 1988). Whereas spatial correlation is a summary index describing the degree of abnormal locations that are adjacent, cluster analysis specifically describes the clusters themselves. Cluster size (SIZ), depth (CLUS), centroid (mean x-y co-ordinate), the number of clusters and the total size and depth may be determined (Chauhan et al. 1989a). Furthermore, PCLUS quantifies the percentage of the mean defect that is clustered. The sensitivity and specificity of the cluster indices, SIZ, CLUS and PCLUS, have been compared with the global indices MD and CLV. CLV and PCLUS were more able to differentiate between visual field stability and progression (Chauhan et al. 1990). In addition, the cluster indices were more effective in determining progression from normal to abnormal fields than further deterioration in already abnormal fields (Chauhan et al. 1990), particularly when the significance of the superior hemifield defects were accounted for (Åsman & Heijl 1993; Åsman et al. 1992). Consideration of the depth of loss in conjunction with adjacency of stimulus locations equates more readily with clinical evaluation than adjacency alone. However, in the presence of severe visual field loss cluster analysis becomes less effective (Fankhauser et al. 1993).

1.7.10. Defect Volume (DV) index.

Defect volume describes the reduction in volume of the normal visual field due to the presence of visual field defects (van den Berg et al. 1985):

$$DV = VOL_{norm} - VOL_{meas} \qquad \text{Eq. (1.22)}$$

VOL_{norm} represents the volume of the normal age-matched visual field and VOL_{meas} that of the measured visual field. The normal visual field volume was considered to be a conic section with a sensitivity gradient of 0.25dB per degree of eccentricity. The volume of the visual field has also been used to document the learning effect in static perimetry (Wild et al. 1987a; Wood et al. 1987b) and in determining the change of visual field profile with age (Jaffe et al. 1986; Suzumura et al. 1985).

1.7.11. Learners Index (LI).

Naïve patients undertaking visual field examination often produce artefactual reductions in sensitivity due to unfamiliarity with the examination procedure (Heijl et al. 1989b). This

phenomenon, the learning effect, has been illustrated in normal, ocular hypertensive and glaucoma subjects (Marchini et al. 1991; Werner et al. 1988; Werner et al. 1990; Wild et al. 1989; Wood et al. 1987a) and can confound the diagnosis of glaucoma in addition to determining visual field progression. The Learners Index (LI) is a discriminate linear function, based upon the variability across five concentric zones of the visual field exhibited by patients who had retrospectively demonstrated a learning effect. The LI index tends towards a value of 1 in subjects illustrating 'learning' and towards a value of zero in those exhibiting 'non-learning fields' (Åsman et al. 1993).

1.7.12. General Height (GH) index.

The general height (GH) index is based on the assumption that locations exhibiting the highest values of sensitivity fall beyond the bounds of any localised loss (Åsman 1992). The GH is defined as the seventh most sensitive stimulus location out to an eccentricity of 24° and excluding the blind spot locations (Åsman 1992; Åsman & Heijl 1995). The GH index is similar to the Individual General Sensitivity (IGS) proposed by Langerhorst (1988) and forms a within-subject visual field reference height. The IGS index excludes the two highest sensitivity values to eliminate any bias errors (Langerhorst et al. 1985) and includes any locations within 3dB of the third highest sensitivity in a normal population and, in a glaucomatous population, any location with a difference of ≤6dB between the first and second determinations of threshold (Langerhorst 1988). These criteria are based upon the expected variability found in each population using the Octopus perimeter. It has been postulated that univariate linear regression of the GH index against time, when compared with the corresponding linear regression of MD against time, provides a method of separating general visual field loss from localised visual field loss (Åsman et al. 1995).

1.7.13. Diffuse Loss (DL) index.

The Diffuse Loss index (DL) indicates the reduction of generalised visual field sensitivity and is a numerical determination based upon the 18th deviation of the Bebié curve (Bebié et al. 1989) falling in a region of generalised depression (Funkhouser et al. 1992a; Funkhouser 1991; Funkhouser et al. 1992b).

1.7.14. Glaucoma Hemifield Test (GHT).

The prevalence of localised glaucomatous visual field defects occurring in one hemifield before presenting in the other is well documented (Hart & Becker 1982; Mikelberg & Drance 1984). A number of hemifield comparative analyses have been proposed (Åsman 1992; Åsman & Heijl 1992a; Åsman & Heijl 1992b; Caprioli & Spaeth 1985; Duggan et al. 1985; Heijl & Drance 1981; Heijl et al. 1980; Sommer et al. 1987). The advantage of the hemifield comparison analysis lies in the patient providing their own reference level. The technique has been shown to have greater sensitivity and specificity in recognising glaucomatous loss than the visual field indices MD_H and PSD (Enger & Sommer 1987). The Glaucoma Hemifield Test compares the probability scores of five sectors in the superior hemifield with the probability score of the mirror image sectors in the inferior hemifield. The sectors are derived from retinal nerve fibre layer distributions. The probability scores of the standard GHT are based upon the pattern deviation analysis and as such are not sensitive to diffuse field loss. A more recent development introduces a colour-coded probability map to illustrate both diffuse and localised loss (Åsman 1995). The GHT does, however, detect losses that are symmetrical about the horizontal meridian due to the difference in gradient between the inferior and superior hill of vision in the normal eye (Åsman & Heijl 1992a; Katz & Sommer 1986). Glaucoma patients exhibiting four or more abnormal GHT sectors have also exhibited a reduced general height index to that of a normal population. In contrast, between 9% and 32% of patients whose fields exhibit less than four abnormal sectors derived by the GHT also exhibit supernormal values of general height with respect to a normal population (Åsman & Heijl 1995). These findings support the hypothesis that glaucomatous visual field damage is not always accompanied by diffuse visual field loss (Åsman & Heijl 1994; Åsman & Heijl 1995).

1.8. Analysis of visual field progression.

1.8.1. Box and whisker plots.

The box plot represents a summary of the pointwise distribution of the deviation between the measured sensitivities and that of the age-matched normal sensitivities across the visual field. The upper level of the box signifies the eighty-fifth percentile and the lower the fifteenth percentile of the distribution. The end of the upper whisker signifies the most positive deviation from the normal age-matched reference field and, likewise, the lower whisker signifies the

most negative deviation. A generalised reduction in sensitivity of the given visual field will depress the boxplot relative to that of the normal display, but the shape will be remain generally unaffected. An increase in depth of the scotoma would be signified by an increase in the length of the negative tail alone. An increase in the area of the scotoma results in a lengthening of the box and a shortening of the whiskers. Classification of glaucomatous visual field defects based upon the appearance of the box plot has also been developed (Shin et al. 1991).

1.8.2. Univariate linear regression.

Univariate linear regression against time to follow-up may be utilised for the entire visual field, a specific region of the visual field or a single stimulus location to evaluate progression (Heijl et al. 1991; Holmin & Krakau 1980; Holmin & Krakau 1982; O'Brien & Schwartz 1990). This technique will be more fully reviewed in Chapter 6.

1.8.3. Glaucoma change probability analysis(GCPA).

The Glaucoma Change Probability analysis (GCPA) determines whether any location of the given field illustrates a value of sensitivity, outside the limits encountered for the between-test variability exhibited in stable glaucoma. The GCPA will be discussed in more detail in Chapter 5.

1.8.4. Graphical Analysis of Topographical Trends (GATT).

Graphical analysis of topographical trends (GATT) is included in Peridata and illustrates serial topographic changes in sensitivity, derived from superimposing two or four measured field greyscales (Brusini et al. 1991; Weber & Krieglstein 1989). In a similar format to that of GATV, regions of visual field change are illustrated by stripes: horizontal stripes indicate deterioration, vertical stripes indicate improvement and areas of high variability are illustrated with a chequerboard pattern.

1.8.5. Octosmart.

The Octosmart program includes the Bebié Curve in conjunction with statements evaluating the extent of progression of each individual field. A one-dimensional graphic display (an

'intelligent box plot') is used to describe the reliability of the visual field. The progression criteria of Octosmart have been shown to exhibit good agreement with human observation in clear cases of visual field loss (Funkhouser et al. 1991). The use of Octosmart can remove the effect of inter-individual differences in clinical opinion with borderline decision-making (Hirsbrunner et al. 1990), however early visual field damage which may not adversely affect the statistical results may be determined only by observation of the original data (Kaufmann et al. 1990).

1.8.6. Program Delta.

Designed for the Octopus perimeter, Program Delta (Bebié & Fankhauser 1981b) was amongst the first analysis programs to incorporate serial visual field analysis in addition to single visual field analysis. Deterioration was determined from the results of a paired comparison *t*-test between the mean sensitivities of consecutive visual field examinations (Bebié 1985; Bebié & Fankhauser 1981a). The use of the *t*-test in this respect, however, was subsequently shown to be very sensitive to generalised depression of the visual field, but to be unable to detect small to moderate localised scotoma (Hills & Johnson 1988).

1.9. Incidental factors influencing the differential light threshold.

The differential light threshold can be influenced by a variety of extraneous factors. These include the age of the subject, pupillary miosis, age-related changes in media optical density and less efficient neural transmission (Johnson et al. 1989a; Marshall 1985).

1.9.1. Age.

An increase in age produces an overall contraction of the isopters in manual kinetic perimetry (Drance et al. 1967; Ferree et al. 1929; Goldmann 1945), which is more pronounced centrally (Suzumura et al. 1985). The nature of this contraction is equivocal: the contraction has been observed to occur linearly until 80 years of age (Drance et al. 1967) or only after 40 years of age (Ferree et al. 1929; Suzumura et al. 1985). In automated perimetry, an increase in age results in a general reduction in sensitivity (Brenton & Phelps 1981; Collin et al. 1988; Haas et al. 1986; Jaffe et al. 1986; Katz & Sommer 1986) accompanied by a steepening of the sensitivity gradient (Heijl et al. 1987a; Heijl et al. 1988; Jaffe et al. 1986; Katz & Sommer

1986). The pericentral area has been found to deteriorate less than both the central and the peripheral visual field out to 30° eccentricity (Haas et al. 1986); the upper hemifield deteriorates to a greater extent than the lower hemifield (Haas & Flammer 1985; Katz & Sommer 1986).

1.9.2. Systemic condition and medication.

Transitory visual field artefacts may be noted at any given examination as a consequence of the patient's general health and are frequently considered as exclusion criteria in clinical studies. When an episode of migraine is accompanied by visual aura, peripheral differential light sensitivity may be depressed for up to the subsequent ten days (Drummond & Anderson 1992). Extensive physical exercise preceding the visual field examination results in an improvement in Mean Deviation (Koskela et al. 1990).

The effects of alcohol on the differential light threshold are equivocal. A small, but statistically significant, decrease in sensitivity has been found centrally for a low blood alcohol level (<0.08%) by some authors (Wild et al. 1990) and not by others (Zulauf et al. 1986) and peripherally for a high dose of alcohol (>1.00%) (Riedel et al. 1985). Both studies investigating the influence of a low blood alcohol level on the visual field reported an increase in the number of stimulus presentations required and an increase in the recorded number of false-responses (Wild et al. 1990; Zulauf et al. 1986).

Systemic medication can also affect the visual field. Acetazolamide, used in the treatment of autosomal dominant retinitis pigmentosa and glaucoma, produces an improvement in overall sensitivity (Chen et al. 1990; Flammer & Drance 1983). This increase was most evident in those glaucoma patients with greatest visual field disturbance (Flammer & Drance 1983). Cumulative treatment with Chlorquine and Hydroxychloroquine over 8 months showed no measurable defect in visual function (Mann et al. 1988). Short-term 5mg and 10mg doses of Diazepam in young, normal individuals produces a small overall reduction in sensitivity although this was found not to be statistically significant (Haas & Flammer 1985). A short-term dose of 100mg of Diazepam produces a contraction of the visual field which is sustained for the duration of the treatment (Elder 1992).

1.9.3. Pupil Size.

Pupil size decreases linearly with age, the rate of which is independent of gender and refractive error (Winn et al. 1995). In the normal eye, pilocarpine produces a constriction of the isopters and the percentage change in isopter area is significantly correlated with the percentage change in pupil area (McCluskey et al. 1986). In automated perimetry, pupillary constriction produces a more negative mean deviation of 0.7dB in the normal eye (Lindenmuth et al. 1989) and 1.5dB in glaucoma (Webster et al. 1993). Conversely, in normals an improvement in mean sensitivity has been reported (Wood et al. 1988). Similarly, pharmacological mydriasis produces a more negative mean deviation and a more negative corrected pattern standard deviation in normals (Lindenmuth et al. 1990), probably due to the increase in the Stiles-Crawford effect. In glaucoma patients treated with pilocarpine, an improvement in MD of 3.14dB and an improvement in CPSD of 1.73dB has been demonstrated following dilatation with 10% phenylephrine (Rebolleda et al. 1992). The depth of focus (Mikelberg et al. 1987), its interaction with refractive defocus (Herse 1992), and diffraction (Lindenmuth et al. 1989; Mikelberg et al. 1987) are all sequelae associated with a change in pupil size and as such have a bearing on the differential light threshold.

1.9.4. Media Optical Density.

Changes in the ocular media frequently result in degradation of the retinal image (Bettleheim & Ali 1985). Age-related cataract results from a change in physiology of the lens proteins (crystallins) and the formation of lens discontinuities (Davson 1980b). Although the image degradation produced by cataract results from both light absorption and light scatter, its effect on visual function is often clinically determined solely by the level of visual acuity. However, a high contrast vernier acuity task does not correlate well with the presence of perimetric attenuation produced by cataract (Elliott et al. 1990; Guthauser & Flammer 1988).

Light absorption by the ocular media causes a reduction of the effective level of light reaching the retina. Light scatter describes the dispersion of a point source of light as it passes through the ocular media. Light absorption is considered to have a lesser effect in attenuating the conventional perimetric response than that of light scatter (Bettleheim & Ali 1985; Greve 1980b). It is wavelength selective, with short wavelengths being more affected (Sample et al.

1988) and attenuates the blue-on-yellow visual field (Moss et al. 1995). Light scatter is largely independent of wavelength.

Light scatter can be subdivided into light scattered forward towards the retina (straylight) and light scattered backward away from the crystalline lens. Forward light scatter produces a veiling luminance superimposed on the retina and causes a reduction in retinal contrast. Backscatter is assumed to be proportional to forward light scatter. However, due to a large degree of variability between individuals, backscatter cannot be used to derive the degree of forward light scatter (de Waard et al. 1992). Image degradation caused by cataract is considered to be due to an increase in forward light scatter (Bettleheim & Ali 1985). In the presence of a glare source, the forward light scatter factor (μ) may be described as (Paulsson & Sjöstrand 1980):

$$\mu = \frac{L}{E}\left(\frac{M_2}{M_1} - 1\right) \qquad \text{Eq. (1.23)}$$

where L is the screen luminance, E is the illuminance of the glare source in the plane of the pupil and M_2 and M_1 are the contrast thresholds with and without the glare source respectively. The forward light scatter factor (μ) has been modified with a correction factor (CF) to compensate for the change in retinal adaptation due to the presence of a glare source (Abrahamsson & Sjöstrand 1986). At background luminance levels of $2cdm^{-2}$ the uncorrected light scattering factor greatly overestimates the amount of forward light scatter (Thaung et al. 1995).

The magnitude of forward light scatter has also been investigated using the Point Spread Function (PSF) which mathematically describes the dispersion of a point source as it passes through the ocular media (van den Berg 1987). By this method, light scattered over a wide and a narrow angle causes an attenuation of perimetric sensitivity, the degree of which is lessened with increase in target size (van den Berg 1987). The PSF has the same general shape in glaucoma as in normals, but the peak of the distribution is kurtosed and the peripheral tails are longer.

Cataract has been found to be highly correlated with forward light scatter both for a narrow and a wide angle glare source (Dengler-Harles et al. 1990), producing an overall reduction in sensitivity as the degree of light scattering increases (Dengler-Harles et al. 1990; Moss & Wild 1994; Moss et al. 1995). Loss variance under the same conditions, however, shows a decreasing curvilinear relationship that disappears with the correction of the age-matched normal reference data for light scattering (Dengler-Harles et al. 1990). In glaucoma the effects of cataract are difficult to separate using the total, mean (Stewart et al. 1995) and pattern deviations (Heider et al. 1991; Stewart et al. 1995).

Neural function declines more markedly than the pre-retinal factors and is the principal cause of normal age-related visual field decay (Johnson et al. 1989; Morrison & Jay 1993). However, the presence of cataract has a greater effect on visual function than that due to age-related neural deterioration (Morrison & Jay 1993).

1.9.5. Refractive error.

Uncorrected or inappropriately corrected ametropia reduces sensitivity out to 30° eccentricity for stimulus sizes equal to, or smaller than, Goldmann III (Atchison 1987; Goldstick & Weinrib 1987; Martin-Boglind 1991; Mutlukan 1994; Weinreb & Perlman 1986). However, the increased depth of focus produced by a small pupil minimises the attenuation of sensitivity (Herse 1992). Optical defocus produces a reduction in the visual field height (ie. the MD) whilst the pattern standard deviation and the short-term fluctuation remain unchanged (Goldstick & Weinrib 1987). Within the central 12°, the reduction in sensitivity is in the order of 0.4dB per degree per dioptre (Weinreb & Perlman 1986) and the rate of decline in sensitivity reduces with increasing eccentricity (Atchison 1987; Fankhauser & Bebié 1979). Refractive defocus to 21° eccentricity does not adversely influence the detection of localised glaucomatous loss in supra-threshold perimetry (Henson & Morris 1993).

Inappropriate positioning of the correcting lens may produce artefactual absolute or relative visual field defects due to induced prismatic effects (Atchison 1987; Miller & Gelber 1990) and to the lens rim (Zalta 1989). The use of trial lenses in high hyperopic or aphakic corrections cause optical distortion which may be resolved in part by the use of aspheric contact lenses

(Miller & Gelber 1990; Zalta 1989). Presbyopia should be corrected for the viewing distance of the bowl (Norden 1989).

1.9.6. The learning effect.

Learning may be described as a time-dependent improvement in the visual field (Zulauf & Caprioli 1991) and as such may exist both within an examination and between examinations. In particular, recognition of the learning effect is important in the selection of appropriate baseline fields from which progression is determined. The learning effect has been illustrated in normal subjects (Autzen & Work 1990; Heijl et al. 1989b; Wood et al. 1987a), in glaucoma suspects (Werner et al. 1990; Wild et al. 1989) and in glaucoma patients (Heijl & Bengtsson 1996; Kulze et al. 1990; Werner et al. 1988).

Between examinations, the learning effect results in an improvement in MS of approximately 1-2dB in normals (Autzen & Work 1990; Heijl et al. 1989b; Wild et al. 1989), glaucoma suspects (Wild et al. 1989) and glaucoma (Kulze et al. 1990). Normal subjects with previous experience in manual perimetry show no learning effect (Katz & Sommer 1987). Learning has also been found to increase with increase in eccentricity in normals, glaucoma suspects and glaucoma patients (Heijl & Bengtsson 1996; Heijl et al. 1989b; Wild et al. 1989; Wood et al. 1987a) particularly between 20° and 30° eccentricity (Werner et al. 1990). The learning effect is significantly correlated with the short-term fluctuation (Autzen & Work 1990; Werner et al. 1988; Werner et al. 1990; Wild et al. 1989; Wood et al. 1987a) and the magnitude of the SF has been suggested as an index for determining the suitability of a given visual field for selection as a baseline field (Werner et al. 1988; Werner et al. 1990). The learning effect can be present over the first five examinations (Wood et al. 1987a) and can be minimised by prior training in the visual field examination (Heijl et al. 1989b; Werner et al. 1988; Werner et al. 1990). The extent of the learning effect is independent of age (Heijl et al. 1989a; Kulze et al. 1990) but is related to the magnitude of sensitivity recorded at the initial examination (Heijl & Bengtsson 1996; Heijl et al. 1989b; Wild et al. 1989).

1.9.7. The fatigue effect.

The fatigue effect, whereby sensitivity declines during an examination, has been demonstrated in normals (Searle et al. 1991), ocular hypertension (Wild et al. 1991), glaucoma (Fujimoto & Usami 1993; Heijl & Drance 1983; Johnson et al. 1988; Wild et al. 1991) and in neuro-ophthalmological disorders (Keltner & Johnson 1995). Fatigue within an examination causes a general reduction in sensitivity in the normal eye of between 1dB (Johnson et al. 1988) and 2.5dB (Hudson et al. 1994) which becomes more pronounced with examination durations of greater than 5 to 10 minutes (Marra & Flammer 1991). In ocular hypertension, the overall reduction in sensitivity within an examination is, on average, 2.2dB (Hudson et al. 1994) whilst in glaucoma, it is approximately 3dB (Johnson et al. 1988). Loss variance (LV) increases in magnitude for normals and ocular hypertensives although the increase is greater for normals (Hudson et al. 1994). The reduction in the MD (Hudson et al. 1994), MS (Searle et al. 1991) and the increase in the LV (Hudson et al. 1994) is worse for the second eye examined at any given session. Global short-term fluctuation (SF) remains relatively unchanged over the duration of a single examination (Hudson et al. 1994) in normal and ocular hypertensive subjects. The deterioration in sensitivity is eccentricity dependent (Hudson et al. 1994; Johnson et al. 1988; Wild et al. 1991) particularly in glaucoma (Johnson et al. 1988). Fatigue may be minimised by rest periods within examinations at a single visit (Johnson et al. 1988) and/or by utilising algorithms specifically designed to reduce the examination duration (Flanagan et al. 1993a; Mills et al. 1994).

Chapter 2: Research rationale.

2.1. Research aims.

The aims of the research evolved from research previously undertaken in the Department of Vision Sciences at Aston University. The overall aims of the research were firstly, to refine existing statistical techniques for the evaluation of visual field progression and secondly to develop novel alternative procedures for the analysis of progression. The intention was to develop models that were able to describe progressive deterioration, as exhibited in glaucoma, and progressive improvement, as exhibited in optic neuritis. The detailed aims were:

- to quantify the homogeneous and heterogeneous components of the long-term fluctuation (LF) between successive Humphrey Visual Field Analyzer examinations in stable primary open-angle glaucoma (POAG) as a function of the depth of visual field loss. The evaluation of LF was approached with a view to develop an algorithm that could eliminate the necessity of repeated additional examinations.
- to compare the magnitudes of between-examination variation at each stimulus location for the Standard and FASTPAC threshold algorithms in POAG in order to evaluate the viability of interchanging the two algorithms.
- to investigate the utility of moving the glaucoma change probability analysis baseline in order to identify continual deterioration subsequent to that exhibited with the original baseline.
- to evaluate univariate linear regression (ULR) of absolute sensitivity against follow-up time as a technique for the identification of visual field loss in POAG and to compare the findings with those of the corresponding regression of the pattern deviation.
- to evaluate multivariate linear regression analysis of sensitivity against time to follow-up as a method of forecasting visual field progression in POAG.
- to model the natural evolution of the sensitivity recovery against time to follow-up in optic neuritis.

2.2. Rationale.

2.2.1. Quantification of the long-term fluctuation.

Deterioration of the visual field in primary open angle glaucoma is a fundamental indicator for change in the therapeutic management of the patient. However, the separation of true deterioration from the fluctuation in sensitivity between any two consecutive visual field examinations currently represents a major clinical dilemma. A knowledge of the long-term fluctuation (LF) has been considered a prerequisite for quantitative comparison of visual fields (Flammer et al. 1984) especially when assessing the difference between two consecutive fields and particularly as the long-term variability is reported to be substantially larger in patients with glaucoma than in normal subjects of the same age (Flammer et al. 1983).

As was discussed in Chapter 1, the outcome of any given single visual field examination can be influenced by factors such as pupil size (Lindenmuth et al. 1989; Webster et al. 1993; Wood et al. 1988), refractive error (Goldstick & Weinrib 1987; Heuer et al. 1987; Weinreb & Perlman 1986), media opacities (Dengler-Harles et al. 1990; Guthauser & Flammer 1988; Wood et al. 1987; Wood et al. 1989), learning (Heijl et al. 1989b; Wild et al. 1989), fatigue (Heijl 1977; Heijl & Drance 1983; Hudson et al. 1994; Johnson et al. 1988), drugs (Haas & Flammer 1985; Wild et al. 1990) and random variations in the physiological status of the patient (Anderson 1992). These factors are such that the variability within, and between, any two successive examinations can mask or even mimic the true deterioration in the visual field. To date, true progression has frequently only been recognised retrospectively from a series of visual field examinations often obtained over a period of several years. It is now recognised that confirmation of deterioration between any two consecutive fields may necessitate up to several repeat examinations, carried out over a period of days or weeks (Schulzer 1994). Such a requirement involves additional financial and resource burdens. The criteria for the decision to undertake one or more confirmatory examinations is currently based upon clinical evaluation of the appearance of the visual field rather than upon knowledge of the between-examination variability in the threshold response.

The long-term fluctuation, or between-examination variability, exists in addition to short-term fluctuation, or within-examination variability. LF in its entirety consists of two components: the homogeneous component, LF(Ho), and the heterogeneous component, LF(He) (Bebié et al. 1976). The aim of the study was to derive the LF(Ho) and LF(He) components using the statistical model of Flammer (1983) in each of two samples of stable POAG patients. The first sample comprised three stable consecutive visual fields, separated by approximately 6 to 9 months, from each of thirty patients who had undergone automated static perimetry. The outcome measures of each component of the LF were compared with those from a second sample of thirty patients. These latter patients each underwent three visual field examinations each separated by a period of approximately two weeks. The two samples were matched for age and were of an age range (54 to 73 years) typical of that encountered in glaucoma. The samples were also matched for the extent of visual field loss as defined by their visual field indices.

2.2.2. Evaluation of between-examination variability as a function of thresholding strategy.

The thresholding strategy used to determine the differential light threshold employs a modified staircase procedure. The Standard strategy follows a 4-2dB staircase in which a 4dB step is reduced to a 2dB step after the first crossing of threshold and the 2dB step size is retained for a subsequent crossing of threshold. The duration of a perimetric threshold examination of this type is approximately 10-15 minutes. Previous studies have demonstrated a fatiguing effect, whereby a decline in overall sensitivity is exhibited as the examination progresses. A curtailed staircase strategy (FASTPAC) has been introduced in an effort to reduce the examination duration and concurrently minimise the fatigue effect. The FASTPAC strategy follows a continuous 3dB staircase with a single crossing of threshold. The examination time is reduced by 30-40% compared to the Standard strategy (Flanagan et al. 1993a; Flanagan et al. 1993b; Mills et al. 1994; O'Brien et al. 1994; Schaumberger et al. 1995). However, the reduction in time is at the expense of the accuracy of the estimation of the threshold (Glass et al. 1995). Comparative investigation of the between-examination behaviour of the Standard and

FASTPAC algorithms has shown an increase in the short-term fluctuation in normals (Flanagan et al. 1993a; Mills et al. 1994) and in glaucomas (Flanagan et al. 1993b; Mills et al. 1994; Schaumberger et al. 1995). In addition, the increase in SF becomes more pronounced with advancing age and with severity of defect (Flanagan et al. 1993b). It has been suggested that the limitations of the FASTPAC strategy may result in a greater between-examination variation and, compared with the Standard strategy, further hamper the identification of progressive visual field loss (Flanagan et al. 1993b; Schaumberger et al. 1995). The aim of the study was to compare and contrast the degree of between-examination variability exhibited by each strategy at stimulus locations of similar sensitivities.

The assessment of between-examination variability followed a similar protocol to that of Heijl and co-workers in a previous study of the Standard algorithm (Heijl et al. 1989a). The sample comprised sixty stable POAG patients who were divided into two age-matched groups of thirty patients. The study followed a standard cross-over design, each patient performing both a Standard and a FASTPAC strategy examination at each visit.

2.2.3. Evaluation of repositioning the baseline in the GCP analysis.

The Glaucoma Change Probability Analysis (GCPA) (Heijl et al. 1991) defines the first two fields in any given series of visual fields as a baseline. At each subsequent visual field examination the change in sensitivity from the baseline at each stimulus location, expressed as the total deviation, is determined. The change at each stimulus location from the baseline pair of fields is compared with the between-examination variation exhibited in stable glaucoma. A level of probability ($p<0.05$) indicates the statistical likelihood that such a change would be observed in a stable glaucomatous population. A stimulus location can exhibit a reduction in sensitivity from the baseline pair of fields that is sufficient for the GCPA plot to indicate deterioration at consecutive examinations. At the following examinations, the change in sensitivity from the original baseline may continue to increase without any change in the appearance of the GCPA plot. Moving the original baseline to the two fields of the plot at which progressive loss is first shown should allow any further deterioration to be indicated.

The aim of the study was to investigate the efficacy of repositioning the baseline to determine the presence of any deterioration in sensitivity at those stimulus locations exhibiting deterioration from the original baseline. The sample comprised 16 primary open-angle glaucoma patients exhibiting progressive visual field loss over a minimum of seven examinations.

2.2.4. Evaluating ULR of sensitivity against time to follow-up to describe visual field progression in POAG.

Various statistical methods have been proposed to enable delineation of visual field progression. Progression may be analysed by comparison with baseline fields (Heijl et al. 1991; Morgan et al. 1991), intuitive evaluation of empirical probability maps (Åsman 1995; Heijl & Åsman 1989), a *t*-test between the distributions of sensitivities from two fields (Bebié & Fankhauser 1981) and linear regression of summary measures of the visual field as a whole against time to follow-up (Heijl et al. 1991; Holmin & Krakau 1982) or on a pointwise basis (Birch et al. 1995; Noureddin et al. 1991; O'Brien & Schwartz 1990; O'Brien & Schwartz 1993).

Pointwise univariate linear regression of absolute sensitivity against time to follow-up describes the rate of change at each stimulus location. The technique treats each stimulus location as independent such that spatial analysis may be achieved only by graphical presentation of the outcome at each stimulus location (Fitzke & McNaught 1994; Noureddin et al. 1991). Linear regression analysis of the pattern deviation at each stimulus location against time to follow-up yields information relating to the change in shape of the visual field. The shape of the visual field is particularly important in glaucoma due to the localised nature of the visual field defects (Hart & Becker 1982).

The efficacy of pointwise univariate linear regression analysis in determining a trend of deterioration in both absolute sensitivity and pattern deviation was investigated in glaucomatous patients. The outcome at each location was compared with the results of linear regression analysis of the Mean Deviation against time to follow-up (Heijl et al. 1991) and with

the GCPA (Heijl et al. 1989a; Heijl et al. 1991). The sample comprised 38 primary open-angle glaucoma patients who had been followed with automated perimetry for at least five years.

2.2.5. Multivariate forecasting of visual field progression in glaucoma.

The pointwise topographical and longitudinal model described by Wild et al (1993) represents a novel approach to identifying progressive visual field loss. The model forecasts the sensitivity at a given stimulus location based upon the sensitivity at that location in the preceding examinations. The percentage difference between the forecasted sensitivity at a given stimulus location and at a given examination was compared retrospectively to the measured sensitivity at the corresponding examination. A method of determining an abnormally high percentage error of the forecasted sensitivity was developed, based upon the 95% confidence limit of the percentage errors exhibited by a sample of 23 normal subjects over a series of five visual field examinations. The suitability of the 95% confidence limit to minimise the number of false-positive indicators of progression over a similar number of examinations was tested in a sample of 12 ocular hypertensive patients. The outcome of the multivariate forecasting was then compared with the GCPA in two samples of POAG patients. The first POAG sample comprised 11 patients exhibiting progressive loss (determined by intuitive criteria) over at least two of a selected series of five consecutive visual field examinations. The second POAG sample comprised 11 patients exhibiting stability over a selected series of five visual field examinations. All of the characteristics of the stable POAG sample were matched as closely as possible to the progressing POAG sample.

2.2.6. Modelling the visual field recovery in optic neuritis.

Optic neuritis typically presents with an acute reduction of both the visual field sensitivity and of the visual acuity (O.N.S.G. 1991; Rizzo III & Lessell 1991). Traditionally, the most common visual field defect at presentation was thought to be a central or centrocaecal scotoma. However, more recent studies report a wide variety of visual field defects (Celesia et al. 1990; Keltner et al. 1993; Trobe & J.S. 1978), the most common of which is diffuse loss (Keltner et al. 1993). Unlike glaucoma, the reduction in sensitivity of the visual field typically improves

over the time to follow-up. Qualitative evaluation of the visual field recovery reveals that approximately 50% of patients return to normal 6-12 months after the attack. No clear pattern of visual field recovery is apparent, either in the greyscale appearance or the magnitude of the MD, over the follow-up period. Quantitative evaluation of the rate of recovery of the entire visual field and, in addition, any differential rate of recovery between individual locations within the field could provide insight into the evolution of the visual field recovery. At present the relationship between the rate of the recovery over time to follow-up and the extent of that recovery is unknown.

The aim of the pilot study was to develop a mathematical model to describe the rate of recovery of the Mean Deviation and the sensitivity at each stimulus location against time to follow-up. The sample comprised thirteen subjects aged between 18 and 45 years, examined over an approximate follow-up period of 2.5 years. Each subject presented with severe diffuse loss at the initial visual field examination and received no pharmacological treatment over the follow-up period. Seven subjects subsequently recovered to clinically normal sensitivity and six subjects exhibited a residual visual field defect at the final examination of their series. The model was to be used to evaluate any relationship between the rate of recovery and the level of recovery. In addition, possible applications of the model to forecasting the extent of the recovery were explored.

2.3. Logistics.

The research was carried out in the Department of Vision Sciences, Aston University, Birmingham. The work relating to POAG was undertaken in conjunction with the Toronto Hospital (Western Division), Ontario, Canada and the School of Optometry, University of Waterloo, Ontario, Canada. The clinical material for the ocular hypertensive and primary open-angle glaucoma patients was obtained from the database of the Glaucoma Service of the Toronto Hospital, under the auspices of Dr Graham Trope. The studies were approved, and complied with the constraints of, the Toronto Hospital ethical committee. The Glaucoma Service of the Toronto Hospital offered a more extensive patient database and, more

particularly, a longer follow-up period with automated perimetry than any Hospital Eye Service facility in the United Kingdom.

Full access to the medical and ophthalmological records of the patients was given by the Hospital and the technical support staff were extremely supportive in providing any further information and/or additional visual field examinations.

The statistical analysis software was developed in conjunction with Mr James Cassidy of the School of Optometry, University of Waterloo, Canada. Each item of software formed an add-on module to a suite of programs (HFA Tools©), initially developed as a result of previous collaboration with the Department of Vision Sciences, for use with the Humphrey Field Analyzer (HFA). Dr John Flanagan, associate Professor at the School of Optometry, University of Waterloo, was instrumental in assisting the development of the programs. In each instance, a written document outlining the desired statistical and data-handling procedures together with details of the information and presentation of the program output required from the software was sent to Mr Cassidy. Following clarification of the requirements by electronic mail, a β-program was transferred via the UNIX FTP (file transfer protocol) to the Department of Vision Sciences. Each β-program was extensively tested and then transferred between the two institutions for modification of any ensuing software faults. By these methods, two of the existing modules dealing with conversion (HDISK.EXE) and organisation (FLIST.EXE) of the HFA formatted data were modified. Six additional modules were also developed: LF.EXE, REGRESS.EXE, PREDICT.EXE, VPCONV.EXE, DEVIATE.EXE and PERROR.EXE (see appendix).

The optic neuritis study was carried out in conjunction with Dr Chris Johnson of the Department of Ophthalmology, University of California at Davis, California, USA. The data formed part of the Optic Neuritis Treatment Trial; a nation-wide clinical trial carried out in the United States. The data was transferred on floppy disks and was converted to IBM compatible ASCII files. The VPCONV.EXE module was developed specifically to read this data and

convert it to a format compatible with the other modules of the HFA Tools©. The majority of patients had undergone at least ten visual field examinations at the stipulated intervals of the treatment trial. All data regarding the visual fields, treatment regimes and visual field classifications was provided by Dr Johnson.

The use of electronic means to transfer the statistical software between the institutions was an expedient method of developing and transferring the software. However, the time required to clarify, develop and test the statistical programs delayed the data analysis. In addition, further delays were encountered in the collation of clinical details from Toronto General Hospital.

Chapter 3: Threshold fluctuation in the visual field.

3.1. Introduction.

3.1.1. The frequency-of-seeing ogive.

Fluctuation in sensitivity occurs both within a single examination and between examinations and is attributable to measurement error, sampling error and physiological variation (Anderson 1992; Zulauf & Caprioli 1991). The presence of both within- and between-examination fluctuation is inherent to the dichotomous decision process involved in determining the differential light threshold. Specifically, the differential light threshold represents the stimulus brightness at which the stimulus is perceived as 'seen' on half the total number of presentations against a stipulated background luminance and thus, incorporates some region of uncertainty around the true threshold. The probability that the stimulus will be 'seen' or 'not-seen' may be represented by the frequency-of-seeing ogive, which graphically describes the probability distribution and, in turn, the local threshold variability (Langerhorst 1988). The probability that the stimulus is 'seen' increases as the incremental difference between the stimulus luminance and that of the actual threshold is increased. Practically, the probability that the stimulus is 'seen' or 'not-seen' does not reach either 1.0 or zero as a result of false-negative and false-positive responses respectively (see Chapter 1.5.2).

An early study found that two-thirds of the data points examined did not exhibit monotonicity and thus were unable to be described by an ogive function (Lynn et al. 1985). However, this study principally examined, and was limited by, the algorithm employed to determine the supra- and sub-threshold data. Frequency-of-seeing ogives are approximately symmetrical around the differential light threshold and the slope and confidence interval of the linear inter-quartile range forms the region of interest (Chauhan et al. 1993a; Chauhan et al. 1993b; Weber & Rau 1992). Despite the uncertainty of the Gaussian or exponential nature of the frequency-of-seeing ogive (Green & Swets 1966), the clinical interpretation of an ogive is minimally affected by the difference between these distributions which are at the extremities (Weber & Rau 1992). The slope of the linear region describes the degree of short-term fluctuation exhibited by a stimulus location. The slope of the frequency-of-seeing ogive flattens

as the variability around the measured threshold increases (Chauhan et al. 1993b; Weber & Rau 1992).

Central stimulus locations (out to 29° eccentricity of fixation) of normal subjects describe steeper linear regions of the ogive than both ocular hypertensives (Chauhan et al. 1993a; Chauhan et al. 1993b) and glaucomatous patients (Chauhan et al. 1993a; Chauhan et al. 1993b; Weber & Rau 1992). In normal subjects, the ogives of peripheral stimulus locations described flatter linear regions than their central counterparts. The slope of the ogive is correlated with the level of the differential light threshold, but is less steep in glaucomatous (Chauhan et al. 1993a; Weber & Rau 1992) and ocular hypertensive (Chauhan et al. 1993b) patients than in normals, even at stimulus locations of the same sensitivity (Chauhan et al. 1993b). Furthermore, although the slope of the linear region is similar between peripheral locations of normals and the central locations of glaucomas, normals exhibit less variability in the periphery than the corresponding central stimulus locations of the glaucomatous patients (Weber & Rau 1992).

The extent of overlap of the linear regions of the frequency-of-seeing ogive at a stimulus location between examinations describes the contribution of the short- and long-term fluctuation to the measurement variability. Both the short- and long-term fluctuation are confounding factors in the interpretation of visual field progression.

3.1.2. Short-term fluctuation.

Clinically, the short-term fluctuation (SF) is derived from the variance between two or more threshold determinations at a single stimulus location (ie. local variability) or by the root mean square (RMS) of the variance of two or more determinations at each location across the field as a whole (ie. global variability). Local SF increases as the number of threshold determinations increases to five, after which it remains relatively unchanged (Chauhan et al. 1991). However, global SF appears to be independent of the number of threshold determinations (Chauhan et al. 1991). Therefore, a global index based upon the two

determinations of threshold may underestimate the magnitude of the SF. Similarly, using a sample of the total number of stimulus locations at which the determination of threshold is repeated only once underestimates the SF both in normals (Bebié et al. 1976) and glaucoma (Flanagan et al. 1993c). It has been suggested that a more representative measure of the SF may be obtained by multiple repeated threshold determination of a small sample of apparently normal stimulus locations (Casson et al. 1990; Chauhan et al. 1991) and of stimulus locations in close proximity to regions of visual field progression (Chauhan et al. 1991).

The accuracy of the estimation of the differential light threshold and, as a consequence, the magnitude of the SF is dependent upon the algorithm employed in the thresholding staircase (Flanagan et al. 1993a; Flanagan et al. 1993b) and upon the start- and end-point of that staircase relative to the true threshold value (Fankhauser et al. 1988; Johnson et al. 1992). Indeed, the higher global SF for the Octopus perimeter compared to that of the Humphrey Field Analyser (Brenton & Argus 1987) is attributed to the difference in the thresholding algorithms employed by the two perimeters (Fankhauser et al. 1988).

An increase in SF may be considered a pre-cursor to visual field loss in glaucoma patients (Gloor et al. 1980; Rabineau et al. 1985; Sturmer et al. 1985; Werner & Drance 1977). The magnitude of SF in ocular hypertensives is, in general, similar to that of normal subjects (Flammer 1985; Flammer et al. 1984c). It is larger in glaucoma than in ocular hypertensives (Flammer 1985; Flammer et al. 1984c) or normals (Flammer 1985; Flammer et al. 1984c; Flanagan et al. 1993a; Flanagan et al. 1993b). The SF is in the order of 1.0dB to 2.0dB in normals and may increase by 2dB or more in glaucoma. Interestingly, the Advanced Glaucoma Intervention Study (AGIS) only considered a glaucomatous field to be unreliable in terms of the SF when it was larger than 6dB (AGIS 1994).

The influence of the stimulus size and of the patient age on the magnitude of the SF is equivocal. SF has been found to increase with reduction in the stimulus size over the range from Goldmann size V to size I by some authors (Gundersen et al. 1993) or from size III to

size I (Gilpin et al. 1990) whilst others have found no difference (Dengler-Harles et al. 1993). The reason for the discrepancy in these findings is unclear. The SF has been found to increase with increase in age (Autzen & Work 1990; Chauhan et al. 1990; Haas et al. 1986), whilst other studies find age to have little influence (Brenton & Phelps 1981; Flammer et al. 1984a; Heijl et al. 1987a). The duration of the perimetric stimulus (100-200msecs) has little or no effect on the magnitude of the global SF (Pennebaker et al. 1992). Furthermore, SF had been found to be largely independent of background luminance in normals (Crosswell et al. 1991) and in early glaucoma (Dengler-Harles et al. 1993). The SF decreases as a result of the learning effect (Autzen & Work 1990; Werner et al. 1990; Werner et al. 1989; Wood et al. 1987) but increases as a result of examination fatigue (Hudson et al. 1994; Searle et al. 1991).

The magnitude of the SF is higher at the border of a scotoma (Haefliger & Flammer 1989; Haefliger & Flammer 1991) and is greater at the less defined edges of a glaucomatous scotoma than at the edge of the physiological scotoma of the blind spot (Haefliger & Flammer 1991). It has been postulated that the increase in SF at the border of scotoma may be due to fixation instability (Eizenman et al. 1993; Henson & Bryson 1991). The local SF increases with increasing eccentricity (Brenton & Phelps 1981; Heijl et al. 1987b; Heijl et al. 1987c) and in glaucoma is greater in the superior field than in the inferior field (Flammer 1985). In normal subjects, the SF ranges from 1.7dB to 2.3dB out to eccentricities of 15° and from 2.6dB to 6.1dB from 15° to 30° (Heijl et al. 1987a). SF increases as mean sensitivity reduces but may show a subsequent decrease as the mean sensitivity approaches absolute loss (Haefliger & Flammer 1989; Heijl et al. 1987b). This is due to the lack of available stimulus brightness (ie. the perimeter dynamic range) when operating at low sensitivities.

Alternative techniques of determining the SF have been suggested. By fitting a least squares polynomial surface to the entire field from single measures of the differential light threshold at each stimulus location, a reference level is provided from which the residual of the measured threshold at each location may be determined. The square root of the residual mean square estimate can then be used to provide a measure of the SF (Schulzer et al. 1990). This

measure shows a good correlation with traditional methods of estimating the SF (r>0.66) (Mills et al. 1991). The advantage of this estimation technique lies in the reduction of the examination duration since only one determination of threshold is made and the polynomial surface fit accounts for the intrinsic relationship between adjacent locations in the visual field (Heijl et al. 1989a; Lachenmyer et al. 1994). Spatial filtering, utilising a Gaussian 3 by 3 filter, is another alternative method of determining the within-examination variability from a single estimation of threshold (Fitzke et al. 1995). This method defines weighted local variability as the residual of the difference between the sensitivity at a given stimulus location and the average sensitivity of all the adjacent locations (Crabb et al. 1995). A measure of global variability, termed local spatial variability (LSV), can then be derived by the root mean square of the residuals at all stimulus locations across the visual field (Crabb et al. 1995). The LSV is closely correlated with the visual field index PSD in normals (ϱ=0.74) and in glaucoma (ϱ=0.66) than with the SF (ϱ=0.46 and ϱ=0.52 respectively). This is, perhaps, a slightly surprising finding given that the PSD index is weighted for the increase in variability with increase in eccentricity and is derived by comparison to an empirical database of normal subjects.

3.1.3. Long-term fluctuation.

The long-term fluctuation (LF) is the variance additional to that of the SF and is present between two or more examinations. It is divided into two components: the homogeneous component, LF(Ho), which affects all locations equally and the heterogeneous component, LF(He), which varies between locations (Flammer et al. 1983). The two components each represent summary measures of the fluctuation occurring across all the specified locations and, as such, are global measures. The LF is not routinely quantified in clinical perimetry despite the overriding need to separate fluctuation from true change (Bebié et al. 1976).

The LF(Ho) and LF(He) components are calculated by a two-factor analysis of variance (ANOVA) with replications which utilises the sensitivities from the double determination of threshold at each of a given number of stimulus locations that are common between the two

examinations (Flammer et al. 1983; Flammer et al. 1984b; Flammer et al. 1984c). The procedure assesses the difference in the average overall sensitivity between the two examinations, LF(Ho), and whether the difference varies between stimulus locations, LF(He). The two components are separately derived from the root of the corresponding mean square estimate of the ANOVA corrected for the aggregate measurement across the two examinations (Flammer et al. 1983; Flammer et al. 1984b; Flammer et al. 1984c). However, negative values of both components have been reported (Flammer et al. 1984c) when mathematically the components can only be positive or zero. Analysis of variance (ANOVA) is a convenient method in which to describe the long-term fluctuation and the outcome measures will be influenced by the type of ANOVA used. A two-factor ANOVA with replications is advantageous in that it accounts for the interactive relationship between the components of variance and, in addition, is able to incorporate co-variate factors (Flammer et al. 1984b). However, it is perhaps due to the computational complexity of the calculation that the long-term fluctuation is not defined clinically in this manner.

Several alternative measures of between-examination variation have been proposed for the field as a whole (Flammer et al. 1983; Flammer et al. 1984b; Flammer et al. 1984c; Katz & Sommer 1987; Pennebaker et al. 1992; Young et al. 1990). A linear nested ANOVA model has been advocated by several authors (Crosswell et al. 1991; Gilpin et al. 1990; Pennebaker et al. 1992; Young et al. 1990). This type of model estimates the global components of LF(Ho) and LF(He) and can also include co-variate factors. However, the linear nested ANOVA is a simplified model that may not describe the data well (Stewart & Hunt 1993). In addition, each component of LF is not corrected for the measurement error which contributes approximately 25% of the total variability across examinations (Katz & Sommer 1987). The global long-term fluctuation has also been expressed as the standard deviation of the variance exhibited at each location across all locations in the visual field (Katz & Sommer 1987). This measure describes the total between-examination variation at all stimulus locations and therefore does not differentiate between the two components, LF(Ho) and LF(He), of between-examination variation. The model did, however, include a term for measurement error and as such

corrected for the within-test variability. An alternative global measure of between-examination variance is the range variability which is defined as the absolute difference between the highest and lowest threshold measures at each stimulus location, averaged across the entire field (Werner et al. 1989). The range variability expresses total variability (ie. including SF), is similar to the confidence intervals for visual field change computed by Hoskins et al (1988), and should be used for regions of the visual field rather than for the field as a whole (Hoskins et al. 1988; Werner et al. 1989). A sensitivity reduction of between 5dB and 9dB (depending on the location of the given region) is indicative of visual field progression (Hoskins et al. 1988; Werner et al. 1989). In addition, the probability of actual visual field progression is increased if the specified reduction of sensitivity occurs in more than one region (Werner et al. 1989).

The variability between examinations for an individual stimulus location has also been variously defined (Boeglin et al. 1992; Heijl et al. 1987a; Katz & Sommer 1987; Rutishauser et al. 1989; Werner et al. 1989; Zulauf et al. 1991). The LF has been designated as the variance of the serial threshold determination at each location in the visual field, in dB^2 (Boeglin et al. 1992; Zulauf et al. 1991). This definition includes the measurement error at each determination of threshold; it is perhaps not surprising therefore that this measure of LF correlated with the SF in stable glaucoma (Boeglin et al. 1992). Similarly, Werner et al (1989) define total variability as the square root of the variance of the serial threshold determinations at each stimulus location. This term 'total variability' acknowledges the contamination of SF (Werner et al. 1989) and expresses variability in dBs which is easier to interpret clinically. A component of the ANOVA model which determines the pointwise between-examination variability has been proposed (Rutishauser et al. 1989) which incorporates a term for the measurement error. Further, an empirical method of pointwise between-examination variability has been quantified in glaucoma patients as the difference in threshold deviation between two examinations as a function of the threshold deviation from normal at the first examination (Heijl et al. 1987a). An additional pointwise measure of LF has been suggested in which the estimate is made from the change in the number of 'not-seen' stimulus presentations in supra-threshold (5dB above estimated threshold) perimetry (Henson & Darling 1995).

The effect of perimetric examination parameters on the global estimates of LF have been studied using the inappropriate linear-nested ANOVA model. Gilpin et al (1990) investigated threshold variability as a function of stimulus size at between 15° vertical and 20° horizontal eccentricity in ten young, healthy individuals. Their findings indicate that both the LF(He) and the SF is greater for Goldmann stimulus sizes I and II, but are similar for stimulus size III to size V. The LF(He) was 2.4dB for stimulus size I and 2.2dB for stimulus size II and ranged from 1.0dB to 1.5dB for stimulus size III to size V. In contrast, the LF(Ho) was similar across all five stimulus sizes and was of a lesser magnitude than the LF(He), ranging from 0.3dB to 0.7dB. Moreover, the between-individual component of variability was larger for stimulus sizes IV and V. The effect on the LF of a change in stimulus size in glaucoma is unknown and, since the LF comoponents are reported to be higher in this patient group (Flammer et al. 1984c), assumes particular importance with respect to the use of larger stimulus sizes when the visual field tends towards absolute loss with stimulus size III (Takashima et al. 1993; Wilensky et al. 1986). Using the linear-nested ANOVA, no difference has been observed in the magnitude of either the LF(Ho) or LF(He) at the background intensities commonly employed in static perimetry ($10.0cdm^{-2}$ and $1.26cdm^{-2}$) (Crosswell et al. 1991) or across differing stimulus durations (65ms and 100ms to 500ms in 100ms steps) (Pennebaker et al. 1992). However, the LF(He) and the SF are increased by 1.0 to 1.5dB at mesopic background intensities of $0.10cdm^{-2}$ and $0.01cdm^{-2}$ (Crosswell et al. 1991).

The effect of an increase in age on the between-examination variability in threshold is equivocal. Katz et al (1987) found that, over an eighteen month period, the standard deviation of the variances across stimulus locations were, on average, twice as large in normal subjects of 60 years of age and above than in younger subjects. Conversely, no increase in threshold variability as a function of age has been found over a two month period (Heijl et al. 1988) or over a five year period (Boeglin et al. 1992). Out to 30° eccentricity the pointwise between-examination variation increases with increasing eccentricity both within and between normal individuals (Heijl et al. 1987a). The increased variation exhibited by normal subjects is greater between 20° and 30° than within 20° eccentricity (Rutishauser et al. 1989; Wilensky &

Joondeph 1984) and with the exception of the temporal quadrant is also greater between 30° and 60° (Young et al. 1990). Increased between-examination variability with increasing eccentricity has also been described in glaucoma, and is of a similar extent to that in normals (Boeglin et al. 1992). Between-examination variability increases as pointwise sensitivity decreases (Heijl et al. 1989b; Henson & Darling 1995; Werner et al. 1989), although the variability is greatest at moderately elevated thresholds (where sensitivity is reduced by between 10dB and 20dB) than at locations exhibiting sensitivity either near normal or of absolute loss (Heijl et al. 1989b).

Evaluation of the long-term fluctuation between a pair of examinations is an essential procedure in determining visual field progression. In deriving the LF, the required model should be able to differentiate between the two components of LF and correct for the measurement error. A pointwise approach to the evaluation of LF describes the total long-term fluctuation at each location without accounting for either the amount of variance that is identical at all locations or, in general, the measurement error. Of the current global measures of LF, the linear-nested ANOVA model does not include a correction for the measurement error and the expression of range variability does not separate the components of LF. Nevertheless, these various measures have also been labelled long-term fluctuation. However, despite their limitations these models do represent a mathematical attempt to quantify what is normally achieved by intuitive inspection of a series of visual fields.

The LF(Ho) should not be confused with the difference in the Mean Deviations (MD) between two successive examinations since both measures represent different descriptions of the sensitivity occurring across the entire field. The MD is readily available from the perimeter printout and represents a summary of the differences between the *measured* values of sensitivity and the corresponding age-matched normal values. The difference in the MDs therefore provides a convenient, clinically available, measure of deterioration in the height of the visual field. The resultant value represents the difference between two linear averages of measured values; however, the difference from the true average is distorted by the weighting

function (Heijl et al. 1987b) applied to the MD which adjusts for the variability of the threshold at each stimulus location. In contrast, the LF(Ho) component derived by ANOVA is not available from the perimeter and is an expression of the *variability* of the measured values based upon a linear model involving an interaction term that allows for the inherent error in the measured threshold.

Similarly, the LF(He) between two successive fields should not be confused with the difference in the corrected pattern standard deviation (CPSD) between the two fields. The CPSD is readily available from the perimeter printout and is a summary measure, corrected for the effect of the SF, of the deviation in the shape of the measured field from that of the normal age-matched field. The difference between the CPSDs therefore provides a clinically available measure of deterioration in the shape of the visual field. The resultant value is dependent on the difference between two standardised statistical variances. In contrast, the LF(He) component represents the difference in the *variability* of the measured shape of the visual field. The quantitative relationships between the LF(Ho) component and the difference in the MDs and between the LF(He) component and the difference in the CPSDs are unknown. Such knowledge would further contribute to the identification of visual field progression.

The standard full threshold 4-2dB algorithm of the Humphrey Field Analyser (HFA) (Humphrey Instruments Inc., San Leandro, Ca.) with programs 30-2 or 24-2 undertakes a double determination of threshold at each of ten specified stimulus locations within 21° eccentricity. The SF is calculated from these ten specified locations but the corresponding LF, as calculated by ANOVA, has never been specified. The HFA algorithm undertakes more than ten double determinations of threshold in cases of decreased patient reliability or of irregularity of the field loss between adjacent locations (Heijl et al. 1987b). The magnitude of the components of the LF calculated from all available double determinations of threshold is also unknown.

3.2. Aims.

The study had five aims. Firstly, to compare the magnitudes and distributions of the LF(Ho) and LF(He) components, in a stable glaucomatous sample, between pairs of successive examinations carried out over a routine (long) follow-up of 6-9 months and also over a confirmatory (short) follow-up of three weeks. Secondly, to determine the degree of similarity in the magnitudes of the components derived from the immediate next pair of examinations carried out over similar follow-ups. Thirdly, to relate the LF(Ho) component to the difference in the corresponding MDs for the two successive examinations and the LF(He) component to the difference in the corresponding CPSDs. Fourthly, to determine the influence of the indices MD, SF and CPSD on the magnitude of the LF(Ho) and LF(He) components. In addition, to investigate the relationship between the magnitude of the LF components and the level of sensitivity of the stimulus locations from which they are derived. Finally, to determine the influence of the number of double determinations of threshold on the magnitude of the LF(Ho) and LF(He) components. Subsequently, to utilise the knowledge gained about the LF to develop an algorithm that could be used to determine the clinical necessity of a follow-up examination to confirm visual field progression.

3.3. Methodology.

Two experimental protocols were used to determine the components of the LF. The first protocol was concerned with the derivation of the LF from pairs of consecutive fields separated by a long follow-up. The second protocol was concerned with the derivation of the LF from pairs of consecutive fields separated by a short follow-up. Informed consent was obtained from all patients after the nature and possible consequences of the procedure had been fully explained and the study had approval from the ethical committee of the Toronto Hospital.

3.3.1. Long follow-up.

The protocol for the derivation of the LF over the long follow-up involved a retrospective study. The sample comprised 30 patients with stable primary open angle glaucoma drawn from the Glaucoma Service of the Toronto Hospital (Western Division). The sample was selected to

provide the broadest possible range of field loss (HFA Program 30-2; stimulus size III). Three consecutive visual fields, separated by 6-9 months, were selected from the randomly assigned eye of each patient. The three fields were chosen on the basis that they had been preceded by at least two earlier examinations in order to minimise the effects of learning, that the visual fields were stable and that the optic nerve head appearance and intraocular pressures remained unchanged during the period in question. All patients had a distance visual acuity of 6/12 or better and were experienced in automated perimetry. Cases of clinically significant cataract, of pilocarpine therapy, or of an ocular history other than glaucoma were excluded from the study. The sample was not controlled for the type of ocular therapy, with the exception of pilocarpine, and the treatment remained unchanged for each patient over the time period. The protocol for examination of the visual field was strictly followed and all fields were deemed to be reliable in terms of the incidence of false-responses to the catch trials. The mean age of the sample was 64.8 years (SD 11.4). The MD at the initial presentation ranged from -0.2dB to -23.7dB (mean -8.3dB; SD 7.3) and the PSD from 1.3dB to 16.5dB (mean 6.7dB; SD 3.4). The group mean intraocular pressure over the three examinations was 15.0mmHg (SD 2.3).

The mean interval between each of the three examinations was 7.9 months. Stability of the visual field for the sample as a whole over each of the three examinations was confirmed statistically in terms of the stability of the visual field indices MD, CPSD and SF (Flanagan et al. 1993c). Three separate measures of the MD were evaluated: the weighted MD of all 76 locations derived from the HFA print-out, the corresponding unweighted MD, and the unweighted MD derived from the 10 standard stimulus locations at which a double determination of threshold is undertaken. The unweighted indices were calculated as the weighting function has not been published. The indices based upon the 10 standard stimulus locations were calculated for compatibility with the locations at which the two components of the LF were determined. The unweighted indices based upon all 76 locations were calculated to provide a link between the weighted index derived from the print-out and the unweighted index representing the 10 standard stimulus locations. Two separate measures for the SF

were analysed: the weighted SF derived from the HFA print-out and the unweighted SF derived from the 10 standard locations. Similarly, three measures of the CPSD were analaysed: the weighted CPSD from the HFA print-out, the unweighted 76 location CPSD and the unweighted CPSD derived from the 10 standard locations. The normal values necessary for the calculation of the unweighted indices were provided by Humphrey Instruments Inc. and were identical to the normal data used in the STATPAC software (Heijl et al. 1987b). The values were similar to the subset of that data published previously (Heijl et al. 1987a). A separate repeated measures analysis of co-variance (ANCOVA) was undertaken for each of the three indices. Analysis of co-variance is a modification of analysis of variance and accounts for the presence of confounding factors which may influence the outcome of the factors of interest. Age was considered as a co-variate, and subtype of index (ie. weighted, unweighted, or unweighted based upon the 10 stimulus locations) and examination order (ie. first to second and second to third) as within-subject factors. The three separate indices (including all subtypes) were stable over the three examinations (MD p=0.148; SF p=0.644; CPSD p=0.475). The summary table for the ANCOVA outcomes for each of the three indices MD, SF and CPSD, respectively, are shown in Tables 3.1.-3.3.

3.3.2. Short follow-up.

The protocol for the derivation of the LF over the short examination interval involved a prospective study. The sample also comprised 30 patients with primary open angle glaucoma selected from the database of the Glaucoma Service of the Toronto Hospital (Western Division). Each patient was individually matched as closely as possible to a patient in the retrospective study on the basis of the visual field indices MD, SF and CPSD in the designated eye (*t*-test: p=0.79; p=0.83; p=0.76) and in terms of IOP (group mean 15.4mmHg; SD 2.21; *t*-test: p=0.11) and of age (group mean 67.8 years; SD 7.14; *t*-test: p=0.53). The mean deviation against the corrected pattern deviation for the first of the three examinations in each arm of the study is illustrated in Figure 3.1. All patients were experienced in automated perimetry having had numerous previous examinations. Identical inclusion criteria were utilised to that of the retrospective study. Each patient underwent three Humphrey Field Analyser Program 30-2

MD (long follow-up)

SOURCE	df	SUMS OF SQUARES	MEAN SQUARE	F-VALUE	p-VALUE
Index	2	6.933	3.466	0.132	0.876
Exam	2	21.546	10.773	0.412	0.663
Age	1	79.795	79.795	3.049	0.082
Index * Exam	4	179.115	44.779	1.711	0.183
Index * Age	2	34.013	17.006	0.650	0.523
Exam * Age	2	89.200	44.600	1.704	0.184
Index * Exam * Age	4	97.726	24.432	0.934	0.445
Residual	252	659.854	26.170		

MD (short follow-up)

SOURCE	df	SUMS OF SQUARES	MEAN SQUARE	F-VALUE	p-VALUE
Index	2	0.325	0.162	0.005	0.995
Exam	2	20.302	10.151	0.326	0.722
Age	1	114.719	114.719	3.686	0.056
Index * Exam	4	37.496	9.374	0.301	0.877
Index * Age	2	11.532	5.766	0.185	0.831
Exam * Age	2	10.794	5.397	0.173	0.841
Index * Exam * Age	4	51.297	12.824	0.412	0.800
Residual	252	9354.907	31.123		

Table 3.1. Summary table of the repeated measures ANCOVA for the three types of Mean Deviation (MD) derived from the three examinations of the long follow-up (top) and short follow-up (bottom).

SF (long follow-up)

SOURCE	df	SUMS OF SQUARES	MEAN SQUARE	F-VALUE	p-VALUE
Index	1	0.276	0.276	0.187	0.666
Exam	2	1.992	0.996	0.676	0.510
Age	1	5.302	5.302	3.597	0.060
Index * Exam	2	1.300	0.650	0.441	0.644
Index * Age	1	0.119	0.119	0.081	0.776
Exam * Age	2	5.074	2.537	1.721	0.182
Index * Exam * Age	2	1.594	0.798	0.541	0.583
Residual	168	247.611	1.474		

SF (short follow-up)

SOURCE	df	SUMS OF SQUARES	MEAN SQUARE	F-VALUE	p-VALUE
Index	1	0.086	0.086	0.069	0.793
Exam	2	0.490	0.245	0.197	0.821
Age	1	0.724	0.724	0.582	0.447
Index * Exam	2	5.215	2.608	2.097	0.126
Index * Age	1	0.002	0.002	0.002	0.965
Exam * Age	2	6.071	3.036	2.442	0.090
Index * Exam * Age	2	0.352	0.176	0.142	0.868
Residual	168	208.872	1.243		

Table 3.2. Summary table of the repeated measures ANCOVA for the two types of short-term fluctuation (SF) derived from the three examinations of the long follow-up (top) and short follow-up (bottom).

CPSD (long follow-up)

SOURCE	df	SUMS OF SQUARES	MEAN SQUARE	F-VALUE	p-VALUE
Index	2	3.485	1.743	0.259	0.772
Exam	2	3.294	1.647	0.245	0.783
Age	1	36.288	36.288	5.394	0.021
Index * Exam	4	23.744	5.936	0.882	0.475
Index * Age	2	7.373	3.686	0.548	0.579
Exam * Age	2	3.473	1.736	0.258	0.773
Index * Exam * Age	4	8.653	2.163	0.322	0.863
Residual	252	1695.231	6.727		

CPSD (short follow-up)

SOURCE	df	SUMS OF SQUARES	MEAN SQUARE	F-VALUE	p-VALUE
Index	2	3.011	1.506	0.145	0.866
Exam	2	43.345	21.673	2.081	0.127
Age	1	41.888	41.888	4.021	0.046
Index * Exam	4	93.843	23.461	2.252	0.064
Index * Age	2	9.142	12.421	0.439	0.645
Exam * Age	2	24.842	0.654	1.192	0.305
Index * Exam * Age	4	2.616	10.417	0.063	0.993
Residual	252	2625.032			

Table 3.3. Summary table of the repeated measures ANCOVA for the three types of corrected pattern standard deviation (CPSD) derived from the three examinations of the long follow-up (top) and short follow-up (bottom).

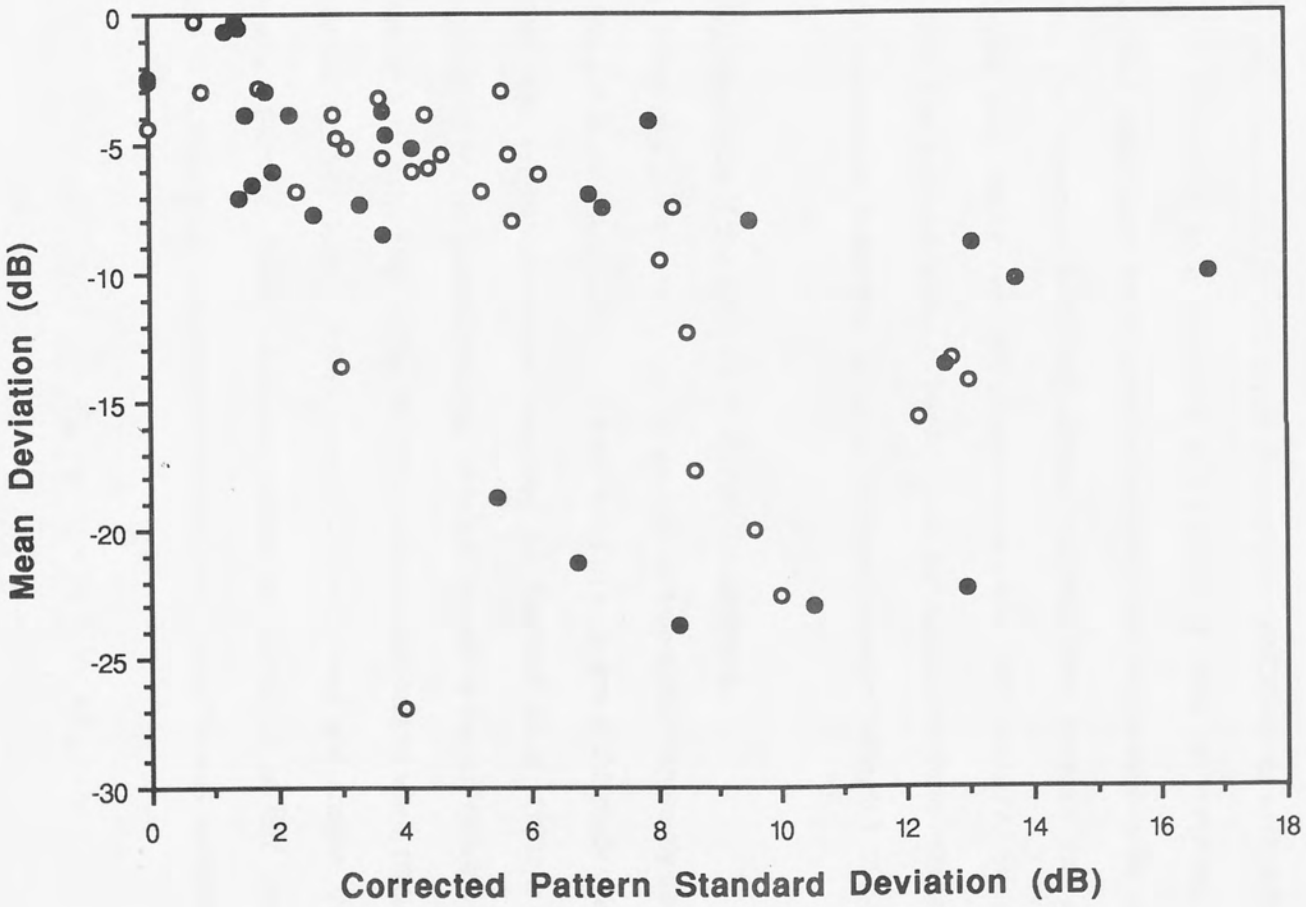

Figure 3.1. The type of visual field loss at the first visual field examination in terms of the mean deviation (dB) against the corrected pattern standard deviation (dB) for the long (filled circles) and short (open circles) follow-up arms of the study.

threshold fields (stimulus size III) in the designated eye over a period of six weeks with an interval of three weeks between each examination. The short follow-up examinations were all carried out by one experienced perimetrist. All fields were deemed to be reliable in terms of the incidence of false-responses to the catch trials.

Stability of the three fields over the six week period was confirmed statistically by undertaking a separate repeated measures analysis of covariance (ANCOVA) for each of the three indices. Age was considered as a co-variate, and subtype of index (ie. weighted, unweighted, or unweighted based upon the 10 stimulus locations) and examination order as within subject factors. The respective ANCOVAs showed that the three separate indices (including all subtypes) were stable over the three examinations (MD p=0.877; SF p=0.126; CPSD p=0.064). The summary tables of the ANCOVA for each of the three indices of MD, SF and CPSD, respectively, in the short follow-up study are shown in Tables 3.1. to 3.3.

3.3.3. Calculation of the LF(Ho) and LF(He) components.

The LF(Ho) and LF(He) components for each patient were then separately calculated between the first and second, and second and third, fields of each arm of the study using the two-factor ANOVA with replications model described by Flammer et al. (1983). The replications comprised the double determinations of threshold at each of the ten stimulus locations utilised by the HFA for calculation of the SF. The within-subject factors were stimulus location and examination order. Custom software was used to convert and analyse the HFA datafiles (Cassidy & Flanagan 1989) to a format suitable for analysis by an IBM compatible PC. The model for estimating the components of the long-term fluctuation was described by:

$$Y_{jkl} = \mu + L_j + V_k + LV_{jk} + E_{jkl} \qquad \text{Eq. (3.1)}$$

where Y is the threshold determination at each individual location, μ is the overall mean value of sensitivity which is related to MD by an aggregate constant, L_j is the effect of the test locations, V_k is the effect of each visual field examination, LV_{jk} is the interaction of L_j and V_k,

and E_{jkl} is the experimental error. The integers j, k and l represent, respectively, the number of considered stimulus locations with a double determination of threshold (j=1,2, ...n), the number of examinations (k=2) and the number of determinations of threshold at each considered location (l=2). The LF(Ho) component can be attributed to V_k, the LF(He) component can be attributed to the interaction term LV_{jk} and the short-term variance across both examinations can be attributed to the experimental error, E_{jkl}, normally distributed with an expected value of zero such that E_{jkl} is not correlated with any other error terms and is independent of the independent variables L_j, V_k and LV_{jk}.

The mean square estimates (MSE) for V_k and LV_{jk} were then reduced to their constituent variances in order to remove the accompanying error variance E_{jkl} by the hypothesis (Paradine & Rivett 1966):

$$MSE(V_k) = jl\sigma_k^2 + l\sigma_{jk}^2 + \sigma^2 \qquad \text{Eq. (3.2)}$$

$$MSE(LV_{jk}) = l\sigma_{jk}^2 + \sigma^2 \qquad \text{Eq. (3.3)}$$

$$MSE(E_{jkl}) = \sigma^2 \qquad \text{Eq. (3.4)}$$

The LF(He) component (σ_{jk}) was calculated by substituting the mean square error of the error term, σ^2, from equation 3.4 into equation 3.3. The LF(Ho) component (σ_k) was calculated in a similar manner by substituting equation 3.3 into equation 3.2.

In cases where either or both of the variance estimates σ_k^2 and σ_{jk}^2 corresponding to the LF(Ho) and LF(He) components, respectively, were found to be negative, the mean square estimate V_k and LV_{jk} of either σ_k^2 or σ_{jk}^2 was combined with the mean square estimate of E_{jkl} to give a corrected error variance, $\hat{\sigma}^2$. The resultant root mean square of $\hat{\sigma}^2$ was considered to be more representative of the actual aggregate error. This corrected error variance was achieved by adding the sums of squares of the original error estimate to the sums of squares of the source of the negative value:

$$\hat{\sigma}^2 = \frac{SS_{error} + SS_x}{df_{error} + df_x} \qquad \text{Eq. (3.5)}$$

where $\hat{\sigma}^2$ is the corrected aggregate error, SS_{error} and df_{error} are the sums of squares and degrees of freedom of the error variance, respectively, and SS_x and df_x are the sums of squares and degrees of freedom of the source of the negative value (ie either LV or V). Since the estimate of σ^2 becomes $\hat{\sigma}^2$, the interaction variance, σ^2_{jk}, was recalculated by substitution into equation 3.3. Since $\sigma^2 = \hat{\sigma}^2$, then:

$$\hat{\sigma}^2_{jk} = \frac{MSE(LV) - \hat{\sigma}^2}{I} \qquad \text{Eq. (3.6)}$$

Therefore, $\hat{\sigma}^2_{jk}$ was a more accurate assessment of σ^2_{jk} from which to calculate the LF(He). Since the magnitude of the aggregate error variance masks the statistical effect of the negative value, the corrected aggregate error variance is the most representative value of the negative effect. If both σ^2_k and σ^2_{jk} were found to be negative, then the combined error estimate calculation (equation 3.5) included the sums of squares of both V_k and Lv_{jk} from which they are derived. In all cases, the components of LF were expressed in decibels as the square root of the given variance estimate.

3.3.4. Analysis.

Stability of the LF(Ho) and LF(He) components and of the error term between the three successive examinations of each arm of the study were determined using a separate repeated measures analysis of covariance (ANCOVA) for each component. Age was considered as a co-variate and examination order as a within-subjects factor and type of study as a between-subjects factor.

The influence of the depth of loss described by the stimulus locations used to derive the LF components was investigated by collapsing the average sensitivity at each of the ten standard double determinations of threshold across the thirty subjects in each group. The sensitivities were collated into three groups describing mild, moderate and severe reductions in sensitivity. Each sensitivity group embodied an interval of twelve decibels ranging from 36dB to 0dB. The decibel width of each sensitivity group was taken such that each group contained,

approximately, the same number of stimulus locations. Locations which exhibited a threshold of 0dB for each determination at both examinations were excluded. Each component of the LF was derived in a similar manner to that of the ten standard double determinations excepting the integer j which represented the number of stimulus locations contained within each sensitivity group. The consideration of sensitivity across individuals in this manner is similar to that of Heijl et al. (1989b).

3.2.3. Results.

The group means, medians, SDs and ranges for each component of the LF derived from the 10 locations featuring a double determination of threshold are given in Table 3.4 for each arm of the study. The magnitudes of the LF(Ho) and LF(He) and of the error term remained constant over each of the three examinations in each of the two studies (LF(Ho) p=0.940; LF(He) p=0.426; error p=0.652). The magnitudes of the LF(Ho) and of the error term were greater in the short follow-up study (p=0.008 and p=0.005 respectively) than in the long follow-up study and this difference was present for both the first and second pairs of examinations (p=0.263 and p=0.856 respectively). The summary tables for the ANCOVA of each component of LF and the aggregate error are shown in Table 3.5. The discrepancy between the LF(Ho) values for the two studies can be attributed to the increased number of patients in the short follow-up group exhibiting a measurement error across the given pair of examinations initially producing a negative value of the LF(Ho) component. In these cases the negative value was combined with the measurement error across the two examinations, thereby skewing the LF(Ho) towards a more positive value. The cumulative frequency distributions for the second pair of examinations of each arm of the study are shown in Figure 3.2 for each component of LF and the aggregate error respectively. The positive shift of the cumulative frequency curve of both the LF(Ho) and aggregate error components can be clearly seen.

A construction of the limits of agreement (Bland & Altman 1986) for each component of LF and the aggregate error are illustrated in Figure 3.3. The 95% limits of agreement were +2.2dB to -2.6dB and +2.1dB to -2.5dB for the LF(Ho) component of the long and short follow-up studies

	LONG FOLLOW-UP			SHORT FOLLOW-UP		
	Mean (SD)	**Median**	**Range**	**Mean (SD)**	**Median**	**Range**
LF(Ho)						
1st - 2nd	1.72 (1.06)	1.47	0.08 - 4.79	2.19 (1.04)	2.18	0.38 - 5.29
2nd - 3rd	1.50 (0.75)	1.32	0.37 - 2.96	1.95 (0.91)	2.08	0.19 - 3.39
LF(He)						
1st - 2nd	2.02 (1.23)	1.51	0.70 - 5.05	2.00 (1.27)	1.76	0.33 - 5.32
2nd - 3rd	1.70 (1.03)	1.50	0.41 - 5.16	2.05 (1.08)	1.82	0.49 - 5.48
Aggregate Error						
1st - 2nd	1.93 (0.87)	1.74	1.00 - 4.79	2.31 (0.97)	2.09	1.21 - 5.29
2nd - 3rd	1.80 (0.98)	1.58	0.77 - 5.98	2.35 (0.84)	2.20	1.24 - 5.48

Table 3.4. Group means, SDs, medians and ranges (dB) for each of the LF components corresponding to each successive pair of fields for the long and short follow-up arms of the study.

LF(Ho)

SOURCE	df	SUMS OF SQUARES	MEAN SQUARE	F-VALUE	p-VALUE
Age	1	2.743	2.743	2.735	0.101
Study	1	7.314	7.314	7.292	0.008
Exam pair	1	1.269	1.269	1.266	0.263
Age * Study	1	0.490	0.490	0.489	0.486
Study * Exam pair	1	0.006	0.006	0.006	0.940
Age * Exam pair	1	0.113	0.113	0.112	0.738
Age * Study * Exam pair	1	0.048	0.048	0.048	0.827
Residual	112	112.306	1.003		

LF(He)

SOURCE	df	SUMS OF SQUARES	MEAN SQUARE	F-VALUE	p-VALUE
Age	1	4.031	4.031	3.039	0.084
Study	1	3.220	3.220	2.428	0.122
Exam pair	1	1.678	1.678	1.266	0.263
Age * Study	1	1.259	1.259	0.949	0.332
Study * Exam pair	1	0.846	0.846	0.638	0.426
Age * Exam pair	1	0.524	0.524	0.395	0.531
Age * Study * Exam pair	1	0.415	0.415	0.313	0.577
Residual	112	148.498	1.326		

Aggregate Error

SOURCE		SUMS OF SQUARES	MEAN SQUARE	F-VALUE	p-VALUE
Age	1	2.039	2.039	1.723	0.192
Study	1	9.704	9.704	8.201	0.005
Exam pair	1	0.039	0.039	0.033	0.856
Age * Study	1	0.704	0.704	0.595	0.442
Study * Exam pair	1	0.242	0.242	0.204	0.652
Age * Exam pair	1	0.26	0.256	0.216	0.643
Age * Study * Exam pair	1	0.162	0.162	0.137	0.712
Residual	112	132.522	1.183		

Table 3.5. Summary table for the repeated measures ANCOVA of the LF(Ho) (top), LF(He) (middle) and aggregate error (bottom) components of the long-term fluctuation for each pair of examinations for the long and short follow-up studies.

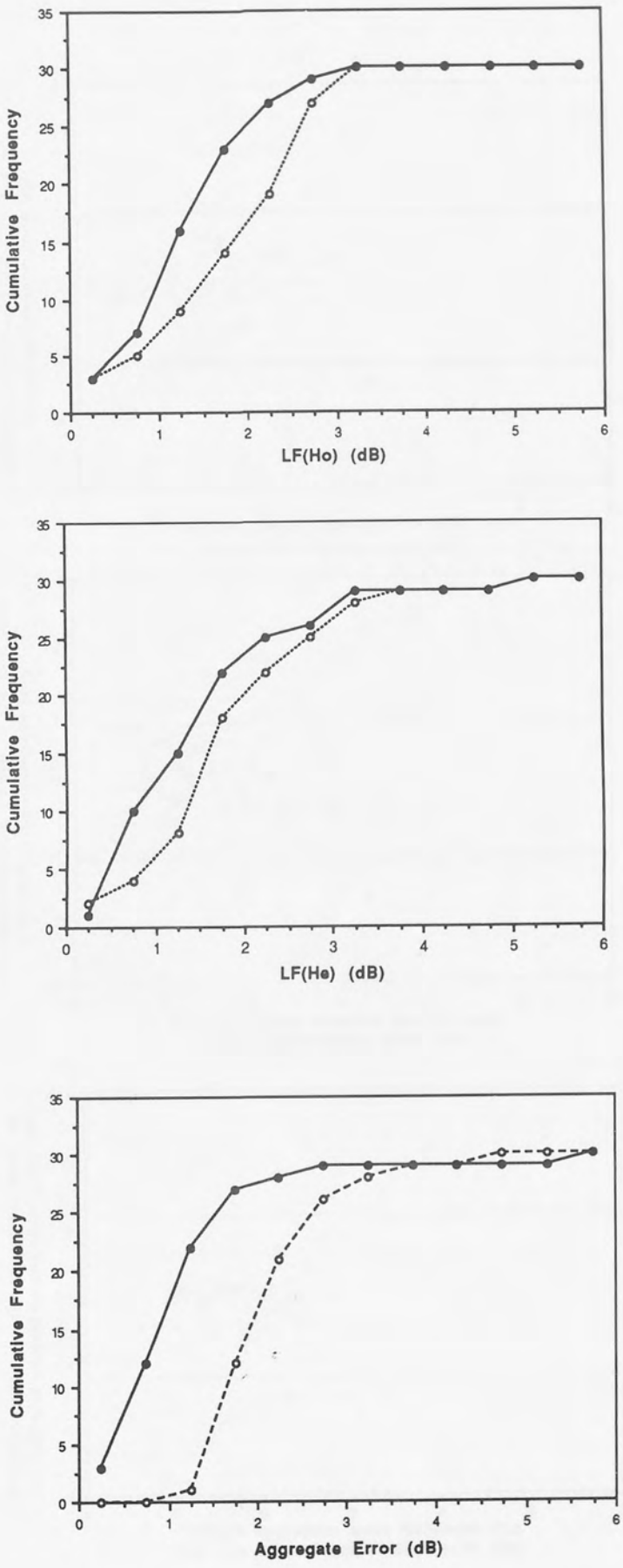

Figure 3.2. The cumulative frequency distributions of the LF(Ho) (top), LF(He) (middle) and aggregate error (bottom) components between the second and third examinations for the long (solid line) and short (broken line) follow-up arms of the study.

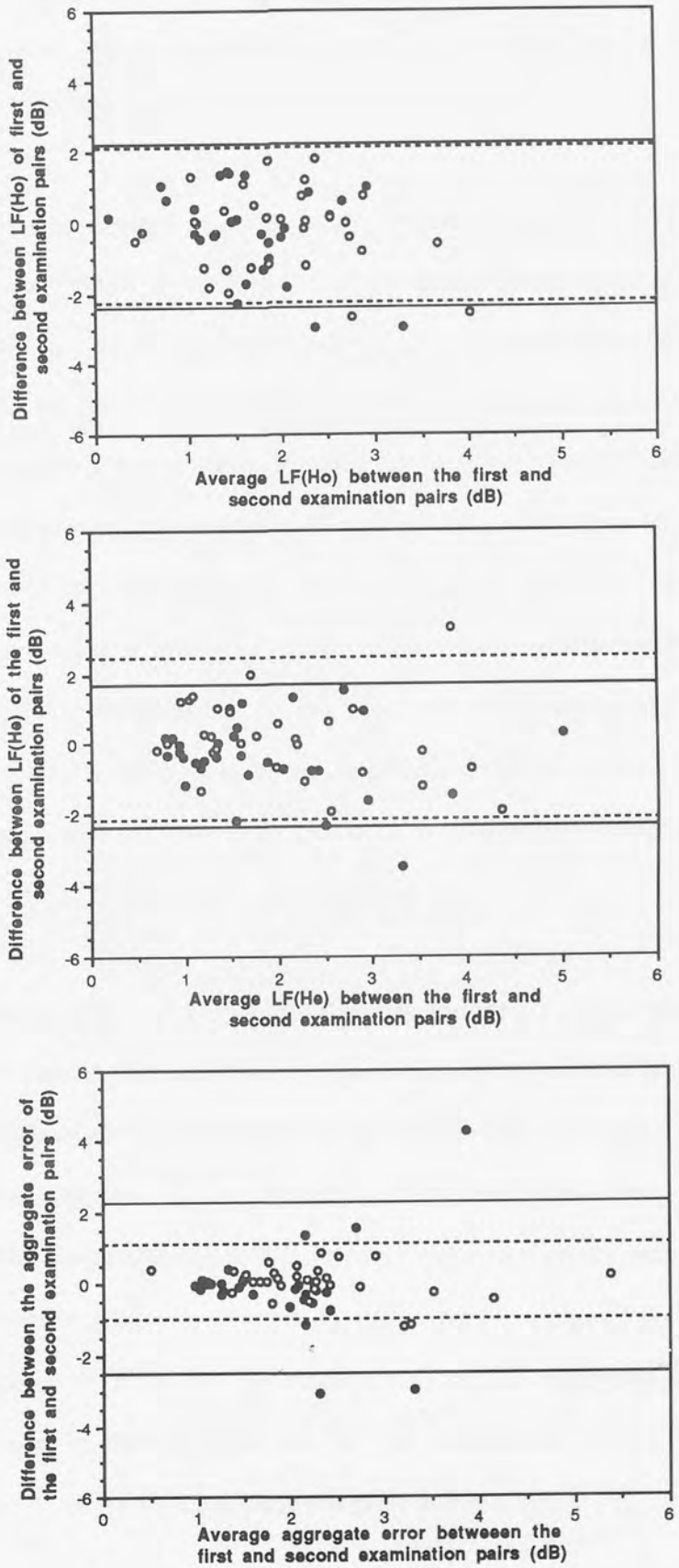

Figure 3.3. The 95% limits of agreement of the LF(Ho) (top), LF(He) (middle) and aggregate error (bottom) components for the long (solid line/filled circles) and short (broken line/open circles) follow-up arms of the study.

respectively. Similarly, the limits of agreement were +2.4dB to -2.3dB and +1.8dB to -2.4dB for the LF(He) component and +1.0dB to -0.9dB and +2.3dB to -2.5dB for the aggregate error of the long and short follow-up studies, respectively.

Little relationship was present in either study between either the LF(Ho) or the LF(He) component derived from the 10 locations featuring a double determination of threshold and the modulus difference in each of the various types of MD. The magnitudes of the coefficients of determination with the LF(Ho) component ranged from 1.1% to 32.4% for the three types of MD index across each of the two pairs of examinations in each study (Table 3.6). The larger values were evident in the second ppair of examinations of the long follow-up study. The magnitudes of the coefficients of determination for the LF(He) component ranged from 3.9% to 23.7% for the three types of MD index across each of the two pairs of examinations in each study. The larger values obtained for the coefficient of determination with the LF(He) component were clearly attributable to the presence of obvious outliers. The LF(Ho) and LF(He) components against the modulus difference in the weighted MD for the second pair of examinations in both studies are illustrated in Figures 3.4.

Similarly, little relationship was present for the corresponding functions between the LF(Ho) and the LF(He) components and the modulus difference in the three types of CPSD. The magnitudes of the coefficients of determination for the LF(He) ranged from 1.7% to 31.7%. The magnitudes of the coefficients of determination for the LF(Ho) ranged from 1.3% to 10.8%. The LF(Ho) and LF(He) components against the modulus differences in the weighted CPSD for the second pair of examinations in both studies are illustrated in Figures 3.5. The coefficients of determination for each of the two LF components and the aggregate error between the modulus difference in the weighted and in the unweighted indices for each pair of examinations and in each arm of the study are given in Table 3.6.

Little relationship was present in either arm of the study between the LF(Ho) or the LF(He) component derived from the 10 locations featuring a double determination of threshold and

MODULUS DIFFERENCE INDEX TYPE	LONG FOLLOW-UP						SHORT FOLLOW-UP					
	LF(Ho)		LF(He)		Aggregate Error		LF(Ho)		LF(He)		Aggregate Error	
	1st - 2nd	2nd - 3rd	1st - 2nd	2nd - 3rd	1st - 2nd	2nd - 3rd	1st - 2nd	2nd - 3rd	1st - 2nd	2nd - 3rd	1st - 2nd	2nd - 3rd
MD												
Weighted 76	1.7	32.4	16.0	6.2	1.7	1.9	1.4	1.2	6.0	4.9	0.9	2.2
Unweighted 76	1.1	25.9	12.7	5.9	0.5	2.0	5.9	1.9	7.1	5.0	1.6	2.1
Unweighted 10	5.8	26.8	3.9	23.7	4.0	2.4	1.9	0.7	6.7	6.9	0.2	1.4
CPSD												
Weighted 76	1.8	2.1	1.7	7.1	1.0	2.1	1.8	3.9	3.9	31.7	11.4	9.4
Unweighted 76	3.0	2.8	4.7	7.2	1.3	1.8	1.3	4.3	6.0	30.0	6.6	7.2
Unweighted 10	4.9	5.1	6.3	7.5	1.2	1.9	10.8	6.8	6.4	20.0	7.1	7.0
SF												
Weighted 10	4.9	6.4	12.2	10.5	1.2	4.6	10.9	8.8	3.6	5.7	7.1	6.8
Unweighted 10	2.1	3.9	13.4	11.3	1.1	4.4	13.6	5.4	3.8	4.9	8.5	5.0

Table 3.6. Coefficients of determination, expressed as a percentage, between the LF(Ho), LF(He) and aggregate error components and the modulus difference in the weighted and unweighted indices MD, CPSD and SF for each pair of examinations.

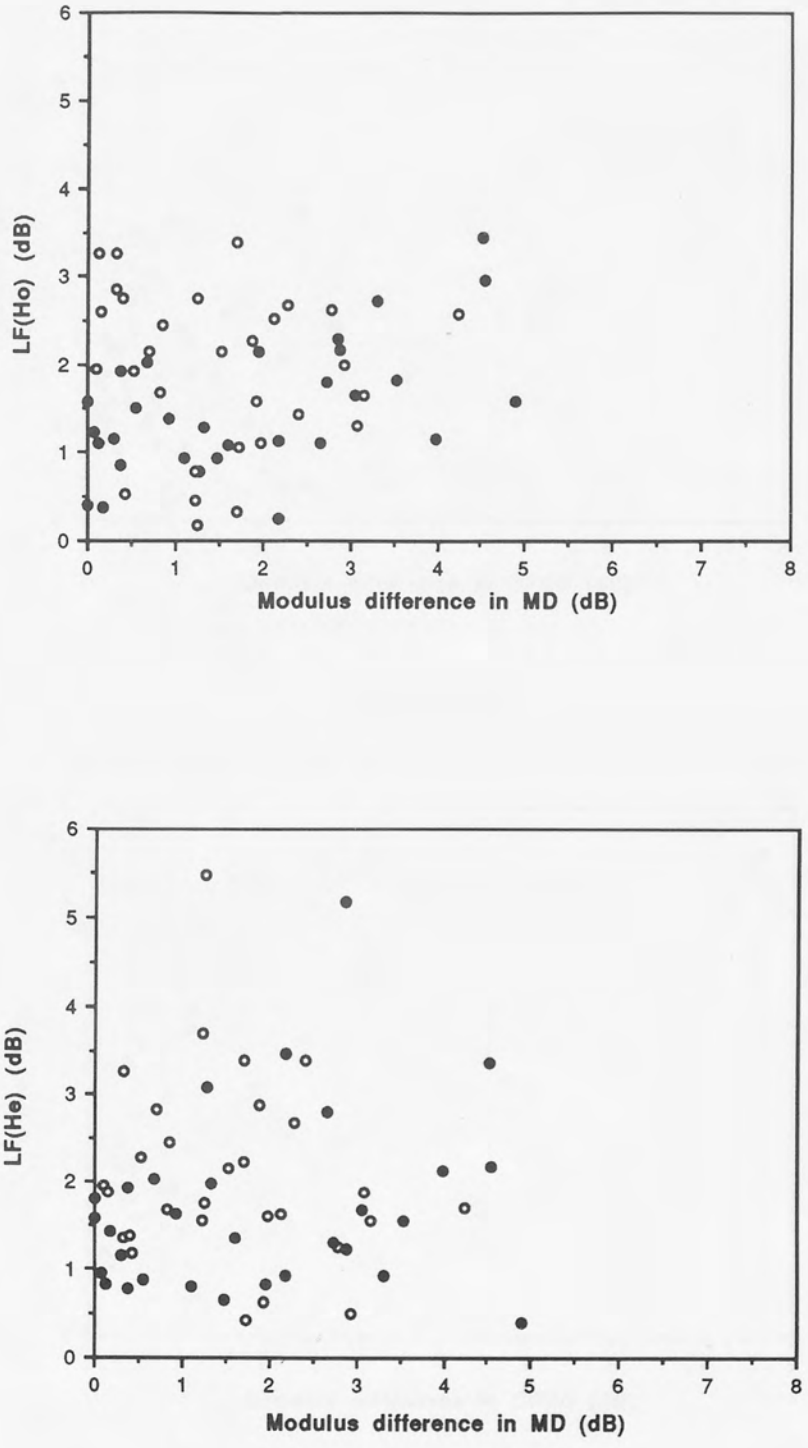

Figure 3.4. The LF(Ho) (top) and the LF(He) (bottom) components between the second and third examinations against the modulus difference in weighted mean deviation (MD) for the long (filled circles) and short (open circles) follow-up arms of the study.

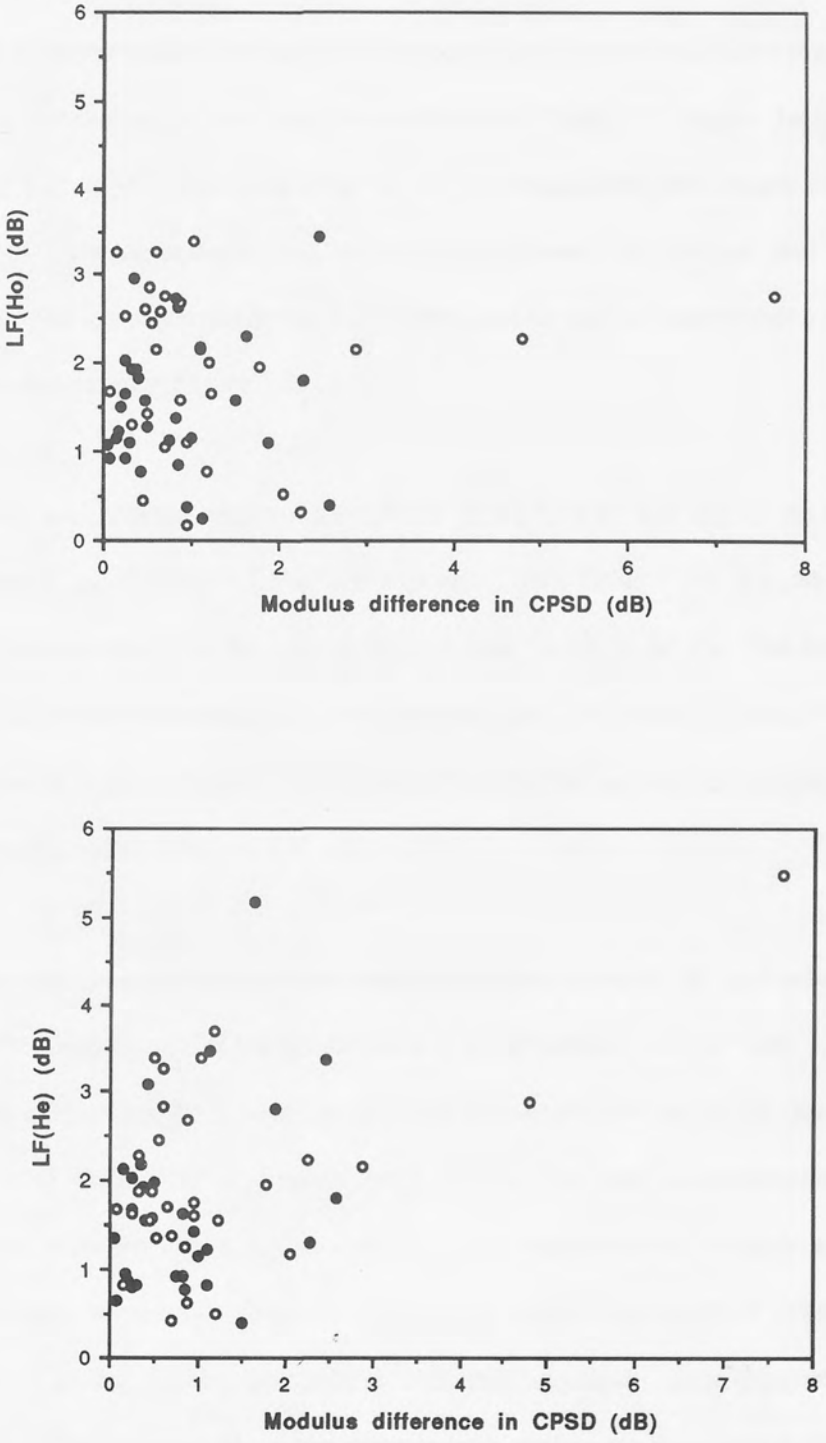

Figure 3.5. The LF(Ho) (top) and the LF(He) (bottom) components between the second and third examinations against the modulus difference in weighted corrected pattern standard deviation (CPSD) for the long (filled circles) and short (open circles) follow-up arms of the study.

any of the three MD indices expressed as a mean of the corresponding two fields. The magnitudes of the coefficients of determination for the LF(Ho) ranged from 1.8% to 32.5% for the three types of MD index across each of the two pairs of examinations. The magnitudes of the coefficients of determination for the LF(He) ranged from 1.0% to 45.2% for the three types of MD index across each of the two pairs of examinations (Table 3.7). Again, the larger values for the coefficient of determination and either of the LF components were clearly attributable to the presence of obvious outliers. The relationship between the LF(Ho) and the LF(He) components against the mean weighted MD for the second pair of examinations of each arm of the study are illustrated in Figure 3.6.

Little relationship was present between the LF(Ho) or the LF(He) and any of the three CPSD indices expressed as a mean of the corresponding two fields. The magnitudes of the coefficients of determination for the LF(He) ranged from 14.5% to 32.7%. The magnitudes of the coefficients of determination for the LF(Ho) ranged from 1.0% to 6.5%. The LF(Ho) and the LF(He) components against the mean weighted CPSD for the second pair of examinations in both studies are illustrated in Figure 3.7.

No relationship was present between the mean of the two types of SF and either of the LF components. The magnitudes of the coefficients of determination ranged from 1.2% to 9.8% across the two studies for the LF(Ho) component and from 1.3% to 41.9% for the LF(He) component (Table 3.7). The aggregate error across the two examinations correlated moderately well with the mean SF across the two examinations in both studies. The magnitudes of the coefficients of determination ranged from 48.6% to 60.5% (Table 3.7). The LF(Ho) component, the LF(He) component and the aggregate error against the mean weighted SF for the second pair of examinations in both studies are illustrated in Figures 3.8.

The magnitude of each component of LF as a function of the level of sensitivity is shown in Table 3.8. In general, both the LF(Ho), LF(He) components and the aggregate error increased in magnitude as the level of sensitivity decreased.

MEAN INDEX TYPE	LONG FOLLOW-UP						SHORT FOLLOW-UP					
	LF(Ho)		LF(He)		Aggregate Error		LF(Ho)		LF(He)		Aggregate Error	
	1st - 2nd	2nd - 3rd	1st - 2nd	2nd - 3rd	1st - 2nd	2nd - 3rd	1st - 2nd	2nd - 3rd	1st - 2nd	2nd - 3rd	1st - 2nd	2nd - 3rd
MD												
Weighted 76	8.8	8.4	13.5	3.8	7.4	1.3	21.5	6.4	17.1	45.2	48.1	39.1
Unweighted 76	5.4	1.8	7.5	2.1	5.2	0.9	19.8	5.4	17.9	42.3	46.3	36.9
Unweighted 10	5.7	2.9	14.5	1.0	10.4	1.0	32.5	10.1	18.4	38.1	43.9	34.0
CPSD												
Weighted 76	5.5	1.0	29.0	15.7	16.3	6.5	2.8	1.0	18.0	15.0	9.6	1.5
Unweighted 76	4.9	2.0	32.7	15.8	21.0	6.2	4.9	6.5	14.5	16.7	0.9	1.1
Unweighted 10	1.5	3.6	22.7	17.8	5.8	7.8	2.6	1.2	25.1	17.3	16.4	4.7
SF												
Weighted 10	3.2	1.2	10.4	12.6	49.9	48.6	4.3	9.8	2.8	41.9	60.2	60.5
Unweighted 10	1.6	2.2	3.9	5.5	48.7	48.9	3.8	1.8	1.3	38.2	58.8	54.0

Table 3.7. Coefficients of determination, expressed as a percentage, between the LF(Ho), LF(He) and aggregate error components and the mean weighted and unweighted indices MD, CPSD and SF for each pair of examinations.

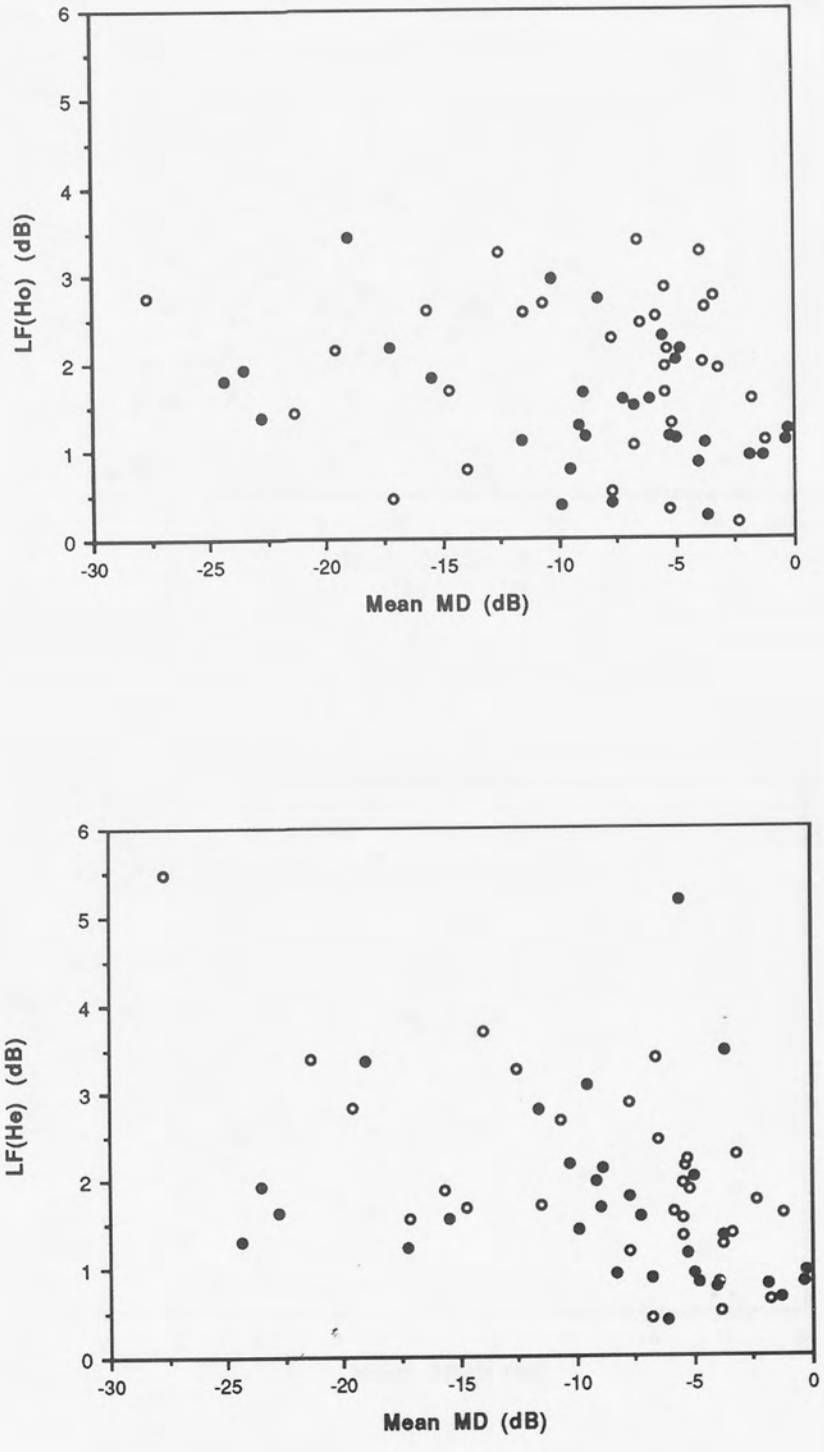

Figure 3.6. The LF(Ho) (top) and the LF(He) (bottom) components between the second and third examinations against the mean weighted mean deviation (MD) for the long (filled circles) and short (open circles) follow-up arms of the study.

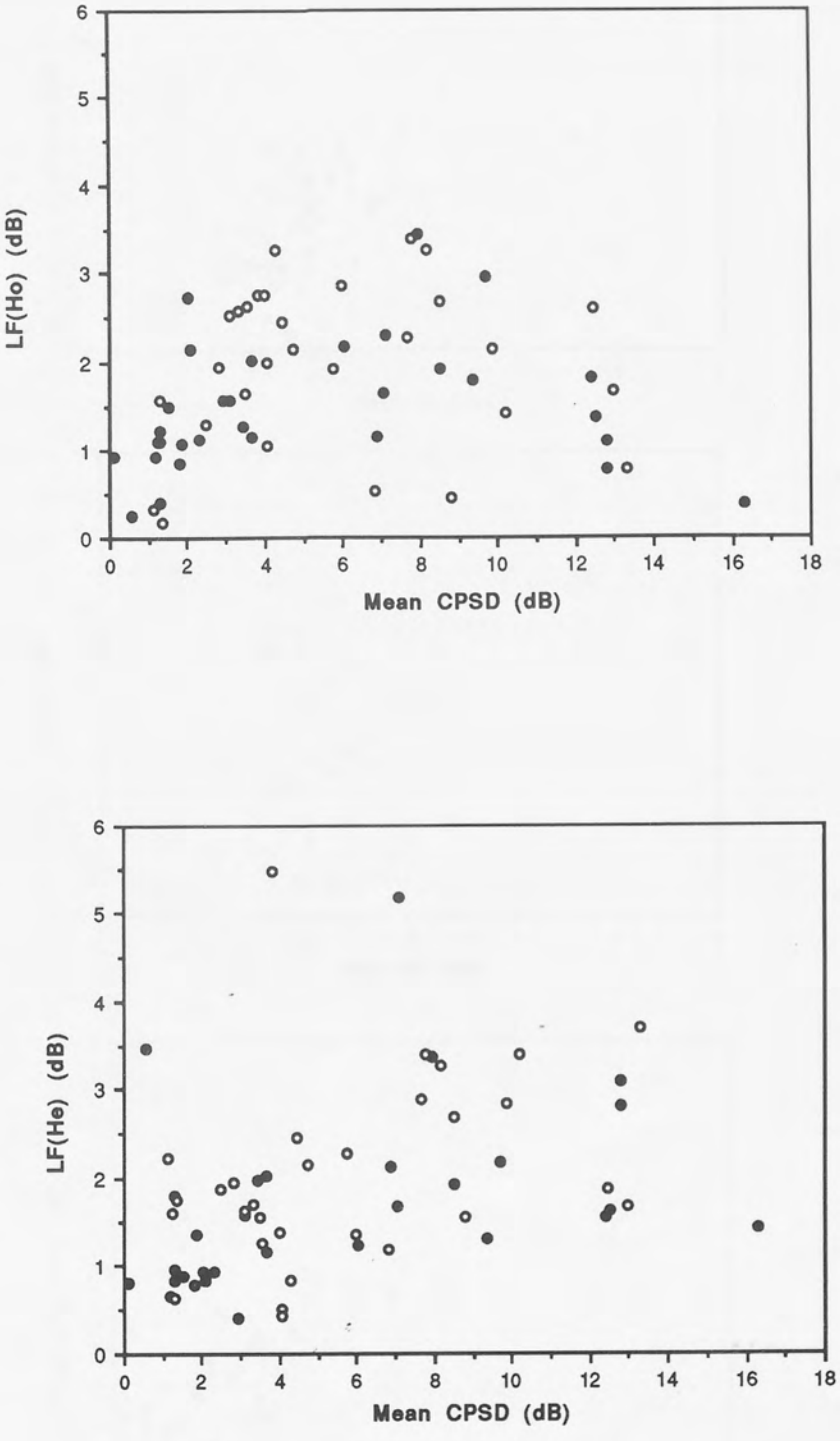

Figure 3.7. The LF(Ho) (top) and the LF(He) (bottom) components between the second and third examinations against the mean weighted corrected pattern standard deviation (CPSD) for the long (filled circles) and short (open circles) follow-up arms of the study.

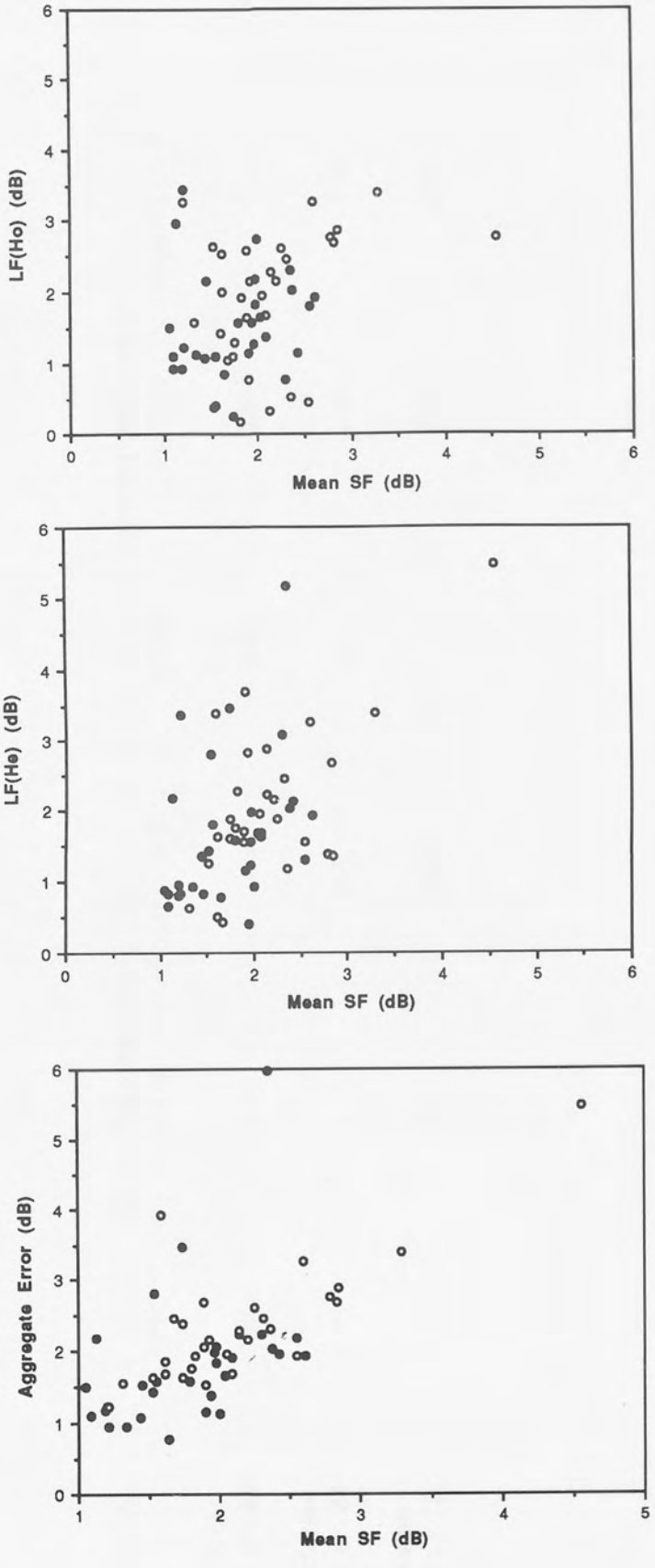

Figure 3.8. The LF(Ho) (top), the LF(He) (middle) and the aggregate error (bottom) components between the second and third examinations against the mean weighted short-term fluctuation (SF) for the long (filled circles) and short (open circles) follow-up arms of the study.

INTERVAL	LONG FOLLOW-UP			SHORT FOLLOW-UP		
	LF(Ho)	LF(He)	Aggregate Error	LF(Ho)	LF(He)	Aggregate Error
Mild $24 \leq z \leq 36$	0.34	0.68	0.38	0.48	0.55	0.32
Moderate $12 \leq z \leq 24$	1.25	1.73	3.72	1.57	2.33	4.56
Severe $0 < z \leq 12$	1.61	2.04	3.96	1.89	2.73	4.01

Table 3.8. The magnitude of the LF(Ho), LF(He) and aggregate error (dB) as a function of the mean level of sensitivity of the stimulus locations.

In the long follow-up study only 14 of the 30 patients exhibited additional double determinations of threshold common to the first and second examinations and 16 patients additional double determinations common to the second and third examinations. The corresponding figures for the short follow-up study were 29 and 25 patients respectively. The group means, SDs and ranges for each component of the LF derived from the 10 locations featuring a double determination of threshold and from all available double determinations of threshold for these subgroups are given in Table 3.9 for each arm of the study. The LF(Ho) and LF(He) components derived from all available double determinations were, in general, larger than those derived from the ten standard double determinations of threshold but these differences did not reach statistical significance (LF(Ho) p=0.132; LF(He) p=0.082) for either pair of examinations (LF(Ho) p=0.671; LF(He) p=0.357) or time of follow-up (LF(Ho) p=0.622; LF(He) p=0.461) (Table 3.10). The number of additional determinations ranged from 2.2 to 2.9. The higher value of the LF components derived from all available double determinations of threshold would be expected since a second threshold determination is undertaken at a stimulus location exhibiting either decreased patient reliability and/or irregularity of the field loss between adjacent locations (Heijl et al. 1987b). The relationship between the LF components derived from the ten standard double determinations and those derived from all available double determinations of threshold are shown in Figure 3.9.

3.5. Discussion.

One of the most difficult problems in the management of glaucoma is the identification of the disease progression. The LF can be calculated for any number of visual fields. However, in this study, the LF was calculated between pairs of consecutive visual fields since the identification of visual field progression is particularly difficult when the second field of any given pair of successive fields shows an apparent deterioration compared to that of the preceding field. The deterioration may be due to the LF or to change resulting from the disease progression. In such a case, a third examination is frequently required to confirm the results of the second field. As a consequence, additional clinic time is required and the appropriate therapeutic intervention may also be delayed. Similarly, when the second of any given pair of

	LONG FOLLOW-UP			SHORT FOLLOW-UP	
	Mean (SD)	Range		Mean (SD)	Range
LF(Ho)					
Determinations			1st - 2nd		
Ten	2.00 (1.21)	0.65 - 4.79		2.05 (1.26)	0.33 - 4.41
All	1.83 (1.37)	1.59 - 5.46		1.99 (1.11)	0.13 - 4.45
Determinations			2nd - 3rd		
Ten	1.74 (0.71)	0.77 - 3.44		1.76 (0.87)	0.19 - 3.39
All	2.16 (1.19)	1.30 - 5.67		2.12 (1.03)	0.35 - 3.85
LF(He)					
Determinations			1st - 2nd		
Ten	2.65 (1.48)	0.95 - 5.05		2.24 (1.02)	0.38 - 5.29
All	2.75 (1.21)	1.01 - 4.38		2.21 (1.07)	0.53 - 5.23
Determinations			2nd - 3rd		
Ten	1.96 (1.19)	0.41 - 5.16		1.99 (1.06)	0.44 - 5.48
All	2.54 (1.11)	0.97 - 4.30		2.78 (1.27)	0.97 - 4.98

Table 3.9. The group means, SDs and ranges (dB) for those patients exhibiting additional double determinations of threshold common between pairs of successive examinations.

LF (Ho)

SOURCE	df	SUMS OF SQUARES	MEAN SQUARE	F-VALUE	p-VALUE
Study	1	0.296	0.296	0.244	0.622
Exam pair	1	0.218	0.218	0.181	0.671
Index	1	2.779	2.779	2.299	0.131
Study * Exam pair	1	0.951	0.951	0.786	0.377
Study * Index	1	0.625	0.625	0.517	0.473
Exam pair * Index	1	1.755	1.755	2.122	0.147
Study * Exam pair * Index	1	0.793	0.793	0.656	0.419
Residual	160	193.467	193.467		

LF (He)

SOURCE	df	SUMS OF SQUARES	MEAN SQUARE	F-VALUE	p-VALUE
Study	1	0.747	0.747	0.546	0.461
Exam pair	1	1.166	1.166	0.853	0.357
Index	1	4.178	4.178	3.056	0.082
Study * Exam pair	1	4.274	4.274	3.126	0.079
Study * Index	1	0.097	0.097	0.071	0.791
Exam pair * Index	1	3.451	3.451	2.524	0.114
Study * Exam pair * Index	1	0.478	0.478	0.350	0.555
Residual	160	218.712	218.712		

Table 3.10. Summary table of the repeated measures ANOVA for the LF(Ho) (top) and LF(He) (bottom) components derived from all double determinations and from the ten standard double determinations of threshold for the long follow-up (top) and short follow-up (bottom).

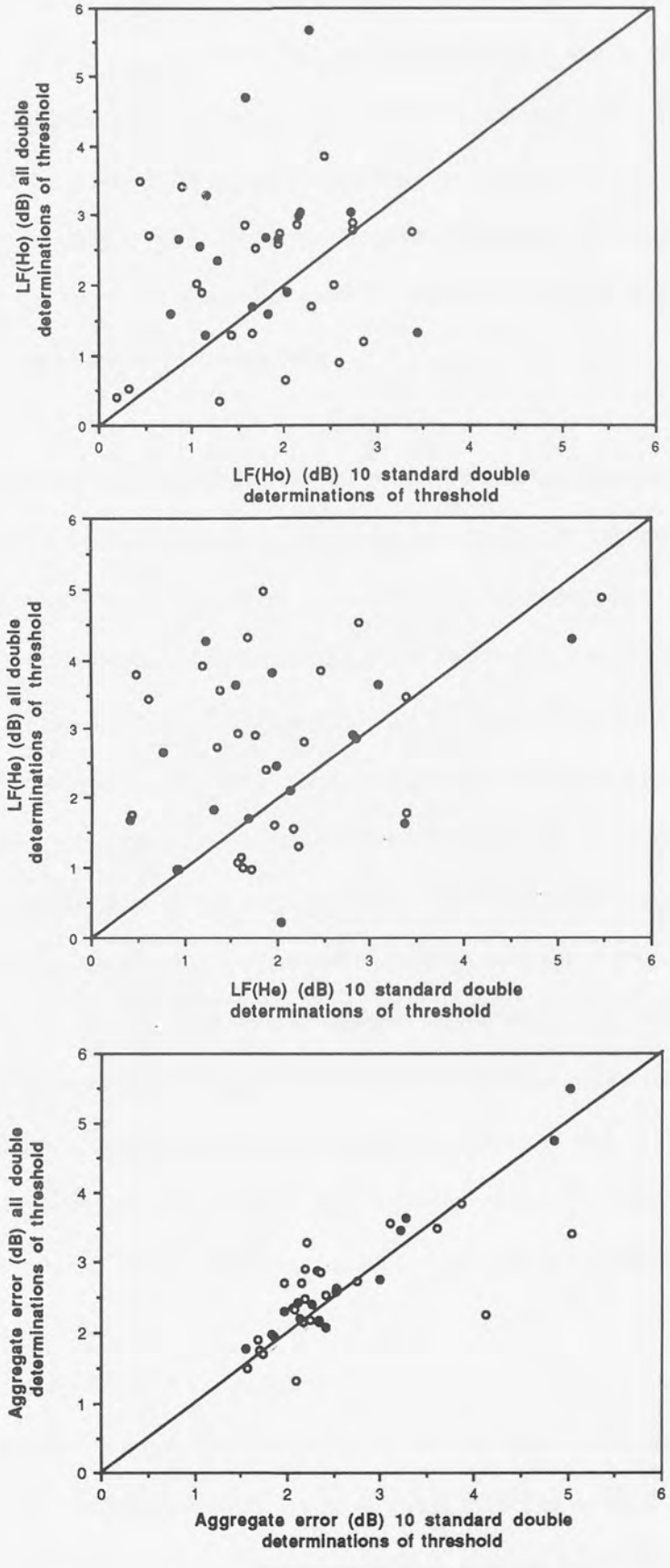

Figure 3.9. The LF(Ho) (top) component between the second and third examinations derived from the ten standard double determinations of threshold against that derived from all available double determinations. The corresponding relationship for the LF(He) (middle) and the aggregate error (bottom) components.

fields exhibits an apparent improvement compared to that of the preceding field, the validity of either field is called into question. The calculation of numerous values of LF based upon comparisons of multiple pairs of visual fields must be treated with caution since each comparison has a finite probability of being incorrect. The likliehood of an incorrect inference increases with an increase in the number of comparisons made and, as such, the comparisons should be used sparingly. However, the most important comparison is always that of the current field with the immediate previous field.

The mean values of the LF(Ho) and LF(He) components are larger than those calculated by a similar method and published previously. The early theory relating to the components of the LF was based upon results from Program JO of the Octopus automated perimeter (Interzeag AG, Schlieren-Zurich, Switzerland) which determined the threshold twice at each of 49 stimulus locations within 26° eccentricity. The values for the LF(Ho) and LF(He) were estimated to be in the region of 0.5 dB and 0.2 dB, respectively, in normals; 0.9 dB and 0.4 dB in suspected glaucoma and 1.2 dB and 0.5 dB in glaucoma (Flammer et al. 1984c). The differing approaches to the handling of the aggregate error term accounts to some extent for the disparity between the previously reported values and the findings of the present study. The inclusion of the error term in place of the negative values skews the distribution towards a higher value and is evident in the cumulative frequency distributions of the LF(Ho) in Figure 3.2. An alternative approach would have been either to allocate a value of zero to the negative values or to omit such values from the summary distributions. The former was considered inappropriate as it would have ignored the influence of the measurement error but would have resulted in smaller estimates, whilst the latter would not have been representative of the clinical reality. The precision of the calculation of the LF between the Humphrey and Octopus perimeters might also be expected to differ due to two important methodological differences. The endpoint taken as threshold with the HFA 4-2dB algorithm is such that the difference between two determinations of the same threshold in a single examination can only be an even number whereas the Octopus can produce both odd and even differences (Fankhauser et al. 1988). The number of stimulus locations incorporating a double determination of

threshold is greater for Octopus Program JO, and its successor Program G1, compared with HFA programs 30-2 or 24-2 particularly at the extremities of the central field. The differences in the stimulus parameters between the two instruments such as the adaptation level and the stimulus duration might conceivably produce minor differences in the magnitude of the LF in glaucoma patients (Lewis et al. 1986).

The lack of relationship between the LF(Ho) component and the difference in the MD and between the LF(He) and the difference in the CPSD, emphasises the distinction between the change in measurement (ie. the index) and the variability present across the visual field between examinations. This finding may appear surprising given that previous studies have shown that a large degree of global variability relates to a clinically significant change in the visual field status (Hoskins et al. 1988; Werner et al. 1989). The lack of relationship may result from a comparison between a visual field index derived from the entire number of stimulus locations in the visual field and an LF component derived from ten stimulus locations. However, this is unlikely given that the unweighted indices derived from the ten standard stimulus locations also exhibited little relationship with the LF components.

Calculation of the LF with the Humphrey Field Analyser is effectively limited to the ten standard double determinations of threshold situated within 21° eccentricity. The use of ten locations merely samples the extent of the fluctuation occurring across the field and it is assumed that the estimate based upon the ten locations is representative of the field as a whole. Such an approach ignores the influence of the relatively greater within-test fluctuation of sensitivity at the more peripheral locations (Heijl et al. 1987a). The precision of the estimate of the LF for the field as a whole will be affected by the degree of similarity in the position and the depth of the field loss for the complete field compared with that manifested at the ten locations. However, the sampling procedure based upon the ten locations is constant between any two tests of the same program (Programs 30-2 and 24-2) for any given patient. An alternative would be to increase the number of stimulus locations at which a double determination of threshold is routinely undertaken. The resulting LF would be more representative of the LF for

the field as a whole but would be acquired at the expense of an increased examination time. The longer examination duration would produce a greater fatigue effect (Hudson et al. 1994), particularly in the second eye examined, with the consequent reduction in the accuracy of the estimate of the true threshold. In terms of statistical accuracy, the precision of any estimation is a function of the square root of the number of measurements in the sample. Increasing the number of locations incorporating a double determination of threshold from 10 to 76 would increase the accuracy of the LF measurement by $\sqrt{(7.6)}$ times but at the expense of a 7.5 times increase in the duration of the examination. However, increasing the number of locations from 10 to 20 would increase the accuracy by $\sqrt{2}$ times. Moreover, it could be argued that the programs used for the detection of glaucomatous visual field loss should incorporate a greater number of stimulus locations and fewer double determinations whilst programs used for the evaluation of visual field progression should incorporate fewer stimulus locations and a greater number of double determinations. The accurate documentation of the remaining areas of high sensitivity within the visual field is of more concern than documentation of the progression of near absolute loss. Inclusion of all double determinations of threshold consistent between any two consecutive fields would seem to offer a more representative estimate of the various components. However, these supplementary double determinations are seldom common between the second field of the given pair and the following field and, in any event, did not yield an LF component which was statistically different from that based upon ten double determinations.

The magnitude of the LF components might be expected to change as a function of the severity of field loss due to ceiling and floor effects of the measured sensitivity. This has been found in several studies where the expression of LF is derived on a pointwise basis (Heijl et al. 1989b; Henson & Darling 1995; Werner et al. 1989). The global components of LF, calculated using the two-factor ANOVA using only stimulus locations of a similar sensitivity, also showed an increase in magnitude with decreasing sensitivity. This outcome is in contrast to the relationship between the LF components based upon the ten double determinations and the visual field indices of MD and CPSD. The relationship between sensitivity and the LF

components may be difficult to discern due to the range of sensitivities encompassed by the ten double determinations. However, the number of double determinations embodied by each or any defined sensitivity group within a single or series of visual fields might be insufficient to compute the LF components. The comparison between the LF components and the visual field indices is therefore more appropriate in a clinical context.

The lack of relationship between the SF and either of the LF components emphasises the importance of the LF as an aid in determining visual field progression. The relationship between the aggregate error and the SF is unremarkable in that the aggregate error expresses the average measurement error across the two examinations in question. The aggregate error exhibited by the short follow-up study was, on average, larger than that exhibited by the long follow-up study. However, the limits of agreement between the first and the second examination pair of the long follow-up study were 2.5 times wider.

The stability of both LF components over the long follow-up interval together with the lack of any relationship with the severity of field loss suggests that the confidence limits associated with each LF component could be used as a reliability index of the relationship between the two consecutive fields. Such an index would be based upon the variability inherent in the stable glaucomatous visual field rather than on the basis of the variability inherent in the normal field. It can be argued that having confirmed the presence of glaucomatous field loss by reference to the properties of the normal visual field, glaucomatous progression should be evaluated by reference to the properties of the stable glaucomatous visual field. Indeed, this latter approach has been adopted in the Glaucoma Change Probability Analysis of the HFA STATPAC 2 (Heijl et al. 1989c). The resulting values for each component of the LF were therefore separately bootstrapped (Efron & Tibshirani 1993) for each pair of successive fields in order to identify the error distribution associated with the 90th percentiles (ie the empirical confidence limits). Bootstrapping is a recently described statistical technique for increasing the maximum information content from a given sample size. It involves the selection, and subsequent replacement, of random sub-samples of values from the original data set. The size

of the sub-sample should be such as to obtain the maximum number of possible combinations from the data set and the data set itself is generally sampled between 50 and 200 times. A sub-sample size of 27 was utilised for each LF component giving 4060 possible combinations of values and each data set was sampled 200 times. The 90% confidence limits are given in Table 3.11. The construction of the 95th percentile based upon a sample of thirty patients was felt to be inappropriate.

It is proposed that the LF as a parameter for reliability between the two examinations would be used in conjunction with those indicating reliability within each examination, particularly that of the SF. The particular type of between-examination variability, ie. general or location/shape specific, would be indicated by the specific component lying outside the confidence limit. In the current study the most conservative estimate of the 90% confidence limit for the LF(Ho) would be 3.3dB and for the LF(He) 3.6dB (Table 3.11). The utility of the technique is illustrated in Figure 3.10.

3.6. Conclusion.

The homogeneous and heterogeneous components of the long-term fluctuation calculated from the ten standard double determinations of threshold of the Humphrey Field Analyser Program 30-2 are larger in stable primary open angle glaucoma than those values previously reported with the Octopus automated perimeter (Flammer et al. 1984c). Both components remained unchanged over three separate examinations separated by a mean interval of approximately 16 months and were essentially independent of the severity of field loss. A knowledge of the LF components in stable glaucoma and of the corresponding confidence limits yields an expression of between-examination variability which provides an objective basis as to whether a confirmatory follow-up field is necessary and facilitates separation of fluctuation from true progression in the determination of visual field progression in glaucoma. In those cases where the LF components fall within the designated limits for the typical follow-up period encountered in a clinical environment, the examination results can be considered

	LONG FOLLOW-UP		SHORT FOLLOW-UP	
	LF(Ho)	LF(He)	LF(Ho)	LF(He)
1st - 2nd	2.95 (0.38)	3.70 (0.49)	3.30 (0.26)	3.60 (0.44)
2nd - 3rd	2.43 (0.36)	3.00 (0.56)	2.97 (0.23)	3.40 (0.55)

Table 3.11. The bootstrapped mean and standard deviation of the 90% confidence limits associated with the distribution of the LF(Ho) and LF(He) components for each pair of examinations and for the long and short follow-up arms of the study.

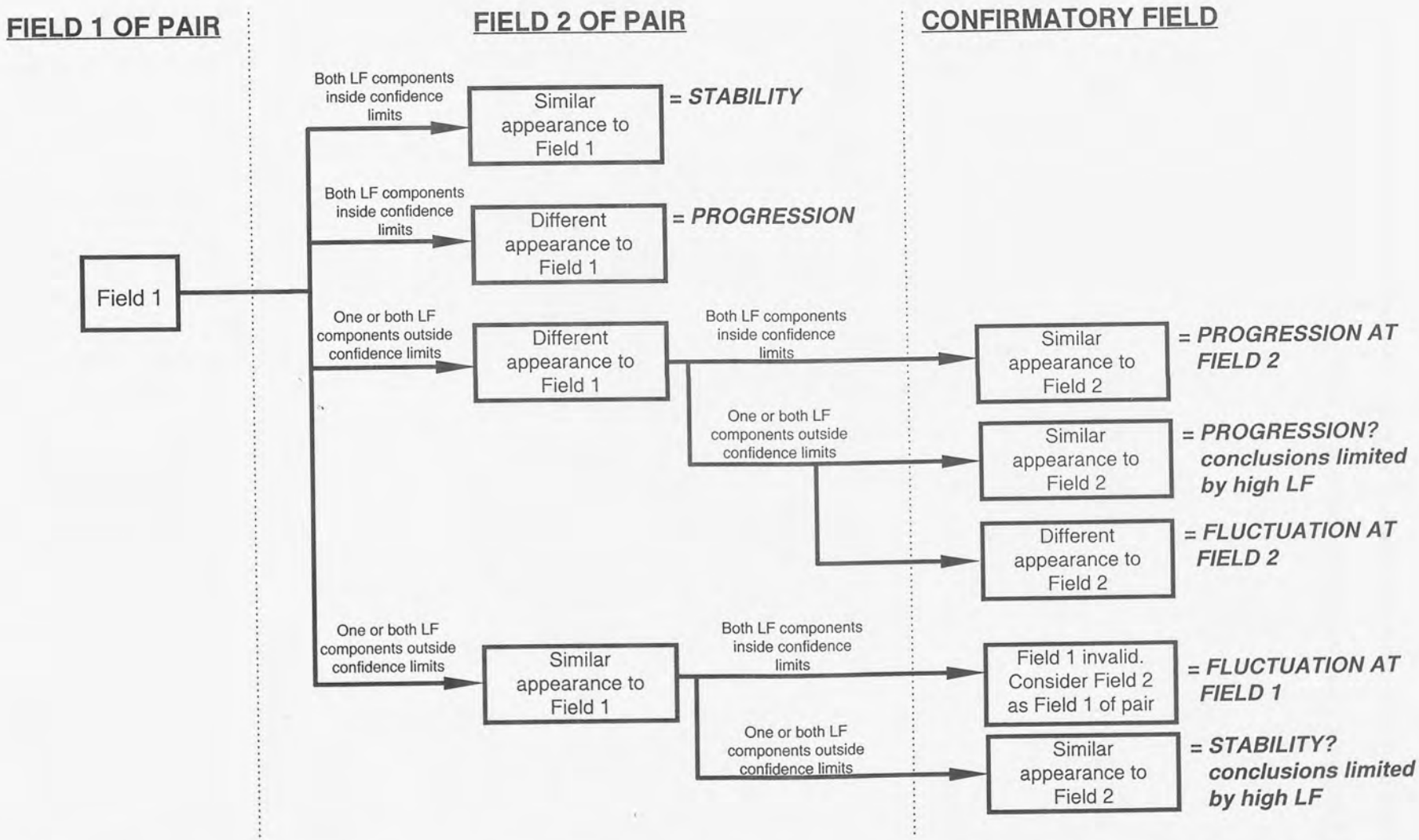

Figure 3.10. The algorithm to determine the necessity of a follow-up examinations based upon the magnitude of the components of long-term fluctuation (LF).

without the need for a confirmatory examination. In this way, the LF in conjunction with the algorithm for determining the validity of an examination may be used to reduce the number of examinations required to determine the presence or absence of visual field progression. The various perimeter manufacturers should be encouraged to incorporate such a measure in their visual field print-out.

Chapter 4: Between-examination variability as a function of the thresholding strategy.

4.1. Introduction.

4.1.1. Staircase procedures.

The sensitivity at any stimulus location is determined by the use of a staircase algorithm. Staircase procedures are an established psychophysical technique for the estimation of threshold, since they require less stimulus presentations than other techniques (Cornsweet 1962). The full staircase procedure requires multiple presentations of successively brighter or dimmer stimuli, dependent on the patient response at each presentation and the ideal algorithm obtains maximum information for each stimulus presentation (Cornsweet 1962; Feeny et al. 1966). The full staircase procedure provides the most accurate estimation of threshold but is extremely time consuming when applied to automated perimetry due to the large number of stimulus locations at which threshold must be estimated. In addition, factors such as the fatigue effect (Hudson et al. 1994; Searle et al. 1991; Wild et al. 1991), and the demands of clinical scheduling (Dalenbach 1966) have necessitated a reduction in the number of stimulus presentations from the ideal algorithm. The truncated staircase procedure represents a practical, non-parametric method of determining threshold. The step-size is fixed prior to the examination and the patient response falls into two categories - 'seen' and 'not-seen'. The direction of the staircase is changed when the patient response to a series of stimulus presentations changes from one response category to the other (Treutwein 1995). The stepping of the threshold algorithm is described mathematically as:

$$X_{n+1} = X_n - \delta(2Z_n - 1) \qquad \text{Eq. (4.1)}$$

where X_{n+1} and X_n represent the stimulus luminance at presentations n+1 and n respectively; δ represents the step-size of the chosen algorithm and Z_n the response category to presentation n. A negative response (ie. stimulus 'not-seen') assigns a value of zero to Z_n and a positive response assigns a value of 1 to Z_n. In this way the stimulus luminance is increased and decreased respectively (Treutwein 1995).

The earliest studies in computer simulation of the ideal observer, found the most favourable truncated staircase to begin with an initial step size of 4dB (up to and including the first staircase reversal), followed by a 2dB step size for a subsequent crossing of threshold (Fankhauser 1979; Spahr 1975). In addition, the estimated threshold was deemed to be the threshold at the final presentation corrected by ±1dB according to the response category of the observer at this presentation (Spahr 1975). In the absence of false-positive and false-negative responses, the frequency distribution of repeated estimates of threshold is narrower when the estimate is based upon the mean of the stimulus threshold either side of the reversal, than when based upon the threshold represented by the last 'seen' stimulus (Heijl 1977).

More recently, other computer simulation models have been used to determine the properties of the staircase procedures used in automated perimetry. The KRAKEN computer simulation procedure had two modes of operation - a patient module and a perimeter module. The perimeter module allowed modification of the examination parameters and strategies whilst the patient module incorporated response characteristics and topographic data based upon the fields both from normal subjects and from a variety of ocular disorders (Shapiro et al. 1989). A modified binary search method (MOBS) (Tyrrell & Owens 1988), adapted for perimetric testing, has also been described. In this technique, each staircase reversal is taken as the bracketing midpoint of the preceding interval between a change in responses (Treutwein 1995; Tyrrell & Owens 1988). The MOBS procedure has been found to be more time consuming than the conventional 4-2dB staircase algorithm simulated with the KRAKEN program, but to be more accurate across differing response variables (Johnson & Shapiro 1989).

A further use of the MOBS procedure has been incorporated into a three-pass heuristic perimetric strategy, RIOTS (Real-time Interactive Optimized Test Sequence) (Johnson & Shapiro 1991). In the RIOTS strategy, a MOBS procedure determined the threshold at twelve threshold 'seed' locations and two blind spot locations. These values were then used to estimate the threshold at all other stimulus locations in the given program. Each pass

consisted of a single presentation at each stimulus location and the response agreement was evaluated and adjusted by heuristic decision rules derived from the sensitivity at the location and from the relationship between adjacent stimulus locations (Johnson & Shapiro 1991). In contrast to MOBS, the duration of a Standard HFA 30-2 program is approximately halved with the RIOTS examination and, unlike that of the 4-2dB Standard staircase, the examination duration does not vary greatly between normal and abnormal subjects (Johnson & Shapiro 1991).

The truncated staircase procedure represents a compromise between accuracy and rapidity of the estimation of the 'true' value of sensitivity (Anderson 1992). The Octopus perimeters employ the 4-2dB strategy with the final ±1dB correction described by Spahr (1975) as the Standard algorithm. The Humphrey Field Analyzer (HFA) employs a similar 4-2dB staircase but does not make the final decibel correction, taking threshold as the last 'seen' stimulus (Haley 1987). In addition, methodological differences exist in the starting point of the staircase procedure between the two perimeters. Theoretically, the selection of the last 'seen' stimulus as threshold represents a determination of threshold that is unaffected by the initial choice of stimulus (Feeny et al. 1966). However, investigations utilising computer simulations and normal subjects found that the starting point of the staircase influenced the estimate of threshold, and that this relationship was more evident with staircase strategies terminating after a single crossing of threshold (Glass et al. 1995; Johnson et al. 1992). A single reversal staircase terminates following an incorrect response and the error in the estimation of threshold increases as a function of the difference between the starting point of the staircase and the true threshold (Glass et al. 1995). In addition, the starting position of the staircase influences its efficiency which reduces as the difference between the starting point of the staircase and the actual threshold increases, particularly when this difference is greater than 4dB (Johnson et al. 1992).

4.1.2. Current threshold staircasing algorithms in automated perimetry.

The time necessary for examination of the 76 stimulus locations contained within the central field out to an eccentricity of 30° (Program 30-2) using the HFA Standard thresholding strategy is in the region of 15 minutes during which time the stimulus will be presented between approximately 350-500 times. The type of staircase procedure employed represents a trade-off between accuracy of the threshold estimation and the efficiency of the strategy, which follows a reciprocal function (Johnson et al. 1992).

The fatigue effect, whereby sensitivity decreases as the examination duration increases, has been demonstrated in normal subjects and in ocular hypertension (Hudson et al. 1994; Langerhorst et al. 1987; Rabineau et al. 1985; Wild et al. 1991), glaucoma (Wild et al. 1991) and optic neuropathy (Johnson et al. 1988; Keltner & Johnson 1995; Wildberger & Robert 1988). The effect occurs both within- and between-eyes at a single visit (Hudson et al. 1994), is more pronounced in areas adjacent to visual field defects (Heijl & Drance 1983; Holmin & Krakau 1979) and increases with increasing eccentricity (Johnson et al. 1988; Langerhorst et al. 1987; Suzumura 1988) and increasing age (Hudson et al. 1994; Langerhorst et al. 1987) and defect depth (Hudson et al. 1994; Suzumura 1988). Minimising the examination duration has been shown to produce a concurrent reduction in the effects of fatigue.

A 4-2dB staircase is also utilised by programs G1 and G1X of the Octopus perimeter in the first phase of a two phase program (Flammer 1987; Zulauf 1994). The initial stimulus is presented at 4dB brighter than the age-corrected normal value at each location in the visual field. The second phase of the examination utilises a 2-1dB staircase, presented at the threshold estimation of the first phase, to obtain a second estimation of threshold. The G1X program represents a modification of the G1 program in that each phase is separated into four stages. The locations thresholded within each stage are prioritised such that, at the end of stage 2, the thirty stimulus locations which produce the best agreement with the Mean Defect derived from the four stages of the first phase have been thresholded (Funkhouser et al.

1989a; Funkhouser et al. 1989b). By these means, the examination may be terminated for a patently normal visual field (Messmer & Flammer 1991).

More recently, a dynamic strategy has been introduced in which the step size employed is determined by the sensitivity of the stimulus location. The width of the frequency-of-seeing curve increases both as a function of eccentricity and of reducing sensitivity. The fixed step size employed by the traditional strategies takes no account of these factors. The dynamic strategy of the Octopus perimeter (dG1X) selects the step-size by referring to the width of the frequency-of-seeing curve at a stimulus location of a given sensitivity. The step-size can range between 2dB and 10dB and is utilised in a single step-size strategy with a single crossing of threshold (Weber 1990). The dynamic strategy has exhibited a reduction in the duration of a perimetric examination by, on average, 46% (Weber & Klimaschka 1995). The reduction in examination duration is accompanied by increased within-examination variability when compared to the Standard strategy (Weber & Klimaschka 1995; Zulauf et al. 1995). However, the variance of the SF between-examinations for the dynamic and Standard strategy of the Octopus perimeter is not significantly different (Zulauf et al. 1995). The utility of dG1X has been analysed by the benefit-cost ratio. This ratio expresses the 'benefit' of reproducibility in the estimated threshold (1/variance) as a function of the number of presentations ('cost'). The findings indicate that across sensitivity levels, stratified at intervals between 1dB and 30dB, the benefit-cost ratio was always better for the dG1X strategy in comparison to that of the Standard strategy (Weber & Klimaschka 1995).

In recent years, the FASTPAC strategy has been introduced for the HFA perimeter as an alternative to the established 4-2dB threshold strategy in an attempt to reduce the examination duration without loss of measurement accuracy (Flanagan et al. 1993a). Both the Standard and FASTPAC strategies determine threshold at four seed points located at (9,9) along the 45°, 135°, 225° and 315° meridians. These four threshold estimations form the basis of predicted values of threshold at locations adjacent to the seed points and their subsequent adjacent locations. Whereas the 4-2dB algorithm presents the initial stimulus at 2dB higher

than the predicted threshold at all locations, the FASTPAC strategy presents an initial stimulus at 1dB higher than the estimated threshold at half of the locations and 2dB lower at the other half. The last 'seen' stimulus is taken as the estimated value of threshold after a double crossing of threshold by the Standard strategy and a single crossing of threshold by the FASTPAC strategy. Any locations at which the measured threshold deviates from the predicted threshold by ≥4 dB are re-thresholded by both strategies.

The 3dB step size with a single crossing of threshold employed by the FASTPAC strategy has demonstrated a reduction in the number of stimulus presentations and, consequently, the examination time of approximately 35% (Flanagan et al. 1993a; Flanagan et al. 1993b; Iwase et al. 1993; Moss et al. 1992; O'Brien et al. 1994; Schäfer et al. 1993). The saving in time, however, is at the expense of a possible reduction in the accuracy of the threshold estimate. The SF is generally considered to be higher with FASTPAC although similarity between the two values has also been reported (O'Brien et al. 1994). In addition, the increase in measurement error with the FASTPAC strategy became more distinct with advancing age (Flanagan et al. 1993b) and severity of defect (Flanagan et al. 1993b; Schaumberger et al. 1995).

The relationship between the remaining visual field indices derived by the two strategies is equivocal. The mean deviation (MD) index is considered, variously, to be similar (Schaumberger et al. 1995), more negative (Flanagan et al. 1993b; O'Brien et al. 1994), or more positive (Iwase et al. 1993) with the Standard strategy; the pattern standard deviation (PSD) to be either similar (Flanagan et al. 1993b) or lower (Hoop et al. 1993; Schaumberger et al. 1995) with FASTPAC; and the corrected pattern standard deviation (CPSD) to be smaller (Hoop et al. 1993; O'Brien et al. 1994; Schaumberger et al. 1995) with FASTPAC. The magnitudes of any differences between the indices, however, are such as to be clinically identical. In addition, the visual field indices of FASTPAC have been found to lie inside the range encountered for the test-retest variability of the corresponding index obtained with the Standard strategy in both ocular hypertension and glaucoma (O'Donnell et al. 1995).

The visual field indices merely provide an expression of the composite field, and the MD in particular exhibits a low sensitivity and specificity in the determination of glaucomatous visual field progression (Birch et al. 1995; Chauhan et al. 1990). The Glaucoma Change Probability Analysis (GCPA) is an established method for use with the Standard strategy of the HFA that identifies progressive visual field loss at each individual stimulus location (Heijl et al. 1991). The technique, which is based on the test-retest pointwise variability in sensitivity exhibited in stable glaucoma patients, compares the sensitivity at a given examination with that of a baseline (Heijl et al. 1991; Morgan et al. 1991). In this manner, the range of between-test variability exhibited by stimulus locations with a similar loss of sensitivity can be examined. Little is known about the test-retest variability of the FASTPAC strategy at each stimulus location and consequently no such analysis of progressive field loss exists for FASTPAC.

The FASTPAC strategy has been advocated variously as an alternative to suprathreshold strategies (Mills et al. 1994), for examination of low/high risk ocular hypertensives, for the reduction of fatigue effects (Flanagan et al. 1993a; Flanagan et al. 1993b) and to increase the through-put of patients. Clinical situations can therefore arise whereby a patient is changed from the Standard strategy to FASTPAC and vice versa. However, the impact of such a decision is limited by the lack of information concerning the pointwise test-retest variability of FASTPAC in relation to that of the Standard strategy.

4.2. Aim.

The aim of the study was to determine the pointwise test-retest variability of the FASTPAC strategy in stable primary open angle glaucoma and to compare the findings with those of the Standard strategy. The outcome of the study would thus determine whether the two strategies could be considered as interchangeable in the evaluation of progressive visual field loss.

4.3. Methodology.

The sample consisted of 60 patients with primary open angle glaucoma randomly selected from the Glaucoma Service, Toronto Hospital (Western Division). Forty-eight of the 60 patients

were being treated with topical beta blockers only, 32 had undergone previous argon laser trabeculoplasty and 7 had received YAG laser iridotomies. The mean age of the sample was 67.5 years (SD 8.5 years) and all patients were experienced in automated static perimetry. The group mean intraocular pressure over the series of examinations was 20.6mmHg (SD 3.2). Exclusion criteria comprised ametropia of greater than ±5.00 DS and/or greater than ±2.50 DC; use of mydriatics; pupils of less than 3mm in diameter; history of amblyopia; history of non-glaucomatous eye disease, trauma or surgery; medical history of diabetes mellitus, neurologic or psychiatric illness; and use of central nervous system depressants. The methods of recruitment, including proper consent and approval, and the research protocol were approved by the ethical committee of the Toronto Hospital.

The sample was divided into two age-matched groups each of 30 patients. Perimetry was undertaken on one randomly assigned eye of each patient using program 30-2 of the Humphrey Field Analyser. Where necessary, the appropriate optical correction was worn for the viewing distance of the perimeter. The study employed a standard cross-over design. The first group of patients was examined with the Standard 4-2 dB strategy followed by the FASTPAC strategy. The order of the two threshold strategies was reversed for the second group. A rest period of between two and five minutes was given between examinations. All patients were re-examined on two further occasions, after intervals of three and six weeks from baseline, respectively, using an identical procedure to that of the initial examination session. All left eye data was converted to right eye format.

4.3.1. Data Analysis.

The first examination session was used as an opportunity for familiarisation with the test procedures and the data was discarded accordingly. The results for the remaining two examination sessions were analysed separately between the two groups of patients. The fields recorded at the second examination session were considered in terms of the total deviation at each stimulus location, i.e. the defect depth - the difference between the measured threshold and the age-corrected normal threshold contained within the STATPAC

and FASTPAC software respectively. The locations immediately above and below the blind-spot were omitted from the analysis. The total deviation at each stimulus location across all patients was separately ranked in order of magnitude for each thresholding strategy. The ranked defect depths were then divided into 19 intervals each of 2dB width covering the complete range of deviations. In this way, groups of stimulus locations were identified which exhibited a similar total deviation. The intervals at the extreme ends of the sensitivity range (more negative than -36dB and more positive than +2dB) were omitted from any further analysis as the limited number of data contained within each of these intervals precluded calculation of percentiles. For each strategy in each of the two patient groups, the total deviation at the third examination session at each stimulus location across all patients was then calculated and expressed as a function of the extent of the total deviation at the second session. In this way, the frequency with which a given amount of variability occurred between any two consecutive visual field examinations was determined as a function of the defect depth recorded at the first of the pair of examinations. The 95%, 90%, 50%, 10% and 5% confidence limits of the between-examination variability at each 2dB sensitivity interval were calculated for each thresholding strategy.

The influence of stimulus eccentricity on the difference in the between-examination variability between the two strategies was investigated by dividing the stimulus locations into three annuli extending between 0° and 15°, 15° and 21° and 21° and 27° respectively (Figure 4.1). The total deviation at each stimulus location across all patients was again separately ranked into intervals each of 2dB for each thresholding strategy. The total deviations at the second examination session were then categorised as to eccentricity and expressed as a function of the extent of the total deviation at the third session.

4.3.2. Statistical analysis.

The confidence limits of the between-examination variability for each thresholding strategy underwent two separate statistical analyses for each group of patients. Firstly, the differences between the 95% confidence limits for the Standard and FASTPAC strategy across all the 2dB

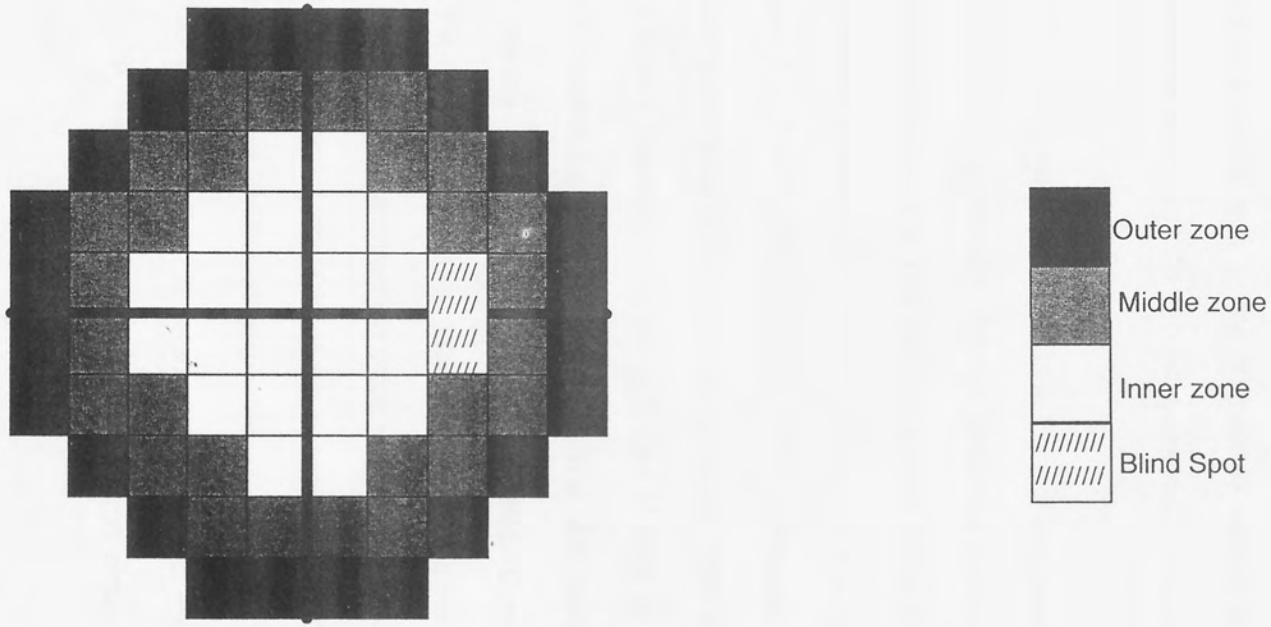

Figure 4.1. The three eccentricity zones used to investigate between-test variability as a function of pointwise total deviation.

intervals were tested as to whether they were statistically different from zero using a Student's t-test. Secondly, a Runs test on the mean of any given differences was undertaken to determine whether any such differences varied systematically across the 2dB intervals. The analysis was then repeated for the corresponding 5% confidence limits and for each zone of eccentricity.

4.4. Results.

The type and extent of field loss for the 60 patients defined in terms of the results for the Standard thresholding strategy at the second examination session is shown in Figure 4.2.

The 5%, 10%, 50%, 90% and 95% confidence limits of the between-examination variability at each 2dB sensitivity interval for each strategy, classified in terms of the sequence of the two strategies, are given in Figure 4.3. The confidence limits of the between-examination variability at each 2dB sensitivity interval for each strategy regardless of the examination order are also shown in Figure 4.3. The magnitude of the 95% confidence limit increased as the total deviation increased upto a defect depth of approximately 20dB magnitude after which the rate of the increase slowed appreciably. At defect depths of 30dB or more, the magnitudes of the 50% and 95% confidence limits converged. The 5% confidence intervals increased approximately linearly as the defect depth increased. Consequently, the between-test variability with the Standard strategy for locations exhibiting a measured sensitivity equal to, or near, the age-corrected normal threshold value ranged between approximately +2.0dB and -8.5dB from the normal value on 90% of the occasions. The 90% prediction interval then increased between defect depths of approximately 5dB and 21dB, ranging for example between -7.90dB and -29.15dB for a defect depth of 21dB. For defect depths greater than approximately 26dB, the prediction interval narrowed. A similar trend was present for the FASTPAC strategy.

The 95% confidence limits of the between-examination variability at each 2dB sensitivity interval for the two thresholding strategies are shown in Figure 4.4. For the patients who underwent the Standard strategy followed by the FASTPAC strategy, the 95% confidence

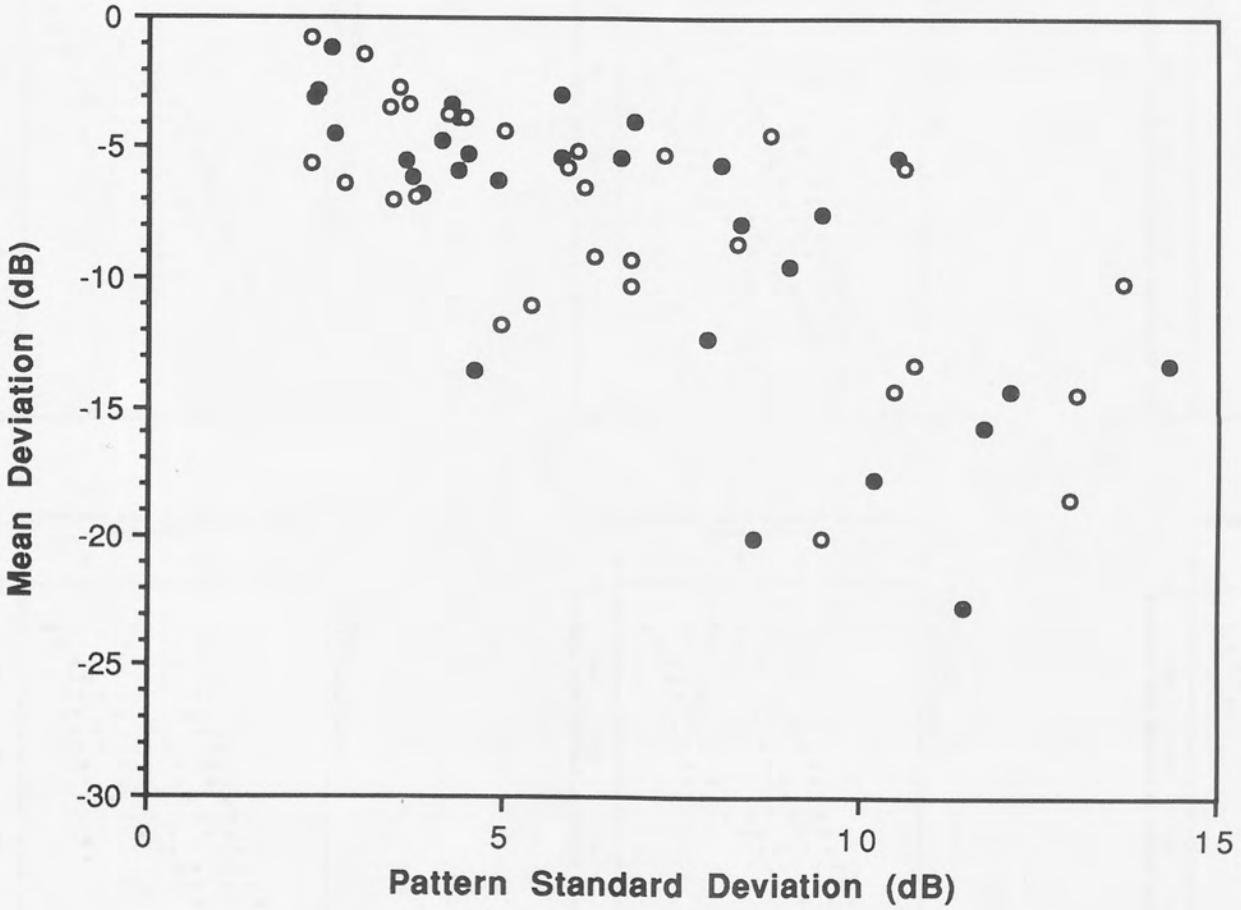

Figure 4.2 The type of visual field loss illustrated in terms of the Mean Deviation (dB) and the Pattern Standard Deviation (dB) at the second examination. The filled circles indicate the 30 patients undergoing the Standard strategy followed by the FASTPAC strategy and the open circles indicate the 30 patients in whom the order of the strategies was reversed.

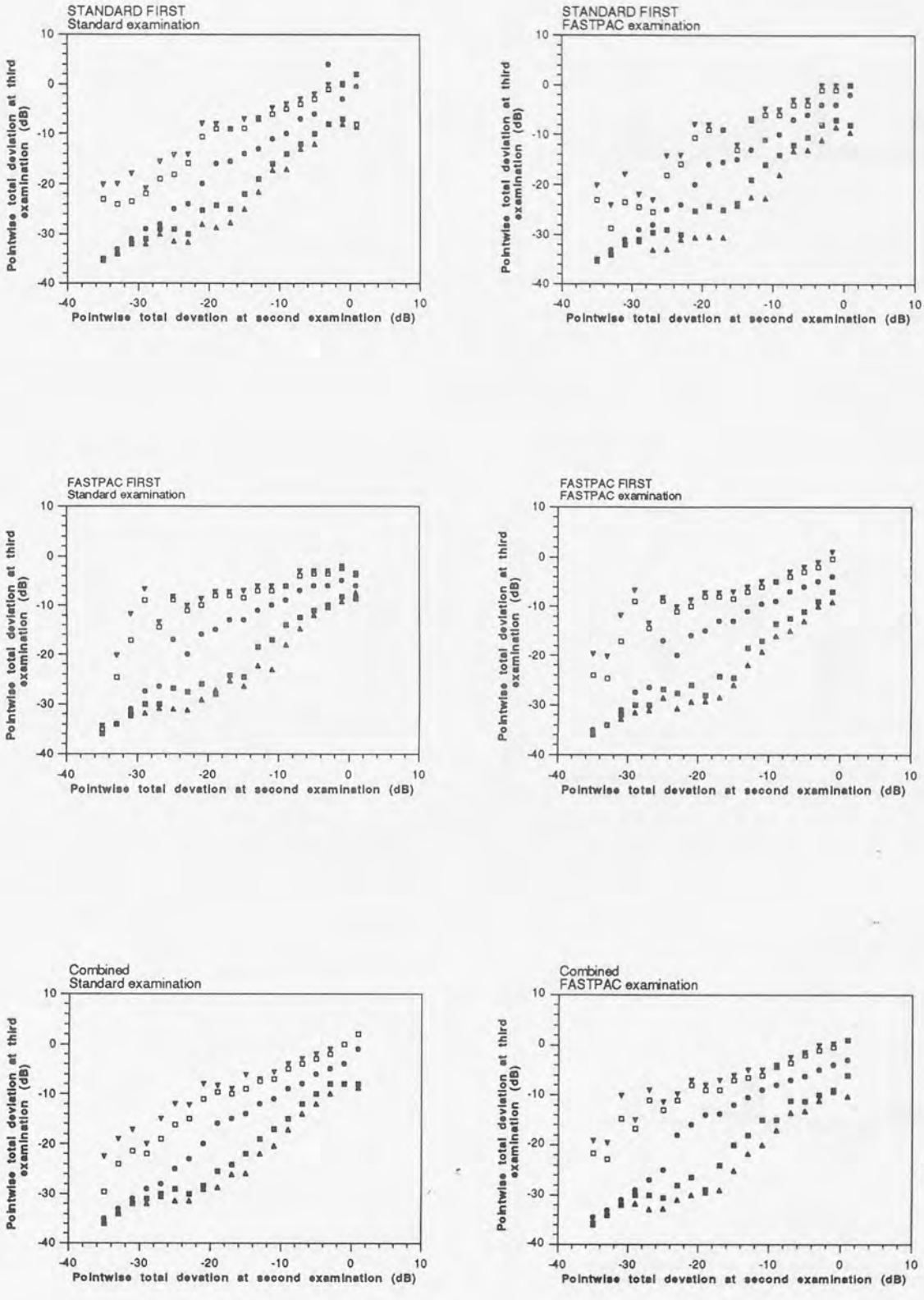

Figure 4.3. The 5% (inverted triangles), 10% (open squares), 50% (filled circles), 90% (filled squares) and 95% (upright triangles) confidence limits of between-examination variation at each 2dB total deviation interval for the Standard (top left) and for the FASTPAC strategy (top right) in the patient group undergoing the Standard strategy followed by the FASTPAC strategy. The corresponding data in the patient group undergoing the FASTPAC strategy followed by the standard strategy (middle left and right) and, similarly, for the two patient groups combined (bottom left and right).

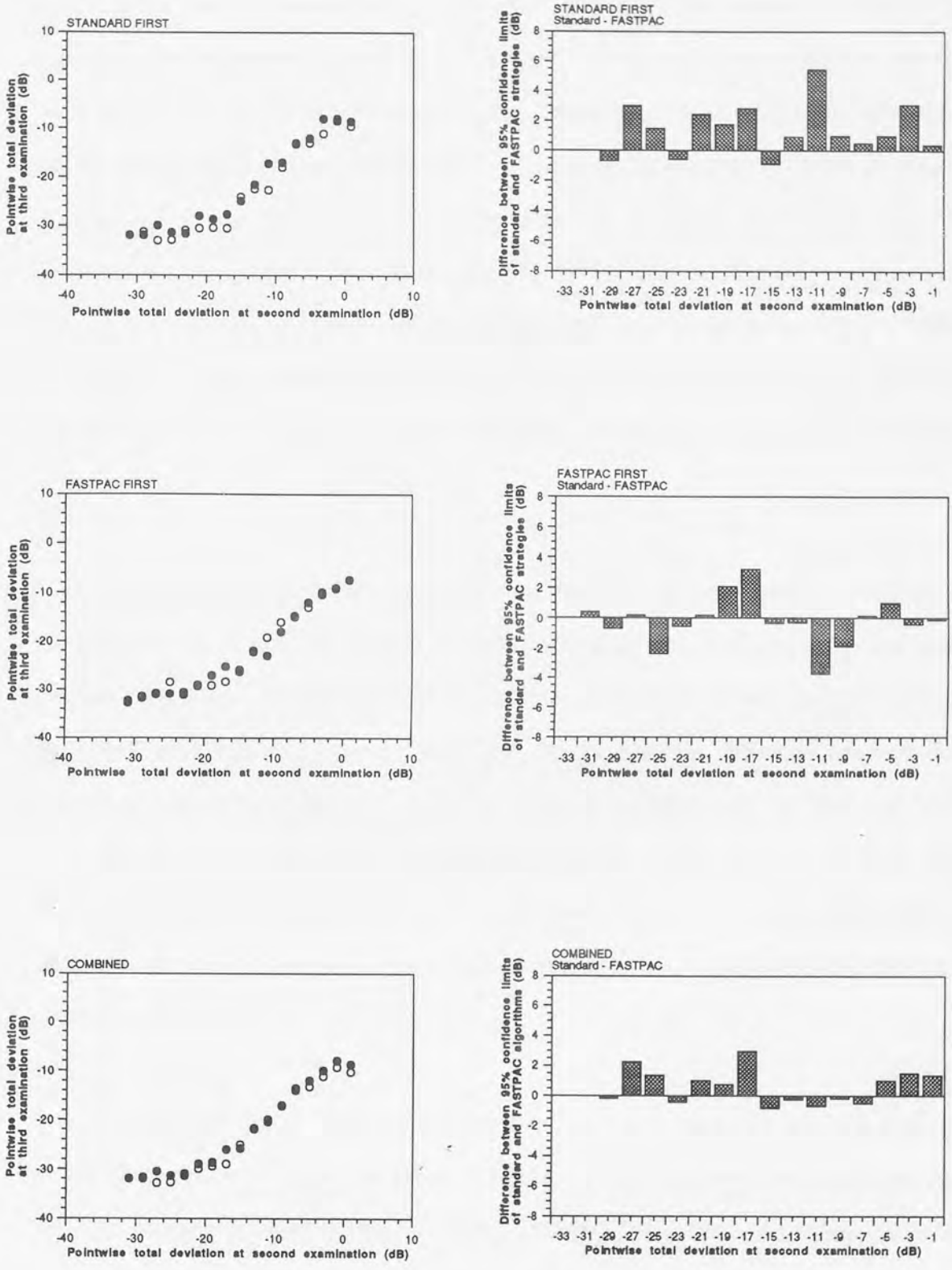

Figure 4.4. The 95% confidence limits of between-examination variation of the Standard (filled circles) and FASTPAC (open circles) strategies for the patient group undergoing the Standard strategy followed by the FASTPAC strategy (top left). The bar chart (top right) illustrates the difference between these 95% confidence limits across the sensitivity intervals. The corresponding data is illustrated for the patient group undergoing the FASTPAC strategy followed by the Standard strategy (middle left and right) and for the two patient groups combined (bottom left and right).

limits for the FASTPAC strategy were wider (ie exhibited greater between-examination variability) than for the Standard strategy (p=0.007). The difference between the confidence limits for the two strategies (Standard minus FASTPAC) across the 2dB intervals in this patient group ranged from -0.70dB to 5.40dB with a mean difference of 1.27dB (SD 1.66). The Runs test, however, showed that no particular trend in the differences was present across the range of sensitivity intervals (p=0.977). The corresponding 95% confidence limits for the patients who underwent the FASTPAC strategy followed by the Standard strategy are also shown in Figure 4.4. The difference between the 95% limits for the two strategies ranged from -3.75dB to 3.20dB with a mean difference of -0.19dB (SD 1.58) which was not significantly different from zero (p=0.624). The Runs test showed no particular trend across the range of intervals (p=1.000).

The 95% confidence limits for each strategy, for the two patient groups, combined, are shown in Figure 4.4. The differences between the 95% limits for the two strategies across the 2dB intervals ranged from -0.68dB to 3.00dB with a mean difference of 0.54dB (SD 1.09) which was significantly different from zero (p=0.029). No trend in the difference between the confidence limits of each strategy across the range of sensitivity intervals was observed (p=0.135). The 95% limits with the FASTPAC strategy were, in general, wider than with the Standard strategy for those sensitivities which deviated from normal by upto approximately 20dB. However, such differences were clinically insignificant lying mostly within the step size of the two strategies.

The 5% confidence limits of the between-examination variability at each 2dB sensitivity interval for both thresholding strategies are shown in Figure 4.5 for the patients who underwent the Standard strategy followed by the FASTPAC strategy. The difference between the 5% confidence limits, overall, reached statistical significance (p=0.028) and the Standard confidence limit was wider than that corresponding to FASTPAC. The difference across the 2dB intervals ranged from 0dB to 7.5dB with a mean difference of 1.16dB (SD 2.20). Although there was no systematic trend in the differences across the 2dB sensitivity intervals (p=0.378), the difference between the two strategies was more marked for those sensitivities which

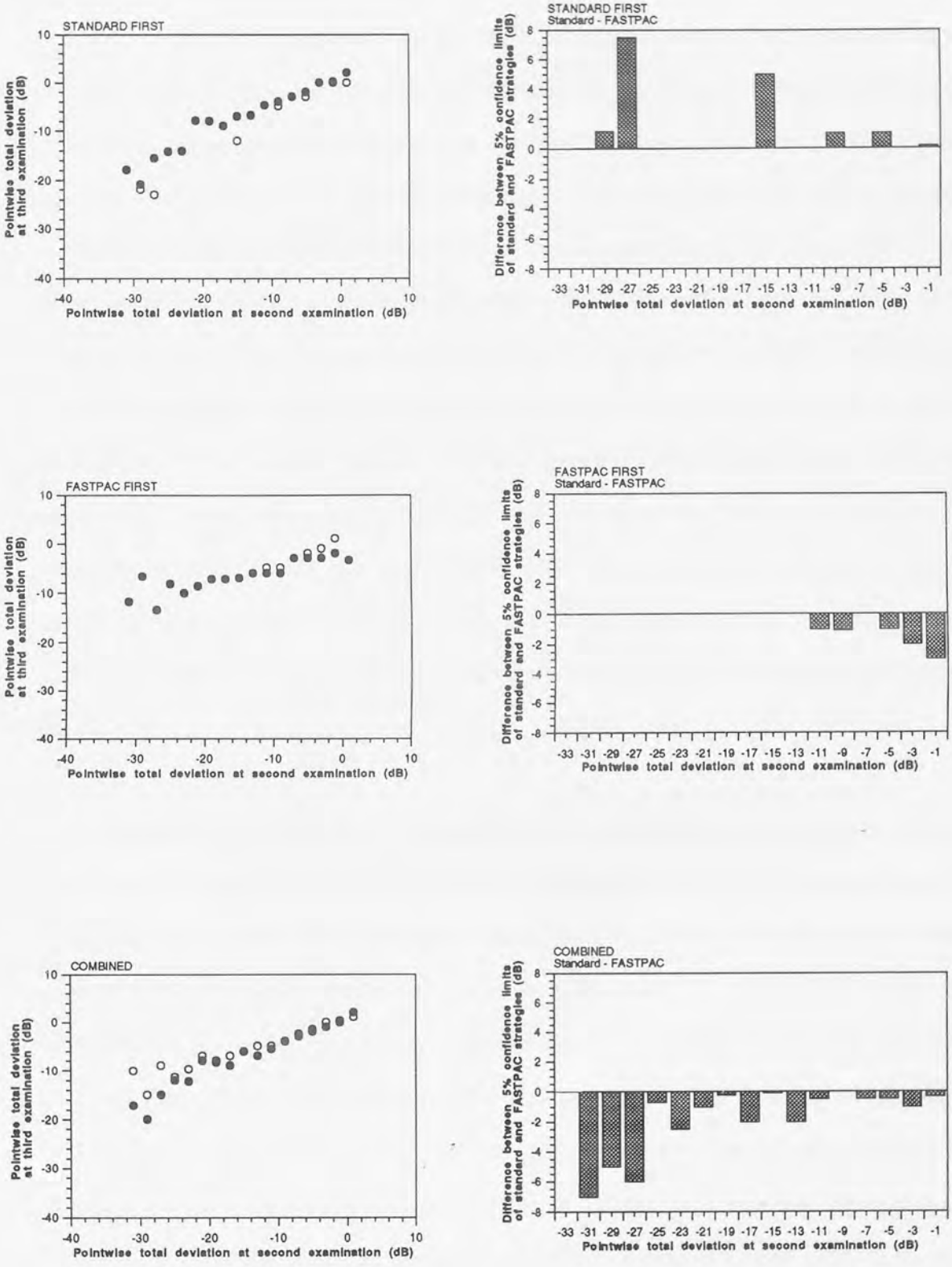

Figure 4.5. The 5% confidence limits of between-examination variation of the Standard (filled circles) and FASTPAC (open circles) strategies for the patient group undergoing the Standard strategy followed by the FASTPAC strategy (top left). The bar chart (top right) illustrates the difference between these 95% confidence limits across the sensitivity intervals. The corresponding data is illustrated for the patient group undergoing the FASTPAC strategy followed by the Standard strategy (middle left and right) and for the two patient groups combined (bottom left and right).

deviated from normal by approximately 24dB or more. The corresponding 5% confidence limits for the patients who underwent the FASTPAC strategy followed by the Standard strategy are also shown in Figure 4.5. The difference between the 5% confidence limits, overall, was small in this patient group but, nevertheless reached statistical significance (p=0.040). This was largely attributable to the marked differences between the confidence limits for those sensitivities which deviated from normal by between approximately 0dB and 12dB. The difference across the 2dB intervals ranged from -3dB to 0dB; with a mean difference of -0.36dB (SD 0.66). The Runs test showed that this trend across the sensitivity intervals was statistically significant (p=0.030). The difference between the 5% confidence limits of each strategy for the two patient groups, combined, reached statistical significance (p=0.005) (Figure 4.5). The difference across the 2dB intervals ranged from -7.03dB to 0.53dB with a mean difference of -1.70dB (SD 2.23). The greatest differences again occurred for those sensitivities which deviated from normal by approximately 24dB or more. The trend of the differences across the sensitivity intervals, however, failed to reach statistical significance (p=1.00).

The confidence limits for each zone of eccentricity were computed for each strategy combined across the two patient groups. The total deviation groups that deviated more negatively than -32dB and more positively than -2dB were excluded from the analysis since the 2dB intervals contained an insufficient number of stimulus locations from which to compute the confidence limits. There was no statistical difference between the 95% confidence limits of the Standard and FASTPAC strategies for either the outer (p=0.90), the middle (p=0.36) or the inner (p=0.82) zones of eccentricity. The 5%, 50% and 95% confidence limits for each strategy are shown for the outer, middle and inner zones in Figure 4.6. For each zone, the corresponding differences between the strategies (Standard - FASTPAC) averaged -0.06dB (SD 2.0) for the outer, 0.33dB (SD 2.25) for the middle and 0.13dB (SD 2.2) for the inner zone.

For each of the strategies, the difference between the 95% confidence limit of the outer and middle zones of eccentricity was significantly different from zero (Standard p=0.03; FASTPAC p=0.08). The 95% confidence limit was wider for the middle zone than that of the outer zone

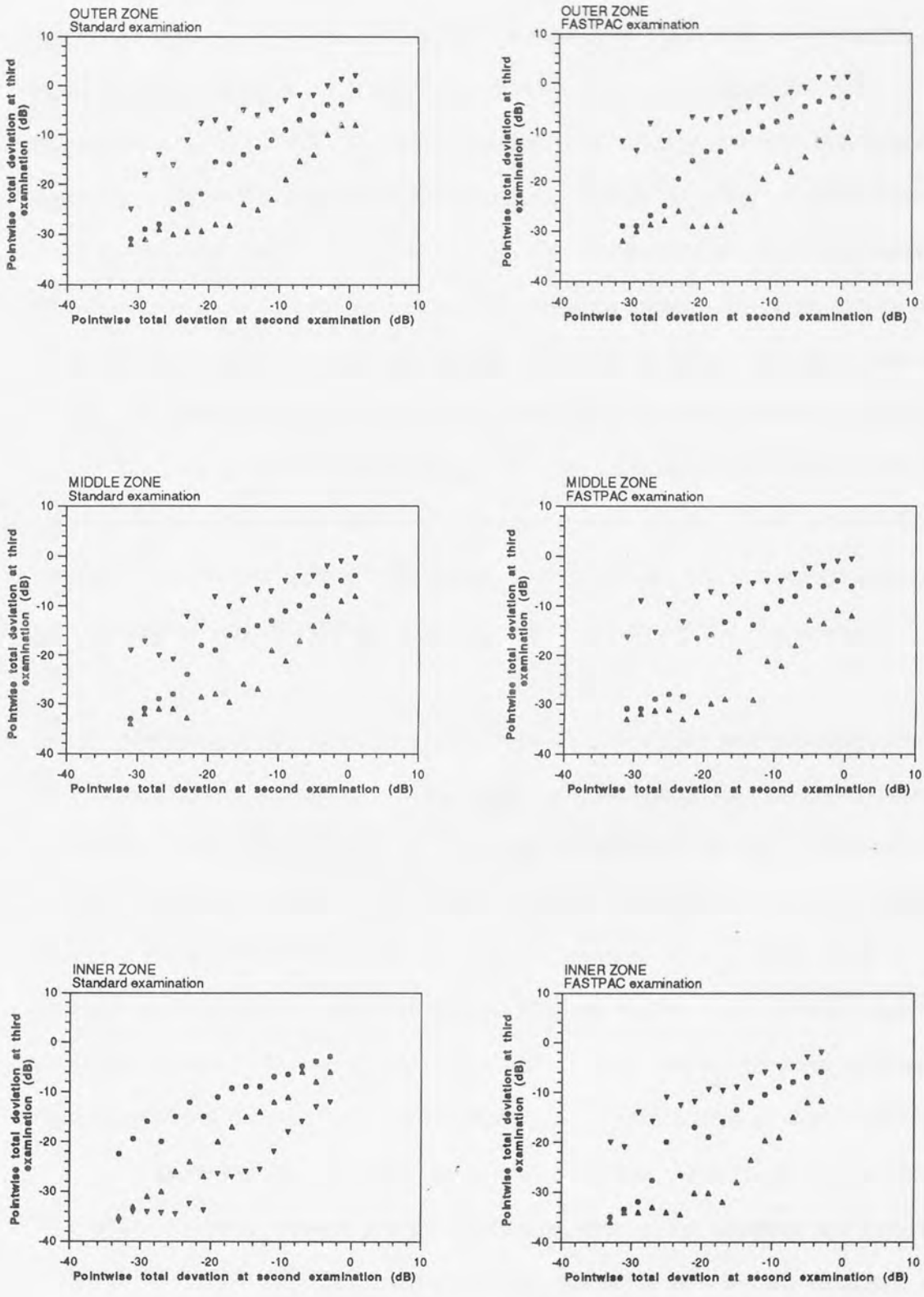

Figure 4.6. The 5% (inverted triangles), 50% (filled circles), and 95% (upright triangles) confidence limits of between-examination variation of the outer, middle and inner eccentricity zones at each 2dB total deviation interval for the Standard (left) and for the FASTPAC strategy (right) combined across the two patient groups.

for both strategies. In each strategy the 95% confidence limit exhibited a total deviation that was more negative in the middle zone across the majority of the 2dB sensitivity classes. The mean difference between the zones (outer minus middle) was 1.05dB (SD 1.73) for the Standard strategy and 1.62dB (SD 3.32) for the FASTPAC strategy. The Runs test showed no significant trend in the variability across sensitivity classes for either strategy (Standard p=0.612; FASTPAC p=0.341). Similarly, the 95% confidence limit of the inner zone was wider than the middle zone for each strategy but the difference between the zones did not reach statistical significance (Standard p=0.56 and FASTPAC p=0.75). The mean difference between the zones (middle minus inner) was 0.38dB (SD 2.44) for the Standard strategy and 0.29dB (SD 3.38) for the FASTPAC strategy. The wider confidence limit was evident at more negative total deviations than -18dB in the Standard strategy and than -13dB in the FASTPAC strategy. The Runs test reached statistical significance for the trend in these differences for both examination strategies (Standard p=0.042 and FASTPAC p=0.033, respectively).

The 5% confidence limits of the Standard and FASTPAC strategies were statistically different from each other for the outer (p=0.05), middle (p=0.006) and inner (p=0.005) zones of eccentricity. The FASTPAC strategy 5% confidence limit was wider for each of the three annuli than the Standard strategy. For the outer zone, the differences between the strategies (Standard minus FASTPAC) across the 2dB total deviation groups from -34dB to -2dB averaged -2.13dB (SD 3.59) and were greatest when the deviation from normal sensitivity at the second examination was greater than -24dB. Likewise, the middle zone exhibited an average difference between each strategy of the 5% confidence limits of -2.87dB (SD 3.35) and the difference was greatest at total deviations of -20dB or more. The inner zone showed an average difference between the 5% confidence limits of the Standard and FASTPAC strategies of -1.28dB (SD 1.65) and the greatest differences between the strategies were observed when the total deviation at the second examination was greater than -18dB.

The Standard strategy exhibited a significant difference between the 5% confidence limits of the outer and middle zones of eccentricity (p=0.026). No such difference was found for the

FASTPAC strategy (p=0.125). Neither strategy exhibited a significant trend across the sensitivity intervals by the Runs test (Standard, p=0.578; FASTPAC, p=0.867). Conversely, the FASTPAC strategy exhibited a significant difference between the 5% confidence limit of the middle and inner zones (p=0.001) where no such difference was found for the Standard strategy (p=0.751). Again, neither strategy exhibited a significant trend across the sensitivity intervals by the Runs test (Standard, p=0.986; FASTPAC, p=0.478). The mean width and range of the 90% confidence intervals for each strategy and for each zone, averaged across the 2dB sensitivity groups, is shown in Table 4.1.

In order to investigate the influence of depth of defect on the between-examination variability, the two patient groups were combined and separated into those with a Mean Defect of less than 5.7dB and those with a Mean Defect of greater than 5.7dB for the second Standard examination. Two patients from each group were omitted due to the severity of their visual field loss. The corresponding confidence limits were computed for each Mean Defect group and for each strategy across the 2dB sensitivity classes and are shown in Figure 4.7. There was no significant difference between the Standard and FASTPAC strategies for either the 5% or 95% confidence limits (p=0.494 and p=0.939, respectively) across the 2dB total deviation intervals from +2dB to -20dB in the group with a Mean Defect of -5.7dB or more positive. The width of the 90% confidence interval increased as the magnitude of the total deviation at the second examination increased. For example, the width of the 90% confidence interval was 6.80dB for the Standard strategy and 7.35dB for the FASTPAC strategy at normal or near normal sensitivities; the width of the 90% confidence interval was 20.30dB for the Standard strategy and 20.20dB for the FASTPAC strategy at stimulus locations deviating from normal sensitivity by approximately 19dB. There was also no significant difference between the Standard and FASTPAC strategies for either the 5% and 95% confidence limits (p=0.067 and p=0.129, respectively) across the 2dB total deviation intervals from 0dB to -34dB in the group with a Mean Defect more negative than -5.7dB. The width of the 90% confidence intervals was similar between the Standard and FASTPAC strategies at stimulus locations deviating from normal by up to -10dB. At stimulus locations with a sensitivity of greater than -10dB the

ZONE	STRATEGY			
	Standard		FASTPAC	
	Mean (SD) (dB)	Range (dB)	Mean (SD) (dB)	Range (dB)
Outer	15.79 (4.25)	7.0 - 21.6	17.58 (3.19)	12.8 - 22.0
Middle	14.96 (3.91)	10.0 - 20.7	18.05 (4.50)	10.3 - 23.7
Inner	15.17 (3.65)	9.1 - 20.3	16.58 (4.76)	9.0 - 23.1

Table 4.1. The mean width of the 90% confidence interval (dB) across the range of total deviation groups for the standard and FASTPAC strategies and for each of the outer, middle and inner zones.

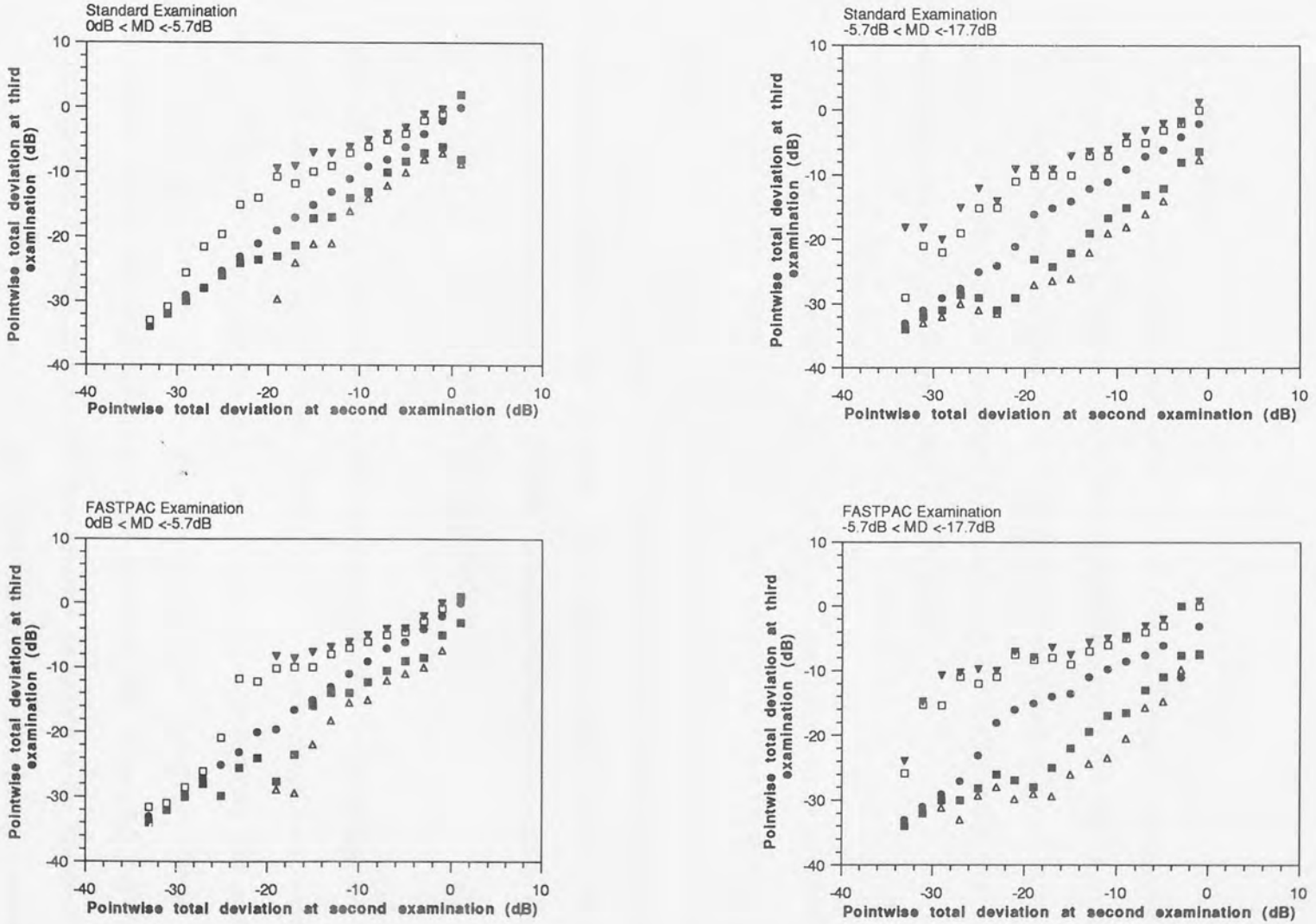

Figure 4.7. The 5% (inverted triangles), 10% (open squares), 50% (filled circles), 90% (filled squares) and 95% (upright triangles) confidence limits of between-examination variation at each 2dB total deviation interval for the Standard (top) and for the FASTPAC strategy (bottom) combined across the two patient groups as a function of the Mean Deviation (MD) at the second examination.

FASTPAC 90% confidence interval was wider than that of the Standard. At stimulus locations with a total deviation of greater than -26dB the Standard strategy exhibited greater convergence of the 5% and 95% confidence limits.

4.5. Discussion.

The findings for the between-examination variability of the Standard strategy are in good agreement with those of Heijl and co-workers (1989b) who found that the magnitude of the 95% confidence limit increased as the total deviation increased up to a defect depth of approximately 18dB after which it subsequently plateaued. The plateau effect is an artefact of the limited dynamic range of the HFA (Heijl et al. 1989a).

When the two groups of patients were considered separately, the total deviations at the third examination were more negative, overall, for the strategy undertaken as the second in the pair regardless of the strategy order. This was particularly evident when the Standard strategy was followed by the FASTPAC strategy. The increased total deviations may be attributable to the fatigue effect, resulting in a lower sensitivity for the second strategy (Hudson et al. 1994). However, the differences in the total deviation between the strategies in either group were small despite, in some cases, reaching statistical significance.

The FASTPAC strategy exhibited greater between-examination variability than the Standard strategy when the 60 patients were considered as a single group, irrespective of the examination order. The magnitude of the discrepancy was approximately 2dB and may be attributed to an interaction between the difference in the strategy staircases and the stratification at the second examination of the pointwise total deviations. The FASTPAC strategy exhibits a greater error for the total deviation compared to the Standard strategy (Flanagan et al. 1993b; Schaumberger et al. 1995) due to the single crossing of threshold and to the larger step size at the final crossing. The difference between the pointwise total deviations obtained with each strategy at the second examination was minimised when the stimulus locations were condensed into 2dB intervals. However, the data obtained at the third

examination was represented as a continuous scale, thereby emphasising the difference between the strategies. The difference between the FASTPAC and Standard between-examination variability is of minimal clinical consequence, particularly when the benefits of the reduced examination duration are considered. Furthermore, the characteristics of the between-examination variability across the sensitivity intervals was similar between strategies; greater between-examination variability was exhibited by those stimulus locations deviating moderately from the normal sensitivity than by those of near normal sensitivity or of absolute loss.

The width of the 90% confidence interval was greater for the FASTPAC strategy than for the Standard strategy across the sensitivity intervals for each eccentricity zone. Other studies have found an increase in between-examination variability with increasing eccentricity in glaucoma subjects (Boeglin et al. 1992; Heijl et al. 1989b). However, in this study neither the Standard nor the FASTPAC strategy showed such a trend. The greatest between-examination variability was again evident at stimulus locations exhibiting a sensitivity that deviated moderately from the normal sensitivity for all three eccentricity zones and this finding is in agreement with that of Heijl et al (1989b).

The magnitude of the pointwise between-examination variability has been previously been shown to increase with the severity of the visual field defect (Boeglin et al. 1992; Heijl et al. 1989b; Henson & Darling 1995). Together with the reported increase in the FASTPAC Short-term Fluctuation at advancing defect depths (Flanagan et al. 1993b; Schaumberger et al. 1995), it might be expected that the FASTPAC strategy would exhibit greater between-examination variability in advanced loss. Indeed, this was found to be the case when the MD was more negative than -5.4dB and the stimulus location sensitivity deviated by 10dB or more from the normal sensitivity. The between-examination variability was otherwise similar between the strategies.

4.6. Conclusion.

The FASTPAC algorithm shows greater between-examination variability than the Standard algorithm as a function of sensitivity at the first examination. The magnitude of the disparity may be attributed to the differing staircases of the two strategies. The FASTPAC between-examination variability was also greater at all eccentricities, although neither strategy showed increasing variability with an increase in eccentricity. The greatest magnitude of FASTPAC and Standard between-examination variability was most evident at stimulus locations exhibiting moderate loss within a visual field of moderate to severe MD. However, the difference between the strategies was small enough to render them clinically similar in the detection of progressive visual field loss.

Chapter 5. The influence of repositioning the baseline in the Glaucoma Change Probability Analysis on the detection of progressive visual field loss.

5.1. Introduction.

Delineation of progressive visual field loss in glaucoma is generally carried out using criteria based upon a comparison of the combined appearances of the greyscales, the total and pattern deviation probability plots, and the visual field indices. This type of analysis is arbitrary, is based upon the experience of the clinician and often there is little agreement between clinicians (Werner et al. 1988).

More objective criteria for determining progressive visual field loss at a given stimulus location utilise a reduction in sensitivity of an arbitrary number of decibels from a pre-determined baseline visual field. An apparent reduction in sensitivity at a stimulus location can also be evaluated in relation to the magnitude of the short-term fluctuation (AGIS 1994; Morgan et al. 1991). Additional criteria may also stipulate that any stimulus locations exhibiting deterioration are adjacent to one another (AGIS 1994; Johnson et al. 1993a). A mathematical algorithm has also been introduced which, by scoring the empirical criteria at each examination, attaches a statistical probability of progressive loss to the pattern of scores over a series of examinations (Schulzer 1994).

The most rigid technique for identifying progressive visual field loss assigns a level of statistical probability to the observed change in sensitivity. Such statistical procedures minimise the variation between clinicians. The Glaucoma Change Probability Analysis (GCPA), contained within the Humphrey Field Analyser (HFA) Statpac 2 software, is one such technique and provides a statistical interpretation of visual field progression at each individual stimulus location. The GCPA compares the sensitivity at the given stimulus location with the sensitivity at the corresponding location in a composite baseline, comprising two fields. The magnitude of the deviation between the measured and the baseline sensitivity is then referenced to a database containing the between-examination variation in sensitivity encountered in a stable glaucomatous population. A reduction or improvement in sensitivity

that falls outside the empirical 95% confidence limit of between-examination variation exhibited by the database is assigned a probability symbol on the graphical display. The baseline fields are usually taken as the initial two fields. However, the GCPA software is able to remove the first field to compensate for the learning effect if the MD at the first examination is worse than at the second examination and if it is an outlier from the linear regression of MD against follow-up time (Heijl et al.1991). The magnitude of the between-examination variation in stable glaucoma becomes greater as sensitivity declines and is also influenced by the spatial location of the stimulus. The inferior nasal region exhibits a greater degree of between-examination variability than the superior nasal region and thus requires a larger apparent deterioration to reach statistical significance. The superior and inferior temporal regions, however, exhibit similar variability between examinations (Heijl et al. 1989b). The graphical display of the GCPA denotes deterioration as a filled triangle and improvement with an open triangle. Confidence limits for deterioration are only included in the database for those stimulus locations which exhibit a baseline sensitivity that differs from normal by between -12dB and +2dB. Improvements in sensitivity can only be determined for stimulus locations with a sensitivity that differs from normal by between -28dB and 0dB at baseline. In addition, confidence limits for change may only be computed when the initial MD is -15dB or better. Progressive deterioration or improvement at a stimulus location whose sensitivity at the baseline falls outside the limits of the database is only indicated if the stimulus location exhibits a deviation that is equal to, or larger than, the deviation required for change at the lowest sensitivity in the database (Heijl et al.1991). In such a case, the deterioration or improvement is indicated by an *x* symbol.

It is possible that the GCPA could indicate statistically significant deterioration at a single stimulus location due to chance because of the presence of random variations. Therefore, clinical progressive loss should be considered to have occurred only when the deterioration in sensitivity at a single location is confirmed at the immediate subsequent examination (Morgan et al. 1991) or if, within a single field, two non-edge locations with a significant deterioration in sensitivity appear adjacent to each other (Birch et al. 1995). The GCPA has been shown to

provide a more reliable indication of visual field progression than intuitive techniques particularly at eccentricities of greater than 24° (Morgan et al. 1991). The relationship between the GCPA and univariate linear regression of sensitivity against time to follow-up is described in Chapter 6.

The GCPA does, however, have some inherent limitations in its use. The comparison of any given field with the baseline pair of fields disregards the information contained within the intervening visual field examinations. In addition, once deterioration from the baseline has been identified, the GCPA is unable to indicate any further progression at that given location. This latter limitation may be overcome by repositioning the baseline at the two fields exhibiting deterioration. However, those locations exhibiting a deviation within the normal between-examination variability when referenced to the initial baseline will also be re-referenced to the repositioned baseline. Once progression has taken place at a stimulus location it can be impossible to detect further change with the same baseline, particularly if the location exhibits minimal variability and a small decline in sensitivity (Chapter 6). In addition, a sensitivity falling within the GCPA database criteria for change may become classed as 'out-of-database' as a result of repositioning the baseline. The utility of modifying the baseline for stimulus locations exhibiting progressive loss whilst maintaining the initial baseline for those exhibiting stability is unknown.

5.2. Aims.

The aim of the study was to determine whether repositioning the baseline to the most immediate pair of fields at which a stimulus location exhibits deterioration could identify further progression at subsequent examinations.

5.3. Methodology.

The sample was selected from 1516 fields of both eyes of 80 consecutive patients with primary open angle glaucoma drawn from the database of the Glaucoma Service, Toronto Hospital (Western Division). All patients were required to have a distance visual acuity of 6/12

or better at the initial visual field in the given series. Cases of clinically significant cataract or of an ocular history other than glaucoma were excluded from the sampling process. The mean age of the patients was 64.66 years (SD 13.3). The MD at the initial field of the series ranged from +0.46dB to -20.86dB (mean -8.24dB; SD 6.34dB) and the PSD from 0.60dB to 13.4dB (mean 4.86dB; SD 4.2dB). Each patient was also required to have a minimum of six (range 6 to 16) HFA Program 24-2 or 30-2 visual fields (stimulus size III) and to have undergone automated perimetry prior to presentation for tertiary care at the Toronto Hospital. The follow-up period ranged from 3.1 years to 8.9 years. The protocol for the examination of the visual field had been strictly followed. All the visual fields were reduced to a 24-2 format and the stimulus locations above and below the blind spot were excluded. The fields of each eye from each patient were classified by a single individual, experienced in automated perimetry, as 'stable' or as 'progressing' using the Overview and Change Analysis print-outs. The individual was both masked to the other clinical criteria and to the outcome of the GCPA. Of the 80 patients examined, 60 were deemed to possess stable visual fields in both eyes over the given visual field series. The fields of one eye from each of the remaining 20 patients exhibiting progressive visual field loss were selected at random. The corresponding GCPA print-outs were then obtained for these twenty patients directly from the perimeter. In all cases, the first two fields in the series were used and confirmed by the GCPA as the baseline. Progression of the visual field from the initial baseline was defined as a stimulus location exhibiting deterioration by the GCPA at two or more consecutive examinations. Four of the twenty patients did not exhibit any stimulus locations at which the GCPA indicated consistent deterioration. These four patients were removed from the analysis.

The baseline of each of the sixteen patients was then repositioned, on a pointiwise basis, to the most immediate pair of fields at which a single stimulus location exhibited visual field progression from the initial baseline. The validity of the fields as an appropriate second baseline was confirmed by the GCPA. The number of stimulus locations exhibiting deterioration from the second baseline was then determined. A similar analysis was carried out for those stimulus locations exhibiting improvement from the initial baseline. An 'out-of-

database' classification was considered as deterioration if the change from the baseline was negative. A stimulus location was considered to be stable if neither deterioration nor improvement was indicated by the GCPA at any of the subsequent fields. A fluctuating stimulus location was defined as the appearance of a symbol denoting deterioration or improvement at a single examination that was not confirmed at the next consecutive examination.

The mean age of the 16 patients was 66.38 years (SD 12.8). The MD of the sub-sample at the initial field in the series ranged from -0.20dB to -14.67dB (mean -6.02dB; SD 5.0) and the PSD from 1.92dB to 13.4dB (mean 5.50dB; SD 3.4dB). The type of defect at the initial examination in the series is shown in Figure 5.1. The mean number of fields was 11.88 (range 7 to 16) over a mean follow-up time of 6.55 years (SD 1.1). The mean interval between examinations was 7.56 months (SD 1.4). Each visual field of each patient's series was deemed reliable in terms of the incidence of false-responses to the catch trials and the magnitude of the short-term fluctuation. The group mean intraocular pressure over the series of examinations was 21.2mmHg (SD 2.3). The sub-sample was not controlled for the type of ocular therapy. However, three patients were receiving pilocarpine therapy. In these three patients the therapy was unchanged throughout the visual field series and each maintained a pupil size within ±1mm of their baseline fields.

5.4. Results.

From a total of 832 stimulus locations, 222 exhibited progressive loss, 14 were classified as 'out-of-database', 22 exhibited improvement, 369 were stable and 205 were fluctuating at the first baseline. The mean, standard deviation and range of each classification per patient is shown in Table 5.1. Eight locations (three patients) exhibited deterioration in two of the last three fields in their series. Further deterioration from a second baseline could not be confirmed due to an insufficient number of subsequent fields. The fourteen locations classified as 'out-of-database' by the GCPA exhibited a reduction in sensitivity were present in five of the sixteen patients.

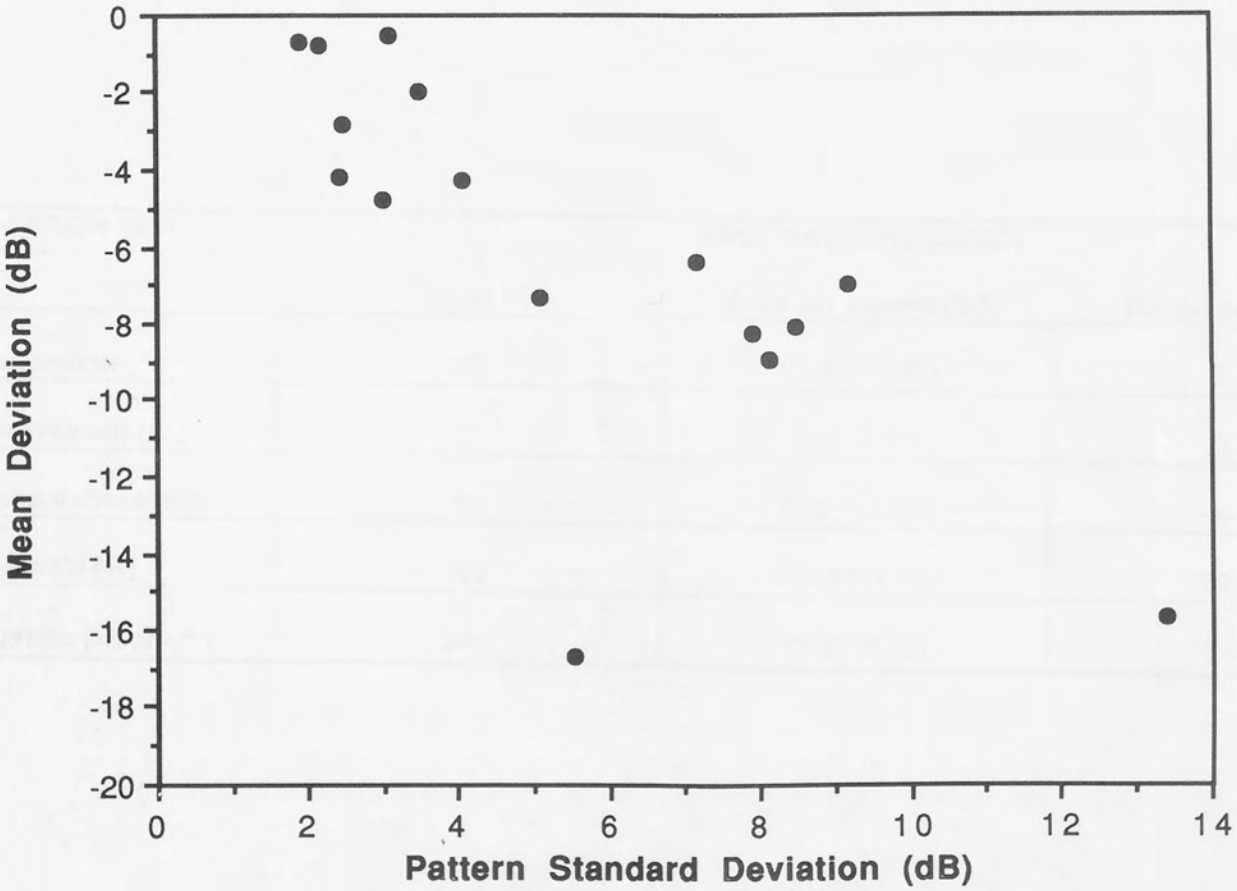

Figure 5.1. The type of visual field defect at the first examination in the series illustrated in terms of the Mean Deviation (dB) against the Corrected Pattern Standard Deviation (dB) for the sixteen glaucoma patients exhibiting visual field progression .

LOCATION TYPE	FIRST BASELINE (n=832)		
	Total	Mean per patient (SD)	Range per patient
Deterioration (▲▲)	222	13.88 (10.54)	2 - 33
Improvement (ΔΔ)	22	1.38 (1.11)	1 - 3
Out of database (xx)	14	0.875 (1.41)	0 - 2
Stable (••)	369	23.06 (12.06)	20 - 46
Fluctuation (•Δ or •▲)	205	12.81 (8.23)	2 - 18

Table 5.1. The outcome at the first baseline at each stimulus location across the sixteen patients.

A total of 13 locations exhibited progressive loss at the second baseline. The thirteen locations were present in five patients (mean of 2.6; SD 1.8 locations per patient; range 2-5). A further 8 stimulus locations (2 patients) exhibited deterioration from the first baseline in two or three of the last three fields in their series and exhibited deterioration when the baseline was repositioned to the pair of fields most immediate to the progressive loss. The combined total of 21 locations exhibiting progressive loss from the initial baseline and from the second baseline were present in seven patients and each patient had a cluster of two or more stimulus locations. All locations were situated within 21° eccentricity of fixation; fourteen of the deteriorating stimulus locations were situated in the superior hemifield and seven in the inferior hemifield.

Twenty-three locations across eleven patients exhibited deterioration from the first baseline but subsequently showed improvement at the second baseline (mean 2.09; SD 1.62; range 1-4 locations per patient). Eleven of these locations were situated outside 21° eccentricity. Two patients had a cluster of two locations exhibiting improvement with the second baseline. Four patients exhibited at least one improving stimulus location coexisting, but not adjacent to, a clustered pair of stimulus locations exhibiting deterioration with their second baseline. Fifteen stimulus locations (six patients) exhibiting deterioration with the initial baseline showed two consecutive 'out-of-database' symbols with the second baseline. The 'out-of-database' symbols all corresponded to negative changes in sensitivity from the second baseline (mean 2.5; SD 2.07; range 1-6). Four of these fifteen locations were isolated and were situated outside 21° eccentricity. Eight of the eleven locations situated within 21° eccentricity formed four clustered pairs. Fifty-one locations that exhibited progressive loss with the first baseline showed fluctuation with the second baseline. The remaining 112 locations were stable at the second baseline. The frequency of each type of outcome at the second baseline is shown in Table 5.2.

The twenty-one stimulus locations exhibiting additional deterioration at the second baseline were identified by nine different positions of the second baseline. The second baseline was

LOCATION TYPE	SECOND BASELINE (n=222)	THIRD BASELINE (n=13)
Deterioration (▲▲)	21	3
Improvement (ΔΔ)	23	1
Out of database (xx)	15	2
Stable (••)	112	5
Fluctuation (•Δ or •▲)	51	2

Table 5.2. The outcome at the second baseline of the 222 stimulus locations exhibiting progressive loss from the first baseline. The corresponding data for the 13 stimulus locations exhibiting progressive loss from the third baseline.

altered by a mean of 1.28 times per patient (SD 0.49). The locations exhibiting subsequent improvement at the second baseline were identified by 15 different positions of the second baseline. Six of the nine different alterations of the second baseline, made for stimulus locations exhibiting progressive loss, were common to the fifteen carried out for stimulus locations exhibiting improvement at the second baseline.

Of the 13 stimulus locations exhibiting deterioration at the second baseline, 3 stimulus locations (two patients) continued to progress and two stimulus locations were out of the database (with a negative change in sensitivity) from a the third baseline. One stimulus location exhibited a subsequent improvement. The outcome of the thirteen stimulus locations at the third baseline is summarised in Table 5.2.

The influence of the defect depth at the initial pair of examinations on the outcome of the GCPA at the second baseline was examined by stratifying the 222 stimulus locations exhibiting progressive loss with the first baseline in terms of their outcome at the second baseline. This resulted in three classifications: progressive loss at the second baseline (n=36); subsequent improvement (n=23) and stability (n=163) at the second baseline. The stimulus locations classified as stable included those locations exhibiting fluctuation at the second baseline. The mean total deviation derived from the first baseline fields of each stimulus location was then determined. The fiftieth percentile of the cumulative frequency distribution of the stimulus locations exhibiting stability at the second baseline occurred at a mean total deviation of -2dB (Figure 5.2). The corresponding fiftieth percentile of the group with progressive loss and the group showing improvement occurred at a mean total deviation of -4dB.

5.5. Discussion.

The determination of visual field progression is a crucial factor in the management of glaucoma. The selection of patients exhibiting progression based upon visual field criteria alone allows this factor to be considered in isolation. Visual field progression was identified by

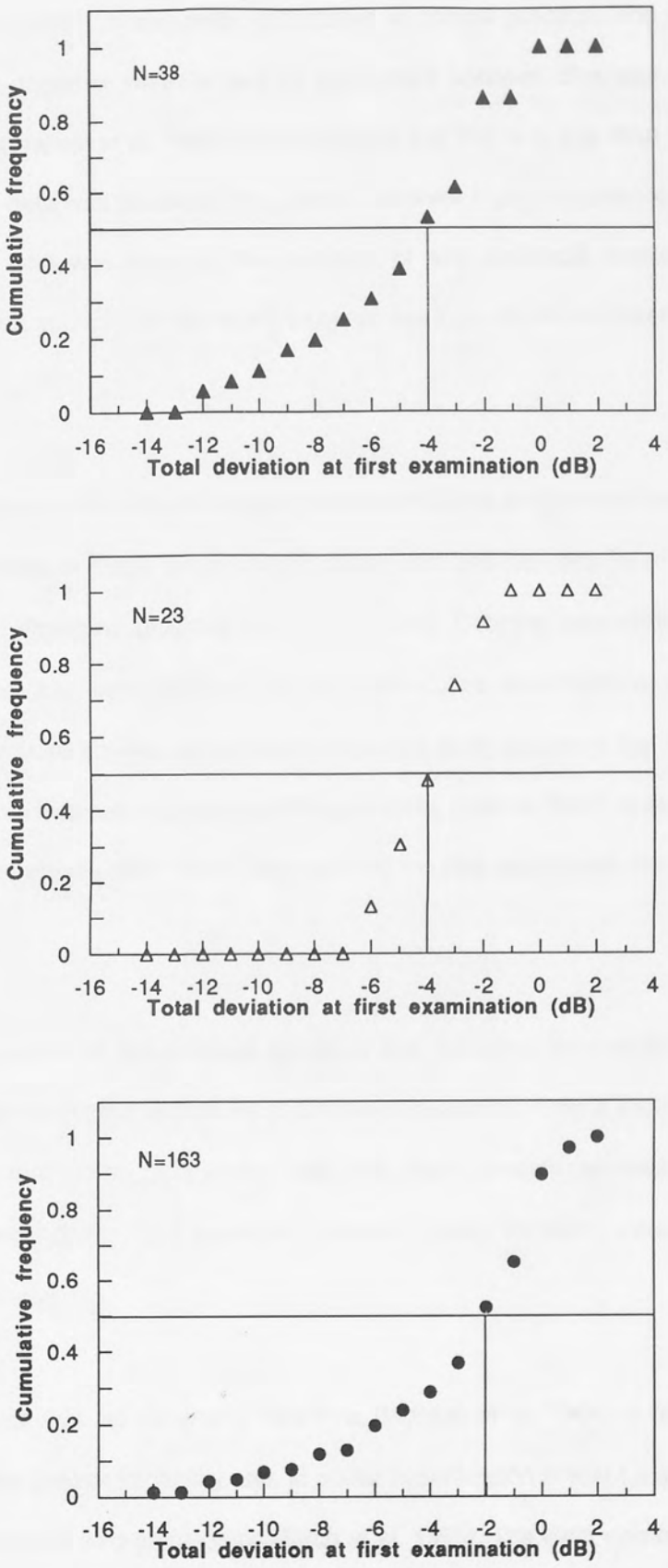

Figure 5.2. The number of stimulus locations, expressed as a cumulative frequency, as a function of depth (dB) for the 36 stimulus locations exhibiting progressive loss (top), the 23 stimulus locations exhibiting improvement (middle) and the 163 stimulus locations exhibiting stability (bottom) at the second baseline.

intuitive criteria of a type which is frequently undertaken in clinical practice. The subjective nature of this approach, together with the lack of agreement between clinicians in studies adopting similar criteria (Werner et al. 1988) would suggest that this is a less than ideal 'gold standard'. However, the data was inspected by a single observer highly experienced in visual field interpretation and who was blind to the outcome of any statistical interpretation of progression. Indeed, good agreement was found between this type of clinical observation and the GCPA.

The use of a criterion of a minimum of one single location exhibiting progressive loss could be considered to be erroneous. A single progressing location can also be considered part of an existing defect or be an emerging separate area of focal loss. Defining deterioration as only those stimulus locations that were repeated at two consecutive examinations was felt to reduce the possibility of false positive occurrences. A recent study suggests that this criteria represents a conservative measure of progression in glaucoma patients (Birch et al. 1995) and good agreement has previously been found with numeric intuitive techniques (Morgan et al. 1991).

Approximately three-quarters of the stimulus locations that exhibited deterioration with the original baseline showed fluctuation or stability at the second baseline. Only a small proportion of stimulus locations that were progressing with the first baseline showed additional progression with the second and third baselines. However, these locations were present in seven of the sixteen patients.

Previous studies suggest that the peripheral locations (Morgan et al. 1991) or 'edge-points' (Birch et al. 1995) exhibit greater variability and, in ocular hypertension present a questionable criteria for determining visual field progression (Birch et al. 1995). The exclusion of peripheral locations, however, overlooks the possibility of deterioration occurring in the more peripheral field (Haas & LeBlanc 1993; Miller et al. 1989; Stewart et al. 1989). Nevertheless, the spatial position of the stimulus locations showing sustained deterioration in this study were situated

within 21° eccentricity. In addition, sixteen of the 21 locations showing additional progression were adjacent to at least one other similarly progressing stimulus location.

A similar number of stimulus locations exhibited subsequent improvement at the second baseline as those with additional progression. The subsequent improvement was, however, observed in almost twice as many patients. It is likely that that localised learning effects are occurring at these locations, the extent of which is not widespread enough to negate the use of the entire visual field as a baseline. The incidence of the stimulus locations exhibiting localised learning at the second baseline appeared to be independent of eccentricity.

Given that the degree of variability increases as a function of sensitivity, it could be expected that some stimulus locations could fall outside the database in a glaucomatous sample. Fifteen stimulus locations converted from progressive loss with the first baseline to 'out-of-database' at the second baseline. This can be attributed to the restricted measurement range of the perimeter creating artificially narrow limits of the GCPA database at depressed sensitivities.

5.6. Conclusion.

The delineation of additional visual field progression at a proportion of stimulus locations following alteration of the baseline advocates movement of the baseline through the series of fields. In contrast to those stimulus locations showing subsequent improvement with the repositioned baseline, the greater majority of locations exhibiting additional progression were adjacent to at least one other similar location. A baseline alteration for the entire visual field may impede the detection of progression at those stimulus locations manifesting deterioration from the original baseline that appear in consecutive examinations proximal to the new baseline. Thus, the outcome of this study proposes baseline repositioning on a pointwise basis at adjacent stimulus locations exhibiting deterioration at the original baseline. In this way, the number of locations showing subsequent improvement with the baseline alteration will be minimised. These enhancements to the GCPA would require additional software development

in order to automate the procedure and to enable the printout to reflect the baseline alterations.

Chapter 6: Pointwise modelling of visual field progression with univariate linear regression of absolute sensitivity and pattern deviation against time to follow-up.

6.1. Introduction.

Glaucomatous visual field progression can be evaluated for the field as a whole, for any region of the field, or for each individual stimulus location. Univariate linear regression (ULR) analysis regresses a summary measure for the given extent of the field against the time to follow-up examination (Heijl et al. 1991). The degree of progression is determined from the slope of the function (Heijl et al. 1991; Holmin & Krakau 1980; Holmin & Krakau 1982; Schwartz & Nagin 1985; Wu et al. 1987).

The early studies of ULR were based upon regression of an index called the performance value (P). The performance value represented the sum of the threshold measurements at each of the stimulus locations examined (Heijl & Bengtsson 1984; Holmin & Krakau 1980; Holmin & Krakau 1982; Holmin & Storr-Paulsen 1984). In normal individuals a decay of 2.61 units/year in the P value was found across an age range of 55 to 71 years. A more rapid rate of decay was found to be present in glaucoma regardless of the level of IOP and the type of treatment (Holmin & Krakau 1980) and the decay was greater in cases of small to moderate field loss than in cases of extreme loss (Holmin & Krakau 1982; Holmin & Storr-Paulsen 1984; Schultz et al. 1987).

With the advent of the visual field indices, ULR of the mean sensitivity against time to follow-up has been used to determine the rate of visual field deterioration. The mean rate of decay in glaucoma patients exhibiting stable visual fields was found to be -0.072 dB/year (O'Brien et al. 1991) which was similar to the decay in normal subjects (-0.058 dB/year) (Haas et al. 1986). The mean rate of decay in primary open-angle glaucoma (POAG) exhibiting visual field progression was estimated variously as -1.39 dB/year (O'Brien et al. 1991) and -0.195 dB/year (Weber et al. 1993), whilst in secondary glaucoma the decay was -0.308 dB/year (Weber et al. 1993). The derived slope is an expression of the average rate of decay across the given extent of the field and subtle localised changes may be missed with this technique. The visual field

indices for the composite field exhibit a low sensitivity and specificity in the determination of glaucomatous visual field progression (Birch et al. 1995; Chauhan et al. 1990). In addition, the presence of diffuse field loss in glaucoma is equivocal (Airaksinen et al. 1985a; Flammer et al. 1985). Moreover, the slope of the regression of MD against time to follow-up has been found to correlate more closely with cataract progression than with visual field progression in glaucoma (Åsman & Heijl 1994). In order to better describe the rate of visual field loss specific to glaucoma it may be more appropriate to consider the slope of the pattern deviation against time to follow-up.

ULR of the mean sensitivity in regions of the visual field against time to follow-up has been suggested as an appropriate way to monitor regional change (Suzuki et al. 1993). As would be expected, POAG (O'Brien & Schwartz 1990) and secondary open-angle glaucoma (Werner et al. 1988b) patients exhibiting deterioration in mean sensitivity for the entire field also show significant loss in a majority of regions. More interestingly, patients deemed stable by regression of the mean sensitivity for the composite field against time to follow-up can show a significant decline in sensitivity in one or more regions (O'Brien & Schwartz 1990; O'Brien et al. 1991; Werner et al. 1988b), particularly if the initial sensitivity of the region is high (O'Brien et al. 1991).

ULR of sensitivity against time to follow-up applied to each individual stimulus location is becoming increasingly popular and is being used for the study of visual field progression in ocular hypertension (Wu et al. 1987) and primary open angle glaucoma (Birch et al. 1995; Hitchings et al. 1994; Noureddin et al. 1991; O'Brien & Schwartz 1990; Wu et al. 1987). The technique enables emphasis to be placed upon local changes in sensitivity that may otherwise have been masked by regression of a single summary statistic for the field as a whole. A statistical software package, PROGRESSOR, displays the outcome of ULR of sensitivity against time to follow-up at each stimulus location over the series of fields examined. The display consists of a single bar at each stimulus location; the length of the bar indicates the magnitude of the regression coefficient and the bars are colour-coded to indicate the statistical

significance of the regression coefficient (Fitzke & McNaught 1994). The regression coefficient at each stimulus location is recalculated after an additional visual field examination. The addition of a single data point has a minimal effect on the magnitude of the regression coefficient in this type of consecutive ULR analysis. There is therefore an increased likelihood of 'regression towards the mean' (Krakau 1986) and, as such, the incidence of false-positive stability is also increased.

The slope (regression coefficient) of the function is used to determine the extent of the progressive loss, yet the criterion for defining progression by ULR is empirical, varies between studies (Hitchings et al. 1994; Noureddin et al. 1991; O'Brien & Schwartz 1990) and to date has not separated the decline in sensitivity due to age from that due to the disease process itself. The simplest criterion for denoting progression is a negative regression coefficient that is significantly different from zero (Araujo et al. 1987; O'Brien & Schwartz 1993). A single stimulus location exhibiting such a criterion may misclassify progressive visual field loss (Oden 1993). Alternative criteria have been adopted such that progression is determined by a negative regression coefficient, which is significantly different from zero and with a rate of decline of greater than either 2.4dB/year (Hitchings et al. 1994; Noureddin et al. 1991) or 1.0dB/year (Baez et al. 1995; Birch et al. 1995). Noureddin et al (1991) and Hitchings et al (1994) also stipulated that a stimulus location should be classified as deteriorating only if two regression coefficients in succession are greater than -2.4dB/year. Progression has also been determined from the pointwise ULR of only three measures of sensitivity against follow-up time (Noureddin et al. 1991), a method of doubtful statistical viability (Krakau 1985).

Various other techniques have been utilised for the evaluation of progression at each individual stimulus location. An established method is that of the Glaucoma Change Probability Analysis (GCPA) which is based empirically on the pointwise variability of stable glaucoma patients and compares the absolute sensitivity at a given examination with that of a baseline (Heijl et al. 1989; Heijl et al. 1991; Morgan et al. 1991). The GCPA and the pointwise ULR technique are based upon distinctly different statistical approaches. Recently, the GCPA has

been compared with both the MD and pointwise ULR techniques in ocular hypertension and glaucoma over a mean follow-up of 40 months (Birch et al. 1995). In general, little agreement was found between the three techniques. However, in ocular hypertension the GCPA detected more than twice as many instances of apparent progression compared to the two ULR techniques; whilst in glaucoma, the pointwise ULR technique detected more than twice as much progression as the GCPA. The application of ULR analysis has certain theoretical advantages in that both the spatial distribution and the rate of the progression can be identified. In addition, by using the second derivative of the function, the rate of change of progression can also be determined (Schwartz 1995).

The reason for the lack of agreement between the two techniques of pointwise analysis is unclear. The regression technique requires a minimum of five to six fields within a series for statistical expediency (Krakau 1985) and the statistical accuracy of the fitted slope of a linear function increases with the square root of the number of examinations within the follow-up. The relationship between the magnitude of the slope and the level of sensitivity is unknown. The slope is also more susceptible to bias from alterations in sensitivity occurring at the initial examinations due to the learning effect (Marchini et al. 1991; Werner et al. 1988a; Werner et al. 1990; Wild et al. 1989). The magnitude of the deterioration in glaucoma increases with the length of follow-up (Hart & Becker 1982; Mikelberg & Drance 1984; Mikelberg et al. 1986) and the deterioration of sensitivity over time has been reported to be non-linear in approximately 27% of cases (Mikelberg et al. 1986). In non-linear progression, ULR may seriously either under- or overestimate the rate of progression and the most immediate deterioration may be more suitably described by the use of the last six fields within the series (Figure 6.1). The outcome of ULR analysis is therefore clearly affected by the type of visual field progression, by the number of examinations selected in a given total visual field series and by the position, or time-frame, of these examinations in the series. A knowledge of the role of these factors in the outcome of ULR would help to explain the relationship between the two techniques of pointwise analysis and would facilitate recognition of visual field progression.

6.2. Aims.

The primary aim of the study was to develop the most appropriate model for pointwise univariate linear regression of sensitivity and to compare, in both a glaucomatous and an ocular hypertensive sample, the results with those of the Glaucoma Change Probability Analysis as a function of the magnitude of the slope of the pointwise regression function. Secondly, to examine the influence of the number and time-frame of the sequential examinations in a glaucomatous sample. Thirdly, to compare the outcome of ULR of the absolute sensitivities with that of ULR of the pattern deviation values in both a glaucomatous sample and an ocular hypertensive sample.

6.3. Methodology.

6.3.1. Glaucoma sample.

The glaucomatous sample comprised the fields from the arbitrarily assigned left eye of 38 patients (17 males) with POAG selected from the data files of the Department of Ophthalmology, The Toronto Hospital (Western Division). The first two fields of each patient were deleted from the analysis to minimise the effects of perimetric learning (Marchini et al. 1991; Werner et al. 1988a; Werner et al. 1990; Wild et al. 1989). The patients were selected to provide a broad range of the type and depth of field loss at the initial examination of the series (Figure 6.2). All patients were required to have undergone a minimum of 6 remaining examinations with the Humphrey Field Analyser (HFA) Program 30-2 or Program 24-2 using stimulus size III. The mean number of remaining fields per patient was 12.0 (SD 2.8) and the mean duration of follow-up 6.0 years (SD 1.6) (Range 3.2 to 8.5 years). The interval between examinations was not controlled between patients and was determined by conventional clinical practice based upon adequacy of intraocular pressure control, stability of the optic nerve head features determined by stereo-observation of the disc, and/or the rate of progression of visual field loss. The mean maximum interval per patient between remaining fields was 10.6 months (SD 4.3) and the mean minimal interval 3.2 months (SD 1.7). The mean age of the sample at the time of enrolment in the study was 59.0 years (SD 12.9). The group mean intraocular pressure in the left eye over the period of follow-up was 17.6mmHg (SD 3.5).

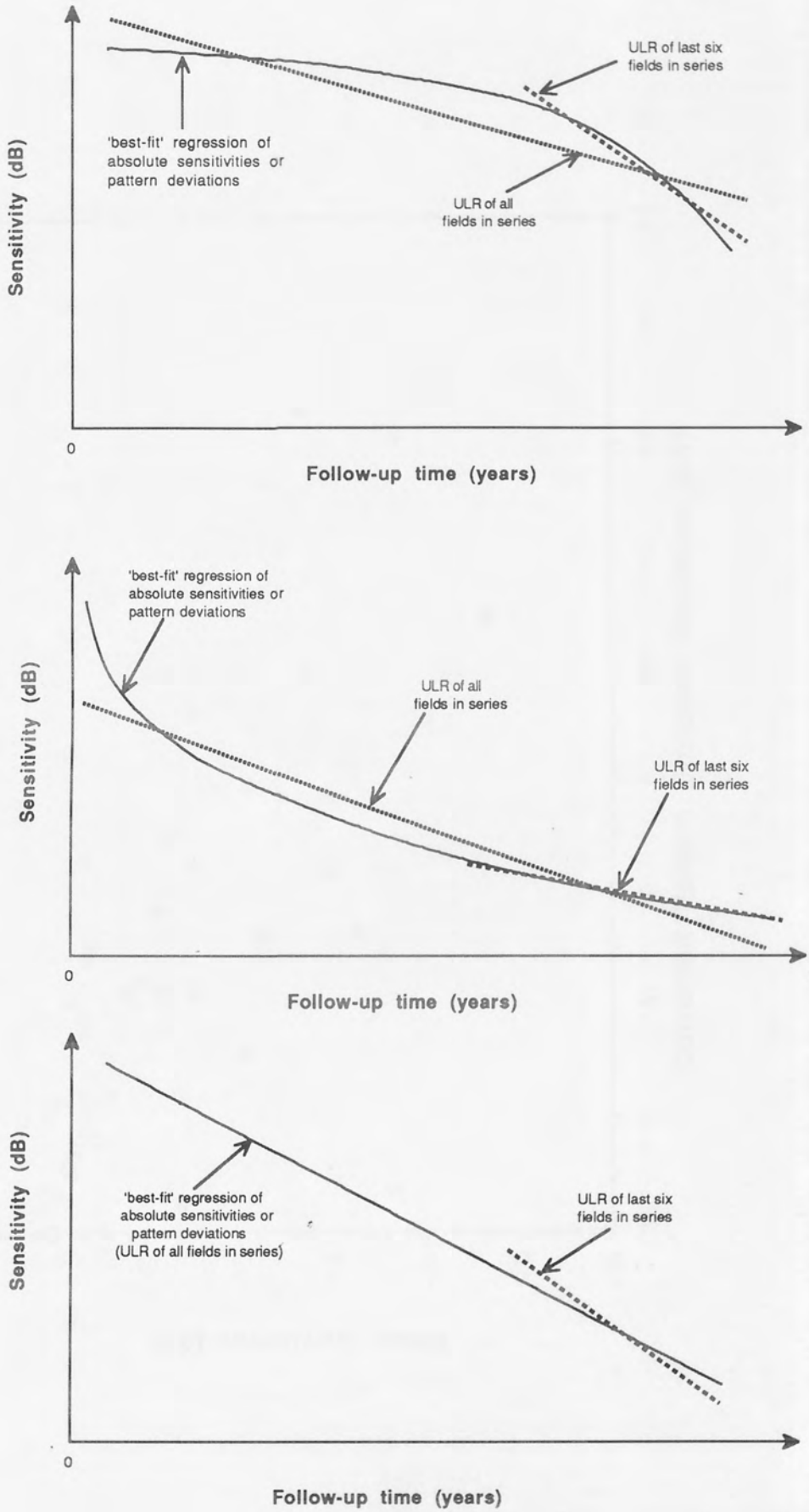

Figure 6.1. A schematic representation of pointwise univariate linear regression against time to follow-up for the entire and for the last six fields of the series illustrating three types of glaucomatous visual field progression.

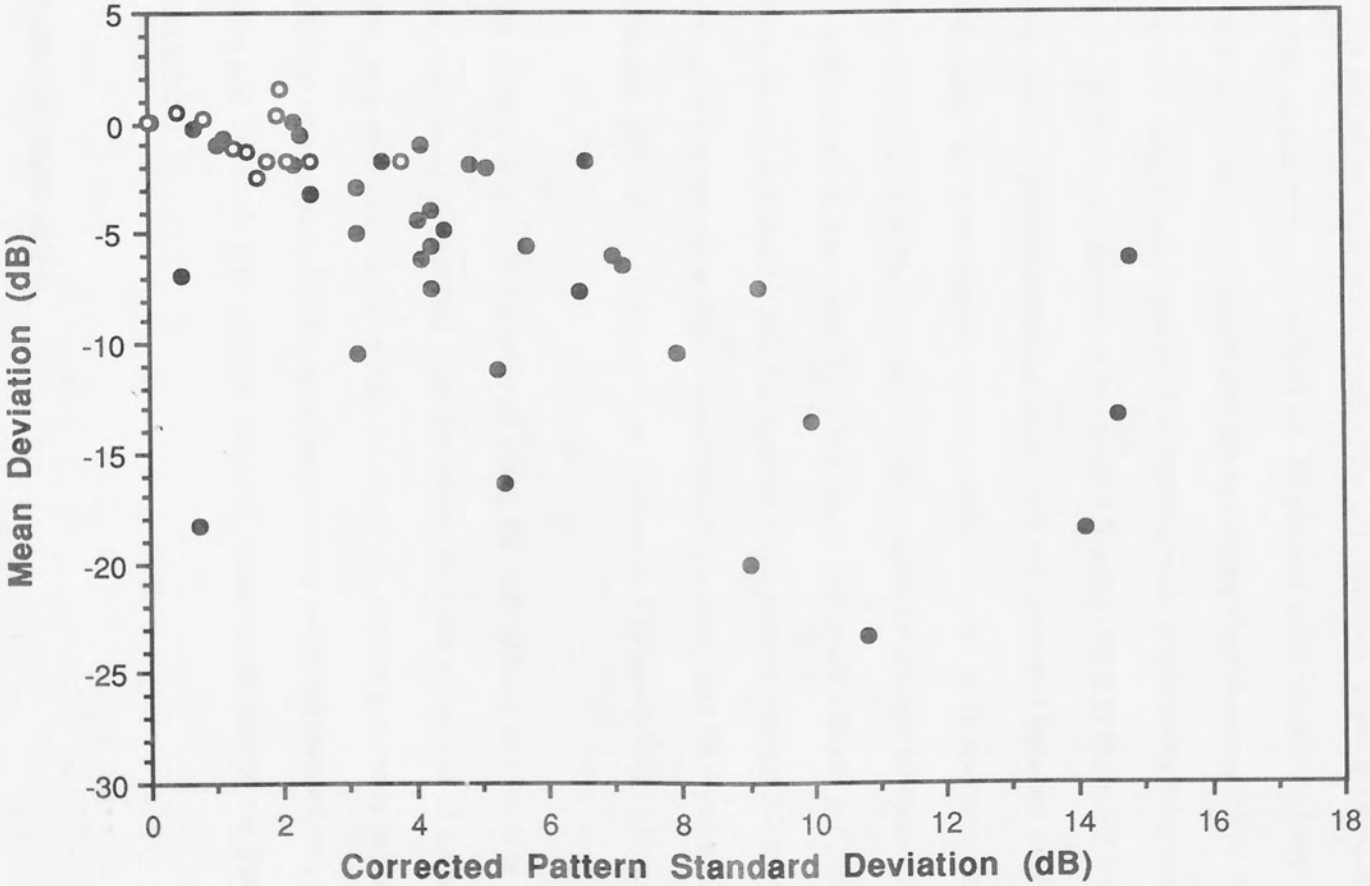

Figure 6.2. The degree of visual field loss at the first examination in the series illustrated in terms of the Mean Deviation (dB) against the Corrected Pattern Standard Deviation (dB) for the 34 glaucoma patients (filled circles) and the 12 ocular hypertensive patients (open circles).

6.3.2. Ocular hypertensive sample.

The sample comprised the fields from the arbitrarily assigned left eye of 12 low-risk ocular hypertensive patients (OHT) (11 males) also selected from the data files of the Glaucoma Service, Toronto Hospital (Western Division). The first two fields were removed from the analysis. The MD at the initial examination of the OHT patients ranged from +0.32 to -2.36 dB and the CPSD ranged from 0.00 to 3.80 dB. All patients were required to have undergone a minimum of 6 remaining examinations with the Humphrey Field Analyser (HFA) Program 30-2 or Program 24-2 using stimulus size III. The mean number of remaining fields per patient was 8.7 (SD 3.2) and the mean duration of follow-up 5.0 years (SD 2.1) (Range 2.9 to 8.3 years). The interval between examinations was once more not controlled between patients and was again determined by conventional clinical practice based upon adequacy of intraocular pressure control, stability of the optic nerve head features determined by stereo-observation of the disc, and stability of the visual field. The mean maximum interval per patient between remaining fields was 8.8 months (SD 2.4) and the mean minimal interval 3.0 months (SD 1.2). The mean age of the sample at time of enrolment in the study was 58.4 years (SD 14.4). The mean intraocular pressure in the left eye over the period of follow-up was 19.5mmHg (SD 3.6).

The visual acuity was 6/12 or better in all cases for both groups and patients with clinically significant cataract were excluded from the study. With the exception of patients receiving pilocarpine, who were also excluded from the study, no attempt was made to control between patients for the type of medical, surgical or laser therapy. Informed consent was obtained from all subjects and the study had approval from the ethical committee of the Toronto Hospital (Western Division).

6.3.3. Statistical manipulation.

The absolute sensitivity, z, at any given stimulus location was regressed against the time to follow-up, t, and the regression line fitted by the method of least squares such that:

$$z_j(t) = a_j + b_j t + \bar{u}_j \qquad \text{Eq. (6.1)}$$

where z_j is the sensitivity (expressed in dB) at visual field location j at time to follow-up t (expressed in years), a_j is a constant, b_j is a coefficient describing the slope of the function and $\bar{u}_j$ is a stochastic disturbance term at location j.

The t-statistic, T_{b_j}, of the derived slope, b_j, for the given stimulus location, j, was then tested as to whether it was statistically different from zero with respect to the Student's t-distribution using the equation:

$$T_{b_j} = \frac{b_j \sqrt{\sum_{i=1}^{i=n} \left(t_i - \bar{t} \right)^2}}{s_{z_j}} \qquad \text{Eq. (6.2)}$$

where t is the time in years at each follow-up examination (i), $\bar{t}$ is the mean follow-up time and s_{z_j} is the standard deviation of the sensitivity values for the given stimulus location j. s_{z_j} was calculated using the equation:

$$s_{z_j} = \frac{\sum_{i=1}^{i=n} \left(z_{ij} - \bar{z}_j \right)}{n-2} \qquad \text{Eq. (6.3)}$$

where z_{ij} is the sensitivity of location j at examination i, and $\bar{z}_j$ is the mean sensitivity at location j over the entire follow-up period consisting of n examinations.

The slopes that were statistically different from zero were further tested to determine whether they were statistically different from the slope of the normal decline of sensitivity with age using a modified t-test. The t-statistic, T'_{b_j}, representing the difference between the slope of the normal decline in sensitivity with age and that due to the disease process over time was calculated using the equation:

$$T'_{b_j} = \frac{\left(b_j - b'_j \right) \left(\sqrt{\sum_{i=1}^{i=n} \left(t_i - \bar{t} \right)^2} \right)}{s_{z_j}} \qquad \text{Eq. (6.4)}$$

where b_j' is the normal deterioration of sensitivity with age at the given location j. The normal values utilised to calculate the slopes of the age-decline in sensitivity were calculated from the normal database incorporated in the STATPAC software. The database was provided by Humphrey Instruments. A subset of the database has been published by Heijl et al (1987) (Heijl et al. 1987a). These procedures are methodologically equivalent to, but not computationally identical with, the regression of MD against time (Heijl et al. 1987b). The statistics T_{b_j} and T_{b_j}' assume that $\tilde{u}_j$ is normally distributed with a mean of zero and a constant variance and is independent of the value of the independent variable, t.

6.3.4. Analysis.

The STATPAC 2 printouts of the univariate linear regression analysis of MD against time to follow-up and of the GCPA were obtained for each patient directly from the instrument. The GCPA compares the result of any given examination with the mean of two stipulated baseline fields. In order to provide a comparable outcome, the baseline fields were designated as the first two in the series of fields utilised by the ULR analysis.

The HFA data were then converted from the HFA formatted diskettes to a DOS format and analysed by a series of custom designed software modules on an IBM compatible PC (Cassidy & Flanagan 1989). The pointwise univariate linear regression was one such module and was labelled regress.exe. The two stimulus locations directly above and below the blindspot were omitted from the analysis. In cases where patients had been examined with both Programs 30-2 and 24-2 over the follow-up period, the Program 30-2 fields were converted to the Program 24-2 format. The regress.exe file had two modes of operation. First, the absolute sensitivity at each stimulus location was regressed against the time to follow-up and the regression line fitted by the method of least squares. Second, the unweighted pattern deviation at each stimulus location was calculated as a measure of the deviation of sensitivity from that of a normal subject, standardised across the whole field. The pattern deviation at each stimulus location was then regressed against time to follow-up and the regression line

fitted by the method of least squares. The mean value of sensitivity was taken at any stimulus location for which the sensitivity had been determined twice.

The ULR of absolute sensitivity against time to follow-up identified four categories of slope. A Type I slope was considered to result from a stable sensitivity: the slope was negative and statistically different from zero ($p<0.05$) but did not deteriorate at a rate greater than that of the normal decline of sensitivity with age. A Type II slope was considered to result from a true deterioration due to the disease process: the slope of the regression line was negative, significantly different from zero and the decline of sensitivity was greater than that due to age. A Type III slope resulted from an improvement in sensitivity: the slope of the regression line was positive and significantly different from zero. A Type IV slope indicated that the function of sensitivity against follow-up time could not be described by ULR: the slope of the regression line was either negative or positive and was not significantly different from zero. A stimulus location at which the sensitivity exhibited the same value throughout the series of visual field examinations manifested a mathematically indeterminate regression coefficient. These locations were categorised as a Type I location, i.e. clinically stable.

To assist in the clinical evaluation of the severity of any deterioration in sensitivity, the Type II locations were further tested to determine whether the regression slopes differed significantly from 2.5, 5 or 10 times the magnitude of the normal decline of sensitivity with age. Such an approach was an empirical expression and was intended to be a clinical reference only (Figure 6.3).

The pattern deviation values incorporate a correction for age; therefore the derived slopes were only required to be tested as to whether they were statistically different from zero. This was achieved in an identical manner to that of the absolute sensitivity. ULR of the pattern deviation was categorised three types of slope. Type II slopes were considered to result from a deterioration due to the disease process. Similar to that of the absolute sensitivity, Type III locations resulted from an improvement in the pattern deviation: the slope of the regression

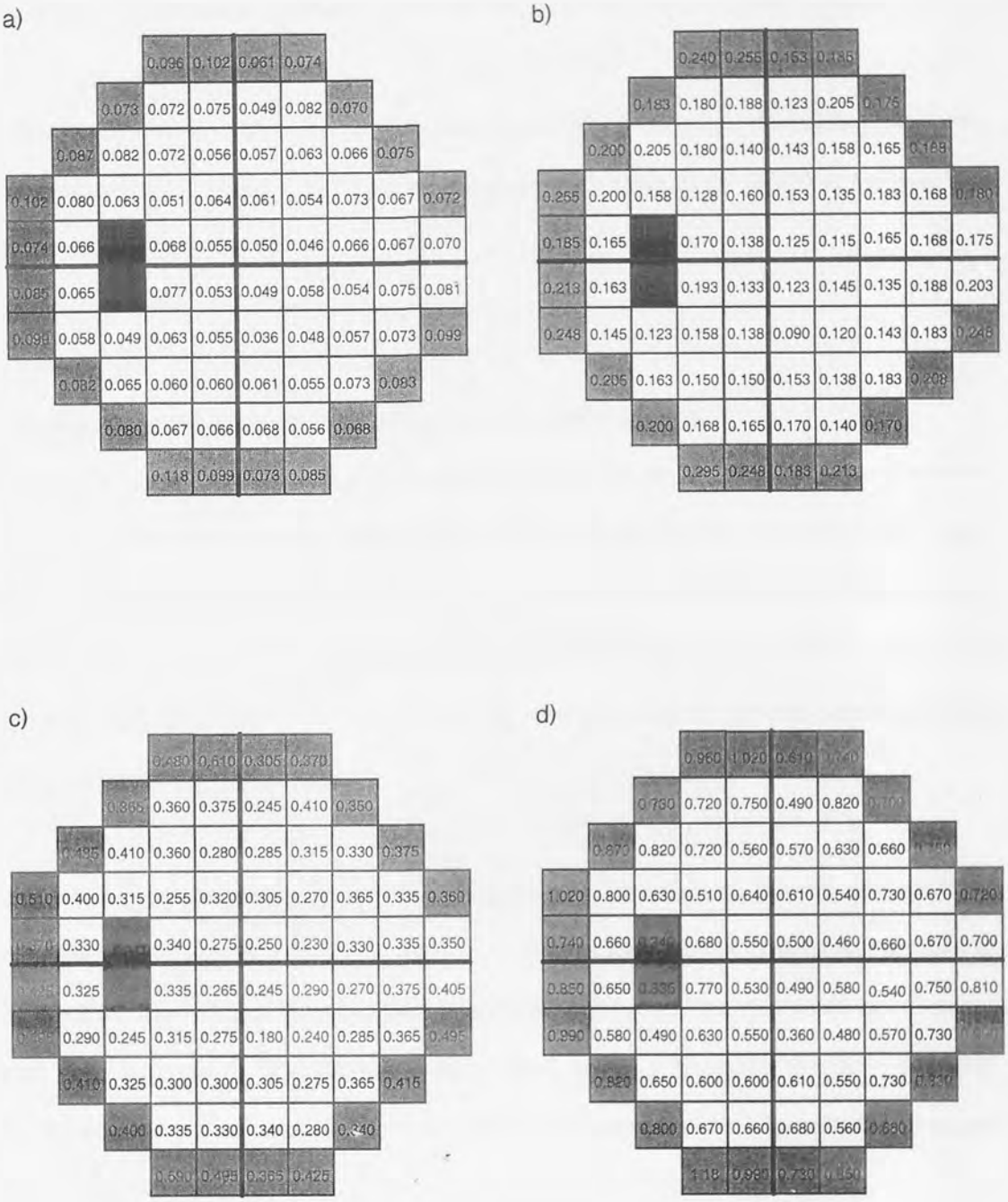

Figure 6.3. Loss of sensitivity (dB/year) at each stimulus location is illustrated for a) the normal rate of decline in sensitivity with age, b) 2.5 times, c) 5 times and 10 times the normal rate of the decline in sensitivity with age. Based upon data from: *Heijl et al (1987). Arch Ophthalmol. 105:1544.*

line was positive and statistically different from zero. A Type IV slope resulted from either a positive or negative regression coefficient that was, statistically, not significantly different from zero. A Type IV slope classification also incorporated those stimulus locations exhibiting a value of zero for the pattern deviation across all the visual field examinations in the series.

The results generated by the ULR of absolute sensitivity and of pattern deviation against time to follow-up were compared at each stimulus location with those of the GCPA at the final field of the series for each patient.

6.4. Results.

6.4.1. Regression of absolute sensitivity against follow-up time.

Four patients showed statistically significant MD slopes: two deteriorated and two improved. Of the two patients manifesting a significantly deteriorating MD slope, one patient (MD slope -0.59 ± 0.50 dB/yr; $p<0.05$) exhibited 6 Type I (ie. stable) locations, 24 Type II (ie. deteriorating) locations and 22 Type IV (ie. non-fitted) locations whilst the other (MD slope -0.82 ± 0.28 dB/yr; $p<0.01$) had 12 Type I, 22 Type II and 18 Type IV locations. Neither patient exhibited any Type III (ie. improving) locations.

The outcome of the slope at each stimulus location for the 34 glaucoma patients who exhibited non-significant MD slopes is shown in Table 6.1. The glaucoma patients exhibited a mean of 2.9 Type II (ie deteriorating) locations per patient and 46.7 Type IV (ie. non-fitted) locations per patient from the total of 52 available Program 24-2 stimulus locations. Similarly, the OHT patients exhibited a mean of 0.3 Type II locations per patient and 49.7 Type IV locations per patient (Table 6.1).

Fifteen of the 34 patients exhibited one or more clusters of at least two adjacent deteriorating (Type II) stimulus locations (comprising a total of 81 locations). Within this subcategory of 15 patients, the mean number of Type II locations per patient was 5.4 (Table 6.1). Approximately 60% of the Type II locations exhibited a decline in sensitivity within five times that of the

SLOPE TYPE	GLAUCOMA		OCULAR HYPERTENSION
	TOTAL SAMPLE (n=34) (Non-significant MD slope)	SUB-SAMPLE (n=15/34) (Two or more clustered, deteriorating locations)	TOTAL SAMPLE (n=12) (Non-significant MD slope)
	Mean (SD)	Mean (SD)	Mean (SD)
TYPE I	1.0 (1.9)	2.3 (4.3)	0.8 (1.4)
TYPE II	2.9 (3.7)	5.4 (2.4)	0.3 (0.7)
TYPE III	1.4 (2.8)	1.8 (3.8)	1.2 (1.5)
TYPE IV	46.7 (5.5)	42.5 (5.8)	49.7 (2.0)

Table 6.1. The mean incidence per patient of the four types of slope against time to follow-up for the 34 glaucoma patients and 12 ocular hypertensive patients who exhibited a non-significantly deteriorating MD slope. The corresponding data for the sub-sample of 15 glaucoma patients who each exhibited one or more clusters of at least two adjacent deteriorating (Type II) stimulus locations.

normal age-decline (Table 6.2). The magnitude of the slope was largely independent of sensitivity (R^2=0.201) (Figure 6.4). The locus of the Type II locations was more prominent in the inferior field compared to their mirror image locations in the superior field (p=0.017) (Figure 6.5). None of the OHT patients exhibited one or more clusters of two deteriorating locations by ULR of sensitivity against time to follow-up.

The results of the ULR in the subgroup of 15 glaucoma patients exhibiting one or more clusters of at least two adjacent deteriorating (Type II) stimulus locations compared to those for the GCPA analysis are shown in Table 6.2. Thirty-six of the 81 Type II locations were identified as deteriorating by both ULR and GCPA; the remaining 45 Type II locations were identified by ULR alone. The majority of the locations at which only the ULR identified deterioration tended to exhibit slopes which lay within five times of the normal decline in sensitivity (Table 6.2). The GCPA identified 63 stimulus locations (in 12 of the 15 patients) (mean 5.3 locations per patient; SD 4.9) as deteriorating which were not identified by ULR analysis. Of these 12 patients, 6 exhibited two or more clustered deteriorating locations by GCPA. Fifty-four of the 63 deteriorating locations identified by GCPA, alone, were adjacent to Type II locations identified by ULR and involved all 12 patients.

The ULR analysis and GCPA both identified 42 Type III locations (ie. improving). Six Type III locations were identified by ULR analysis, alone, and 21 locations were identified by GCPA alone. The Type III locations identified by GCPA alone involved six patients (mean 3.5 locations per patient; SD 4.2). Of these six patients, three exhibited a clustered pair of improving locations.

The remaining 19 patients from the sample of 34 glaucoma patients did not exhibit Type I locations by ULR. Of the 18 isolated Type II locations by ULR, 11 were also identified by GCPA (Table 6.3). Eleven patients exhibited 38 deteriorating locations by GCPA alone (mean 3.5 locations per patient; SD 1.6). Of these 11 patients, six exhibited a cluster of two or more deteriorating locations identified by GCPA. Three of the six patients exhibited either a single or

ANALYSIS	GLAUCOMA SUB-SAMPLE (n=15/34) (Two or more clustered, deteriorating locations)						
	TYPE I	TYPE II TOTAL	MAGNITUDE OF TYPE II SLOPES >AGE	≥2.5x	≥5x	≥10x	TYPE III
ULR and GCP	7	36	8	10	10	8	42
ULR Only	27	45	12	19	9	5	6
GCP Only	0	63	-	-	-	-	21

Table 6.2. The incidence of Type I, II and III slopes identified by ULR of absolute sensitivity against time to follow-up and by GCPA, together with the magnitude of the slope of the Type II locations for the sub-sample of 15 glaucoma patients.

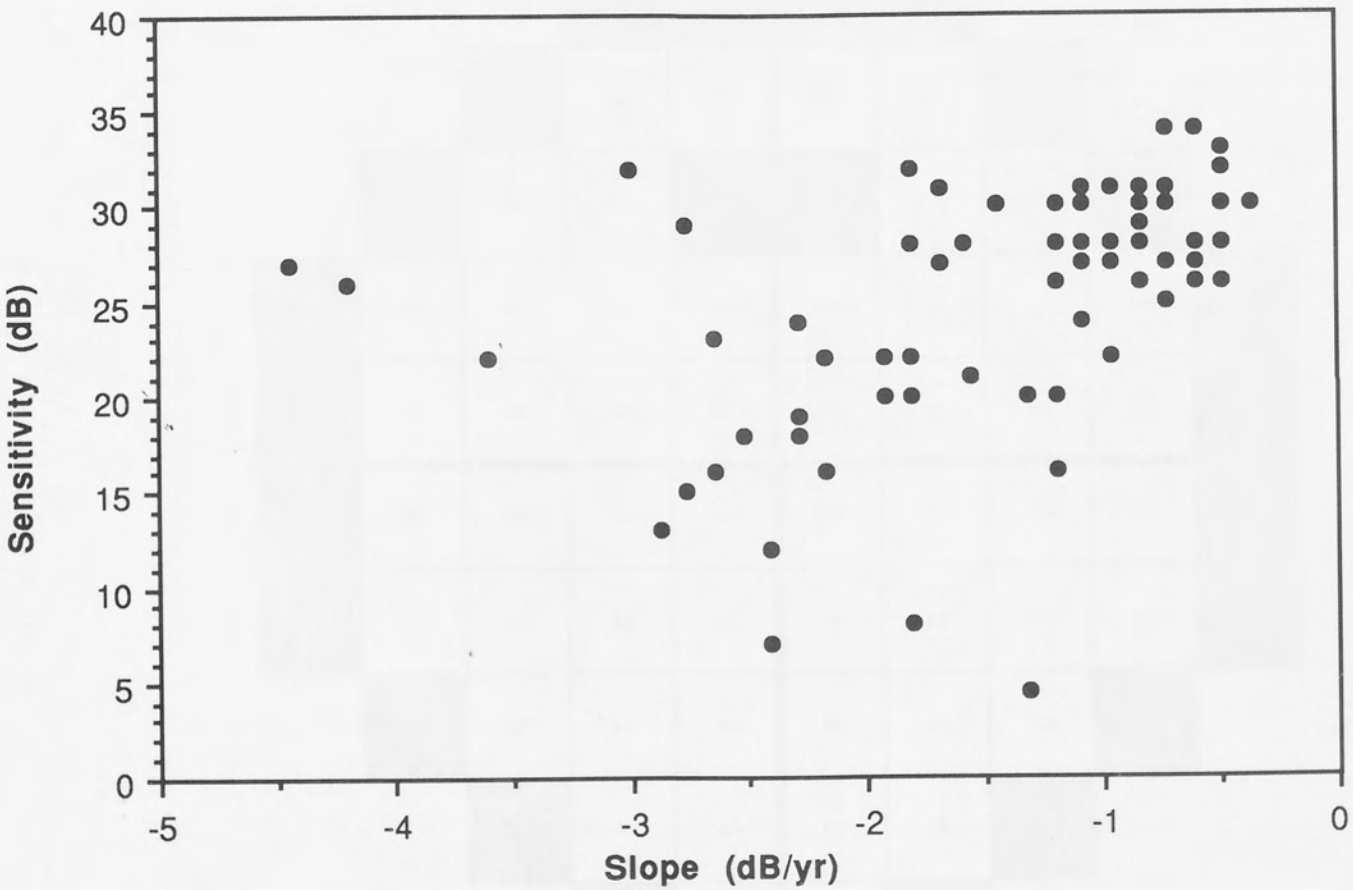

Figure 6.4. The absolute sensitivity (dB) against the slope (dB/yr) for the 81 locations deteriorating at a rate greater than the normal age-related decline in sensitivity (Type II slope). Sensitivity is arbitrarily illustrated for the third examination of the given series.

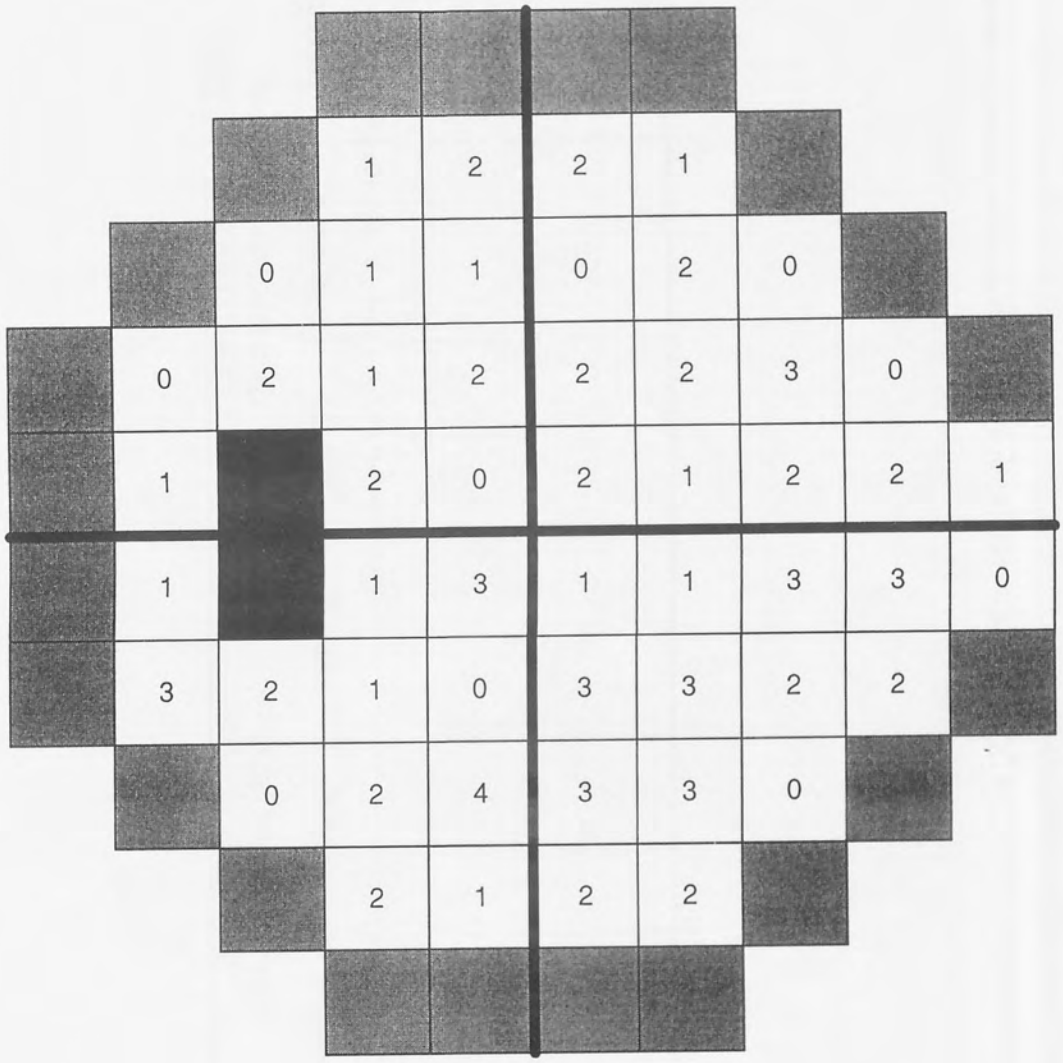

Figure 6.5. The locus of the Type II locations identified by regression of the absolute sensitivity against time to follow-up in the fifteen glaucoma patients with two or more adjacent deteriorating locations.

ANALYSIS	GLAUCOMA (n=19/34) (Non-significant MD slope)			OCULAR HYPERTENSIVE (n=12) (Non-significant MD slope)		
	TYPE I	TYPE II	TYPE III	TYPE I	TYPE II	TYPE III
ULR and GCP	0	11	20	3	4	14
ULR Only	0	7	7	7	0	0
GCP Only	-	38	20	-	17	23

Table 6.3. The incidence of Type I, II and III slopes identified by the ULR of absolute sensitivity against time to follow-up and by the GCPA for the 19 glaucoma and 12 ocular hypertensive patients exhibiting a non-significant MD slope.

a cluster of deteriorating locations adjacent to an isolated deteriorating location identified by ULR. Of the Type III locations, 20 were identified by both ULR and GCPA, 7 by ULR analysis, alone, and 20 by GCPA alone (Table 6.3). The improving locations identified by GCPA, alone, involved six patients (mean 1.8 locations per patient; SD 1.0). Five of the 19 patients exhibited a single cluster of two or more improving locations.

Of the ten stable locations (Type I) exhibited by the twelve OHT patients, 3 were identified by the GCPA. All four isolated Type II (deteriorating) locations were identified by GCPA (Table 6.3). Seventeen deteriorating locations (7 patients) were identified by the GCPA which were not identified by the ULR analysis. Of these 7 patients, four exhibited two separate clusters of two locations. In two patients, the clustered locations appeared adjacent to an isolated Type II location determined by ULR. All fourteen of the Type III locations identified by ULR analysis were identified by the GCPA (Table 6.3). GCPA identified 23 additional locations as improving. The twenty-three locations were dispersed across nine patients; three patients exhibited a cluster of two improving locations (Table 6.3).

6.4.2. The influence of the number and time-frame of the sequential examinations.

The types of slope derived from the complete series of fields compared to those obtained from the last six fields of the same series for 13 of the subgroup of 15 glaucoma patients exhibiting one or more clusters of at least two adjacent deteriorating (Type II) stimulus locations are shown in Table 6.4. The 13 patients were selected on the basis that all had undergone a minimum of eleven or more fields over a minimum follow-up of 6.0 years (mean 6.84 SD 0.59) and all had demonstrated a non-significant MD slope for the last six fields.

The mean number of Type I locations per patient identified by the last six fields was lower than that identified by the complete series of fields (Table 6.4). Both analyses each yielded 69 Type II locations (mean 5.3 per patient). However, of these 138 Type II locations only 10 locations were common to both analyses. These 10 locations manifested a continuous uniform decline in sensitivity. The 59 locations that exhibited a Type II slope for the complete series of fields,

SLOPE TYPE	GLAUCOMA SUB-SAMPLE (n=13/15) (Two or more deteriorating locations; 11 or more fields) REGRESSION SERIES	
	ALL FIELDS OF SERIES	LAST 6 FIELDS OF SERIES
	Mean (SD)	Mean (SD)
TYPE I	2.5 (2.5)	0.6 (0.7)
TYPE II	5.3 (4.6)	5.3 (5.5)
TYPE III	2.0 (4.0)	0.5 (0.9)
TYPE IV	42.2 (6.2)	45.6 (5.6)

Table 6.4. The mean incidence per patient of the four types of slope derived from the regression of absolute sensitivity against time to follow-up of all the fields of a series against that derived from the last six fields in the same series for 13 of the sub-sample of 15 glaucoma patients exhibiting two or more adjacent deteriorating (Type II) locations.

only, manifested an initial continuous linear decline in sensitivity which tended to plateau over the later examinations. This plateau tended to occur at sensitivities of approximately 6dB or less. The regression line based upon the complete series of fields exhibited a greater proportion of shallower/flatter slopes at these locations (ie less than 5 times the normal age-related decline in sensitivity) than that based upon the last six fields (Table 6.5). Conversely, the 59 locations at which a Type II slope was present for the last six fields, only, all exhibited a decline in sensitivity the rate of which increased over the later follow-ups. The regression line based upon the last six fields exhibited a greater proportion of steeper slopes (ie greater than 5 times the normal age-related decline in sensitivity) than that based upon the complete series of fields (Table 6.5).

A graphical modelling packeage (Tablecurve 2D, Jandel Scientific) was used to fit curvilinear functions based upon all fields in the series. The models were applied to each of the 59 locations at which the regression slope of the last six fields deteriorated at a greater rate than that for all the fields in the complete series. The goodness of fit for the best curvilinear function improved, on average, twofold compared to the linear function (Figure 6.6. Top). A similar approach was applied to the 59 locations which exhibited a slope greater than that for the normal age decline in sensitivity for all fields in the series only. The goodness of fit for the curvilinear function improved, on average, by one third (Figure 6.6. Bottom). Such improvements can be compared to the minimal improvement in the goodness of fit (1.6%) arising from the use of a curvilinear function to describe the sensitivities at the 10 locations at which the decline in sensitivity was present for both the last six fields and the entire series of fields.

The relationship of the GCPA to the slope derived from the complete series of fields and to the slope derived from the last six fields of the same series in the 13 patients from the subgroup of 15 exhibiting one or more clusters of at least two adjacent deteriorating (Type II) stimulus locations is also shown in Table 6.5. The GCPA detected 35 of the 59 locations which exhibited a Type II slope for the complete series of fields. The magnitudes of the Types II

REGRESSED FIELDS IN SERIES	GLAUCOMA SUB-SAMPLE (n=13/15) (Two or more deteriorating locations; 11 or more fields) DETECTED BY GCP					GLAUCOMA SUB-SAMPLE (n=13/15) (Two or more deteriorating locations; 11 or more fields) NOT DETECTED BY GCP				
	TOTAL	>AGE	≥2.5x	≥5x	≥10x	TOTAL	>AGE	≥2.5x	≥5x	≥10x
ALL	**35**	7	9	12	7	**24**	4	15	4	1
LAST 6 FIELDS	**18**	0	2	4	12	**41**	5	12	14	10
ALL & LAST 6 FIELDS	**8**	2	2	3	1	**2**	2	0	0	0
All	4	1	2	0	1	2	2	0	0	0
Last 6	4	1	0	3	0	0	0	0	0	0

Table 6.5. The magnitude of the slope of the deteriorating (Type II) locations derived from the regression of absolute sensitivity against time to follow-up all the fields in a series against that derived from the last six fields in the same series for 13 of the sub-sample of 15 glaucoma patients.

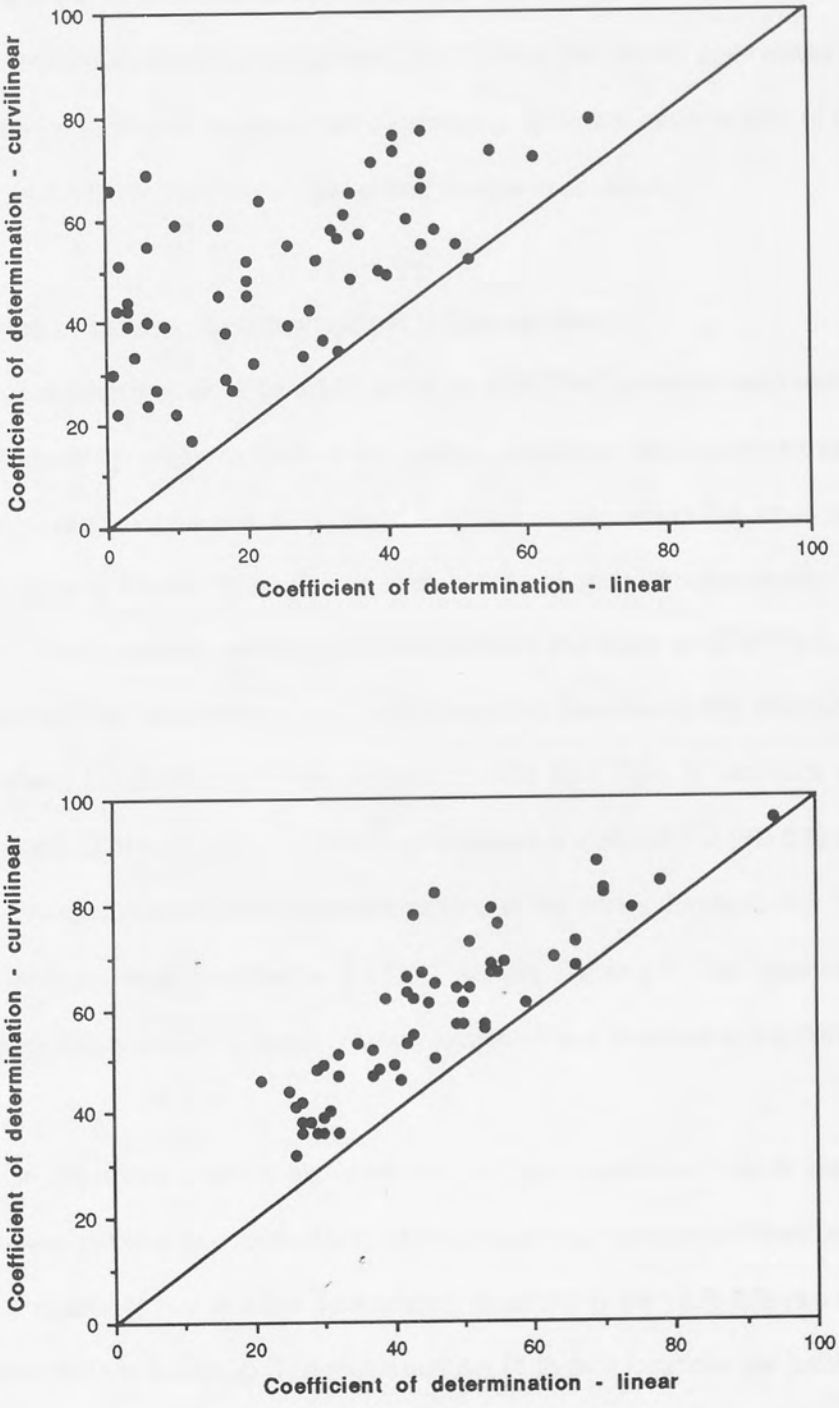

Figure 6.6. The relationship between the coefficient of determination (R^2) derived from a curvilinear function and that derived from univariate linear regression of sensitivity against follow-up time for the 59 stimulus locations deteriorating over the last six fields (top) and the entire series of fields (bottom).

slopes were distributed approximately evenly across these 35 locations. Conversely, the analysis failed to detect 24 locations exhibiting Type II slopes; of these, 19 locations manifested slopes within 5 times the normal age-related decline in sensitivity. The GCPA detected only 18 of the 59 locations which exhibited a Type II slope for the last six fields alone; of these, 16 locations manifested slopes greater than 5 times the normal age-related decline in sensitivity. Of the remaining 41 locations not detected by GCP, the majority (36) of the slopes were greater than 2.5 times the normal age-related decline in sensitivity.

6.4.3. Regression of pattern deviation against follow-up time.

The two patients exhibiting a significant MD slope by STATPAC analysis each exhibited one Type II (ie. deteriorating) slope by ULR of the pattern deviation. One patient exhibited three Type III (ie. improving) slopes and 48 Type IV (unfitted) slopes whilst the other exhibited 5 Type III and 46 Type IV slopes. The outcome of the slopes at each stimulus location for the 34 glaucoma and 12 OHT patients exhibiting a non-significant MD slope by STATPAC analysis is shown in Table 6.6. The mean number of Type II locations identified in the glaucoma sample was 1.8 per patient. In addition, 0.1 Type III locations and 50.1 Type IV locations per patient were also identified. Of the 50.1 Type IV stimulus locations a mean of 1.2 (SD 5.5) per patient with a pattern deviation of zero for all the examinations in the series. Similarly, 0.3 Type II and 51.7 Type IV locations were identified in the OHT sample (Table 6.6). No Type III slopes or stimulus locations with a pattern deviation of zero across all examinations in the OHT sample.

Seven of the 34 glaucoma patients exhibited one or more clusters of two or more Type II locations. All seven patients had formed part of the original sub-sample of fifteen patients who had exhibited a cluster of two or more deteriorating locations in the ULR analysis of absolute sensitivity against time to follow-up. The mean number of Type II locations per patient was 5.7 (SD 3.6). No Type III slopes were identified in this sub-sample of seven patients.

SLOPE TYPE	GLAUCOMA		OCULAR HYPERTENSION
	TOTAL SAMPLE (n=34) (Non-significant MD slope)	**SUB-SAMPLE (n=7/34)** (Two or more clustered, deteriorating locations)	**TOTAL SAMPLE (n=12)** (Non-significant MD slope)
	Mean (SD)	**Mean (SD)**	**Mean (SD)**
TYPE II	1.8 (2.5)	5.7 (3.6)	0.3 (0.7)
TYPE III	0.1 (0.3)	0	0
TYPE IV	50.1 (5.5)	46.3 (3.4)	51.7 (0.9)

Table 6.6. The mean incidence per patient of the three types of slope of the pattern deviation against time to follow-up for the 34 glaucoma patients and 12 ocular hypertensive patients who exhibited a non-significantly deteriorating MD slope. The corresponding data for the sub-sample of 7 glaucoma patients who each exhibited one or more clusters of at least two adjacent deteriorating (Type II) stimulus locations.

The total of 40 deteriorating locations identified across the seven patients by ULR of the pattern deviation, contrasts with 81 deteriorating locations identified by ULR of the absolute sensitivity across all patients in the sub-sample of 15. Twenty-one Type II locations were common to both the absolute sensitivity and the pattern deviation regression analysis. A comparison with the age related decline in the absolute sensitivity at those locations common between the two analyses is shown in Table 6.7.

Of the 40 locations identified by regression of the pattern deviation, 16 were identified as deteriorating by the GCPA. All but one of these 16 locations were also identified by the ULR of the absolute sensitivity against time to follow-up. The GCPA alone identified 24 locations as deteriorating in these seven patients. The Venn diagram in Figure 6.7 illustrates the agreement between the outcome of the pattern deviation ULR analysis, the absolute sensitivity ULR analysis and the GCPA.

6.4.4. The influence of the number and time-frame of the sequential examinations.

The comparison of the pattern deviation ULR between all fields and the last six fields was undertaken on the original 13 patients who had eleven or more fields in their series. The pattern deviation ULR identified two or more clustered Type II (deteriorating) stimulus locations in eight patients (comprising 39 deteriorating locations in total). The mean and standard deviation of each type of slope for these eight patients is shown in Table 6.8. The remaining five patients did not exhibit any deteriorating locations by ULR of pattern deviation against follow-up time.

Two patients exhibited a cluster of two deteriorating stimulus locations in the pattern deviation ULR against time to follow-up for all fields and for the last six fields. All four of these locations were also identified by the ULR of absolute sensitivity against time to follow-up of the last six fields. The Venn diagram in Figure 6.8 illustrates the 39 Type II slopes for the pattern deviation ULR of the last six fields against time to follow-up across six patients that were also identified by the absolute sensitivity ULR analyses and the GCPA. All of the stimulus locations identified

MAGNITUDE OF SLOPE BY REGRESSION OF ABSOLUTE SENSITIVITY	NUMBER OF TYPE II LOCATIONS BY REGRESSION OF PATTERN DEVIATION
>AGE	2
>2.5 x AGE	6
>5 x AGE	6
>10 x AGE	7

Table 6.7. The magnitude of the slope by univariate linear regression of absolute sensitivity against time to follow-up (entire series of fields) at those stimulus locations also classified as deteriorating (Type II) by regression of the pattern deviation against time to follow-up.

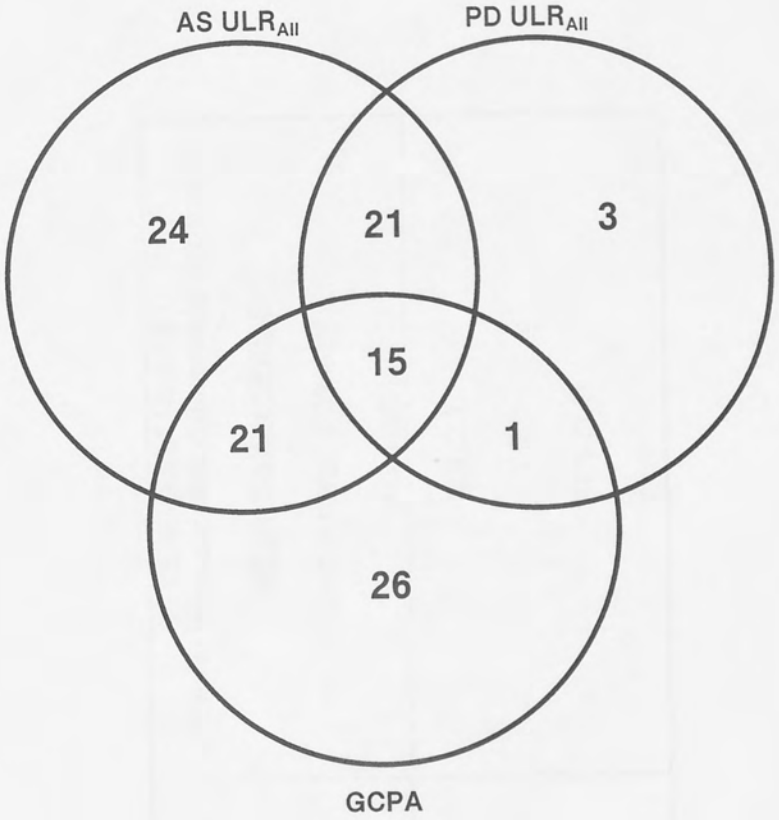

Key:	
AS ULR$_{All}$	Absolute sensitivity ULR of all fields in a series against time to follow-up
PD ULR$_{All}$	Pattern deviation ULR of all fields in a series against time to follow-up
GCPA	Glaucoma Change Probability Analysis

Figure 6.7. The Venn diagram illustrates the number of progressing stimulus locations detected by the absolute sensitivity ULR analysis, the pattern deviation ULR analysis and the GCPA over time to follow-up.

SLOPE TYPE	GLAUCOMA (n=8/13) (Two or more clustered deteriorating locations) REGRESSION SERIES LAST 6 FIELDS OF SERIES Mean (SD)
TYPE II	4.9 (2.3)
TYPE III	0
TYPE IV	47.1 (3.1)

Table 6.8. The mean incidence per patient of the three types of slope derived from the univariate linear regression of the pattern deviation against time to follow-up of the last six fields in each series of eight patients who had exhibited two or more deteriorating (Type II) stimulus locations.

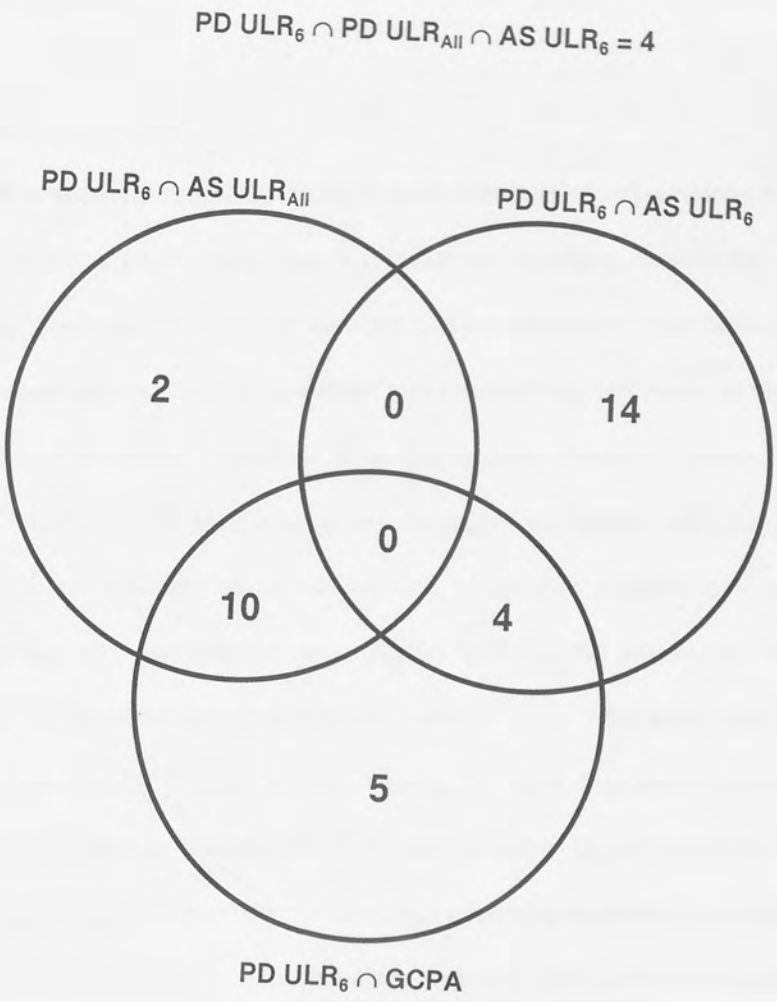

Key:	
$PD\ ULR_6$	Pattern deviation ULR of last six fields in a series against time to follow-up
$PD\ ULR_{All}$	Pattern deviation ULR of all fields in a series against time to follow-up
$AS\ ULR_6$	Absolute sensitivity ULR of last six fields in a series against time to follow-up
$AS\ ULR_{All}$	Absolute sensitivity ULR of all fields in a series against time to follow-up
GCPA	Glaucoma Change Probability Analysis

Figure 6.8. The Venn diagram illustrates the number of progressing locations detected by both of the absolute sensitivity ULR analyses against time to follow-up and by the GCPA of the 39 Type II slopes (eight patients) identified by ULR of the pattern deviation against time to follow-up of the last six fields in a series.

by the pattern deviation ULR of the last six fields against time to follow-up were identified by at least one other analysis.

6.5. Discussion.

The use of ULR to estimate the parameters of large numbers of two-variable models such as that presented in the current study has a number of statistical drawbacks. The classical regression model assumes that the time variable, t, is independent in that there is no statistical association between subsequent measurements of the variable. However, at any given stable stimulus location, it is highly likely that a temporal dependency is present and that the sensitivity derived at a given examination will be highly correlated with that at a previous examination. Such an outcome would violate one of the basic tenets of linear regression theory. Furthermore, although there is no reason to question the assumption of symmetry in the underlying hypothetical error distribution, there is a possibility that the level of measurement error may be of such a magnitude as to mask any two significant differences between the regression coefficients. Such criticisms relate to the outcome at any single location. Any such temporal dependency should not affect the mathematical expectation of the regression estimates but would merely influence their precision. An alternative to the use of standard classical regression techniques might profitably involve bootstrapping (ie. resampling with small sample reuse techniques) the regression estimates to obtain empirical error measurements. Such a procedure would not then rely upon the validity of the classical regression model. However, traditional time series analysis frequently employs the use of regression methods to fit trend lines where similar theoretical limitations exist and, since the technique produces acceptable results, the application of the procedure to visual field progression in this respect can be justified.

It is possible that a further violation occurs when the visual field is evaluated as a whole since the sensitivities between adjacent stimulus locations at any given examination are likely to be highly correlated (Lachenmyer et al. 1994). As with the temporal dependency, the existence of any spatial intercorrelations will only affect the precision of the regression estimates and not

their expected values. An additional violation might result from the interaction of the temporal and spatial dependency. As confidence limits are not used for estimation or prediction purposes, the validity of the procedure should not be in doubt. Nevertheless, given the influence of the temporal and spatial dependencies together with their potential interaction effect on the 52 individual regressions, the use of a multivariate model would seem more apposite. Indeed, the presence of the spatial correlation has been used to advantage in the topographical component of the multivariate linear regression approach (Wild et al. 1993; Chapter 7).

6.5.1. Regression of absolute sensitivity against time to follow-up.

The study illustrates the inability of the regression of the summary index MD to define localised change in sensitivity. The findings demonstrate that even clusters of statistically significant deteriorating locations are overlooked by MD slope analysis. Furthermore, of the two cases which exhibited significantly deteriorating MD slopes, both manifested at least 20 individually significantly deteriorating locations by ULR. These latter findings are in agreement with those of others that the regression of MS and MD against time to follow-up is a poor indicator of visual field progression (Birch et al. 1995; Chauhan et al. 1990; O'Brien & Schwartz 1990; O'Brien et al. 1991; Werner et al. 1988b).

The majority of the stimulus locations exhibited a slope which could not be distinguished from zero. This could imply that the follow-up time in the present study of six years is insufficient to identify the normal age-related decline in sensitivity or that the statistical criteria by which the regression slopes are fitted were too stringent and are inappropriate for the inherent variability present in visual field measurements. Indeed, the within-test variance at each stimulus location ie. the local short-term fluctuation (SF) undoubtedly hinders the identification of any underlying deterioration in sensitivity. An increased within-test local variability (SF) may arise as a precursor to established field loss (Flammer et al. 1984a; Flammer et al. 1984b). It is also present at locations of reduced sensitivity and of increasing stimulus eccentricity (Flammer et al. 1984a; Flammer et al. 1984b). The influence of the local SF could be reduced by increasing

the number of examinations within the given time-frame. However, the adverse effect of the SF only decreases by the square root of the number of additional examinations. The logistical expediency of numerous additional examinations within this time-frame is therefore questionable. However, image processing techniques (Crabb et al. 1995; Fitzke et al. 1995) have been proposed for reducing the influence of the local SF (O'Brien & Wild 1995). Such a manipulation of the within-test variance, with the inevitable reduction of the between-test variance, will consequently mask some real local change, particularly episodic deterioration, in spite of enhancing the apparent utility of ULR. This potential masking effect must be considered in relation to the number of locations that cannot be modelled (Type IV). There is an advantage to knowing the locations that cannot be modelled prior to a smoothing procedure being applied. The masking effect must also be considered in relation to an outcome based solely upon the total fields in a given series. An episodic change at a given location manifested only at the final two fields of the series would have a profound effect on the slope derived from the final six fields, would have a lesser effect on the slope derived from all fields and an even lesser effect on a smoothed data set. As the time-frame lengthens for a given patient and assuming the decay is linear, the ULR technique theoretically becomes more useful in that the influence of the within-test error is reduced with the greater number of examinations.

Three of the 15 patients who exhibited clustered deteriorating locations also exhibited clustered improving locations. This outcome has also been found in other pointwise regression analyses (O'Brien & Schwartz 1993) and indicates that improvement can coexist with progressive loss. Clearly, this finding is likely to be an artefact arising from the local short-term fluctuation; an unrepresentative low value of sensitivity is obtained for the initial fields. Subsequently, more consistent estimates of the sensitivity are obtained which results in a positive slope. At those stimulus locations exhibiting deterioration, the progressive loss in sensitivity is of greater magnitude than the local short-term fluctuation and, consequently, reduces its influence on the outcome of the slope analysis.

The decline in sensitivity of the normal eye with increasing age varies as a function of stimulus location and lies between approximately 0.04 and 0.12 dB/year (Figure 6.3.) (Heijl et al. 1987a). This variation across the field steepens the hill of vision with increase in age. Previous studies which have utilised pointwise ULR have not accounted for age in the definition of visual field progression (Birch et al. 1995; Hitchings et al. 1994; Noureddin et al. 1991). If the criteria for progression were to be defined purely as a slope that is statistically different from zero, then the Type I locations in the current study would be classified as deteriorating. From the ratio of the number of Type I to Type II locations in the current study, it would appear that approximately 25% of the locations designated as deteriorating in other studies may in fact have been decaying within the normal age-decline in sensitivity.

Some studies have introduced a constraint on the presence of a significantly deteriorating slope in that the slope is required to be significantly different from zero and to be deteriorating at a rate greater than -0.1dB per month (Baez et al. 1995; Birch et al. 1995) or, alternatively, -0.2dB per month (Hitchings et al. 1994; Noureddin et al. 1991). However, this constraint does not account for the variation in the age-related decline in sensitivity across the field. The criterion for abnormality of -0.1dB and -0.2dB deterioration per month are at least 10 and 20 times, respectively, the maximum rate for the age-related decline at any given location in the central visual field (Heijl et al. 1987a) and must, as a consequence, only provide an indication of relatively severe visual field progression. The current study identified 68 locations by ULR analysis that deteriorated at a rate between that due to age and that of 10 times the rate of age and 13 locations were deteriorating at a rate of at least 10 times the rate of age (Table 6.2). Sixty-eight of the 81 locations in the current study would be classified as stable if the criteria of Birch et al (1995) and Baez et al (1995) were adopted and 75 of the 81 as stable if that of Noureddin et al (1991) and Hitchings et al (1994) were utilised.

A comparison of the change in absolute sensitivity against follow-up time with the change in sensitivity with age could have been achieved by the regression of the total deviation against follow-up time. This approach, however, would preclude any comparison with other ULR

studies. In addition, the total deviation regression slope could not describe the magnitude of the difference between the rate of change in absolute sensitivity due to the disease process and that due to age against follow-up time. In addition, the GCPA utilises absolute values of sensitivity to determine change from the baseline fields.

The use of a criterion of one or more clusters of at least two adjacent deteriorating stimulus locations was utilised to reduce the possibility of emphasis being erroneously placed on a stimulus location which exhibited a statistically significant slope due to chance. Indeed, for a 95% confidence limit, it would be expected that two or three of the 52 stimulus locations analysed in Program 24-2 would exhibit a statistically significant slope due to chance. However, it would be extremely unlikely that such slopes occurring due to chance would arise at adjacent locations. In addition, the slopes associated with any chance findings would be more likely to be significantly different from zero rather than different from the normal age-decline in sensitivity. Techniques which only classify abnormality as being different from a slope of zero therefore have a far higher risk of producing erroneous results due to chance. Those studies utilising simple, empirical criteria of a loss of sensitivity between examinations also advocate that two contiguous locations should be considered clinical deterioration (AGIS 1994; Schulzer 1994). The statistical significance of the trend in decay of sensitivity both augments the empirical criteria and enables significant decay to be determined at an earlier stage.

6.5.2. Comparison of absolute sensitivity ULR with GCPA outcome.

The results of ULR were compared to existing methods for establishing change within the visual field rather than to any change in structural abnormality since the relationship between the appearance of the optic nerve head and the nature of the glaucomatous visual field loss at any single examination is tenuous (Airaksinen et al. 1985b; Airaksinen et al. 1985c; Airaksinen et al. 1985d; Funk et al. 1988; Sommer et al. 1991). Furthermore the relationship between changes in the optic nerve appearance and changes in the extent of the visual field loss is

equally tenuous, particularly in early stage glaucoma (Birch et al. 1995; Funk 1991; Zeyen & Caprioli 1993).

The relationship between the ULR and the GCPA at any given stimulus location is a complex interaction of the quality of the collected data, the magnitude of the baseline sensitivity, the extent and type of the subsequent visual field progression, and of the position of the fields within the examination series. As would be expected, locations that exhibited a Type I slope (ie that which was less than or equal to the normal rate for age) were not generally identified by GCPA. ULR identified a higher frequency of locations than GCPA in those cases where the slope was within 5 times the normal decline with age. The agreement between the two techniques was more apparent for the steeper slopes. Conversely, the GCPA identified progression in a substantial number of cases where the regression slope could not be fitted (Type IV slopes). GCPA is dependent upon the magnitude of sensitivity; the range of test-retest variation in stable glaucoma is proportionately large at locations exhibiting moderate loss and smaller at locations of either high or low sensitivity (Heijl et al. 1989). In addition, the GCPA is more susceptible to random fluctuations in sensitivity which are smoothed by fitting a least squares univariate regression line. The technique of ULR is based upon the description of trend. At locations of high baseline sensitivity, ULR is clearly capable of modelling a progressive decline in sensitivity the reduction of which lies inside the range of the pointwise test-retest variability encountered. Indeed, it has been observed that ULR of mean sensitivity is more able to determine a trend in sectors of the visual field with higher sensitivity (O'Brien et al. 1991). With steeper slopes, the reduction in sensitivity generally lies outside the test-retest variation in sensitivity; the location is identified as abnormal by GCPA and there is good agreement between the two techniques of analysis. At locations exhibiting a moderate reduction in baseline sensitivity, only steeper gradients are detected by GPCA since the associated reduction in sensitivity has to be proportionately greater to lie outside the wider range of the test-retest variation. The agreement between the two techniques at stimulus locations exhibiting a moderate reduction in sensitivity is influenced by the degree of local SF and the number of examinations to which the regression line is fitted. Similar to the GCPA,

ULR analysis will have difficulty determining progressive visual field loss at a location exhibiting high local SF. The influence of the high local SF will reduce as the number of examinations increases. The results would therefore suggest that pointwise ULR is better than GCPA in defining early deteriorations in sensitivity provided that the quality of the data is sufficient to permit the derivation of a regression slope which is significantly different from the normal rate for age.

6.5.3. The influence of the number and time-frame of the sequential examinations.

The discrepancy between the pointwise ULR for all fields in the given series compared with pointwise ULR of the last six fields highlights the limitations of using a single mathematical function to describe the pattern of glaucomatous visual field progression occurring at each location across the visual field within a given patient. It is clear that since the type of progression differs across the field, and between patients, any trend analysis should attempt to describe all the various potential modes of glaucomatous visual field progression. Indeed, progression at a particular location or cluster of locations may be under or over-estimated by the relative stability of the locations pre- or proceeding, respectively, the more rapid phase of the deterioration. Clearly, the positioning of the sequence of fields and the number of fields selected within the series for a given patient assumes considerable importance in the identification of glaucomatous visual field progression by ULR. Recently, a complex polynomial function has been found to more suitable than linear regression for modelling the pointwise decline of sensitivity in normal tension glaucoma (McNaught et al. 1995). However, the lack of accuracy in the predictive power of the polynomial model suggests that the function describes the between-examination variation in sensitivity rather than the actual decline in sensitivity.

6.5.4. Regression of pattern deviation against time to follow-up.

Regression of the pattern deviation at each stimulus location against time to follow-up describes a change in sensitivity that is independent of both the height, and also the change in height, of the visual field. In this manner, the technique offers an expression of the change in localised visual field loss.

The fewer locations exhibiting statistically significant deterioration by ULR of the pattern deviation against time to follow-up in comparison to the ULR of absolute sensitivity against time to follow-up demonstrates the separation of progressive localised loss from that of progressive generalised loss. Indeed, the two patients exhibiting a significantly deteriorating MD slope each exhibited only one deteriorating stimulus location in pattern deviation ULR analysis compared with 24 and 22 in absolute sensitivity analysis. The incidence of Type III locations was also less in the pattern deviation analysis. Clearly, the presence of height in the regression analysis influences both the positive and negative slope directions. A surprising finding in the ocular hypertensive sample was the absence of stimulus locations exhibiting a zero pattern deviation across all fields. This can be attributed to increased local short-term fluctuation contaminating the calculation of the pattern deviation. However, the Type IV slope classification will necessarily include locations exhibiting low variability but with a trend of either decay or improvement which cannot be distinguished from zero.

Three theoretical permutations of progression can be identified by comparison of the outcome of the absolute and the pattern deviation ULR analyses. Agreement between the two analyses indicates a non-uniform reduction in the height of the visual field (ie. the height reduction is different between stimulus locations). Progression identified by the pattern deviation ULR analysis, alone, indicates a localised reduction in sensitivity that is different between locations. Stimulus locations identified as progressing by the absolute sensitivity ULR analysis, alone, show a more uniform deterioration in visual field height. From our results, the latter event would appear to occur twice as often as the other possible outcomes. However, the relatively large number of Type IV locations (ie. those that were not modelled) in the ULR analysis of absolute sensitivity against time to follow-up would indicate that this is outcome is greatly influenced by measurement inaccuracy.

6.5.5. Comparison of pattern deviation ULR with GCPA.

Just over half of the Type II stimulus locations identified by the pattern deviation ULR against time to follow-up were not identified by the GCPA. This represents a similar proportion to that

found in the absolute sensitivity ULR against time to follow-up. The majority of the stimulus locations identified by the pattern deviation ULR were also detected by the absolute sensitivity ULR analysis. A small number of stimulus locations exhibited a reduction in pattern deviation over time to follow-up which lay within the bounds of glaucomatous variability described by the GCPA database. This latter finding further supports the hypothesis that the ULR technique is able to detect small, but significant changes in sensitivity provided the data is of good quality.

6.5.6.The influence of the number and time-frame of the sequential examinations.

The ULR of the pattern deviation of the last six fields in any given series yielded a similar number of Type II slopes to that of the regression of the entire series of fields. However, only two patients exhibited a clustered pair of deteriorating stimulus locations which were common between the two analyses. These four locations exhibit a uniform rate of progressive localised loss. A differing outcome over each time frame indicates the presence of a curvilinear decline in sensitivity. The results show that the pattern deviation is more likely to exhibit decay that has a more rapid phase, either at the early fields or at the later fields.

6.5. Conclusions.

The study shows that ULR of absolute sensitivity and of pattern deviation, when corrected for stimulus eccentricity, was able to describe localised progression which was not manifested by the corresponding regression of the MD index. The combined use of ULR for an entire series of fields together with that based upon a moving time frame of the most immediate six fields provided a more appropriate description of the differing modes of deterioration across the visual field. The combination of the two techniques provides a tool by which the clinician can detect an episodic *and* a constant decline in sensitivity over time to follow-up. ULR techniques utilising the measured sensitivity which do not account for the effects of age and of eccentricity overestimate abnormality by as much as 25%. Similarly, those ULR techniques employing an arbitrary reference for deterioration underestimate the degree of deterioration.

In addition to differing rates of progression at an individual location across a visual field series, different configurations of progression also emerge. Deteriorating stimulus locations can exhibit change in sensitivity that principally affects the height and may, additional to or exclusive from a deterioration in height, also exhibit a localised loss. The delineation of a progressive localised reduction in height is, however, more susceptible to the influence of measurement error.

The differing relationships between both the absolute and pattern deviation ULR analyses and GCPA highlighted the complexity of delineating visual field progression. In cases of good quality data, the ULR technique identified visual field progression prior to that of the GCPA. Conversely, in cases where the data could not be fitted by ULR, the GCPA was capable of identifying progression. Until such time as the inherent variability associated with the visual field examination can be reduced, clinicians should be encouraged to utilise both GCPA and ULR for the delineation of visual field progression.

Chapter 7: Multivariate forecasting of visual field progression in glaucoma.

7.1. Introduction.

Progressive visual field loss in glaucoma is often only delineated by retrospective analysis of a series of visual fields (Chapters 5 & 6). The techniques employed to determine progression involve intuitive and/or statistical approaches. The statistical techniques utilise either descriptive statistics of the visual field as a whole or the sensitivity of the individual stimulus location. The efficiency with which the various techniques identify progressive loss is dependent upon many factors, including the patient reliability and the relatively slow rate of decline in sensitivity.

Pointwise methods of determining progressive loss are currently popular as the global visual field indices have proved insensitive to small amounts of localised change (Chauhan et al. 1990; Chapter 6). Univariate linear regression (ULR) has been widely espoused as a technique to retrospectively determine pointwise change in sensitivity (Chapter 6).

An alternative and novel approach to the identification of progressive visual field loss utilises a knowledge of the sensitivities at a given location derived from previous examinations to forecast the sensitivity at any given future examination.

The efficacy in forecasting the sensitivity at a stimulus location by ULR against time to follow-up has been compared with the corresponding outcome derived by complex polynomial, exponential, cubic and quadratic functions in normal-tension glaucoma (McNaught et al. 1995). The study selected 47 stimulus locations across 12 patients at which a 10dB change in sensitivity from the initial fields had occurred at the last two of a series of fifteen fields. The fifteen fields had been obtained over a mean time to follow-up of 5.7 years. The measures of sensitivity of the first five fields were then used to forecast the sensitivity at a time to follow-up of six years. Despite providing a better model of the decline in sensitivity over time than the pointwise ULR technique, complex polynomial functions did not accurately forecast the sensitivity at the final examination in the series. The pointwise ULR model showed an average

prediction error of 7dB and provided an adequate fit of the data in 25 of the 47 stimulus locations. The complex polynomial function, applied to a single stimulus location best described the variation in sensitivity between pairs of examinations.

A pointwise topographical and longitudinal model has been proposed to overcome the limitations of the pointwise ULR technique (Wild et al. 1993). The topographical component of the model related the sensitivity at each stimulus location to the sensitivity at the adjacent stimulus locations in terms of the respective stimulus co-ordinates. The longitudinal component utilised multiple linear regression to relate the sensitivity at a given location for a given field in terms of the sensitivity measured at that location in the preceding fields. In general, the coefficient of determination (R^2) of the topographical model decreased as the MD decreased and PSD increased. The R^2 of the modelled field utilising the composite topographical and longitudinal model increased as the number of examinations increased. The median and range of the percentage error between the modelled and measured sensitivity increased with an increase in eccentricity in fields with moderate and severe loss. The efficiency of the composite topographical and longitudinal model in forecasting the sensitivity at each stimulus location is unknown. In addition, the level of agreement between the composite model and existing techniques for determining pointwise progressive loss is also unknown.

7.2. Aims.

The aim of the study was firstly to develop the technique for utilising the topographical and longitudinal model to forecast glaucomatous visual field progression and secondly to compare the outcome with established methods for identifying progressive loss.

7.3. Methodology.

7.3.1. Normal subjects.

The sample comprised 23 normal subjects who had had four consecutive HFA Program 30-2 (stimulus size III) examinations, separated by a mean of 12.3 months (SD 1.0) and over a mean time to follow-up of 4.23 years (SD 0.1). Of these 23 subjects, eight had a further fifth

Program 30-2 examination separated from the fourth examination by a mean of 12.38 months (SD 0.9) and at a mean time to follow-up of 5.21 years (SD 0.1). All visual field examinations were carried out by a single perimetrist. The right eye of each subject was arbitrarily selected and the stimulus locations situated above and below the blind spot (+15,±3) were excluded from the analysis. The mean age of the normal subjects at the first examination was 42.70 years (SD 7.6). All subjects were ophthalmologically normal and had a distance visual acuity of 6/6 or better. The appropriate refractive correction was used for the viewing distance of the perimeter. The protocol for examination of the visual field was strictly followed and all fields were deemed to be reliable in terms of fixation losses and false-positive and false-negative responses. The probability maps of each series of fields were examined in order to confirm the absence of a marked learning effect.

7.3.2. Ocular hypertensive (OHT) and primary open angle glaucoma (POAG) patients.

Three patient samples were selected from 91 consecutive patients drawn from the database of the Glaucoma Service, Toronto Hospital (Western Division). All of the selected patients had a minimum of 9 visual field examinations with either Program 24-2 or 30-2 of the HFA using stimulus size III.

The first sample comprised 12 eyes from 12 untreated ocular hypertensive patients. The mean number of visual field examinations was 11.3 (SD 3.5) carried out over a mean period of 8.4 years (SD 2.3). The right eye of each subject was arbitrarily selected and the two stimulus locations situated immediately above and below the blind spot were excluded from the analysis. The first two visual field examinations of each patient were discarded in order to minimise learning effects. Five consecutive visual field examinations were then selected from each patient's series. The reliability of each of the selected examinations fell within normal limits in terms of the magnitude of fixation losses and false-positive and false negative responses. Each subject had a visual acuity of 6/9 or better over the five examinations. The mean age of the OHT sample at the first of the five visual field examinations was 51.48 years (SD 13.67). The mean time to follow-up was 3.15 years (SD 0.51) and the mean interval

between each of the five examinations was 7.55 months (SD 4.54; range 3.4 to 15.6 months). The group mean intraocular pressure over the five examinations was 20.2 mmHg (SD 2.8). The group mean MD at the first of the five examinations was +0.13 dB (SD 0.73; range -0.93 to 1.49 dB) and PSD was 1.85 dB (SD 0.46; range 1.34 to 2.96 dB).

The second sample of patients comprised 11 eyes from 11 POAG patients each exhibiting visual field progression over at least two consecutive Program 24-2 or 30-2 visual field examinations. Progression was determined by the same intuitive criteria defined in Chapter 5. The two or more visual fields exhibiting visual field progression were required to be preceded by at least four examinations yielding a stable sensitivity. The mean number of visual fields was 12.50 (SD 3.31) carried out over a mean period of 10.1 years (SD 4.8). Each eye was converted to the right eye format and the stimulus locations immediately above and below the blind spot were excluded from the analysis. Five consecutive visual field examinations were then selected from the eleven eyes such that the two or more visual fields exhibiting progression were preceded by two examinations of stable sensitivity. The mean number of visual field examinations preceding the series of five examinations in each of the eleven eyes was 6.2 (SD 2.3). The reliability of each of the selected examinations fell within normal limits in terms of the magnitude of fixation losses and false-positive and false negative responses. Each patient had a visual acuity of 6/12 or better over the five examinations. Cases of clinically significant cataract or of an ocular history other than glaucoma were excluded from the sampling process. In order to maintain a sufficiently large sample size, there were no exclusion criteria relating to the pharmacological or surgical control of the intraocular pressure. The mean age of the sample at the first of the five examinations was 59.26 years (SD 14.19). The group mean time to follow-up over the five examinations was 2.93 years (SD 1.03; range 1.83 to 4.3 years) and the group mean interval between each examination was 7.14 months (SD 2.5; range 4.08 to 10.56 months). The group mean intraocular pressure over the five examinations was 18.3 mmHg (SD 3.0). The group mean MD at the first of the five examinations was -5.29 dB (SD 3.01; range +0.97 to -9.28 dB) and PSD was 5.07 dB (SD 1.94; range 1.88 to 8.44 dB).

The third sample of patients comprised 11 eyes from 11 POAG patients with stable visual fields. All characteristics relating to the number of visual fields, the type of loss and the time of follow-up were matched as closely as possible to the 11 eyes with progressive loss. Each eye was converted to the right eye format and the stimulus locations immediately above and below the blind spot were excluded from the analysis. Five consecutive visual field examinations were selected for each patient at random. The mean number of fields preceding the five selected examinations was 4.8 (SD 1.55). The reliability of the selected examinations fell within normal limits in terms of fixation losses and false-positive and false-negative responses. Each patient had a visual acuity of 6/12 or better over the five examinations. Again, there were no exclusion criteria relating to the pharmacological or surgical control of the intraocular pressure. The mean age of the third sample at the first of the five examinations was 60.04 years (SD 16.05). The group mean time to follow-up over the five examinations was 2.67 years (SD 0.60; range 1.21 to 3.65 years) and the group mean interval between examinations was 8.14 months (SD 1.92; range 5.5 to 10.1 months). The group mean intraocular pressure over the five examinations was 20.0 mmHg (SD 2.9). The type of visual field defect at the first examination for the OHT sample and the POAG samples is shown in Figure 7.1.

7.3.3. Statistical analysis.

All visual fields were reduced to the Program 24-2 format. The visual field series of each of the 23 normal subjects was processed by the predict.exe module of the HFA Tools©. This module performs multivariate linear regression analysis using a composite pointwise topographical and longitudinal model described by Wild et al (1993). The model is defined by the general expression:

$$Z_{jt} = \sum_{r=0}^{\infty}\sum_{s=0}^{\infty} {}_{t}M_{rs}x_j^r y_j^s + \sum_{T=1}^{k} N_T z_{j(t-T)} + \bar{W}_t \qquad \text{Eq. (7.1)}$$

where Z_{jt} is the sensitivity of the general stimulus location (x_j, y_j) forecasted at a given time period, t, based upon the sensitivity at each of the previous number of examinations, k, at each time period T. M is the least-squares coefficient term containing $x^r y^s$ at time t and N is the

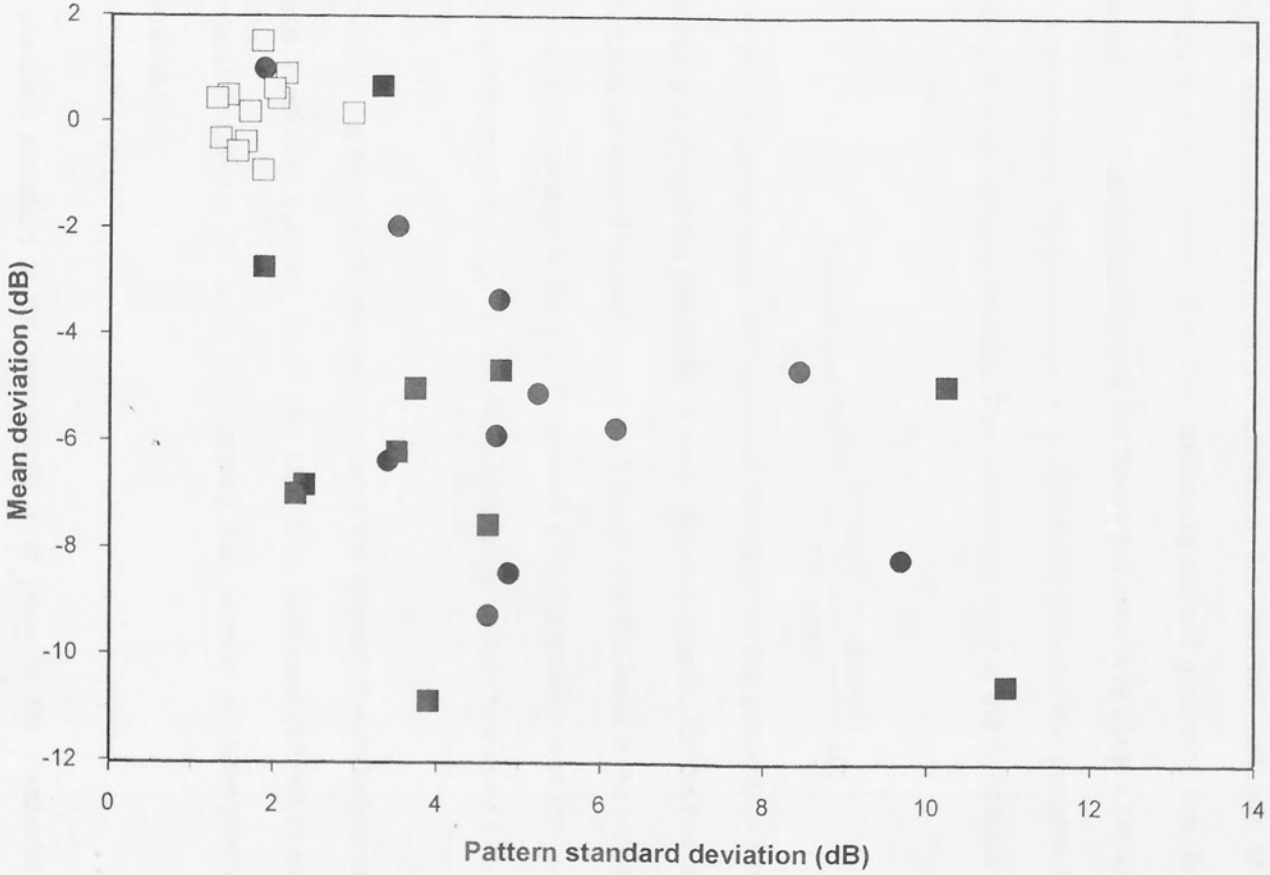

Figure 7.1. The type of visual field defect at the first examination in the series of five for each of the 12 ocular hypertensive (open squares), 11 stable (filled squares) and 11 progressing (filled circles) POAG patients expressed in terms of the mean deviation (dB) and pattern standard deviation (dB).

parameter associated with the value of sensitivity at time (t-T). The stochastic aggregate error term, $\bar{W}_t$, incorporates the short- and long-term fluctuation.

From a minimum of two fields, the model forecasts the pointwise sensitivity at each of the subsequent visual field examinations of the input series, based upon the data from the preceding examinations. The model attributes the greatest variance to the field most immediate to the forecasted field. The predict.exe module generates two files relating to the forecasted field. The first file contains the forecasted sensitivity at each stimulus location. The second file contains the percentage error calculated between the measured and forecasted sensitivity at each stimulus location. The percentage error in the forecasted value is defined as:

$$\text{Percentage Error} = \frac{|\text{forecast} - \text{measured}|}{\text{measured}}.100 \qquad \text{Eq. (7.2)}$$

In this way, a group mean and standard deviation of the percentage error between the measured and forecasted sensitivity at each stimulus location for the normal subjects, as a whole, could be derived for each of the third, fourth and fifth fields in the series. The magnitude of the mean percentage error (± 2SD) at each stimulus location was then used to provide a measure of the normal range of error in the forecasted sensitivity (Figure 7.2).

The suitability of these limits was tested against the forecasted sensitivity encountered at each stimulus location of the third, fourth and fifth visual field examinations in each of the ocular hypertensive patients in order to minimise the number of false-positive indicators of progressive loss.

The standard deviation of the percentage error between the measured and forecasted sensitivity in the normal eyes was modified before being applied to the forecasted sensitivity of the two glaucoma samples. The modification was necessary to account for the greater between-examination variability present in the glaucomatous field (Heijl et al. 1989). If x_i

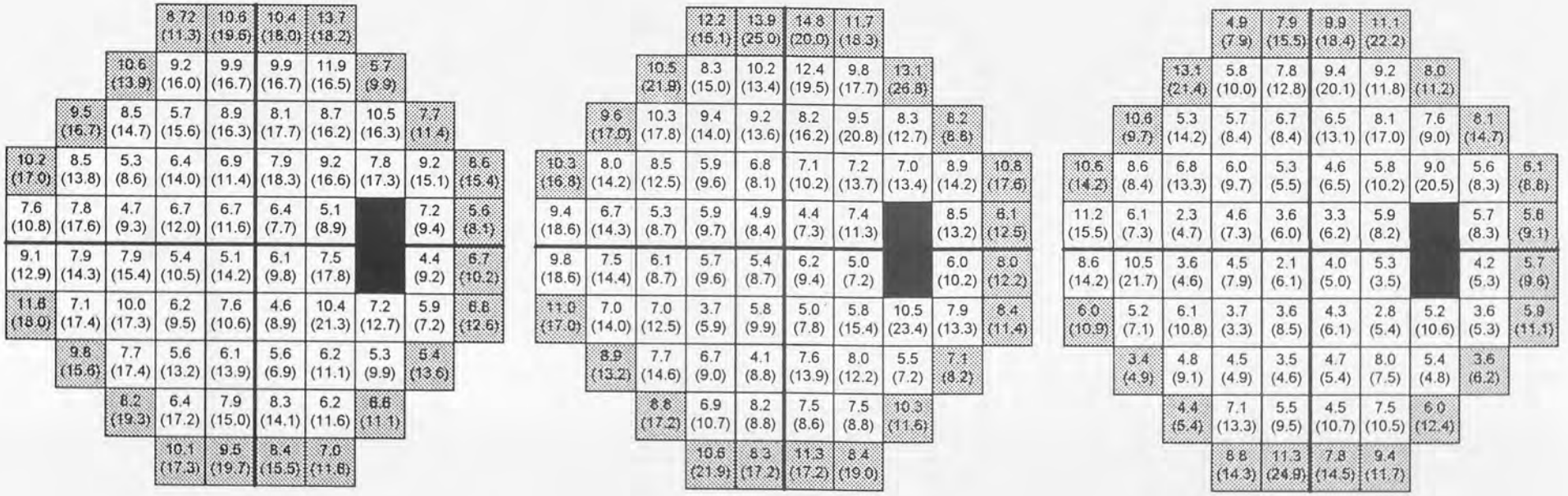

Field 3 Field 4 Field 5

Figure 7.2. The mean (±2 SDs) forecasted percentage error at each stimulus location derived by the multivariate model at the third (23 subjects), fourth (23 subjects) and fifth (8 subjects) examinations of the normal sample. The shaded areas illustrate the stimulus locations omitted for Program 24-2 format.

represents the percentage error (between the measured and forecasted sensitivity) at any given stimulus location, of sensitivity i, falling within the limits of the normal sample then:

$$x_i \in (\mu_i - 2\sigma_i, \mu_i + 2\sigma_i) \qquad \text{Eq. (7.3)}$$

where μ_i is the mean and σ_i is the standard deviation at stimulus location i.

The 5% and 95% confidence limits of between-examination variability encountered in a glaucomatous sample, examined with the Standard algorithm of the HFA, was described in Chapter 4. The width of the 90% confidence interval (ie. The difference between the 5% and 95% confidence limits) was determined at each 2dB sensitivity interval across the measurement range of the HFA. The 90% confidence interval at each 2dB sensitivity interval was used to derive a weighting function. Sixteen different widths of the 90% confidence interval were identified across the 2dB intervals between total deviations of +4dB and -34dB. The width of the 90% confidence interval was then normalised with respect to unity to obtain a weighting function for each interval. The average weighting ($\bar{w}$) function can be described as:

$$\bar{w} = \frac{1}{n}\sum_{1}^{n} w_i \qquad \text{Eq. (7.4)}$$

where w_i represents the weighting function of each 90% confidence interval at each sensitivity interval, i (i=1....16). The weighting function w_i was then expressed as a function of the mean weighting function. Thus:

$$w_i' = \frac{w_i}{\bar{w}} \qquad \text{Eq. (7.5)}$$

The weighting function was applied to the standard deviation of the mean percentage error at each stimulus location in the normal sample. This modification of the standard deviation reflected the additional variability in the percentage error of the forecasted value, expected as a result of any reduction in sensitivity exhibited by a stimulus location in a glaucomatous visual field. The modified standard deviation, σ_i', can be described by:

$$\sigma_i' = w_i'\sigma_i \qquad \text{Eq. (7.6)}$$

In order that the modified standard deviation expressed the *additional* variation of the percentage error at stimulus locations of reduced sensitivity, the smallest value of w_i' was assigned a value of 1.0. However, the difference between the weighting function, w_i', at each 90% confidence interval width in glaucoma was maintained. In this way, the limits of the forecasted percentage error at stimulus locations of normal sensitivity were the same as the limits assigned to the normal sample. At stimulus locations of reduced sensitivity, the limits of the forecasted percentage error increased in proportion to the amount of variability exhibited at that sensitivity between examinations. The weighting function at each 2dB sensitivity interval is shown in Table 7.1. Therefore, if x_i' represents the percentage error of the forecasted value in a glaucoma patient, the limits of the percentage error can be described as:

$$x_i' \in (\mu_i - 2\sigma_i', \mu_i + 2\sigma_i' \qquad \text{Eq. (7.7)}$$

Given that a value of zero for the percentage error of the forecasted sensitivity represents optimum accuracy of the model, the lower limit of x_i' (ie. $\mu_i - 2\sigma_i'$) was not considered.

The appropriate weighting function, w_i', at each stimulus location was derived from the sensitivity, expressed as the total deviation, at the given location present for the examination immediately preceding the forecasted field. A forecasted percentage error outside the 95% confidence limit (ie. $\mu_i + 2\sigma_i'$) was considered abnormal and could result from either an unexpected change in the measured sensitivity or from an inability of the model to forecast a stable sensitivity.

Fluctuation was defined as that in which the forecasted sensitivity at a given location was higher or lower than the measured sensitivity, accompanied by an abnormal forecasted percentage error. This was also followed, at the next examination, by a lower or higher forecasted sensitivity than the measured sensitivity together with an abnormal percentage error. A percentage error for the forecasted sensitivity within the 95% confidence limit followed, at the next examination, by an abnormal percentage error for either a higher or lower forecasted sensitivity was also considered as fluctuation. Progressive loss was considered to

Total deviation at field n (dB)	Width of 90% confidence interval (dB)	W_i'
-34	16.3	1.481
-32	13.6	1.305
-30	16.5	1.494
-28	12	1.201
-26	16.2	1.474
-24	16.0	1.461
-22	23.8	1.968
-20	18.8	1.643
-18	21.3	1.805
-16	17.0	1.526
-14	16.8	1.513
-12	13.6	1.305
-10	13.0	1.266
-8	11.0	1.136
-6	10.0	1.071
-4	9.4	1.032
-2	11.0	1.136
0	8.9	1.000
2	8.9	1.000
4	8.9	1.000
6	8.9	1.000

Table 7.1. The weighting function, w_i', applied to the standard deviation of the percentage error between the forecast and the measured sensitivity at the (n+1)th field, in order to account for the differing variability encountered across the range of sensitivities in glaucoma.

have occurred when a higher sensitivity than the measured sensitivity was forecasted at a given stimulus location, was accompanied by an abnormal percentage error and was followed, at the next examination, either by a forecasted sensitivity whose percentage error was within the 95% confidence limit or by a higher forecasted sensitivity than the measured sensitivity, again accompanied by an abnormal percentage error. Improvement was similarly considered with the exception that the forecasted sensitivity on each occassion was lower than the measured sensitivity. The consideration of a percentage error that was within the 95% confidence limit at the second of a pair of examinations was felt to reflect the adjustment of the model to the reduction or improvement in sensitivity encountered at the first examination of the pair. Stability was defined as a forecasted percentage error that was within the 95% confidence limit at two consecutive examinations.

The outcome of the forecasting procedure was compared with the GCPA. The GCPA printouts for the five fields used in the forecasting were obtained directly from the perimeter. The first two fields were selected and confirmed as baseline. Progressive loss at a single stimulus location was defined as two consecutive filled triangles on the GCPA print-out. Improvement was similarly considered as two open triangles. Fluctuation at a single location was indicated by the appearance of a triangular symbol which was opposite in direction or absent at the next examination.

Agreement (either an improvement or a progressive loss) between the GCPA and the forecasting at a stimulus location was considered to indicate a step change in sensitivity across the two examinations under consideration. A reduction or improvement in sensitivity indicated by the GCPA but not by the forecasting was considered to indicate a systematic change in sensitivity that the model was not able to predict. A reduction or improvement in sensitivity indicated by the forecasting but not by the GCPA was considered either to indicate that the model was inaccurate or that the change in sensitivity had occurred within the limits of the GCPA criteria for change.

7.4. Results.

7.4.1. The outcome of the multivariate model in the normal and ocular hypertensive samples.

The mean and SD of the percentage error between the forecasted and measured sensitivity decreased as the number of examinations increased (Figure 7.2). The mean and SD of the forecasted percentage error increased with increasing eccentricity.

The ocular hypertensive sample exhibited 17 stimulus locations (mean 1.4; SD 2.4 per patient) at which the multivariate model indicated progressive loss between the third and fourth fields. The mean number of stimulus locations classified as improving or fluctuating between these fields was 0.5 per patient and 1.6 per patient respectively (Table 7.2). Nine of the stimulus locations exhibiting progressive loss in the OHT sample were not clustered. Between the fourth and fifth fields, a mean of 0.3 stimulus locations per patient (a total of four) were classified as progressive loss, 1.1 as improving, 5.2 as fluctuating and 45.5 as stable (Table 7.2). One patient exhibited eight progressing stimulus locations, three of which were clustered. This cluster of three locations was situated superiorly at the extreme peripheral locations. None of the remaining OHT patients exhibited more than one stimulus location with progressive loss.

7.4.2. The outcome of the multivariate model in the stable POAG sample.

The stable POAG sample exhibited progressive loss at 36 stimulus locations between the third and fourth examinations and at 53 stimulus locations between the fourth and fifth examinations (Table 7.3). The locus of the progressing stimulus locations is shown in Figure 7.3. Of the 36 stimulus locations exhibiting progressive loss between the third and fourth examinations, 18 were clustered with at least one other such stimulus location (Table 7.4). The remaining eighteen were not clustered; two were positioned at the edge of the field and four were adjacent to the blind spot area. Of the 53 stimulus locations exhibiting progressive loss between the fourth and fifth examinations, 34 were clustered with at least one other such stimulus location. Of these, 17 were accounted for by one patient; 13 clustered in the inferior

	MULTIVARIATE MODEL CLASSIFICATION							
	PROGRESSIVE LOSS		IMPROVEMENT		FLUCTUATION		STABLE	
Field Pair	Mean (SD)	Range	Mean (SD)	Range	Mean (SD)	Range	Mean (SD)	Range
3 & 4	1.4 (2.4)	0 - 8	0.5 (1.5)	0 - 5	1.6 (1.8)	0 - 6	48.5 (4.3)	38 - 52
4 & 5	0.3 (0.4)	0 - 1	1.1 (1.4)	0 - 3	5.2 (7.6)	0 - 27	45.5 (8.3)	22 - 52

Table 7.2. The outcome at each stimulus location in the twelve ocular hypertensive patients classified on the basis of the magnitude and direction of the percentage error between the forecasted and measured sensitivity.

	MULTIVARIATE MODEL CLASSIFICATION							
	PROGRESSIVE LOSS		IMPROVEMENT		FLUCTUATION		STABLE	
Field Pair	**Mean (SD)**	**Range**	**Mean (SD)**	**Range**	**Mean (SD)**	**Range**	**Mean (SD)**	**Range**
3 & 4 Progressing POAG	7.1 (7.7)	0 - 23	1.5 (1.3)	0 - 3	10.1 (5.4)	1 - 19	33.3 (10.7)	16 - 48
Stable POAG	3.3 (5.0)	0 - 16	3.3 (5.5)	0 - 18	9.4 (9.0)	0 - 23	36.1 (13.3)	10 - 52
4 & 5 Progressing POAG	6.0 (5.2)	0 - 18	2.1 (2.6)	0 - 9	19.8 (9.0)	9 - 38	24.1 (10.6)	9 - 42
Stable POAG	4.8 (6.5)	0 - 23	2.9 (4.7)	0 - 14	12.9 (8.3)	4 - 34	31.4 (12.2)	14 - 48

Table 7.3. The outcome at each stimulus location in the stable and progressing glaucoma samples classified on the basis of the magnitude and direction of the percentage error between the forecasted and measured sensitivity.

Stable POAG sample

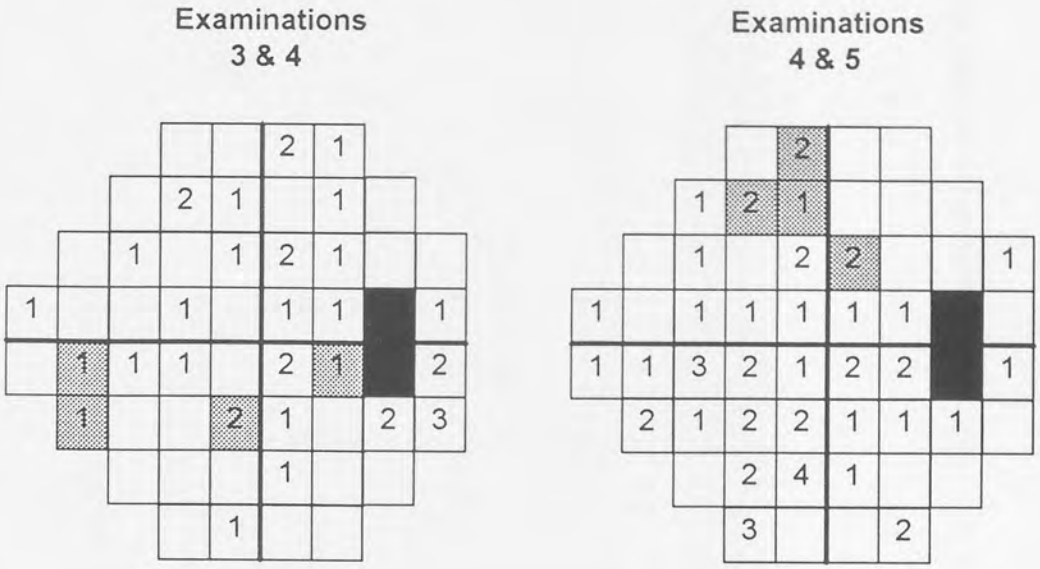

Progressing POAG sample

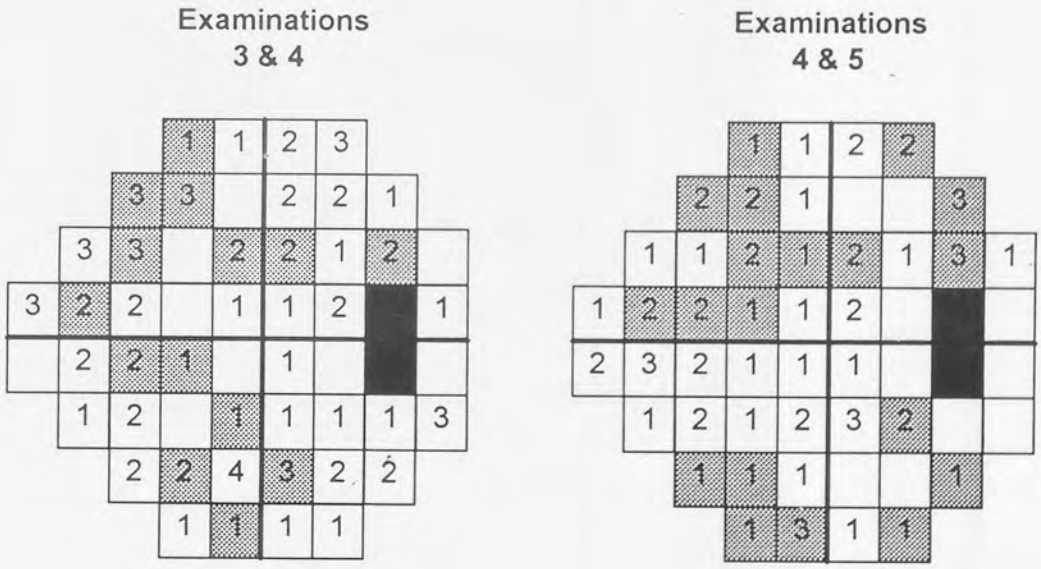

Figure 7.3. The frequency and locus of the stimulus locations classified by the multivariate model as exhibiting progressive loss between the third and fourth (left) and fourth and fifth examinations (right) for the stable (top) and progressing (bottom) POAG samples. The shaded squares illustrate the position of the stimulus locations at which there was agreement with the GCPA.

Spatial extent of stimulus locations in cluster	STABLE Frequency		PROGRESSING Frequency	
	3 & 4	4 & 5	3 & 4	4 & 5
2	2	3	11	5
3	2	2	3	1
4	2	1	1	2
5	0	1	1	2
9	0	0	1	0
13	0	1	0	0

Table 7.4. The frequency and spatial extent of clusters of stimulus locations exhibiting progressive loss in each of the stable and progressing POAG samples.

hemifield and 4 clustered in the superior hemifield. The 17 remaining stimulus locations forming a cluster of two or more were evident in three patients. The 19 stimulus locations that were not clustered were distributed across 9 patients; 10 locations were situated at the edge of the field and 2 were adjacent to the blind spot area.

No stimulus locations exhibiting progressive loss between the third and fourth examination subsequently showed improvement between the fourth and fifth examinations. Progressive loss was identified at three stimulus locations (two patients) both between the third and fourth examinations and between the fourth and fifth examinations.

Thirty-six and 32 stimulus locations exhibited improvement between the third and fourth and the fourth and fifth examinations pespectively. Only one cluster of two improving locations was evident in the sample between the third and fourth examinations and no clustered stimulus locations were evident between the fourth and fifth examinations. Twenty-four of the 36 stimulus locations exhibiting improvement between the third and fourth examinations were situated at the extremities of the field (21° eccentricity or greater) and four were adjacent to the blind spot area. Between the fourth and fifth examinations, 19 of the 32 improving stimulus locations were situated at the extremities of the field and 5 stimulus locations were adjacent to the blind spot area.

7.4.3. The outcome of the multivariate model in the progressing POAG sample.

The multivariate model identified progressive loss between the third and fourth examinations at 78 stimulus locations in the progressing POAG sub-sample. Similarly, 66 stimulus locations were identified between the fourth and fifth examinations (Table 7.3). The locus of the progressing stimulus locations is shown in Figure 7.3. Forty-nine of the 78 stimulus locations progressing between the third and fourth examinations were clustered with at least one other progressing location. Of the stimulus locations exhibiting progressive loss that did not form part of a cluster, eight were situated at 21° eccentricity or beyond and 5 were adjacent to the blind spot area. Between the fourth and fifth examinations, 31 of the 66 progressing stimulus

locations formed part of a cluster of two or more stimulus locations. Thirteen of the 66 stimulus locations were not clustered and were situated at 21° eccentricity or beyond and four were situated adjacent to the blind spot area. Two patients did not exhibit any clustered progressing stimulus locations between either pair of fields. The frequency and spatial extent of the clustered stimulus locations exhibiting progressive loss is shown in Table 7.4.

No stimulus locations exhibiting progressive loss between the third and fourth examination subsequently showed improvement between the fourth and fifth examinations. Progressive loss was identified at eight stimulus locations (four patients) between the third and fourth examinations and between the fourth and fifth examinations.

A total of 16 and 23 improving stimulus locations were identified between the third and fourth and the fourth and fifth examinations, respectively. The majority (12 and 18 respectively) of the improving locations were situated at 21° eccentricity or beyond. One cluster of two improving stimulus locations was present between the third and fourth examinations. No clustered improving stimulus locations were present between the fourth and fifth examinations.

The number of stimulus locations exhibiting progressive loss as a function of the difference between the forecasted percentage error and the 95% confidence limit is illustrated in Figure 7.4. The majority of forecasted percentage errors were up to 30% larger than the 95% confidence limit. The forecasted percentage errors that were more than 30% beyond the 95% confidence limit were mainly evident in the progressing POAG sample. The difference between the forecasted percentage error and the 95% confidence limit for those stimulus locations exhibiting progression as a function of the measured sensitivity at the examination preceding the progressive loss is shown in Figure 7.5. In order to illustrate this relationship more clearly, the aberrant percentage errors greater than 100% are omitted from the figure. Four of the 89 stimulus locations exhibiting progressive loss produced percentage errors of greater than 100% in the stable POAG sample. The mean percentage error of these four stimulus locations was 490.34% (SD 439.1; range 128.96-1048.35) and the mean sensitivity was 3.5 dB (SD 2.9;

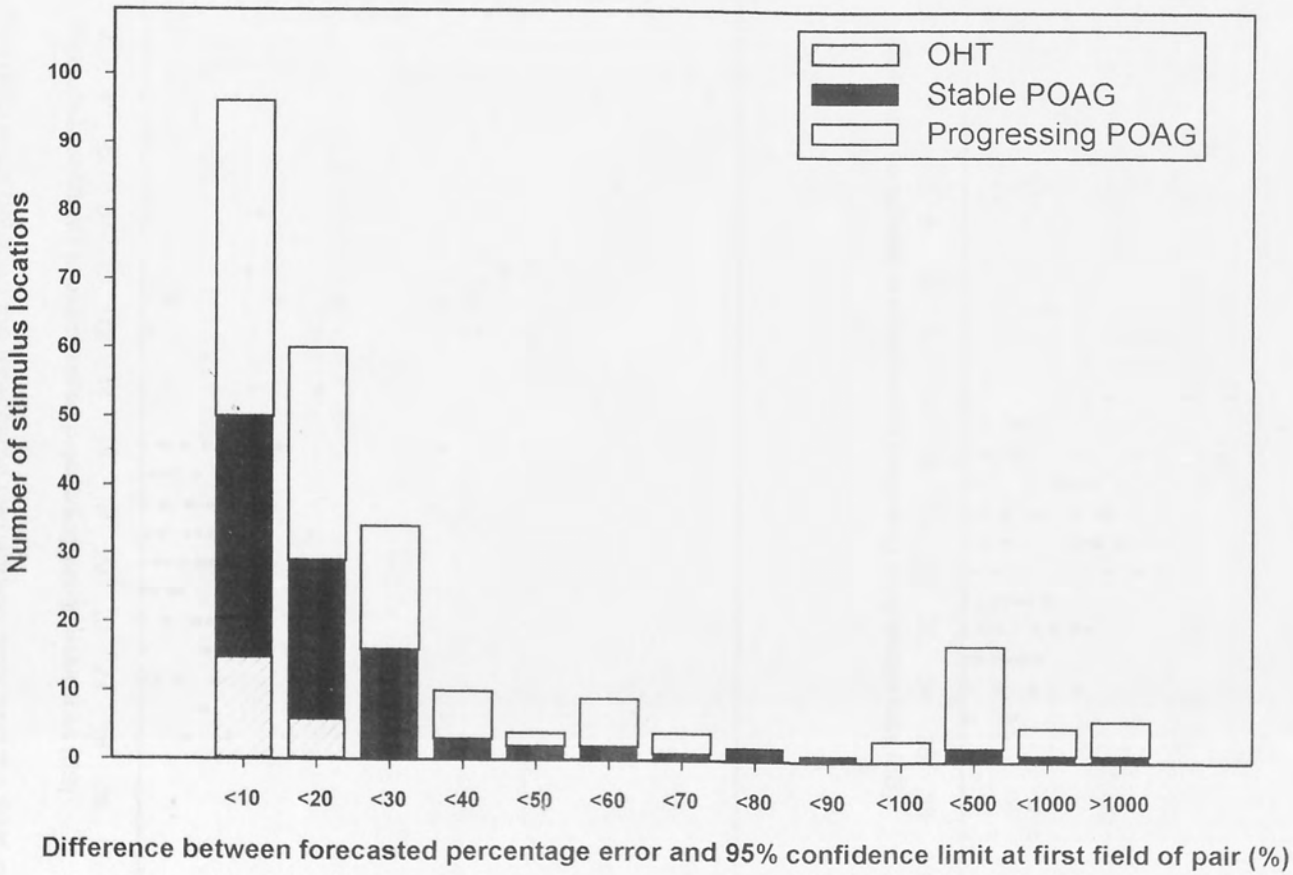

Figure 7.4. The number of stimulus locations exhibiting progressive loss as a function of the difference between the forecasted percentage error and the 95% confidence limit in the ocular hypertensive and POAG samples.

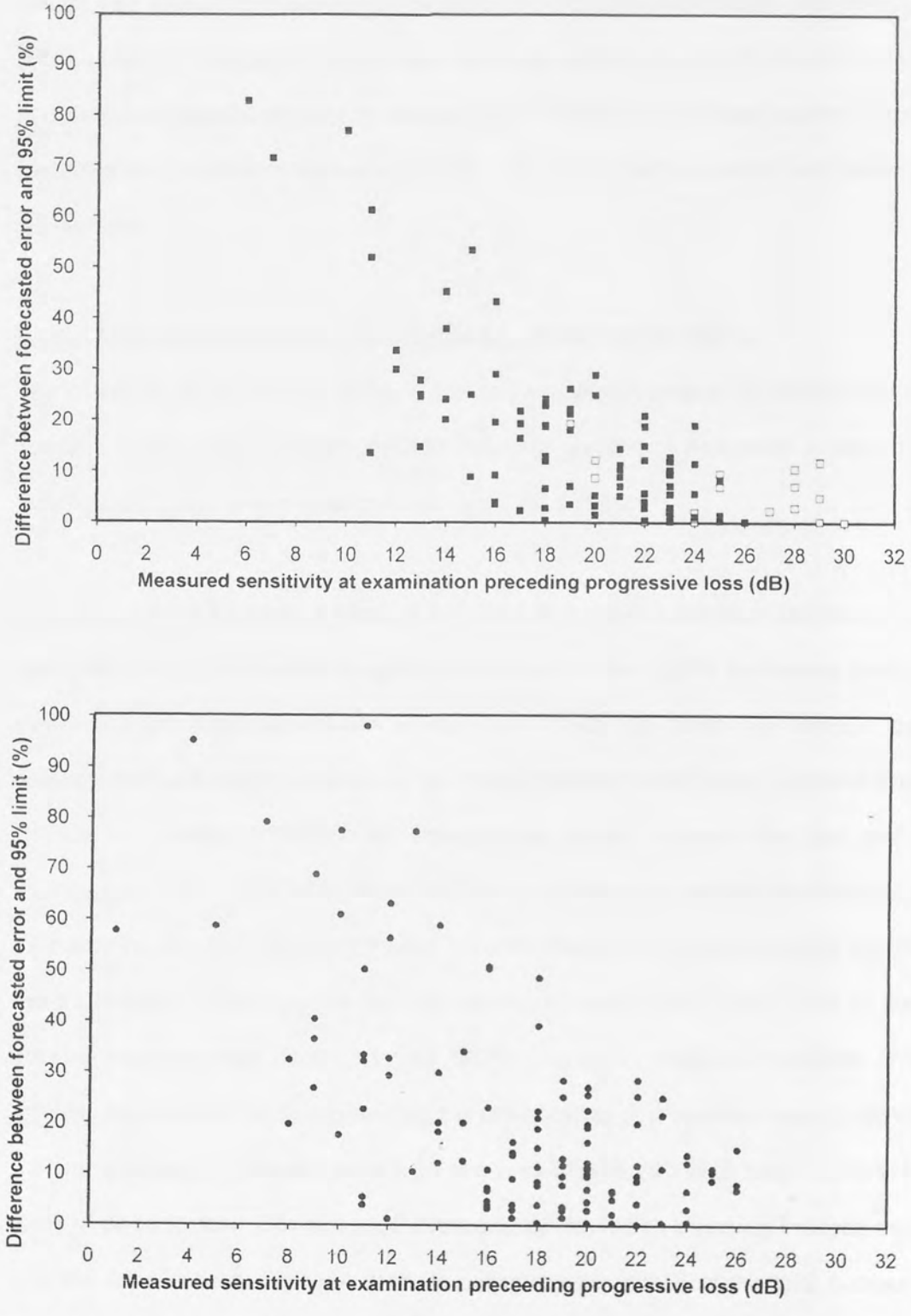

Figure 7.5. The difference between the forecasted percentage error and the 95% confidence limit at the first of a pair of examinations for those stimulus locations exhibiting progressive loss, as a function of the measured sensitivity at the preceding examination. The upper graph illustrates the 21 progressing locations in the ocular hypertensive sample and 85 of the 89 progressing locations in the stable POAG sample. The lower graph illustrates the corresponding data for 120 of the 144 stimulus locations in the progressing POAG sample.

range 1.0-6.0). Similarly, 24 of the 144 stimulus locations exhibiting progression in the progressing POAG sample exhibited percentage errors of the forecast sensitivity that were greater than 100%. The mean percentage error of the 24 stimulus locations was 634.42% (SD 769.9; range 101.2-3252.3) and the mean sensitivity was 4.9 dB (SD 3.1; range 0.5-11.0). Up to 100%, the percentage error increased as the measured sensitivity at the examination preceding the progression decreased (Figure 7.4) in both the progressing and stable POAG sub-samples.

7.4.4. The agreement between the multivariate model and the GCPA.

The extent of the agreement between the multivariate forecasting of progression and the outcome of the GCPA is shown in Table 7.5. Little agreement was found between the two techniques for either pair of fields or for either POAG sample.

In the stable POAG sample, a mean of 0.4 (SD 0.9; range 0-3) stimulus locations per patient were identified as progressing by both the multivariate and GCPA techniques between the third and fourth examinations and a mean of 0.4 (SD 1.0; range 0-4) stimulus locations between the fourth and fifth examinations. The multivariate model, alone, identified a mean of 2.9 (SD 4.0; range 0-13) stimulus locations per patient between the third and fourth examinations and 4.5 (SD 6.6; range 0-23) stimulus locations between the fourth and fifth examinations. A single patient contributed 16 of the total of 32 stimulus locations identified by the multivariate model between the third and fourth examinations. Only three of these 16 stimulus locations were identified by the GCPA. The mean measured sensitivity of the 16 stimulus locations at the field preceding the classification of progression was 21.88 dB (SD 2.5) and the mean forecasted percentage error was 31.61% (SD 11.3; range 14.73 to 51.19). None of these stimulus locations were subsequently classed as improving between the fourth and fifth examinations. Similarly, a single patient contributed 23 of the total number of 49 progressing locations between the fourth and fifth examinations, none of which were identified by the GCPA. The mean measured sensitivity of the 23 locations was 17.57 dB (SD 5.2) and the mean forecasted percentage error was 45.85% (SD 25.8; range 21.28 - 113.85).

	PROGRESSIVE LOSS		IMPROVEMENT		FLUCTUATION		STABLE	
	Field Pair 3 & 4	Field Pair 4&5	Field Pair 3 & 4	Field Pair 4&5	Field Pair 3 & 4	Field Pair 4&5	Field Pair 3 & 4	Field Pair 4&5
Multivariate forecasting & GCPA								
Progressing POAG sample	16	22	0	0	51	89	294	199
Stable POAG sample	4	4	3	1	34	55	355	302
Multivariate forecasting only								
Progressing POAG sample	62	44	16	23	60	129	73	66
Stable POAG sample	32	49	33	31	69	87	42	43
GCPA Only								
Progressing POAG sample	11	29	0	0	82	70	91	140
Stable POAG sample	6	14	5	1	57	47	101	142

Table 7.5. The level of agreement between the number of stimulus locations identified as progressing by the multivariate model and by the GCPA in the progressing and stable glaucoma samples.

Therefore, the error in the forecasted sensitivity was, on average, 7dB in the first patient and 8dB in the second patient. A mean of 0.5 (SD 1.8; range 0-6) stimulus locations per patient were identified as progressing by the GCPA, only, between the third and fourth examinations and a mean of 1.3 (SD 1.9; range 0-5) stimulus locations per patient between the fourth and fifth examinations.

In the progressing POAG sample the level of agreement was slightly better. A mean of 1.5 (SD 2.7; range 0-9) stimulus locations per patient exhibited agreement between the multivariate and GCPA techniques between the third and fourth examinations and a mean of 2.0 (SD2.3; range 0-8) locations per patient exhibited agreement between the fourth and fifth examinations. The mean number of locations per patient exhibiting progressive loss by the multivariate model only in the progressing sample was 5.6 (SD 5.8; range 0-17) between the first pair of examinations and 4.0 (SD 3.6; range 0-10) between the second pair of examinations. Similarly, the GCPA, alone, identified a mean of 1.0 (SD 2.1; range 0-7) progressing stimulus location per patient between the third and fourth examinations and a mean of 2.6 (SD 3.7; range 0-11) between the fourth and fifth examinations. The two patients in the progressing sample in whom a cluster of locations with progressive loss were not identified by the multivariate model each exhibited a pair of clustered deteriorating locations by the GCPA. These two patients therefore exhibited a constant decline in sensitivity that the model was able to forecast.

In the stable POAG sample, the GCPA identified progressive loss at 6 stimulus locations between the third and fourth examinations and at 14 between the fourth and fifth examinations that were not detected by the multivariate technique. Similarly, 11 and 29 such stimulus locations respectively were identified in the progressing POAG sample. In the two patient samples, only two stimulus locations from the progressing POAG sample exhibited progressive loss with GCPA and were also identified as exhibiting progressive loss over both pairs of fields by the multivariate model. The GCPA is unable to indicate either stability at a

third examination following progressive loss over a pair of examinations or to indicate consecutive episodes of progressive loss over three examinations.

In the stable POAG sample, both the multivariate model and the GCPA identified a mean of 0.3 (SD 0.6; range 0-2) improving stimulus locations per patient between the third and fourth examinations and a mean of 0.1 (SD 0.3; range 0-1) improving stimulus locations per patient between the fourth and fifth examinations. The GCPA did not identify any improving stimulus locations between either pair of examinations in the progressing POAG sample.

Seven stimulus locations were classed as 'out-of-database' by the GCPA between the third and fourth examinations of the stable POAG sub-sample. The corresponding number of 'out-of-database' stimulus locations between the fourth and fifth examinations was 6. All but one of these thirteen stimulus locations corresponded to a negative change in sensitivity from the baseline pair of fields. The stimulus location with an increase in sensitivity from the baseline pair of fields was identified as improving by the multivariate model. Eight of the twelve 'out-of-database' locations with a decrease in sensitivity were classified as stable by the multivariate model, whilst 2 were classified as progressive loss and 2 were classified as fluctuating. In the progressing POAG sub-sample, 23 and 22 stimulus locations were classified as 'out-of-database' by the GCPA between the third and fourth and the fourth and fifth examinations, respectively. A single location exhibited an increase in sensitivity from the baseline pair of fields and was identified as improving by the multivariate model. Of the remaining 44 stimulus locations, 34 were classified as stable by the multivariate model, 4 as progressive loss and 6 as fluctuating.

Better agreement between the multivariate model and the GCPA was found at those stimulus locations classed as stable by each technique (Table 7.5). A mean of 32.2 stimulus locations per patient (SD 12.8; range 7-52) and a mean of 27.5 stimulus locations per patient (SD 13; range 11-48) were identified as stable by both techniques between the third and fourth and the fourth and fifth examinations, respectively. In the progressing POAG sub-sample a mean of

26.7 stimulus locations per patient (SD 8.8; range 8-38) and a mean of 18.1 stimulus locations (SD 9.8; range 5-32) were similarly identified as stable between each pair of fields by both techniques.

7.5. Discussion.

The 95% confidence limit of the forecasted percentage error in the normal sample may be considered an expression of the variability in sensitivity between examinations (long-term fluctuation). The increase with increasing eccentricity of the mean and SD of the forecasted percentage error is in agreement with the findings of other investigators (Heijl et al. 1987; Rutishauser et al. 1989; Wilensky & Joondeph 1984). The limited number of stimulus locations exhibiting either progressive loss or improvement in the OHT sample suggests that the 95% confidence limits derived from the normal sample are satisfactory for monitoring the visual field over follow-up time.

The magnitudes of the percentage error of the forecasted sensitivity in all three samples were not comparable to the enormous percentage errors in the forecasted sensitivity previously found with a complex polynomial function (McNaught et al. 1995). The difference in outcomes is attributable both to the form of the composite topographical and longitudinal model and to the application of the model to determining progressive loss. The composite multivariate model utilises an ordinal measure of time and therefore the length of the interval between the last measured values of sensitivity and the forecasted sensitivity have a lesser influence on the forecasted error. However, at stimulus locations exhibiting a significant decrease in sensitivity over time to follow-up, a lengthy period between the first five examinations and the forecasted field would undoubtedly produce an increase in the number of false-positives indicators of progression as well as being unrepresentative of the true rate of decline in sensitivity.

Good agreement between the intuitive criteria utilised for the identification of progression and the outcome of the multivariate model was found in seven of the eleven stable POAG patients. The agreement between the intuitive criteria and the multivariate model in the progressing

sample was also good in nine of the eleven patients. In both samples of POAG patients, the multivariate model classified a similar number of stimulus locations to be exhibiting progressive loss that did not form part of a cluster of two or more locations. Approximately half of these were situated at the extremities of the field or adjacent to the blind spot, which are known to exhibit greater variability (Heijl et al. 1987). Similarly, the stimulus locations identified as improving in both POAG samples were also situated at the extremities of the program 24-2 examination. Across each sample as a whole, the number of stimulus locations per patient that were not clustered and exhibiting progressive loss was, in general, small.

The limited number of stimulus locations exhibiting progressive loss by the GCPA, alone, indicate that few of the stimulus locations exhibited a constant decline in sensitivity. This outcome is in agreement with the findings of ULR of the measured sensitivity against time to follow-up, which also indicated that a constant decline in sensitivity occurred less frequently than an episodic change in sensitivity (Chapter 6).

The 95% confidence limit of the percentage error of the forecasted sensitivity appears to be susceptible to small changes in sensitivity and this is undoubtedly the main factor in the disparity between the outcomes of the multivariate model and the GCPA. The modification of the standard deviation by the weighting function increased the 95% confidence limit used in the POAG samples and the mean magnitude of the increase was 1.5 times the normal 95% confidence limit. Given that the average magnitude of the 95% confidence limit in the normal sample was approximately 20%, the average magnitude of the 95% confidence limit used for the POAG samples was approximately 30%. The majority of abnormal percentage errors encountered in the POAG samples were up to 20% larger than their 95% confidence limit (Figure 7.4) and the magnitude of the percentage error increased as the sensitivity at the examination preceding the forecasted field decreased. Across a 15-25 dB measurement range, a 50% percentage error represents a difference between the forecasted sensitivity and the measured sensitivity of between 7.5 to 12.5 dB. A change in sensitivity of this magnitude between examinations has been attributed to variability in glaucomatous subjects, particularly

if it occurs in the middle sensitivity range and at the extremities of the field (Heijl et al. 1989). Derivation of the 95% confidence limit from the mean and SD exhibited by a stable glaucoma sample at each location would improve the ability of the multivariate model to forecast progressive loss by further minimising the number of false positive indicators of progression.

In addition to a number of false-positive indicators of progressive loss, poor agreement between the multivariate model and the GCPA may also result from a decline in sensitivity that is within the limits of the GCPA criteria for change, but is large enough to produce an abnormal percentage error. At least half of the stimulus locations identified as progressing by the multivariate model were clustered with at least one other progressing location and, as they are clustered, are more likely to be exhibiting progressive loss than variability.

If further modification of the 95% confidence limit used in glaucoma can minimise the incorrect classification of stimulus locations exhibiting variability as progressing, the multivariate model has advantages over the GCPA. The stimulus locations at which the GCPA indicated progressive loss at all three examinations showed little agreement with the multivariate model. This outcome arises from the inability of the GCPA to indicate stability after a step-change in sensitivity or to show consecutive episodes of loss over serial examinations (Chapter 5). Conversely, the emphasis placed by the multivariate model upon the visual field examination immediately preceding the forecasted field determines that the model itself acts as a 'moving' baseline. The multivariate is also able to include the data from all examinations preceding the forecasted field whereas the GCPA ignores any data preceding the two baseline fields.

7.6. Conclusion.

The 95% confidence limit derived from the normal sample was a satisfactory means of determining progressive loss in OHT patients. However, the modified 95% confidence limit appeared to make the multivariate model too sensitive to the magnitude of change that can be exhibited by glaucomatous subjects between examinations. This may be overcome by deriving the 95% confidence limit for the forecasted percentage error from a stable glaucomatous

sample. Little agreement was found between the forecasting technique and the GCPA which was mainly attributable to susceptibility of the multivariate model to large degrees of variability. The GCPA presents a more reliable technique for indicating progressive loss than the multivariate forecasting technique in its current form.

Chapter 8: Modelling of the visual field in optic neuritis.

8.1. Introduction.

Optic neuritis is an inflammatory demyelinating condition of the optic nerve. Typically, patients comprise adolescents and young adults, with proportionally more females (~75%) (O.N.S.G. 1991; Rizzo III & Lessell 1991). It presents as an acute reduction of visual acuity accompanied by periorbital pain (O.N.S.G. 1991; Rizzo III & Lessell 1991). The periorbital pain is considered to be a consequence of mechanical interaction of the inflamed optic nerve sheath with the orbit, and is often worse with eye movements (Lepore 1991). Subsequently, the presenting symptoms frequently resolve. Optic neuritis has an incidence of between 0.6 and 5.1 per hundred thousand of the population (Alter et al. 1973; Kahana et al. 1976; Kinnunen 1983; Percy et al. 1972; Rodriguez et al. 1995). In approximately 24% to 39% of cases, isolated optic neuritis precedes the development of multiple sclerosis within ten years (Alter et al. 1973; Kahana et al. 1976; Kinnunen 1983; Rodriguez et al. 1995). Some studies report a gender bias toward females at the onset of multiple sclerosis (Rizzo III & Lessell 1991; Sandberg-Wolheim et al. 1990) whilst others find little difference in gender (Beck et al. 1993b; Morrissey et al. 1993; Rodriguez et al. 1995).

Following recovery of visual acuity, deficiencies in visual function frequently remain and are subjectively reported by patients. Clinical deficits include localised visual field loss, reduced contrast sensitivity (O.N.S.G. 1991), aberrant colour vision (Beck 1988; O.N.S.G. 1991), prolonged latency in the visual evoked potential (Celesia et al. 1990) and reduced stereopsis (Fleishman et al. 1987).

The outcome of clinical and psychophysical investigation relates to the distribution and extent of damage to the fibres of the anterior visual pathway. Transmission of visual information from the retinal photoreceptors is mediated by two parallel processing structures, the magnocellular and parvocellular pathways. Both the physiological and anatomical characteristics of the two pathways are different and each responds more specifically to particular aspects of visual information (Bassi & Lehmkuhle 1990; Kolb 1991; Livingstone & Hubel 1987; Livingstone & Hubel 1988; Merigan et al. 1991; Merigan & Maunsell 1990; Wiesel & Hubel 1966). The magnocellular pathway constitutes approximately 10% of the optic nerve fibres. These

emanate from the large retinal ganglion cells (M-cells) (Silveira & Perry 1991). The M-cells have large cell bodies, large dendritic trees and project via thick axon fibres to the magnocellular layers of the dorsal lateral geniculate nucleus. The parvocellular pathway approximates 80% of the optic nerve fibres (Perry et al. 1984). These emanate from the small retinal ganglion cells (P-cells). The dendritic fields of the P-cells are about one third smaller than those of the M-cells, are more dense and project via thin axon fibres to the parvocellular layers of the lateral geniculate nucleus. The conduction velocity of neural impulses along the thick axons of the M-pathway is more rapid than along the thin axons of the P-pathway (Gouras 1968; Schiller & Malpelli 1977). The remaining 10% of optic nerve fibres are of a parvocellular type and project to the superior colliculus of the mid-brain where they are utilised in eye movement control. Thin axon (P-cell) fibres are more highly concentrated in the macula region and a greater variation of fibre diameter has been observed with increasing retinal eccentricity (Jonas et al. 1990; Potts et al. 1972; Sanchez et al. 1986).

The response of the magnocellular and parvocellular pathways to stimulus characteristics also differs. The magnocellular pathways are more responsive to achromatic stimuli of low-to-medium spatial frequency. In contrast, the parvocellular pathway is more responsive to high spatial frequency achromatic stimuli and low-to-medium spatial frequency chromatic stimuli (Derrington & Lennie 1984; Merigan et al. 1991; Merigan & Maunsell 1990). It has been suggested that the temporal frequency characteristics of a stimulus are modulated by a collection of temporal channels, the response activity of which are additionally mediated by the stimulus spatial frequency (Hess & Plant 1985; Kulikowski & Tolhurst 1973). Low spatial frequency stimuli (M-cell pathway) are mediated by a high-pass temporal frequency channel (Derrington & Lennie 1984). Medium-to-high spatial frequency stimuli elicit a composite temporal response mediated by two temporal frequency channels - one band-pass and one low-pass (Derrington & Lennie 1984).

Psychophysical investigations of the relationship between loss of visual function and the effects of demyelination are complicated by the difficulty in separating the response from each of the two parallel processing systems. The detection of large stimuli by an optic neuritis patient will necessarily be mediated by both affected and unaffected nerve fibres. Small

localised stimuli will evoke a more specific response, but may not represent the effects of demyelination due to the variation in both fibre type and fibre diameter with retinal eccentricity. Selective damage of the P-cells has been reported in optic neuritis. Recovered optic neuritis patients have shown either normal or mild depression of sensitivity at the central visual field when investigated with kinetic perimetry, whilst static perimetry reveals additional loss in the mid-periphery. This stato-kinetic dissociation indicates greater achromatic luminance detection loss (P-cell) than movement detection loss (M-cells) (Johnson et al. 1989b). A loss of high spatial frequency (1Hz) pattern detection has been reported in human subjects (Wall 1990), similar to that of the macaque with P-cell depletion (Merigan 1989; Merigan & Eskin 1986). An increase in temporal modulation sensitivity has been found with increasing eccentricity out to 10° (Edgar et al. 1990). These findings would appear to match the distribution of the small diameter fibres as a function of retinal eccentricity (Perry et al. 1984; Potts et al. 1972; Sanchez et al. 1986). Conversely, an impaired detection of low spatial frequency gratings at both high and low temporal frequencies has also been reported (Travis & Thompson 1989; Wall 1990; Wright et al. 1987) suggesting both M- and P-cell involvement. Chromatic function, also mediated by the P-cells, has been reported to be impaired in patients presenting with demyelinating disease and the reduction at the fovea is approximately equal to the luminance loss (Foster et al. 1985; Grigsby et al. 1991; Russell et al. 1991). The luminance function would, however, appear to be more affected than the chromatic function when detecting a stimulus of low-to-medium spatial frequency across the border of a scotoma (Phillips et al. 1994). This would appear to suggest that the effects of demyelination are more likely to involve the M-cell fibres which mediate the response to low-to-medium spatial frequency achromatic stimuli. It is possible that the parvocellular losses may simply be due to the greater debilitating effects of demyelination on the physical characteristics of the smaller fibres (Foster et al. 1985). Alternatively, the preferential damage to the magnocellular fibres may be a manifestation of the large extent of damage caused by demyelination (Ulrich & Groebke-Lorenz 1983). The reduced signal transmission of the M-cell fibres may therefore be a chance finding related to the small absolute number of fibres. In any event, the separation of the M- and P- channels would not appear to be absolutely distinct, particularly in the V4 area of the visual cortex (Ferrera et al. 1992).

The optic neuritis treatment trial (ONTT) (Beck 1988; Beck et al. 1993a; Beck & O.N.S.G. 1995; Keltner & Johnson 1994; Keltner et al. 1993a; Keltner et al. 1993b; O.N.S.G. 1991; Trobe 1994) was developed to answer clinical questions regarding the efficacy of oral or intravenous corticosteroid treatment in cases of optic neuritis. The ONTT provided an opportunity to define clinical features of the condition. The early study reports determined that advanced diagnostic techniques, including MRI, appeared to offer little additional clinical insight when reviewed after 6 months and one year of the trial (Beck et al. 1992; Beck et al. 1993a; O.N.S.G. 1991). However, abnormal MRI at the outset did appear to be indicative of multiple sclerosis at two years (Beck et al. 1993b; Beck & O.N.S.G. 1995). Intravenous corticosteroid treatment expedited visual recovery, most noticeably in the first month of treatment and in patients with visual acuity at the outset of less than 20/40 (Beck 1992; Beck et al. 1992; Beck et al. 1993b; Trobe 1994).

Classically, visual field defects associated with optic neuritis are described as central or centrocaecal scotoma. However, both the ONTT and other studies in optic neuritis note a wide variety of visual field defects (Celesia et al. 1990; Chamlin 1953; Trobe & Glaserm 1978). Visual field examination with both the Humphrey Visual Field Analyzer (HFA) and the Goldmann perimeter formed an intrinsic part of the study. The visual field reading centre (VFRC) of the ONTT produced a standardised procedure by which each visual field was read and classified (Keltner & Johnson 1994; Keltner et al. 1993a). The visual field defects presenting at the baseline in the ONTT trial were broadly separated into diffuse loss and localised loss. Based upon the outcome of the HFA results, diffuse loss was classified as mild, moderate or severe and localised loss was classified into fourteen patterns of loss (O.N.S.G. 1991). The most common visual field defect presenting in the affected eye of the 448 patients enrolled in the study was diffuse visual field loss (48.2%) of which 35.5% was severe, 9.7% moderate and 3.0% mild (Keltner et al. 1993b). Altitudinal defects constituted 14.9% of loss at baseline and three quadrant loss, 6% (Keltner et al. 1993b). The patterns of field loss in the remaining patients, including centrocaecal defects, presented with a frequency of less than 5% in the study population. Nearly 70% of patients also presented with a visual field loss in the fellow eye.

The natural course of recovery of either the visual field as a whole or at each stimulus location is unknown. A knowledge of the rate and the magnitude of the recovery could facilitate early recognition of incomplete recovery. In addition, the ability of any derived model to forecast the outcome would present a further clinical guide to the course of recovery.

8.2. Aim.

The aim of the study was, firstly, to develop a mathematical model capable of describing the recovery of optic neuritis; secondly, to determine whether the model was capable of providing additional information concerning the recovery of the field as a whole and at each individual stimulus location; thirdly, to use the model to forecast the visual field recovery.

8.3. Methodology.

The sample was drawn from 448 patients enrolled in the Optic Neuritis Treatment Trial (ONTT). For each patient, the central visual field of both eyes was examined with Program 30-2 of the HFA (stimulus size III) using the Standard 4-2dB strategy. In order to fulfil the perimetric eligibility criteria for the study, the affected eye of each patient had to exhibit a visual field defect in accord with a diagnosis of optic neuritis, a significant reduction in at least one of the summary visual field parameters (MD, CPSD and PSD) or a significant reduction in sensitivity for at least 8 of the 76 individual stimulus locations (Keltner et al. 1993b). The first visual field examination was undertaken within eight days of the onset of the visual symptoms associated with optic neuritis (O.N.S.G. 1991). Subsequent visual field examinations were carried out at time periods of approximately 3, 14 and 29 days after the baseline field and then at time periods of 7, 13 and 19 weeks, 6 and 12 months and then annually (Keltner et al. 1993a). Each visual field examination was carried out by a trained technician, following a strict protocol, and the visual field outcomes underwent additional quality control measures (Keltner et al. 1993a). All visual fields complied with the study reliability criteria of less than 20% fixation losses and less than 30% false-positive and false-negative responses.

The sample selection criteria were based upon the visual field outcome and the treatment regime employed and required the affected eye of each patient to exhibit severe diffuse loss at the initial presentation; to have received no oral or intravenous corticosteroid treatment

throughout the course of the trial; to exhibit no recurrent episodes over the time to follow-up and to have a minimum of nine visual field examinations. No exclusion criteria related to sub-clinical disease changes. The criteria of nine visual field examinations was used to ensure that a sufficient number of degrees of freedom were available to permit the use of complex functions to describe the improvement in sensitivity. Of the 484 patients enrolled in the study, 173 exhibited severe diffuse loss at the baseline examination. Sixty-two of the 173 patients received oral corticosteroid treatment and 59 received intravenous corticosteroid treatment. Twenty of the 52 patients who were untreated had less than nine consecutive visual field examinations and 19 had a recurrent episode of sensitivity reduction. Thirteen patients reached the selection criteria and were separated into two sub-samples. The first sub-sample comprised seven patients who exhibited complete visual field recovery over their series of examinations, as specified by the VFRC. Recovery was defined as: no clusters of two or more stimulus locations whose sensitivity was depressed at $p<0.05$. The second sub-sample comprised six patients who did not exhibit complete visual field recovery by the same classification and manifested a variety of defects at the final field of their series.

8.3.1. Complete recovery sub-sample.

The complete recovery sub-sample consisted of 7 patients. All of the patients were between 18 and 45 years of age. This sub-sample had undergone a mean of 10.00 (SD 1.3) visual field examinations over a period of 2.50 years (SD 1.3; range 1.02 to 4.26). The mean interval between each examination was 95 days (SD 40.3; range 4 to 449). The field at which each subjects visual field was deemed to have recovered by the VFRC classification is shown in Table 8.1. The mean MD of the sub-sample at the initial examination was -27.36dB (SD 3.3; range -20.39 to -30.03).

8.3.2. Incomplete recovery sub-sample.

The incomplete recovery sub-sample consisted of 6 patients aged between 18 and 45 years. This sub-sample had undergone a mean of 10.33 (SD 1.2) visual field examinations over a period of 2.74 years (SD 0.8; range 2.02 to 4.04). The mean interval between each examination was 104 days (SD 28.3; range 2 to 405). The residual visual field defect at the

SUB-SAMPLE	Number of fields in series	Examination	Residual field loss at final field
COMPLETE RECOVERY Subject		Recovery	
A	11	7	None
B	12	5	None
C	9	7	None
D	11	8	None
E	9	7	None
F	9	4	None
G	9	7	None
INCOMPLETE RECOVERY Subject		Residual Field Loss	
A'	11	9	Moderate localised altitudinal
B'	9	6	Minimal diffuse
C'	10	6	Minimal diffuse
D'	11	7	Moderate localised quadrant
E'	12	6	Minimal localised peripheral rim
F'	9	8	Minimal localised popcorn

Table 8.1. Descriptive data for the two sub-samples of patients.

final examination according to the VFRC classification is shown in Table 8.1. The mean MD of the sub-sample at the initial examination was -27.63dB (SD 1.6; range -26.02 to -29.57).

8.3.3. Data Analysis.

The visual field data, expressed as the percentage recovery of the MD from the baseline, was plotted against the logarithm of the time to follow-up. A similar procedure was adopted for the sensitivity at each individual stimulus location. The pointwise analysis excluded the stimulus locations immediately above and below the blind spot.

The Kinetic Formation equation of an automated curve fitting software program (Tablecurve *2D*, Jandel Scientific, Erkrath, Germany) was selected. This family of curves described the rate of recovery at each data point in terms of the amount of recovery that had already occurred. The shape of the Kinetic Formation functions followed the type of recovery frequently exhibited in optic neuritis, ie. a rapid recovery of the sensitivity at the initial examinations which plateaued at the later examinations.

A logistic model was also selected and this function took the form:

$$\frac{\delta y}{\delta t} = y(a - y) \qquad \text{Eq. (8.1)}$$

where y is the percentage recovery of the MD from the baseline, t is the (log) time to follow-up and a is the maximum recovery (dB). This model was chosen as it described the rate of improvement in sensitivity at each examination in terms of the amount still to occur to reach complete recovery.

The first order Formation equation with a zero-intercept exhibited a better coefficient of determination (R^2) than the logistic model for both of the patient sub-samples and was chosen for use in further analysis. The function took the form:

$$y = a(1 - e^{-bx}) \qquad \text{Eq. (8.2)}$$

where a represents the maximum decibel recovery and b is the rate constant.

In addition to the Formation curve, a Gaussian cumulative function was selected. The selection was made on the basis of inspection of the data relating to the percentage recovery in sensitivity against (log) time to follow-up. This equation took the form:

$$y = \frac{a}{2}\left(1 + erf\left(\frac{x-b}{\sqrt{2c}}\right)\right) \qquad \text{Eq. (8.3)}$$

where a is the transition height (ie. the level of recovery), b is the transition centre (ie. the centre of the linear portion of the function), c is related to the transition width and *erf* is the error function. The slope of the transition zone at the transition centre (b=0) is described by:

$$\text{Slope} = \frac{a}{4c\sqrt{\pi}} \qquad \text{Eq. (8.4)}$$

The coefficient of determination (R^2), the level of recovery and the slope of the recovery were recorded for each fit. The function generating the best R^2 for the MD against time to follow-up and for the sensitivity at each stimulus location against time to follow-up was then used to investigate any differences between patients within a sub-sample and then between sub-samples.

A second approach to modelling and forecasting was adopted. The model took the form of a simple probability model based upon the expected number of stimulus locations still to exhibit at least a 90% recovery from baseline at a given visual field examination. For a given stimulus location, i, the probability that a stimulus location is still to recover at the first examination from the baseline is:

$$P_i(1) = p_i \qquad \text{Eq. (8.5)}$$

where i=1,2,3....74 and p_i falls between 0 and 1. As a first approximation, p_i was assumed to be similar at all stimulus locations. Therefore:

$$p_i = p \qquad \text{Eq. (8.6)}$$

and p may be estimated by:

$$\hat{p} = \frac{n}{N} \qquad \text{Eq. (8.7)}$$

where n is the number of stimulus locations exhibiting recovery and N is the total number of stimulus locations in the visual field.

As a further consequence of this assumption, the expected number of stimulus locations still to show recovery at the second examination from the baseline may be expressed as:

$$P(2) = p.q \qquad \text{Eq. (8.8)}$$

and at the third field from the baseline as:

$$P(3) = p.q^2$$

where q is related to p by:

$$q = 1 - p \qquad \text{Eq. (8.9)}$$

The general form of the probability model at the visual field examination of recovery, r, may be written as:

$$P(r) = p.q^{r-1} \qquad \text{Eq. (8.10)}$$

A difference between the observed and estimated values of p is determined by the Chi-squared test. A statistically significant outcome of this procedure indicates that the model does not approximate well to the observed findings.

This expression may also be modified to forecast the expected field at which recovery of all the stimulus locations will occur. The estimated field of recovery, E(r), may be expressed as:

$$E(r) = \sum_{r=1}^{\infty} r.q.p^{r-1} \qquad \text{Eq. (8.11)}$$

$$= q + (2.q.p) + (3.q.p^2) + \ldots\ldots (r.q.p^{r-1})$$

$$= q.(1 + 2.p + 3.p^2 + \ldots\ldots r.p^{r-1})$$

$$= \frac{q}{(1-p)^2} \qquad \text{Eq. (8.12)}$$

substituting from equation 8.8:

$$E(r) = \frac{1}{q} \qquad \text{Eq. (8.13)}$$

The estimated field for recovery was retrospectively compared with the observed field for either complete recovery or for the residual field loss in each of the sub-samples of patients.

8.4. Results.

The coefficient of determination (R^2) for the percentage recovery of MD against (log) time to follow-up with the Formation curve and with the Gaussian cumulative curve are shown in Table 8.2 for each patient in each of the two sub-samples. The mean R^2 of the Formation curve and of the Gaussian cumulative curve was 0.766 (SD 0.09) and 0.974 (SD 0.02), respectively, for the sub-sample exhibiting complete recovery. The corresponding mean values for the sub-sample exhibiting an incomplete recovery was 0.729 (SD 0.09) and 0.932 (SD 0.07), respectively.

The mean, range and median R^2 values for the pointwise analysis for each subject in each of the sub-samples are shown in Table 8.3. In the majority of cases, the Gaussian cumulative curve better described the data for both the MD and the pointwise sensitivity against time to follow-up. An example of a stimulus location that exhibited a better fit with the Gaussian cumulative curve than with the Formation curve is shown in Figure 8.1.

The outcome at each stimulus location with the Gaussian cumulative curve, as a function of the magnitude of the maximum recovery (a) and the slope of the recovery at the transition centre, for each patient in the sub-sample exhibiting complete recovery is shown in Figure 8.2. The corresponding data is shown in Figure 8.3 for the sub-sample exhibiting an incomplete recovery. Some data could not be fitted by the Gaussian cumulative function. This occurred when the slope of the recovery was extremely rapid over a short time period and, as a consequence, the width of the transition zone tended toward zero.

Subject A in the complete recovery sub-sample, exhibited a marked difference in the level of recovery modelled by the Gaussian cumulative curve for the MD compared to that for the pointwise sensitivity. However, in the complete recovery sub-sample most patients showed a magnitude of recovery that was greater for the MD than that exhibited by the sensitivity of the individual stimulus locations. The incomplete recovery sub-sample, in contrast, exhibited a magnitude of recovery for the MD that was similar to the recovery of the sensitivity at the individual stimulus locations. The magnitude of the recovery was, in general, smaller for the peripheral stimulus locations (greater than 21° from fixation) than for those situated more

COMPLETE RECOVERY Subject	FORMATION R^2	GAUSSIAN CUMULATIVE R^2
A	0.859	0.979
B	0.840	0.992
C	0.759	0.985
D	0.661	0.985
E	0.639	0.985
F	0.745	0.969
G	0.858	0.924
INCOMPLETE RECOVERY Subject		
A'	0.632	0.920
B'	0.846	0.997
C'	0.665	0.981
D'	0.688	0.889
E'	0.706	0.808
F'	0.834	0.994

Table 8.2. Coefficient of determination (R^2) of the Formation curve and the Gaussian cumulative curve for the MD against time to follow-up for each patient of each sub-sample.

COMPLETE RECOVERY Subject	FORMATION R^2			GAUSSIAN CUMULATIVE R^2		
	Mean (SD)	Range	Median	Mean (SD)	Range	Median
A	0.783 (0.15)	0.273 - 0.978	0.792	0.866 (0.21)	0.207 - 0.994	0.938
B	0.777 (0.10)	0.580 - 0.980	0.754	0.961 (0.04)	0.800 - 0.996	0.976
C	0.679 (0.15)	0.195 - 0.926	0.681	0.890 (0.11)	0.527 - 0.996	0.919
D	0.629 (0.06)	0.365 - 0.737	0.635	0.944 (0.07)	0.477 - 0.995	0.967
E	0.426 (0.18)	0.062 - 0.857	0.430	0.968 (0.05)	0.784 - 0.999	0.986
F	0.674 (0.20)	0.051 - 0.935	0.747	0.818 (0.24)	0.102 - 0.995	0.906
G	0.680 (0.13)	0.010 - 0.896	0.709	0.888 (0.19)	0.316 - 0.998	0.971
INCOMPLETE RECOVERY Subject						
A'	0.455 (0.16)	0.038 - 0.704	0.462	0.763 (0.19)	0.100 - 0.995	0.814
B'	0.740 (0.17)	0.092 - 0.979	0.755	0.884 (0.18)	0.102 - 0.996	0.932
C'	0.599 (0.18)	0.002 - 0.782	0.656	0.250 (0.22)	0.003 - 0.970	0.205
D'	0.562 (0.22)	0.000 - 0.881	0.576	0.702 (0.28)	0.000 - 0.995	0.770
E'	0.613 (0.18)	0.084 - 0.812	0.675	0.806 (0.24)	0.000 - 0.997	0.914
F'	0.731 (0.14)	0.374 - 0.986	0.719	0.897 (0.13)	0.231 - 0.996	0.946

Table 8.3. Mean, range and median coefficient of determination (R^2) of the Formation curve and the Gaussian cumulative curve for percentage recovery from baseline of the sensitivity against time to follow-up for each patient of each sub-sample.

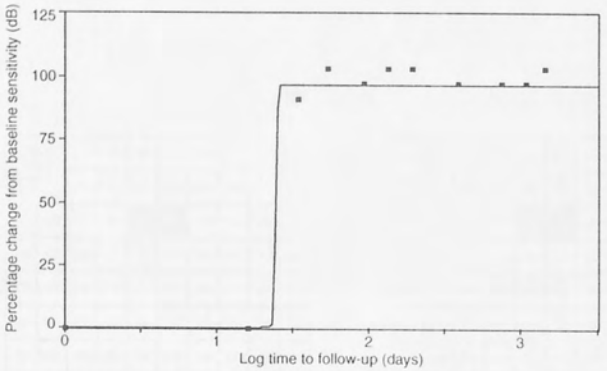

Subject D (+3,+9) Gaussian Cumulative: $R^2 = 0.981$; a = 96.28;

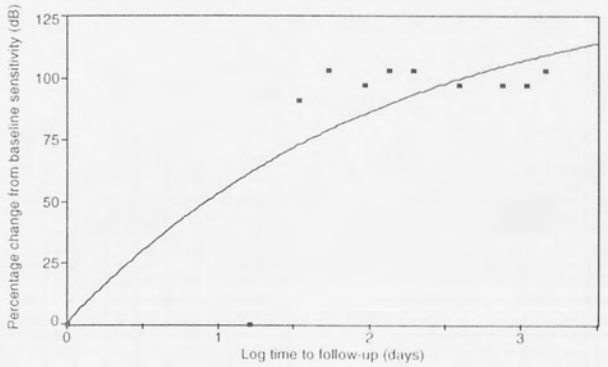

Subject D (+3,+9) Formation curve: $R^2 = 0.590$; a = 140.29;

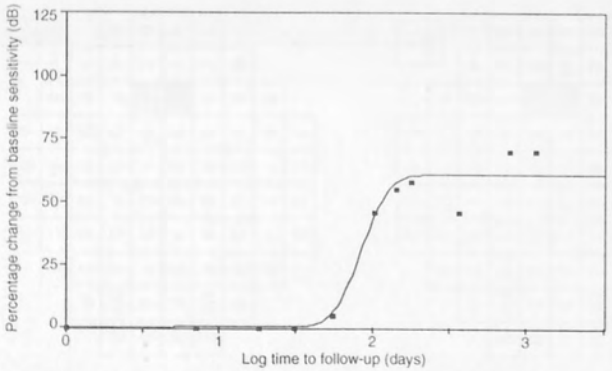

Subject A' (+3,+9) Gaussian Cumulative: $R^2 = 0.936$; a = 60.510;

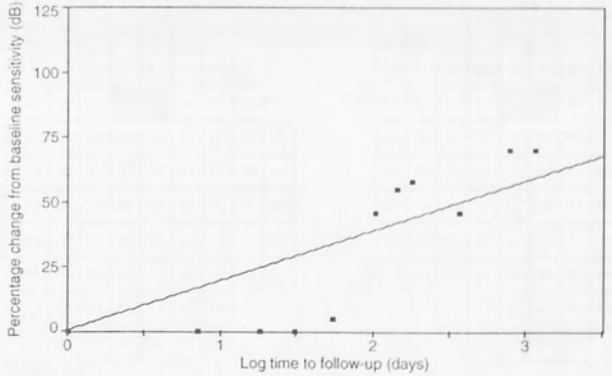

Subject A' (+3,+9) Formation curve: $R^2 = 0.556$; a = 5663.921;

Figure 8.1. Illustration of the better fit of the data by the Gaussian Cumulative function than the Formation curve for a single stimulus location.

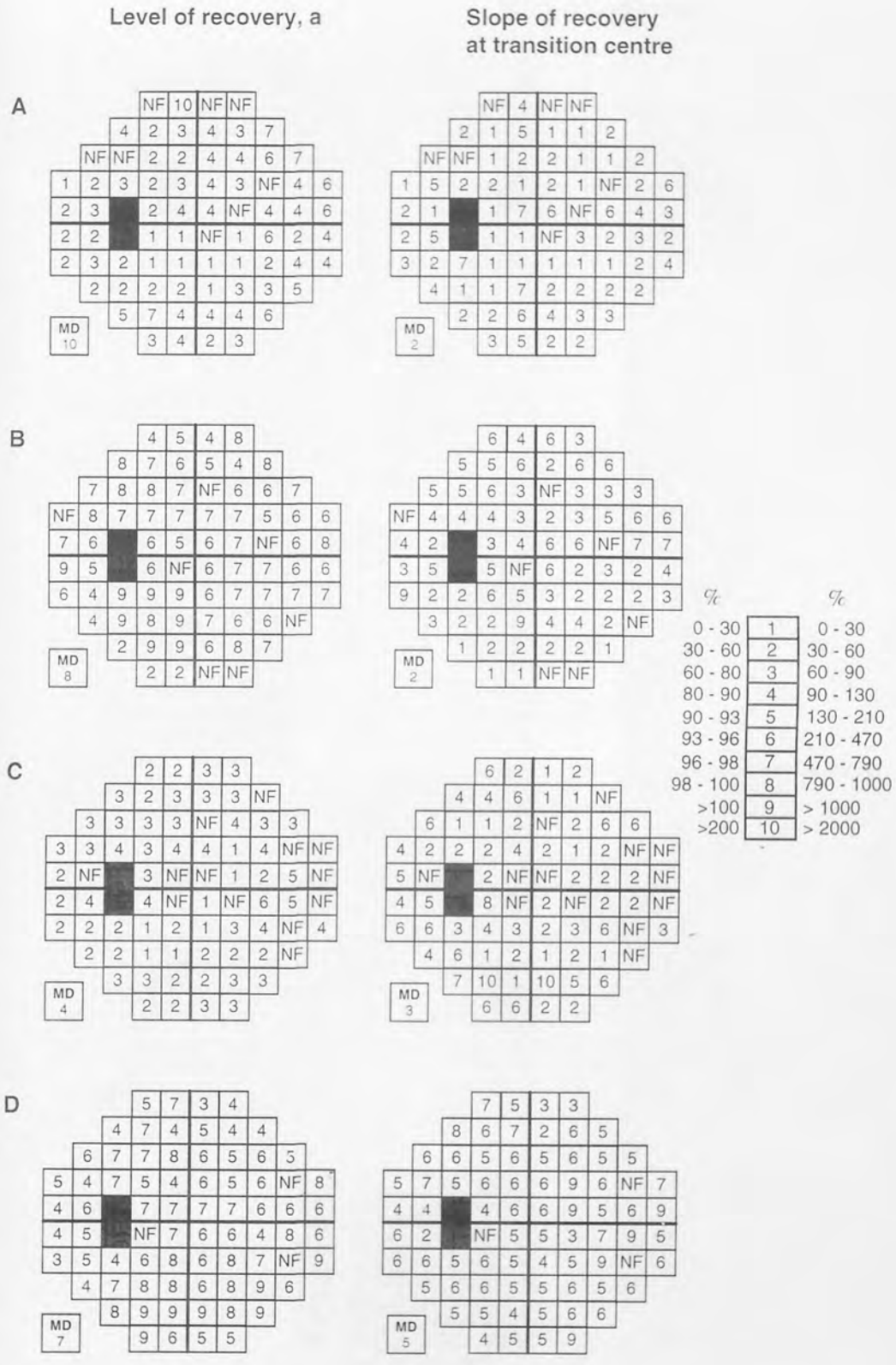

Figure 8.2. The magnitude and slope of the recovery of the Mean Deviation against time to follow-up modelled with the Gaussian cumulative function. The figure shows the respective data of subjects A to D from the sub-sample exhibiting recovery over the series of fields. NF indicates that the data could not be fitted by the Gaussian cumulative function.

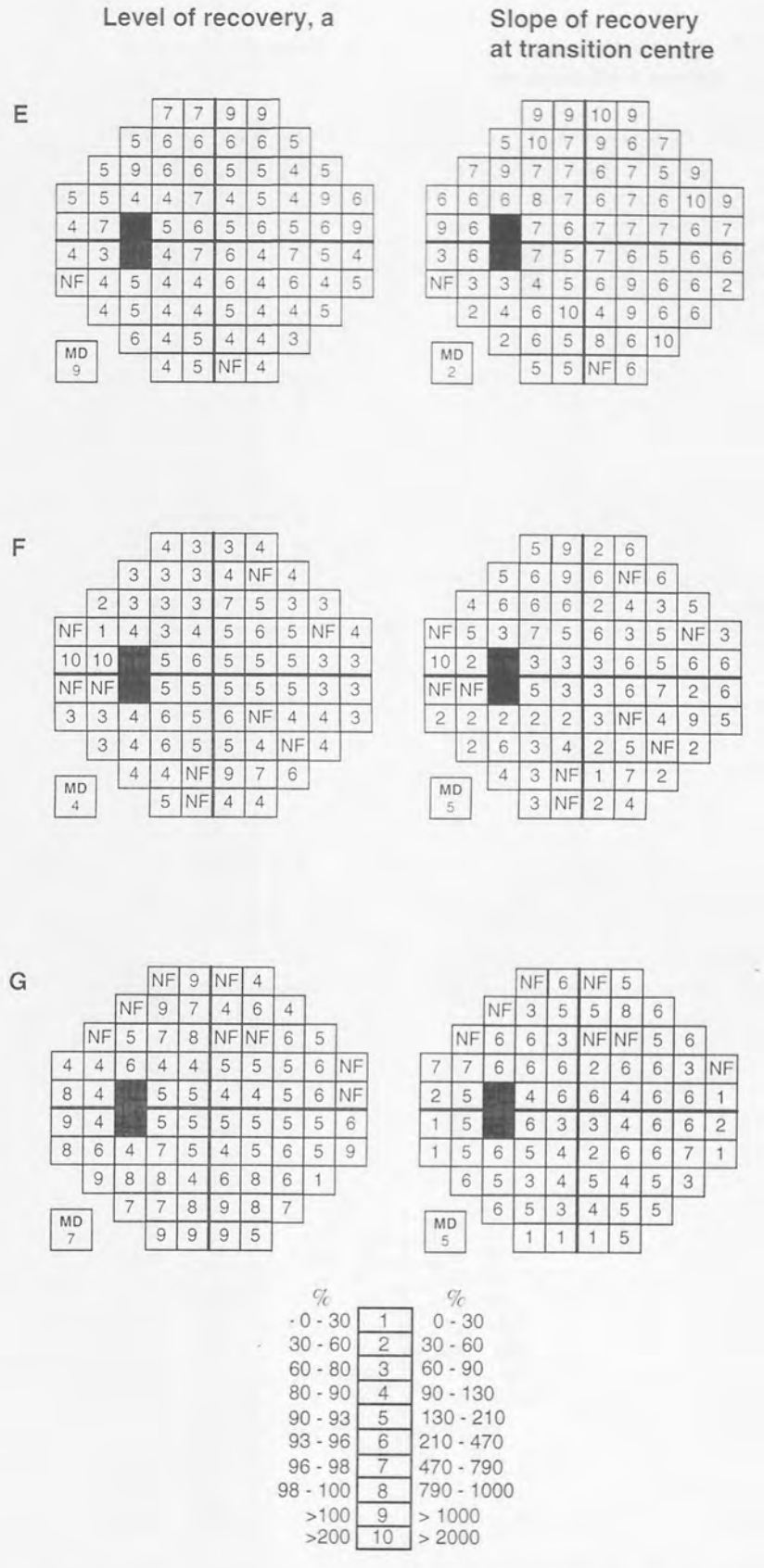

Figure 8.2. (cont.) The magnitude and slope of the recovery of the Mean Deviation against time to follow-up modelled with the Gaussian cumulative function. The figure shows the respective data of subjects E to G from the sub-sample exhibiting recovery over the series of fields. NF indicates that the data could not be fitted by the Gaussian cumulative function.

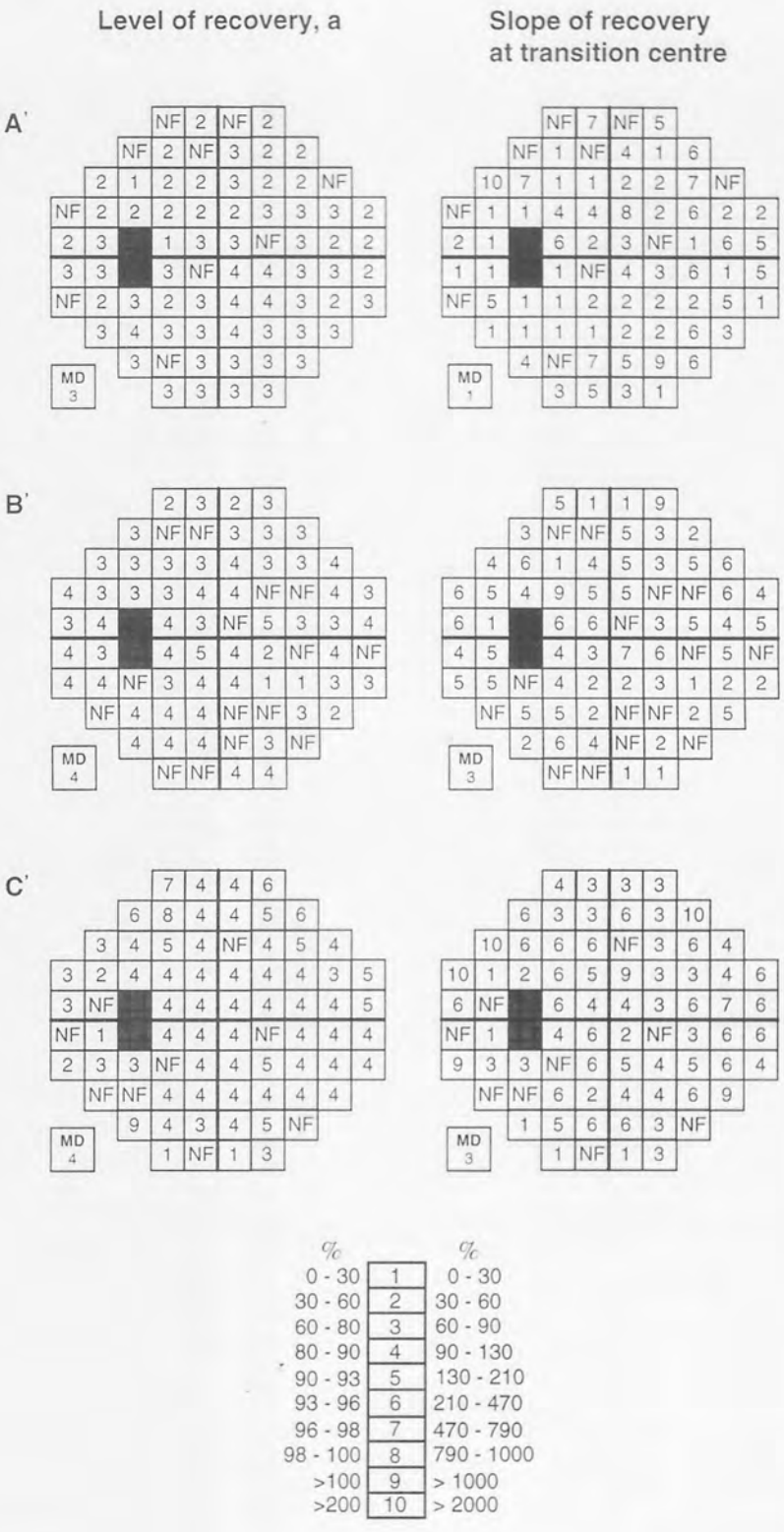

Figure 8.3. The magnitude and slope of the recovery of the Mean Deviation against time to follow-up modelled with the Gaussian cumulative function. The figure shows the respective data of subjects A' to C' from the sub-sample exhibiting incomplete recovery over the series of fields. NF indicates that the data could not be fitted by the Gaussian cumulative function.

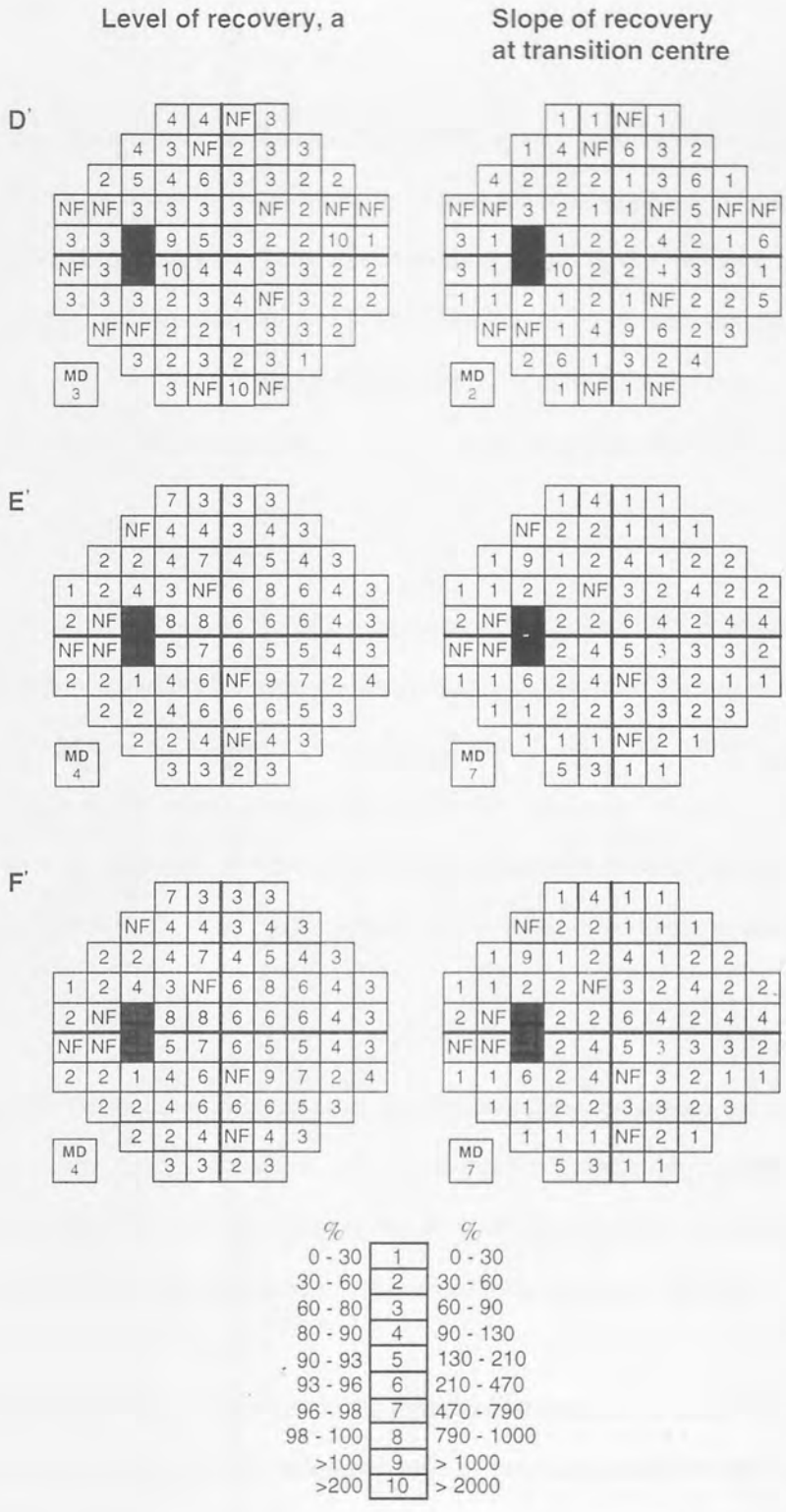

Figure 8.3. (cont.) The magnitude and slope of the recovery of the Mean Deviation against time to follow-up modelled with the Gaussian cumulative function. The figure shows the respective data of subjects D' to F' from the sub-sample exhibiting incomplete recovery over the series of fields. NF indicates that the data could not be fitted by the Gaussian cumulative function.

centrally. This was evident in both sub-samples, but was more noticeable in the incomplete recovery sub-sample.

In both sub-samples, the slope of the recovery for the MD against time to follow-up was similar to, or less than, the slope of the recovery of the individual stimulus locations. The slope of the recovery at the individual stimulus locations was steeper in the complete recovery sub-sample than in the incomplete recovery sub-sample. In the complete recovery sub-sample, the slope of recovery was steeper for stimulus locations situated at eccentricities beyond 21° than for those situated more centrally. No such trend was evident in the incomplete recovery sub-sample.

The Gaussian cumulative curves of the MD against time to follow-up for both sub-samples were plotted together in order to determine if it was possible to separate the sub-samples from one another on the basis of the shape of the function (Figure 8.4). Those patients exhibiting a diffuse residual field defect were inseparable from the complete recovery sub-sample. However, subjects A' and D' who exhibited a moderate localised residual defect showed a departure from the complete recovery sub-sample after a time to follow-up of approximately thirty days.

The outcomes of the Chi-squared test between the observed and estimated values of p are shown in Table 8.4. The results show that the model formed a better approximation of the number of stimulus locations still to recover to 90% of the baseline sensitivity for the incomplete recovery sub-sample compared to the complete recovery sub-sample.

The estimated field of recovery, forecasted by the probability model, is shown in Table 8.5. For the complete recovery sub-sample, the observed field of recovery related to the first field at which the sensitivity had returned to normal. In the incomplete recovery sub-sample, the observed field of recovery was taken as the field at which the residual loss, present at the final examination, was first recorded. The level of agreement between the model and the observed values was similar between the two groups of subjects. The larger disparities between the estimated and observed values relate to the time period at which the majority of stimulus

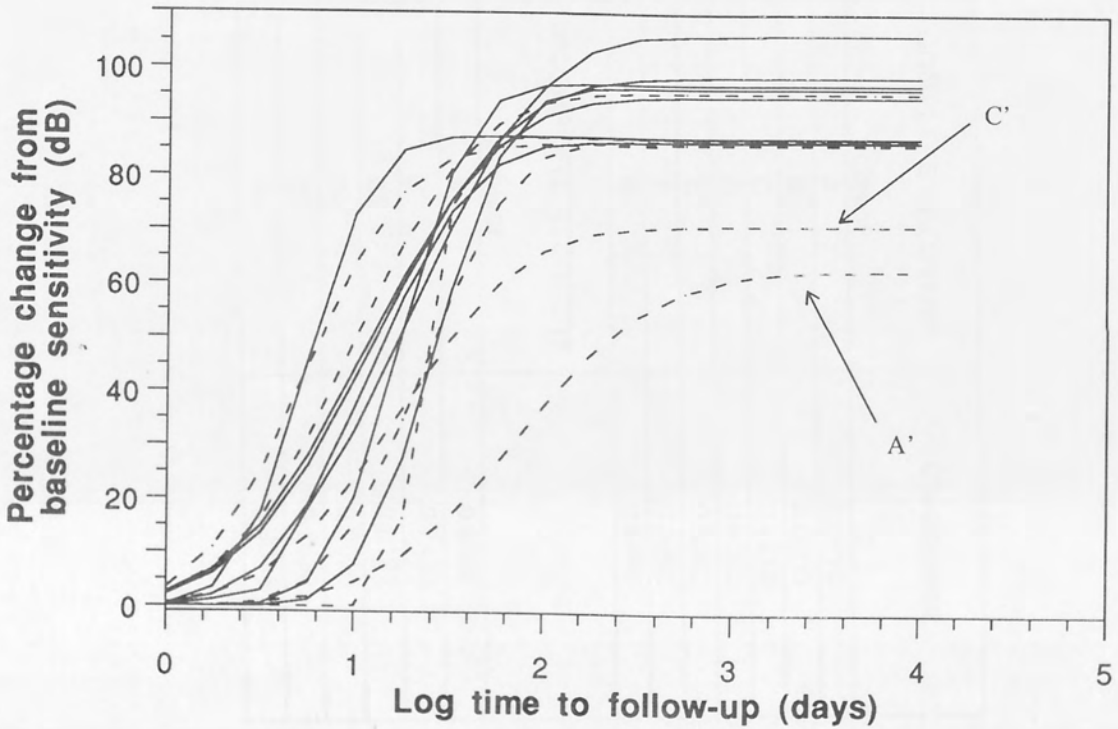

Figure 8.4. The percentage recovery from baseline of the MD against time of follow-up for the complete (solid lines) and incomplete recovery sub-samples (broken lines).

COMPLETE RECOVERY Subject	Chi-Squared p
A	0.0510
B	0.0000
C	0.1210
D	0.0000
E	0.0000
F	0.0292
G	0.6486
INCOMPLETE RECOVERY Subject	
A'	0.9534
B'	0.7423
C'	0.0197
D'	0.9990
E'	0.7630
F'	0.0035

Table 8.4. Chi-squared probability values between the observed and expected values using a simple probability model based upon the number of stimulus locations still to exhibit a 90% recovery from baseline as a function of the two sub-samples of patients.

SUB-SAMPLE	Estimated recovery field	Observed recovery/residual loss field
COMPLETE RECOVERY Subject		
A	37	7
B	6	5
C	74	7
D	15	8
E	6	7
F	4	4
G	2	7
INCOMPLETE RECOVERY Subject		
A'	74	9
B'	8	6
C'	4	6
D'	37	7
E'	8	6
F'	3	8

Table 8.5. The estimated and observed field at which the best recovery to 90% of the baseline sensitivity occurred.

locations exhibit their most rapid phase of recovery. The estimate is based upon a probability value derived from recovery in the first instance, which may not necessarily coincide with the most rapid phase. Similarly, a better level of agreement is reached between the estimated and observed values when these two time periods are coincident.

8.5. Discussion.

The choice of the Gaussian cumulative curve over the Formation curve to describe the natural evolution of the recovery of the global field and of the individual stimulus locations was based upon the coefficient of determination of the respective functions. Clearly, the Formation curve offers a greater number of degrees of freedom as a two parameter function than does the three parameter Gaussian cumulative curve. However, the commencement of the recovery in optic neuritis is often not immediate. The relative inability of the Formation curve to model the recovery when it begins at a later stage was the essential difference between the two functions. The difference between the two models might perhaps be reduced in a sample of patients receiving intravenous corticosteroid treatment as the onset of the recovery phase in these patients is accelerated (Beck 1992; Beck et al. 1992; Beck et al. 1993a; Beck et al. 1993b; Trobe 1994).

The more rapid slope of recovery at the peripheral locations exhibited by the complete recovery group is in agreement with previous perimetric findings. A more rapid improvement of the peripheral sensitivity than the central sensitivity over the time to follow-up has previously been found in patients with a similar initial field loss (Grochowicki et al. 1993). Such a trend was not apparent in the incomplete recovery sub-sample and might not be discernible as a result of their residual visual field defects. That is, a stimulus location exhibiting poor recovery over the time to follow-up will, implicitly, be of lower sensitivity than a location exhibiting good recovery. Such a location may therefore exhibit greater measurement variability (ie. local short-term fluctuation), which will be further increased if the stimulus location is situated at the edge of the field. The magnitude of the measurement variability constitutes the major factor in the fit, level of recovery and slope of the Gaussian cumulative function.

In the sub-sample exhibiting complete recovery, the individual stimulus locations showed a similar magnitude of recovery across the visual field and a steeper slope of recovery at the peripheral stimulus locations. The larger magnitude of the level of recovery for the MD against time to follow-up in comparison to that of the individual stimulus locations may be the result of a smoothing effect caused by the averaging of the different slopes at individual stimulus locations by the MD. In the sub-sample of patients exhibiting incomplete recovery, the individual stimulus locations also showed a similar slope of recovery across the visual field, but showed a smaller magnitude of recovery and greater variability at the peripheral locations. The smoothing by the MD was therefore less pronounced for this sub-sample.

The Gaussian cumulative functions for the MD recovery of the two patients exhibiting a moderate, localised residual field loss departed from the corresponding functions for the complete recovery sub-sample and for the patients with a diffuse or minimal localised residual loss. This finding could be used as a simple technique of forecasting a moderate (or severe) localised residual loss in a patient presenting with optic neuritis. By comparing the magnitude of the MD at each time period with the Gaussian cumulative functions derived from patients exhibiting complete recovery, a moderate or severe localised defect could be revealed at or before approximately thirty days of follow-up.

Both the Formation and the Gaussian cumulative functions represent complex non-linear equations. The number of terms in each function require that a minimum of nine visual field examinations must be undertaken in order to obtain a reasonable description of the data. It is likely that an episode of optic neuritis will exhibit some or even complete recovery over the time to follow-up incorporated by nine examinations. The probability model was devised in order that a forecast from a smaller number of fields could be made.

The probability distribution model exhibited reasonable agreement with the observed outcome in the incomplete recovery group. Subject F' exhibited the greatest departure from the model and the unsystematic nature of recovery in this patient is reflected in the residual field defect. In the complete recovery group, the disagreement between the estimated and observed values results from an inappropriate estimation of p. The agreement between the estimated

field of recovery in both patient groups was moderate. The estimated field of recovery represents an average expression of the recovery and, in addition, includes the assumption that the probability of recovery is similar at all stimulus locations in the visual field. The variance associated with the value of the estimated field of recovery would account for some of the differences between the estimated and observed values. Both the probability distribution models would, however, benefit from refinement that reflected the delay between the presentation of visual symptoms and the rapid phase of recovery.

8.6. Conclusion.

The Gaussian cumulative curve offered the best description, based upon the coefficient of determination, of the MD and pointwise recovery in sensitivity over time to follow-up. Subjects showing complete recovery as classified by the VFRC appeared to exhibit a more rapid slope of recovery at the peripheral stimulus locations than at the central stimulus locations. Subjects with incomplete recovery did not exhibit such a trend. A comparison of the percentage recovery of the MD at each examination with the corresponding Gaussian cumulative function of subjects exhibiting complete recovery presents a promising method of forecasting the likelihood of a moderate or severe residual localised loss at the final examination.

CHAPTER 9: GENERAL SUMMARY OF RESULTS AND CONCLUSIONS AND FUTURE WORK.

9.1. Summary of results and conclusions.

9.1.1. Long-term fluctuation (LF).

There is a pressing need to evaluate the LF(Ho) and the LF(He), in order to separate fluctuation from visual field progression. The computational complexities of the calculation have resulted in the publication of a number of simpler measures which do not truly express the LF. The development of advanced microprocessors and their utilisation in automated perimeters will enable the LF to be routinely quantified.

The homogeneous and heterogeneous components of the LF were calculated between a pair of HFA examinations in a stable glaucomatous population over a long follow-up period (6-9 months) and, for a separate sample, over a short follow-up period (3 weeks). The two LF components were derived from the between-examination variation exhibited by the ten standard double determinations common between the pair of examinations using a 2-Factor ANOVA with replications.

The magnitude of the homogeneous component, LF(Ho), and of the heterogeneous component, LF(He), in the stable glaucomatous population were larger than previously reported. The LF(Ho) ranged between 2.4dB and 3.3dB, and the LF(He) between 3.0dB and 3.7dB across the two time periods. Both components were essentially independent of the depth of visual field loss. However, both the LF(Ho) and LF(He) were greater over the short follow-up period than over the long follow-up period.

The LF is a confounding factor in the identification of visual field progression. The short-term fluctuation (SF) describes the degree of within-examination variation and confounds the interpretation of a single examination. Both the LF components showed little relationship with the SF. The magnitude of the LF between a pair of fields cannot, therefore, be estimated from the extent of the SF at each individual examination.

The LF(Ho) and the LF(He) exhibited stability between two consecutive pairs of fields in the stable glaucomatous population. By using the 90% confidence limits of the LF, the essential separation of visual field fluctuation from progression can be achieved avoiding the necessity of numerous confirmatory follow-up examinations.

9.1.2. Between-examination variability as a function of the thresholding algorithm.

The Standard and FASTPAC strategies are two staircase algorithms incorporated in the HFA and both are in common clinical use. The between-examination variability for each strategy was described by the 5% and 95% confidence limits of the change in defect depth between-examinations, expressed as a function of defect depth at that location for the first examination of the pair. The FASTPAC algorithm exhibited wider confidence limits than the Standard strategy across the range of sensitivities measured by the HFA. In addition, the FASTPAC strategy exhibited wider confidence intervals at all eccentricities out to 30° than the Standard strategy. In both the Standard and FASTPAC algorithms, the greatest change in sensitivity between-examinations was evident at stimulus locations whose sensitivity deviated from the normal sensitivity by between 10dB and 26dB.

The magnitude of the difference between the algorithms was approximately 2dB. This finding may be attributed to the difference in the staircase strategy employed and to the categorisation of the between-examination variability into 2dB intervals. The magnitude of the 2dB difference between the algorithms does, however, have little implication in the delineation of visual field progression in glaucoma. In terms of the between-examination variability, the Standard and FASTPAC strategies can, clinically, be considered the same.

9.1.3. Glaucoma Change Probability Analysis.

By positioning the second baseline to the most immediate pair of fields at which a stimulus location exhibited deterioration from the first baseline, progressive loss from the second baseline was able to be identified in seven of sixteen primary open angle glaucoma patients. The seven patients all showed at least one pair of clustered stimulus locations exhibiting progressive loss.

Across the sample of sixteen patients as a whole, the majority of stimulus locations exhibiting progressive loss with the first baseline showed stability with the second baseline. Localised learning was evident in a proportion of stimulus locations at the second baseline, but these locations tended to be isolated and occurred less often per patient than stimulus locations exhibiting progressive loss.

Currently, the baseline of the GCPA is moved for the visual field as a whole. This operation has negative implications in delineating visual field progression at the earliest opportunity for any stimulus locations undergoing progressive loss within the limits of the GCPA database. Maintaining the first baseline despite the existence of progressive loss at one or more stimulus locations limits the identification of further progressive loss at these locations. Repositioning the GCPA baseline on a pointwise basis for adjacent stimulus locations that exhibit progressive loss at the first baseline would allow identification of progressive loss at the second baseline.

9.1.4. Univariate linear regression.

Univariate linear regression (ULR) of MD against time to follow-up was insensitive to clustered pairs of stimulus locations exhibiting progressive loss identified by pointwise absolute sensitivity ULR against time to follow-up and by pointwise pattern deviation ULR against time to follow-up. This indicates that pointwise ULR against time to follow-up is able to identify small localised changes in sensitivity, whilst the ULR of MD against time to follow-up principally identifies a global reduction in visual field height.

The ability of absolute sensitivity ULR to model the normal decline in sensitivity with age over time to follow-up increased as the number of visual field examinations increased. This was due to a reduction in the influence of the local SF when a greater number of examinations were used to derive the regression coefficient.

The agreement between the pointwise absolute sensitivity ULR against time to follow-up and the GCPA was greater when the slope of the decline in sensitivity with age was five times greater than the normal rate of decline with age. Both the pointwise absolute sensitivity and the

pointwise pattern deviation ULR analyses against time to follow-up identified stimulus locations with progressive loss that were not identified by the GCPA. These stimulus locations exhibited a small, but significant, reduction in sensitivity that lay within the bounds of the GCPA criteria for progressive loss. With good quality data, the ULR technique is able to identify small, uniform reductions in sensitivity earlier than the GCPA. With cases of either moderate or large degrees of variability, the GCPA is able to detect progressive loss; however, the ULR may be unable to fit the data unless the slope of decline is steep. The application of the ULR technique would prove particularly useful if applied to visual fields with high overall sensitivity that tend to exhibit less variability (eg. suspect glaucoma), thus enabling progressive loss to be identified by ULR at the earliest opportunity.

The data frequently exhibited a curvilinear decline in sensitivity. Indeed, the pattern deviation values were more likely to show a curvilinear than a constant decline in sensitivity over the time to follow-up. In addition to the outcome of ULR based upon the entire series of fields, consideration of the most immediate six fields would enhance the detection of a curvilinear decline in sensitivity.

9.1.5. Pointwise multivariate forecasting of visual field progression in glaucoma.

For a series of five examinations, the pointwise multivariate technique forecasted the sensitivity at each stimulus location of the third, fourth and fifth examinations based upon the sensitivity at the given location at the previous two examinations. At each forecasted examination, the magnitude of the percentage error between the forecasted sensitivity and the measured sensitivity described the accuracy of the multivariate model. The 95% confidence limit of the forecasted percentage error was derived from five examinations of 23 normal subjects. The magnitude of this confidence limit showed good agreement with the forecasted percentage errors found in 12 ocular hypretensive patients.

In glaucomatous patients, a weighting function was applied to the 95% confidence limit derived from the normal subjects in order to account for the increased variability encountered at stimulus locations of reduced sensitivity. The agreement between the multivariate forecasting of progression and that of the GCPA was compared. Little agreement between the two

techniques was found, both in a stable and in a progressing sample of glaucomatous patients. The magnitude of the abnormal percentage errors of the multivariate technique increased as the sensitivity at the given stimulus location decreased, particularly at sensitivities of less than 16dB. The lack of agreement between the multivariate technique and the GCPA might be attributable to an inadequate weighting function which did not sufficiently describe the degree of variability typically exhibited by glaucomatous patients. In its current form therefore, the multivariate model would best be applied to the follow-up of ocular hypertensive patients and to regions of high sensitivity in glaucomatous subjects.

9.1.6. Modelling of the visual field in optic neuritis.

The recovery of the sensitivity of the global visual field and at individual stimulus locations in optic neuritis was well described by the Gaussian cumulative function. Two of 6 patients exhibiting incomplete recovery had a residual field loss that involved one or more quadrants. The recovery of the MD against time to follow-up in these two patients showed the greatest departure from the shape of the Gaussian cumulative functions fitted to the MD against time to follow-up in patients showing complete recovery. The likelihood of a residual field defect being present at the next visit could be determined by comparing the magnitude of the MD at each time period with the average cumulative Gaussian function derived from patients exhibiting complete recovery.

The pointwise slope of the recovery modelled by the cumulative Gaussian function increased with an increase in eccentricity in patients exhibiting complete recovery of the visual field. Patients exhibiting a residual visual field defect after the time of follow-up did not exhibit an increase in the slope of recovery with increasing eccentricity.

The probability model exhibited reasonable agreement between the modelled and observed outcome in the sample exhibiting incomplete recovery. The agreement between the model and the observed outcome in those exhibiting complete recovery was less good. Both samples exhibited a moderate degree of agreement between the forecasted field of best recovery and the observed field of recovery. The estimate of the probability (p) that a stimulus location has still to exhibit recovery was determined at the first field at which any recovery was shown. The

most rapid phase of recovery of the sensitivity occurred at the next most immediate field. Inconsistencies between the model and the observed outcome were attributable to the estimate of p inaccurately reflecting the time period at which the rapid phase of recovery occurred.

9.2. Future work.

9.2.1. Long-term fluctuation.

Short-wavelength automated perimetry (SWAP) is increasingly being used in the follow-up of glaucoma (Johnson et al. 1993b; Sample & Weinreb 1992) and neuro-ophthalmic disorders (Keltner & Johnson 1995). The variability of the sensitivity measure is greater with the SWAP technique than with conventional white-on-white perimetry (Wild et al. 1996). The magnitude of the LF in SWAP is unknown. The separation of fluctuation from progression assumes particular importance as no objective statistical procedures for delineating visual field progression have yet been developed.

9.2.2. Between-examination variability as a function of thresholding algorithm.

The described technique of between-examination variability provides a useful insight into the magnitude of variability across the range of sensitivities measured by the perimeter. The mathematical artefact arising from the stratification of the sensitivity into 2dB intervals at the first of a pair of examinations may be removed by considering single decibel intervals. Consideration of single decibel intervals has been limited by the number of sensitivity values contained within each interval. This may be facilitated by the use of re-sampling techniques such as bootstrapping within each sensitivity interval.

The development of rapid thresholding algorithms has improved the efficiency of a perimetric examination by reducing its duration. This is particularly true of the variable step size staircase procedures (Weber 1990). There is concern that the increase in efficiency is at the cost of reduced accuracy. Evaluation of the between-examination variability would provide a measure repeatability and enable the performance of the newer algorithms to be compared with existing techniques.

9.2.3. Glaucoma change probability.

The GCPA analysis provides a satisfactory method of delineating visual field progression, particularly in the areas showing large degrees of variability. Automation of the baseline movement at single stimulus location would enhance the ability of the GCPA to determine progressive visual field loss. The need for this procedure becomes more pronounced as the number of visual field examinations for a given individual increases.

The criteria for change of the GCPA is based upon the total deviation at a stimulus location. The total deviation measure does not differentiate the amount of reduction (or improvement) in sensitivity that is common between all stimulus locations of the visual field. A modified GCPA analysis based upon the pattern deviation measure would improve the detection of localised visual loss. Since localised visual field of loss is of primary interest in the detection and the follow-up of glaucoma, this enhancement of the technique would prove extremely useful.

9.2.4. Univariate linear regression.

The univariate linear regression technique is limited by the extent of measurement error (SF) exhibited in glaucoma. Future work might centre upon the use of ULR on data which has undergone spatial filtering procedures (Crabb et al. 1995; Fitzke et al. 1995). The combination of ULR and spatial filtering techniques could prove to be of particular benefit when the minimum number of examinations (six) are used. A smoothed data set would produce less variation around the regression line and therefore enhance the identification of a significant reduction in sensitivity.

9.2.5. Multivariate forecasting of visual field progression in glaucoma.

The major confounding factor in delineating visual field progression is the inherent 'noise' in the measurement of sensitivity, particularly in glaucoma. The inability of the multivariate technique to model the sensitivity over time in the presence of the degree of variability in this patient group represents its principle drawback. However, the model does appear to be effective in patient groups, such as ocular hypertensives, whose fields are of high sensitivity and, as a consequence, largely exhibit less variability. Future work would involve investigation

of the ability of the multivariate technique to determine visual field progression in ocular hypertensive subjects who, retrospectively, convert to glaucoma.

Modification of the 95% confidence limit is required to enhance the utility of the technique in glaucomatous subjects. This might best be achieved by establishing the values of the 95% confidence limit of the forecast error at each stimulus location of stable glaucomatous patients, rather than that of normal subjects.

9.2.6. Modelling of the visual field in optic neuritis.

The pilot study into techniques to model the recovery of the sensitivity in optic neuritis enabled the development of two techniques. Future work would involve the evaluation of the Gaussian cumulative technique and the probability model both in different treatment groups and in patient groups with an initial field defect other than severe diffuse loss. The increase in the patient sample would enable statistical analysis to be undertaken in order to determine differences between the patient groups. The knowledge gained from the patients who do not exhibit subsequent attacks of sensitivity reduction after the baseline field may also prove useful in differentiating patients susceptible to recurrent episodes of optic neuritis.

REFERENCES

Peridata manual. (v. 6.3α). Interzeag AG, Schlieren, Switzerland.

Abrahamsson M. and Sjöstrand J. (1986). Impairment of contrast sensitivity function (CSF) as a measure of disability glare. *Invest Ophthalmol Vis Sci* 27:1131-1136.

Adler F.H. (1987). *Adler's physiology of the eye.* Eds: R. A. Moses and W. M. Hart. Mosby, St Louis.

Advanced Glaucoma Intervention Study (A.G.I.S.). (1994). Advanced Glaucoma Intervention Study. 2. Visual field test scoring and reliability. *Ophthalmology* 101:1445-1455.

Airaksinen P.J., Drance S.M. and Douglas G.R. (1985a). Diffuse and localised nerve fiber loss in glaucoma. *Am J Ophthalmol* 99:107-110.

Airaksinen P.J., Drance S.M., Douglas G.R. and Schulzer M. (1985b). Neuroretinal rim areas and visual field indices in glaucoma. *Am J Ophthalmol* 99:107-10.

Airaksinen P.J., Drance S.M., Douglas G.R., Schulzer M. and Wijsman K. (1985c). Visual field and retinal nerve fiber layer comparisons in glaucoma. *Arch Ophthalmol* 103:205-7.

Airaksinen P.J., Drance S.M. and Schulzer M. (1985d). Neuroretinal rim area in early glaucoma. *Am J Ophthalmol* 99:1-4.

Alter M., Good J. and Okihiro M. (1973). Optic neuritis in Orientals and Caucasians. *Neurology* 23:631-639.

Anctil J.L. and Anderson D.R. (1984). Early foveal involvement and generalized depression of the visual field in glaucoma. *Arch Ophthalmol* 102:363-370.

Anderson D.R., Feuer W.J., Alward W.L. and Skuta G.L. (1989). Threshold equivalence between perimeters. *Am J Ophthalmol* 107:493-505.

Anderson D.R. (1992a). Basis of quantatative perimetry. *Automated static perimetry.* Ed: K. Kist. Mosby-Year Book Inc., St. Louis. pp.10-29.

Anderson D.R. (1992b). Introductory Concepts. *Automated static perimetry.* Ed: K. Kist. Mosby-Year Book Inc., St Louis. pp. 2-9.

Araujo D., Schwartz B., Takamoto T., Wu D.C. and Manning M. (1987). The relationship of the rate of change of visual fields to the first visual field. *Invest Ophthalmol Vis Sci* 28:269.

Armaly M.F. (1971). Visual field defects in early open angle glaucoma. *Trans Am Ophthalmol Soc* 69:147-162.

Åsman P., Britt J.M., Mills R.P. and Heijl A. (1988). Evaluation of adaptive spatial enhancement in suprathreshold visual field screening. *Ophthalmology* 95:1656-1662.

Åsman P. (1992). Computer-assisted interpretation of visual fields in glaucoma. *Acta Ophthalmol* 70(Suppl 206):1-47.

Åsman P. and Heijl A. (1992a). Evaluation of methods for automated Hemifield analysis in perimetry. *Arch Ophthalmol* 110:820-6.

Åsman P. and Heijl A. (1992b). Glaucoma Hemifield Test. Automated visual field evaluation. *Arch Ophthalmol* 110:812-9.

Åsman P., Heijl A., Olsson J. and Rootzen H. (1992). Spatial analyses of glaucomatous visual fields; a comparison with traditional visual field indices. *Acta Ophthalmol* 70:679-86.

Åsman P., Olsson J. and Heijl A. (1993). Learner's Index (LI) to detect low perimetric experience. *Invest Ophthalmol Vis Sci.* 34(suppl):1262.

Åsman P. and Heijl A. (1993). Arcuate cluster analysis in glaucoma perimetry. *J Glaucoma* 2:13-20.

Åsman P. and Heijl A. (1994). Diffuse visual field loss and glaucoma. *Acta Ophthalmol* 72:303-8.

Åsman P. (1995). Color-coded probability maps: separation of field defect types. *Perimetry Update. 1994/95.* Proceedings of the XIth International Perimetric Society Meeting. Eds: R. P. Mills and M. Wall. Amsterdam & New York. Kugler. pp. 57-58.

Åsman P. and Heijl A. (1995). Is there always reduced sensitivity in the entire visual field in patients with glaucoma? *Vis Res* 35(suppl):S63.

Åsman P., Bengtsson B.M. and Heijl A. (1995). Linear regression analysis in glaucoma: separation of local and diffuse visual field deterioration. *Invest Ophthalmol Vis Sci.* 36 (suppl):S170.

Atchison D.A. (1979). History of visual field measurement. *Aust J Optom* 62:345-354.

Atchison D.A. (1987). Effect of defocus on visual field measurement. *Ophthalmic Physiol Opt* 7:259-65.

Augustiny L. and Flammer J. (1985). The influence of artificially induced visual field defects on the visual field indexes. *Doc Ophthalmol Proc Ser 42.* Proceedings of the Sixth International Visual Field Symposium. Eds: A. Heijl and E. L. Greve. Dordrecht. Dr W. Junk. pp.55-67.

Aulhorn E. (1969). Glaukom-Geisichtsfeld. *Ophthalmologica* 158:469-487.

Aulhorn E. and Harms H. (1972). Visual perimetry. *Visual psychophysics: Handbook of sensory physiology.* Eds: D. Jameson and L. M. Hurvich. Springer-Verlag, Berlin. VII. pp.102-145.

Autzen T. and Work K. (1990). The effect of learning and age on short-term fluctuation and mean sensitivity of automated static perimetry. *Acta Ophthalmol* 68:327-330.

Baez K.A., McNaught A.I., Fowler J.G.F., Poinoosawmy D., Fitzke F.W. and Hitchings R.A. (1995). Motion detection thresholds and field progression in normal tension glaucoma. *Br J Ophthalmol* 79:125-128.

Bahill A.T., Brockenbrough A. and Troost B.T. (1981). Variability and development of a normative data base for saccadic eye movements. *Invest Ophthalmol Vis Sci* 21:116-125.

Ball K. and Sekular R. (1980). Models of stimulus uncertainty in motion perception. *Psychol Rev* 87:435-469.

Baloh R.W., Sills A.W., Kumley W.E. and Honrubia V. (1975). Quantatative measurement of saccadic amplitude, duration and velocity. *Neurology* 25:1065-1070.

Barlow H.B. (1958). Temporal and spatial summation in human vision at different background intensities. *J Physiol* 141:337-350.

Barlow H.B. (1972). Dark and light adaptation: Psychophysics. *Visual Psychophysics: Handbook of sensory physiology.* Eds: D. Jameson and L. M. Hurvich. Springer-Verlag, Berlin, New York. VII. pp.1-28.

Bassi C.J. and Lehmkuhle S. (1990). Clinical implications of parallel visual pathways. *J Am Optom Assoc* 61:98-110.

Bebié H., Fankhauser F. and Spahr J. (1976). Static perimetry: accuracy and fluctuations. *Acta Opthalmol* 54:339-348.

Bebié H. and Fankhauser F. (1981a). *Program Delta manual.* Interzeag AG. Schlieren, Switzerland.

Bebié H. and Fankhauser F. (1981b). Statistical program for the analysis of perimetric data. *Doc Ophthalmol Proc Ser 26.* Proceedings of the Fourth Visual Field Symposium. Eds: E. L. Greve and G. Verriest. The Hague. Dr W. Junk. pp.9-10.

Bebié H. (1985). Computerized techniques of visual field analysis. *Automatic perimetry in glaucoma. A practical guide.* Eds: S. M. Drance and D. Anderson. Grune & Stratton, Orlando. pp.147-160.

Bebié H., Flammer J. and Bebié T. (1989). The cumulative defect curve : separation of local and diffuse components of visual field damage. *Graefe's Arch Clin Exp Ophthalmol* 227:9-12.

Beck R.W. (1988). The optic neuritis treatment trial. *Arch Ophthalmol* 106:1051-1053.

Beck R.W. (1992). Corticosteroid treatment of optic neuritis: a need to change treatment practices. *Neurology* 42:1133-1135.

Beck R.W., Cleary P.A., Anderson M.M. and O.N.G.S. (1992). A randomized, controlled trial of corticosteroids in the treatment of optic neuritis. *N Engl J Med* 326:581-588.

Beck R.W., Cleary P.A. and O.N.S.G. (1993a). Optic Neuritis Treatment Trial: one-year follow-up results. *Arch Ophthalmol* 111:773-775.

Beck R.W., Cleary P.A., Trobe J.D. and O.N.S.G. (1993b). The effect of corticosteroids for acute optic neuritis on the subsequent development of multiple sclerosis. *N Engl J Med* 329:1764-1769.

Beck R.W. and O.N.S.G. (1995). The Optic Neuritis Treatment Trial: three-year follow-up results. *Arch Ophthalmol* 113:136-137.

Bennett G.R., Werner E.B. and Seraydarian L. (1991). Correlation of reliability indices and test-retest reproducibility in normal subjects undergoing automated perimetry on the Humphrey Visual Field Analyzer. *Perimetry Update 1990/91.* Proceedings of the IXth International Perimetric Society Meeting. Eds: R. P. Mills and A. Heijl. Amsterdam, New York & Milano. Kugler & Ghedini. pp.211-215.

Bettleheim F.A. and Ali S. (1985). Light scattering of normal human lens III. Relationship between forward and backscatter of whole excised lenses. *Exp Eye Res* 41:1-9.

Bickler-Bluth M., Trick G.L., Kolker A.E. and Cooper D.G. (1989). Assessing the utility of reliability indices for automated visual fields. Testing ocular hypertensives. *Ophthalmology* 96:616-619.

Birch M.K., Wishart P.K. and O'Donnell N.P. (1995). Determining progressive visual field loss in serial Humphrey visual fields. *Ophthalmology* 102:1227-1235.

Bland J.M. and Altman D.G. (1986). Statistical methods for assessing agreement between two methods of clinical measurement. *Lancet* 307-310.

Boeglin R.J., Caprioli J. and Zulauf M. (1992). Long-term fluctuation of the visual field in glaucoma. *Am J Ophthalmol* 113:396-400.

Brechner R.J. and Whalen W.R. (1984). Creation of the transformed Q statistic probability distribution to aid in the detection of abnormal computerized visual fields. *Ophthalmic Surgery* 15:833-836.

Brenton R.S. and Phelps C.D. (1981). The normal visual field on the Humphrey Field Analyzer. *Ophthalmologica* 193:56-74.

Brenton R.S. and Argus W.A. (1987). Fluctuations on the Humphrey and Octopus perimeters. *Invest Ophthalmol Vis Sci* 28:767-771.

Brusini P., Nicosia S. and Weber K. (1991). Automated visual field management in glaucoma with the PERIDATA program. *Perimetry Update 1990/91*. Proceedings of the IXth International Perimetric Society Meeting. Eds: R. P. Mills and A. Heijl. Amsterdam, New York & Milano. Kugler & Ghedini. pp.273-277.

Caprioli J. and Spaeth G.L. (1985). Static threshold examination of the peripheral nasal visual field in glaucoma. *Arch Ophthalmol* 103:1150-1154.

Cascairo M.A., Stewart W.C. and Sutherland S.E. (1991). Influence of missed catch trials on the visual field in normal subjects. *Graefe's Arch Clin Exp Ophthalmol* 229:437-441.

Cassidy J. and Flanagan J.G. (1989). HFA Tools©. *Microsystems Technology*. Waterloo, Ontario, Canada.

Casson E.J., Shapiro L.R. and Johnson C.A. (1990). Short-term fluctuation as an estimate of variability in visual field data. *Invest Ophthalmol Vis Sci* 31:2459-2463.

Casson E.J., Zackon D.H., Shillingford-Ricketts H. and Lafontaine M. (1995). Changes in spatial summation and SKD in the normal ageing eye. *Perimetry Update 1994/95.* Proceedings of the XIth International Perimetric Society Meeting. Eds: R. P. Mills and M. Wall. Amsterdam & New York. Kugler. pp.65-69.

Celesia G.G., Kaufman D.O., Brigel M., Toleikis S., Kokinakis D., Lorance R. and Lizano B. (1990). Optic neuritis: a prospective study. *Neurology* 40:919-923.

Chamlin M. (1953). Visual field changes in optic neuritis. *Arch Ophthalmol* 50:699-713.

Chauhan B.C., Henson D.B. and Hobley A.J. (1988). Cluster analysis in visual field quantification. *Doc Ophthalmol* 69:25-39.

Chauhan B.C., Drance S.M. and Lai C. (1989a). A cluster analysis for threshold perimetry. *Graefe's Arch Clin Exp Ophthalmol* 227:216-220.

Chauhan B.C., Henson D.B. and Hobley A.J. (1989b). Cluster analysis in suprathreshold perimetry. *Perimetry Update 1988/89.* Proceedings of the VIIIth International Perimetric Society Meeting. Ed: A. Heijl. Amsterdam, Berkeley & Milano. Kugler & Ghedini. pp.217-221.

Chauhan B.C., Drance S.M. and Douglas G.R. (1990a). The use of visual field indices in detecting changes in the visual field in glaucoma. *Invest Ophthalmol Vis Sci* 31:512-520.

Chauhan B.C., House P.H. and Drance S.M. (1990b). A study of intra-test variability in conventional and high-pass resolution perimetry. *Invest Ophthalmol Vis Sci* 30:15.

Chauhan B.C., LeBlanc R.P., Drance S.M., Wijsman K. and Cruz A.M. (1991). Effect of the number of threshold determinations on short-term fluctuation in automated perimetry. *Ophthalmology* 98:1420-1424.

Chauhan B.C., Mohandas R.N., Whelan J.H. and McCormick T.A. (1993a). Comparison of reliability indices in conventional and high-pass resolution perimetry. *Ophthalmology* 100:1089-1094.

Chauhan B.C., Tompkins J.D., LeBlanc R.P. and McCormick T.A. (1993b). Characteristics of frequency-of-seeing curves in glaucoma. *Perimetry Update 1992/93.* Proceedings of the Xth International Perimetric Society Meeting. Ed: R. P. Mills. Amsterdam & New York. Kugler. pp.543-549.

Chauhan B.C., Tompkins J.D., LeBlanc R.P. and McCormick T.A. (1993c). Characteristics of frequency-of-seeing curves in normal subjects, patients with suspected glaucoma, and patients with glaucoma. *Invest Ophthalmol Vis Sci* 34:3534-3540.

Chen J.C., Fitzke F.W. and Bird A.C. (1990). Long-term effect of acetazolamide in a patient with retinitis pigmentosa. *Invest Ophthalmol Vis Sci* 31:1914-1918.

Collin H.B., Han C. and Khor P.C. (1988). Age changes in the visual field using the Humphrey Field Analyzer. *Clin Exp Optom* 71:174-178.

Cornsweet T.N. (1962). The staircase method in psychophysics. *Am J Psychol* 75:485-491.

Crabb D.P., Edgar D.F., Fitzke F.W., McNaught A.I. and Wynn H.P. (1995). New approach to estimating variability in visual-field data using an image-processing technique. *Br J Ophthalmol* 79:213-217.

Crosswell H.H., Stewart W.C., Cascairo M.A. and Hunt H.H. (1991). The effect of background intensity on the components of fluctuation as determined by threshold-related automated perimetry. *Graefe's Arch Clin Exp Ophthalmol* 229:119-122.

Dalenbach K. (1966). The staircase-method critically examined. *Am J Psychology* 79:654-656.

Dannheim F. and Drance S.M. (1971). Studies of temporal summation of central areas in normal people of all ages. *Ophthalmic Res* 2:295-303.

Davson H. (1980a). *Physiology of the eye.* Churchill Livingstone, Edinburgh/London/New York. pp. 395-396.

Davson H. (1980b). *Physiology of the eye.* Churchill Livingstone, Edinburgh/London/New York. pp. 167-177.

de la Rosa M.G., Reyes J.A. and Sierra M.A.G. (1990). Rapid assessment of the visual field in glaucoma using an analysis based on multiple correlations. *Graefe's Arch Clin Exp Ophthalmol* 228:387-391.

de Waard P.W.T., Ijspeert J.K., van den Berg T.J.T.P. and de Jong P.T.V.M. (1992). Intraocular light scattering in age-related cataracts. *Invest Ophthalmol Vis Sci* 33:618-625.

Demirel S. and Vingrys A.J. (1995). Acceptable false response rates for reliable perimetric outcomes. *Perimetry Update 1994/95.* Proceedings of the XIth International Perimetric Society Meeting. Eds: R. P. Mills and M. Wall. Amsterdam & New York. Kugler. pp. 83-88.

Dengler-Harles M., Wild J.M., Cole M.D., O'Neill E.C. and Crews S.J. (1990). The influence of forward light scatter on visual field indices in glaucoma. *Graefe's Arch Clin Exp Ophthalmol* 228:326-331.

Dengler-Harles M., Wild J.M., Cole M.D. and O'Neill E.C. (1993). The influence of stimulus parameters on the visual field indices by automated projection perimetry. *Graefe's Arch Clin Exp Ophthalmol* 231:337-343.

Derrington A.M. and Lennie P. (1984). Spatial and temporal contrast sensitivities of neurons in lateral geniculate nucleus of the macaque. *J Physiol* 357:219-240.

Desjardins D. and Anderson D.R. (1988). Threshold variability with an automated LED perimeter. *Invest Ophthalmol Vis Sci* 29:915-921.

Drance S.M., Wheeler C. and Patullo M. (1967). The use of static perimetry in the early detection of glaucoma. *Can J Ophthalmol* 2:249-258.

Drance S.M. (1991). Diffuse visual field loss in open-angle glaucoma. *Ophthalmology* 98:1533-1538.

Drummond P.D. and Anderson M. (1992). Visual field loss after attacks of migraine with aura. *Cephalalgia* 12:349-352.

Duggan C., Sommer A., Auer C. and Burkhard K. (1985). Automated differential threshold perimetry for detecting glaucomatous visual field loss. *Am J Ophthalmol* 100:420-423.

Edgar G.K., Foster D.H., Honan W.P., Heron J.R. and Snelgar R.S. (1990). Optic neuritis: variations in temporal modulation sensitivity with retinal eccentricity. *Brain* 113:487-496.

Efron B. and Tibshirani R. (1993). An introduction to the bootstrap. *Monographs on Statistics and Applied Probability*. Chapman & Hall, Cambridge.

Eizenman M., Buys Y.M., Nadler M. and Trope G.E. (1993). Increase of short-term fluctuation at the slope of a scotoma. *Invest Ophthalmol Vis Sci* 34:1263.

Elder M.J. (1992). Diazepam and Its Effects On Visual-Fields. *Aus NZ J Ophthalmol* 20:267-270.

Elliott D.B., Hurst M.A. and Weatherill J. (1990). Comparing Clinical-Tests Of Visual Function In Cataract With the Patients Perceived Visual Disability. *Eye* 4:712-717.

Enger C. and Sommer A. (1987). Recognizing glaucomatous field loss with the Humphrey STATPAC. *Arch Ophthalmol* 105:1355-1357.

Fankhauser F. and Schmidt T. (1958). Die unterschung der raümlichen summation mit stehender und bewegter reizmarke nach der methode der quantitativen lichtsunn perimetrie. *Ophthalmologica* 135:409-423.

Fankhauser F. and Schmidt M. (1960). Die optimalen Bedingungen für die Untersuchung der raümlichen Summation mit stehender Reizmarke nach der Methode der quantitaven Lichtsinnperimetrie. *Ophthalmologica* 139:409-423.

Fankhauser F. (1969). Kinetisch Perimetrie. *Ophthalmologica* 158:406-418.

Fankhauser F., Koch P. and Roulier A. (1972). On automation of perimetry. *Albrecht v Graefe's Arch Klin Exp Ophthalmol* 184:126-150.

Fankhauser F., Spahr J. and Bebié H. (1977). Some aspects of automated perimetry. *Ophthalmology* 22:131-141.

Fankhauser F. (1979). Problems related to the design of automatic perimeters. *Doc Ophthalmol* 47:89-138.

Fankhauser F. and Bebié H. (1979). Threshold fluctuations, interpolations and spatial resolution in perimetry. *Doc Ophthalmol Proc Ser. 19.* Proceedings of the Third International Visual Field Symposium. Ed: E. L. Greve. The Hague. Dr W. Junk. pp.295-309.

Fankhauser F. and Haeberlin H. (1980). Dynamic range and straylight. *Doc Ophthalmol* 50:143-167.

Fankhauser F. (1986). Background illumination and automated perimetry. *Arch Ophthalmol* 104:1126.

Fankhauser F., Funkhouser A. and Kwasniewska S. (1986a). Evaluating the applications of the spatially adaptive program (SAPRO) in clinical perimetry : Part I. *Ophthalmic Surg* 17:338-342.

Fankhauser F., Funkhouser A. and Kwasniewska S. (1986b). Evaluating the applications of the spatially adaptive program (SAPRO) in clinical perimetry : Part II. *Ophthalmic Surg* 17:415-428.

Fankhauser F., Bebié H. and Flammer J. (1988). Threshold fluctuations in the Humphrey Field Analyzer and in the Octopus automated perimeter. *Invest Ophthalmol Vis Sci.* 29:1466.

Fankhauser F. (1993). Influence of missed catch trials on the visual field in normal subjects. *Graefe's Arch Clin Exp Ophthalmol* 231:58-59.

Fankhauser F.I., Fankhauser F.H. and Giger H. (1993). A cluster and scotoma analysis based on empiric criteria. *Graefe's Arch Clin Exp Ophthalmol* 231:697-703.

Feeny S., Kaiser P.K. and Thomas J.P. (1966). An analysis of data gathered by the staircase-method. *Am J Psychology* 79:652-654.

Ferree C.E. and Rand G. (1922). An illuminated perimeter with campimeter features. *Am J Ophthalmol* 5:455-465.

Ferree C.E. and Rand G. (1924). Effect of brightness and preexposure and surrounding field on breadth and shape of colour fields for stimului of different sizes. *Am J Ophthalmol* 7:843-850.

Ferree C.E. and Rand G. (1927). Effect of size of stimulus on size and shape of colour fields. *Am J Ophthalmol* 10:399-412.

Ferree C.E., Rand G. and Monroe M.M. (1929). Studies in perimetry: 3, Errors of refraction, age and sex in relation to size and form of the field. *Am J Ophthalmol* 12:659-664.

Ferrera V.P., Nealey T.A. and Maunsell J.H.R. (1992). Mixed parvocellular and magnocellular geniculate signals in visual area V4. *Nature* 358:756-758.

Fitzke F.W. and McNaught A.I. (1994). The diagnosis of visual field progression in glaucoma. *Current Opinion in Ophthalmology* 5:110-115.

Fitzke F.W., Crabb D.P., McNaught A.I., Edgar D.F. and Hitchings R.A. (1995). Image-processing of computerized visual-field data. *Br J Ophthalmol* 79:207-212.

Flammer J. and Drance S.M. (1983). Effect of acetazolamide on the differential threshold. *Arch Ophthalmol* 101:1378-1380.

Flammer J., Drance S.M. and Schulzer M. (1983). The estimation and testing of the components of long-term fluctuation of the differential light threshold. *Docum Ophthalmol Proc Ser. 35.* Proceedings of the Fifth International Visual Field Symposium. Eds: E. L. Greve and A. Heijl. Kluwer Academic. pp.383-389.

Flammer J., Drance S.M., Fankhauser F. and Augustiny L. (1984a). Differential light threshold in automated static perimetry. Factors influencing short-term fluctuation. *Arch Ophthalmol* 102:876-9.

Flammer J., Drance S.M. and Schulzer M. (1984b). Covariates of the long-term fluctuation of the differential light threshold. *Arch Ophthalmol* 102:880-882.

Flammer J., Drance S.M. and Zulauf M. (1984c). Differential light threshold, short- and long-term fluctuation in patients with glaucoma, normal controls, and patients with suspected glaucoma. *Arch Ophthalmol* 102:704-706.

Flammer J. (1985). Fluctuations in the visual field. *Automatic perimetry in glaucoma. A practical guide.* Eds: S. M. Drance and D. Anderson. Grune & Stratton, Orlando. pp.161-173.

Flammer J., Drance S.M., Augustiny L. and Funkhouser A. (1985). Quantification of glaucomatous visual field defects with automated perimetry. *Invest Ophthalmol Vis Sci* 26:176-181.

Flammer J. (1986). The concept of visual field indices. *Graefe's Arch Clin Exp Ophthalmol* 224:389-392.

Flammer J. (1987). The Octopus glaucoma G1 program. *Glaucoma* 9:67-72.

Flanagan J.G., Wild J.M. and Wood J.M. (1988). Stimulus configuration and the format of the normal sensitivity gradient. *Doc Ophthalmol* 69:371-383.

Flanagan J.G., Wild J.M. and Hovis J.K. (1991). The differential light threshold as a function of retinal adaptation - the Weber-Fechner/Rose-de-Vries controversy revisited. *Perimetry Update 1990/91.* Proceedings of the IXth International Perimetric Society Meeting. Eds: R. P. Mills and A. Heijl. Amsterdam, New York & Milano. Kugler & Ghedini. pp.551-554.

Flanagan J.G., Moss I.D., Wild J.M., Hudson C., Prokopich L., Whitaker D. and O'Neill E.C. (1993a). Evaluation of FASTPAC: a new strategy for threshold estimation with the Humphrey Field Analyser. *Graefe's Arch Clin Exp Ophthalmol* 231:465-469.

Flanagan J.G., Wild J.M. and Trope G.E. (1993b). Evaluation of FASTPAC, a new strategy for threshold estimation with the Humphrey Field Analyzer, in a glaucomatous population. *Ophthalmology* 100:949-954.

Flanagan J.G., Wild J.M. and Trope G.E. (1993c). The visual field indices in primary open-angle glaucoma. *Invest Ophthalmol Vis Sci* 34:2266-2274.

Fleishman J.A., Beck R.W. and Linares O.A. (1987). Deficits in visual function after resolution of optic neuritis. *Ophthalmology* 95:131-134.

Foster D.H., Snelgar R.S. and Heron J.R. (1985). Nonselective losses in foveal chromatic and luminance sensitivity in multiple sclerosis. *Invest Ophthalmol Vis Sci* 26:1431-1441.

Fujimoto N. and Adachi-Usami E. (1992a). Effect of number of test points and size of test field in automated perimetry. *Acta Ophthalmol* 70:323-326.

Fujimoto N. and Adachi-Usami E. (1992b). Effect of number of test points in automated perimetry. *Am J Ophthalmol* 113:317-320.

Fujimoto N. and Usami E. (1993). Fatigue effect within 10° visual field in automated perimetry. *Ann Ophthalmol* 25:142-144.

Funk J., Bornscheuer C. and Grehn F. (1988). Neuroretinal rim area and visual field in glaucoma. *Graefe's Arch Clin Exp Ophthalmol* 226:431-434.

Funk J. (1991). Early detection of glaucoma by longitudinal monitoring of the optic disc structure. *Graefe's Arch Clin Exp Ophthalmol* 229:57-61.

Funkhouser A., Fankhauser F. and Hirsbrunner H. (1989a). A comparison of eight test location configurations for estimating G1 mean defect values. *Jpn J Ophthalmol* 33:295-299.

Funkhouser A., Fankhauser F. and Hirsbrunner H. (1989b). A comparison of three methods for abbreviating G1 examinations. *Jpn J Ophthalmol* 33:288-294.

Funkhouser A.T. (1991). A new diffuse loss index for estimating general glaucomatous visual field depression. *Doc Ophthalmol* 77:57-72.

Funkhouser A., Hirsbrunner H.P., Fankhauser F. and Flammer J. (1991). OCTOSMART: a computerized aid for interpreting visual field examination results. *Perimetry Update 1990/91.* Proceedings of the IXth International Perimetric Society Meeting. Eds: R. P. Mills and A. Heijl. Amsterdam, New York & Milano. Kugler & Ghedini. pp.279-280.

Funkhouser A., Flammer J., Fankhauser F. and Hirsbrunner H.P. (1992a). A comparison of five methods for estimating general glaucomatous visual field depression. *Graefe's Arch Clin Exp Ophthalmol* 230:101-106.

Funkhouser A.T., Fankhauser F. and Weale R.A. (1992b). Problems related to diffuse versus localized loss in the perimetry of glaucomatous visual fields. *Graefe's Arch Clin Exp Ophthalmol* 230:243-247.

Gilpin L.B., Stewart W.C., Hunt H.H. and Broom C.D. (1990). Threshold variability using different Goldmann stimulus sizes. *Acta Ophthalmol* 68:674-676.

Glass E., Schaumberger M. and Lachenmayr B.J. (1995). Simulations For Fastpac and the Standard 4-2 Db Full-Threshold Strategy Of the Humphrey Field Analyzer. *Invest Ophthalmol Vis Sci* 36:1847-1854.

Gloor B., Schmied U. and Fassler A. (1980). Changes of glaucomatous visual field defects: Degree of accuracy of measurements with the automatic perimeter OCTOPUS. *Int Ophthalmol* 98:1560-1563.

Glowazki A. and Flammer J. (1987). Is there a difference between glaucoma patients with rather localised visual field damage and patients with more diffuse visual field damage? *Doc Opthalmol Proc Ser 49*. Proceedings of the Seventh International Visual Field Symposium. Eds: E.L.Greve and A. Heijl. Dordrecht. Martinus Nijhoff/Dr W. Junk. pp.317-320.

Goldmann H. (1945). Ein slebstregistrierendes projektionskugelperimeter. *Ophthalmologica* 109:71-79.

Goldmann H. (1946). Demonstration unseres neuen projektionskugelperimeters samt theoretischen und klinischen bemerkungen über perimetrie. *Ophthalmologica* 111:187-192.

Goldstick B.J. and Weinreb R.N. (1987). The effect of refractive error on automated global analysis Program G-1. *Am J Ophthalmol* 104:229-232.

Gouras P. (1968). Identification of cone mechanisms in monkey ganglion cells. *J Physiol* 199:533-547.

Gramer E., Kontic D. and Kriegelstein G.K. (1981). Die computerperimetrische darstellung glaukomatöser gesichtsfelddefekte in abhängigkeit von der stimulusgröße. *Ophthalmologica* 183:162-167.

Gramer E., Steinhauser B. and Kriegelstein G.K. (1982). The specificity of the automated suprathreshold perimeter Fieldmaster 200. *Graefe's Arch Clin Exp Ophthalmol* 218:253-255.

Green D.M. and Swets J.A. (1966). Assumed distribution of signal and noise. *Signal detection theory and psychophysics.* John Wiley & Sons Inc, New York. pp.53-84.

Greve E.L. (1973). Single and multiple stimulus static perimetry in glaucoma, the two phases of perimetry. *Doc Ophthalmol* 36:1-355.

Greve E.L. (1975). Static Perimetry. *Ophthalmologica* 171:26-38.

Greve E.L. and Verduin W.M. (1976). Detection of early glaucomatous damage. Part I: Visual field examination. *Doc Ophthalmol Proc Ser 14.* Proceedings of the Second International Visual Field Symposium. Ed: E. L. Greve. The Hague. Dr W. Junk. pp.103-114.

Greve E.L. (1980a). Peritest. *Docum Ophthalmol Proc Theory 22.* Proceedings of the Glaucoma Symposium: Diagnosis and therapy. Ed: E. L. Greve. Junk. pp.71-74.

Greve E.L. (1980b). Visual fields, glaucoma and cataract. *Docum Ophthalmol Proc Theory 22.* Proceedings of the Glaucoma Symposium: Diagnosis and therapy. Ed: E. L. Greve. Junk. pp.79-88.

Greve E.L. (1982). Performance of computer assisted perimeters. *Doc Ophthalmol* 53:343-380.

Grigsby S.S., Vingrys A.J., Benes A.C. and King-Smith P.E. (1991). Correlation of chromatic, spatial and temporal sensitivity in optic nerve disease. *Invest Ophthalmol Vis Sci* 32:3252-3262.

Grochowicki M., Vighetto A., Berquet S. and Pissavin C. (1993). Evolutive patterns of the visual field in optic neuritis. *Neuro-ophthalmology* 13:269-273.

Gundersen K.G., Heijl A. and Åsman P. (1993). Stimulus size and normal inter-individual variability in static perimetry. *Invest Ophthalmol Vis Sci* 34:1262.

Guthauser U. and Flammer J. (1988). Quantifying visual field damage caused by cataract. *Am J Ophthalmol* 106:480-484.

Haas A. and Flammer J. (1985). Influence of diazepam on differential light sensitivity. *Doc Ophthalmol Proc Ser 42.* Proceedings of the Sixth International Visual Field Symposium. Eds: A. Heijl and E. L. Greve. Dordrecht. Dr W. Junk. pp.527-532.

Haas A., Flammer J. and Schneider U. (1986). Influence of age on the visual-fields of normal subjects. *Am J Ophthalmol* 101:199-203.

Haas A.L. and LeBlanc R.P. (1993). The significance of peripheral visual field in detecting early visual field changes in glaucoma. *Perimetry Update 1992/93*. Proceedings of the Xth International Perimetric Society Meeting. Ed: R.P.Mills. Amsterdam & New York. Kugler. p.269.

Haeberlin H. and Fankhauser F. (1980). Adaptive programs for analysis of the visual field by automatic perimetry - basic problems and solutions. *Docum Ophthalmol* 50:123-141.

Haeberlin H., Jenni A. and Fankhauser F. (1980). Researches on adaptive high resolution programming for automatic perimeter : principles and preliminary results. *Int Ophthalmol* 2:1-9.

Haefliger I.O. and Flammer J. (1989). Increase of the short-term fluctuation of the differential light threshold around a physiologic scotoma. *Am J Ophthalmol* 107:417-420.

Haefliger I.O. and Flammer J. (1991). Fluctuation of the differential light threshold at the border of absolute scotomas. Comparison between glaucomatous visual field defects and blind spots. *Ophthalmology* 98:1529-1532.

Haley M.J., Ed. (1987). *The field analyzer primer*. Humphrey Allergan, San Leandro.

Hardage L. and Stamper R.L. (1989). Reliability indices for automated visual fields. *Ophthalmology* 96:1810-1811.

Harms H. (1952). Die praktische bedeutung quantitatives perimetrie. *Klin Mbl Augenheilk* 121:683-692.

Harms H. and Aulhorn E. (1959). Vergleichende untersuchungen über den wert der quantitativen perimetrie, skiascotometrie und verschinelzungsfrequenz für die erkannung beginnender geisichtsfeldstörungen beim glaukom. *Doc Ophthalmol* 13:303-332.

Hart W.M. and Becker B. (1982). The onset and evolution of glaucomatous visual field defects. *Ophthalmology* 89:268-279.

Hart W.M., Jr. and Hartz R.K. (1982). Computer-generated display for three-dimensional static perimetry. *Arch Ophthalmol* 100:312-318.

Heider H.W., Seez K.J. and Schnaudigel O.E. (1991). Cataract Induced Visual-Field Changes. *Klin Monatsbl Augenheilkd* 198:15-19.

Heijl A. and Krakau C.E.T. (1975a). An automatic perimeter for glaucoma visual field control. Construction and clinical cases. Construction and clinical cases. *Albrecht v Graefe's Klin Exp Ophthalmol* 197:13-23.

Heijl A. and Krakau C.E.T. (1975b). An automatic perimeter, design and pilot study. *Acta Ophthalmol* 53:293-310.

Heijl A. (1977a). Studies on computerized perimetry. *Acta Ophthalmol* 55(suppl. 132):25-32.

Heijl A. (1977b). Time changes of contrast thresholds during automatic perimetry. *Acta Ophthalmol* 55:696-708.

Heijl A., Drance S.M. and Douglas G.R. (1980). Automatic perimetry (Competer): Ability to detect early glaucomatous field defects. *Arch Ophthalmol* 98:1560-1563.

Heijl A. and Drance S.M. (1981). A clinical comparison of three computerized automated perimeters. *Arch Opthalmol* 99:832-836.

Heijl A. and Drance S.M. (1983). Changes in differential threshold in patients with glaucoma during prolonged perimetry. *Br J Ophthalmol* 67:512-516.

Heijl A. and Bengtsson B. (1984). The short-term effect of laser trabeculoplasty on the glaucomatous visual field. A prospective study using computerized perimetry. *Acta Ophthalmol* 62:705-714.

Heijl A. (1985). The Humphrey Field Analyzer, construction and concepts. *Doc Ophthalmol Proc Ser. 42.* Proceedings of the Sixth International Visual Field Symposium. Eds: A. Heijl and E. L. Greve. Dordrecht. Dr W. Junk. pp.77-84.

Heijl A., Lindgren G. and Olsson J. (1987a). Normal variability of static perimetric threshold across the central visual field. *Arch Ophthalmol* 105:1544-1549.

Heijl A., Lindgren G. and Olsson J. (1987b). A package for the statistical analysis of visual fields. *Doc Ophthalmol Proc Ser 49.* Proceedings of the Seventh International Visual Field Symposium. Eds: E. L. Greve and A. Heijl. Dordrecht. Martinus Nijhoff/Dr W. Junk. pp.153-168.

Heijl A., Lindgren G. and Olsson J. (1987c). Reliability parameters in computerized perimetry. *Doc Ophthalmol Proc Ser 49.* Proceedings of the Seventh International Visual Field Symposium. Eds: E. L. Greve and A. Heijl. Dordrecht. Martinus Nijhoff/Dr W. Junk. pp.593-600.

Heijl A., Lindgren G. and Olsson J. (1988). Perimetric threshold variability and age. *Arch Ophthalmol* 106:450-451.

Heijl A. and Åsman P. (1989). A clinical study of perimetric probability maps. *Arch Ophthalmol* 107:199-203.

Heijl A., Lindgren A. and Lindgren G. (1989a). Inter-point correlations of deviations of threshold values in normal and glaucomatous visual fields. *Perimetry Update. 1988/89.* Proceedings of the VIIIth International Perimetric Society Meeting. Ed: A. Heijl. Amsterdam, Berkeley & Milano. Kugler & Ghedini. pp.177-183.

Heijl A., Lindgren A. and Lindgren G. (1989b). Test-retest variability in glaucomatous visual fields. *Am J Ophthalmol* 108:130-135.

Heijl A., Lindgren G. and Olsson J. (1989c). The effect of perimetric experience in normal subjects. *Arch Ophthalmol* 107:81-86.

Heijl A., Lindgren G., Olsson J. and Åsman P. (1989d). Visual field interpretation with empiric probability symbols. *Arch Ophthalmol* 107:204-208.

Heijl A., Lindgren G., Lindgren A., Olsson J., Åsman P., Myers S. and Patella M. (1991). Extended empirical statistical package for evaluation of single and multiple fields in glaucoma: Statpac 2. *Perimetry Update 1990/91.* Proceedings of the IXth International Perimetric Society Meeting. Eds: R. P. Mills and A. Heijl. Amsterdam, New York & Milano. Kugler & Ghedini. pp.303-315.

Heijl A., Lindgren G., Olsson J. and Asman P. (1992). On weighted visual field indices. *Graefe's Arch Clin Exp Ophthalmol* 230:397-400.

Heijl A. (1993). Perimetric point density and detection of glaucomatous visual field loss. *Acta Ophthalmol* 71:445-450.

Heijl A. and Bengtsson B. (1996). The effect of perimetric experience in patients with glaucoma. *Arch Ophthalmol* 114:19-22.

Henson D.B., Chauhan B.C. and Hobley A. (1988). Screening for glaucomatous visual field defects: the relationship between sensitivity, specificity and the number of test locations. *Ophthal Physiol Opt* 8:123-127.

Henson D.B. (1989). Visual field screening and the development of a new screening program. *J Am Optom Assoc* 60:893-898.

Henson D.B. and Bryson H. (1991). Is the variability in glaucomatous field loss due to poor fixation control? *Perimetry Update 1990/91.* Proceedings of the IXth International Perimetric Society Meeting. Eds: R. P. Mills and A. Heijl. Amsterdam, New York & Milano. Kugler & Ghedini. pp.217-220.

Henson D.B. and Morris E.J. (1993). Effect of uncorrected refractive errors upon central visual field testing. *Ophthal Physiol Opt* 13:339-343.

Henson D.B. and Darling M.N. (1995). Detecting progressive visual field loss. *Ophthal Physiol Opt* 15:387-390.

Henson D.B., Evans J. and Lane C. (1995). Fixation accuracy of patients with glaucoma during full threshold perimetry. *Perimetry Update 1994/1995.* Proceedings of the XIth International Perimetric Society Meeting. Eds: R. P. Mills and M. Wall. Amsterdam & New York. Kugler. pp. 249-255.

Herse P.R. (1992). Factors influencing normal perimetric thresholds obtained using the Humphrey Field Analyzer. *Invest Ophthalmol Vis Sci* 33:611-617.

Hess R.F. and Plant G.T. (1985). Temporal frequency discrimination in human vision: evidence for additional mechanism in the low spatial and high temporal frequency region. *Vis Res* 25:1493-1500.

Heuer D.K., Anderson D.R., Feuer W.J. and Gressel M.G. (1987). The influence of refraction accuracy on automated perimetric threshold measurements. *Ophthalmology* 94:1550-1553.

Hills J.F. and Johnson C.A. (1988). Evaluation of the *t*-test as a method of detecting visual field changes. *Ophthalmology* 95:261-266.

Hirsbrunner H.P., Fankhauser F., Funkhouser A.T. and Jenni A. (1990). Evaluating human and automated interpretation of visual field data in perimetry. *Jpn J Ophthalmol* 34:72-80.

Hitchings R.A., Migdal C.S., Wormald R., Poinooswamy D. and Fitzke F. (1994). The primary treatment trial: changes in the visual field analysis by computer-assisted perimetry. *Eye* 8:117-120.

Holmin C. and Krakau C.E.T. (1979). Variability of glaucomatous visual field defects in computerized perimetry. *Graefe's Arch Clin Exp Ophthalmol* 210:235-250.

Holmin C. and Krakau C.E.T. (1980). Visual field decay in normal subjects and in cases of chronic glaucoma. *Graefe's Arch Clin Exp Ophthalmol* 213:291-298.

Holmin C. and Krakau C.E.T. (1982). Regression analysis of the central visual field in chronic glaucoma cases: a follow-up study using automated perimetry. *Acta Ophthalmol* 60:264-267.

Holmin C. and Storr-Paulsen A. (1984). The visual field after trabeculectomy. *Acta Ophthalmol* 62:230-234.

Hoop J., Harris A., Shoemaker J., Sponsel W.E. and Cantor L.B. (1993). A comparison of global indices from the Humphrey 24-2 Statpac and Fastpac programs in normal and glaucomatous eyes. *Invest Ophthalmol Vis Sci* 34:1264.

Hoskins H.D., Magee S.D., Drake M.V. and Kidd M.N. (1988). Confidence intervals for change in automated visual fields. *Br J Ophthalmol* 72:591-597.

Hudson C. and Wild J.M. (1992). Assessment of physiologic statokinetic dissociation by automated perimetry. *Invest Ophthalmol Vis Sci* 33:3162-3168.

Hudson C., Wild J.M. and O'Neill E.C. (1994). Fatigue effects during a single session of automated static threshold perimetry. *Invest Ophthalmol Vis Sci* 35:268-280.

Iwase A., Kitazawa Y. and Kato Y. (1993). Clinical value of Fastpac: A comparative study with the standard full threshold method. *Perimetry Update 1992/93.* Proceedings of the Xth International Perimetric Society Meeting. Ed: R. P. Mills. Amsterdam & New York. Kugler. pp. 112-114.

Jaffe G.J., Alvarado J.A. and Juster P.R. (1986). Age-related changes of the normal visual field. *Arch Opthalmol.* 104:1021-1025.

Jenni F. and Flammer J. (1987). Experience With the Reliability Parameters Of the Octopus Automated Perimeter. *Doc Ophthalmol Proc Ser 49.* Proceedings of the Seventh International Visual Field Symposium. Eds: E. L. Greve and A. Heijl. Dordrecht. Martinus Nijhoff/Dr W. Junk. pp.601-603.

Johnson C.A. and Keltner J.L. (1981). Computer analysis of visual field loss and optimization of automated perimetric test strategies. *Ophthalmology* 88:1058-1065.

Johnson C.A. and Keltner J.L. (1987). Optimal rates of movement for kinetic perimetry. *Arch Ophthalmol* 105:73-75.

Johnson C., Adams A.J. and Lewis R.A. (1988). Fatigue effects in automated perimetry. *App Optics* 27:1030-1037.

Johnson C.A. and Shapiro L.R. (1989). Comparison of MOBS (modified binary search) and staircase test procedures. *Technical Digest Series - Optical Society of America. 7.* Proceedings of the Non-invasive assessment of the visual field system. pp.84-87.

Johnson C.A., Adams A.J. and Lewis R.A. (1989a). Evidence for a neural basis of age-related visual field loss in normal observers. *Invest Ophthalmol Vis Sci* 30:2056-2064.

Johnson C., Adams A.J. and Lewis R.A. (1989b). Automated perimetry of short-wavelength mechanisms in glaucoma and ocular hypertension. *Perimetry Update 1988/89.* Proceedings of the IXth International Perimetric Society Meeting. Ed: A.Heijl. Amsterdam, Berkeley & Milano. Kugler & Ghedini. pp. 31-37.

Johnson C.A. and Shapiro L.R. (1991). A rapid heuristic test procedure for automated perimetry. *Perimetry Update 1990/91.* Proceedings of the IXth International Perimetric Society Meeting. Eds: R. P. Mills and A. Heijl. Amsterdam, New York & Milano. Kugler & Ghedini. pp.251-256.

Johnson C.A., Chauhan B.C. and Shapiro L.R. (1992). Properties of staircase procedures for estimating thresholds in automated perimetry. *Invest Ophthalmol Vis Sci* 33:2966-2974.

Johnson C.A. and Nelson-Quigg J.M. (1993). A prospective three-year study of response properties of normal subjects and patients during automated perimetry. *Ophthalmology* 100:269-274.

Johnson C.A., Adams A.J., Casson E.J. and Brandt J.D. (1993a). Progression of early glaucomatous visual field loss as detected by blue-on-yellow and standard white-on-white perimetry. *Arch Ophthalmol* 111:651-656.

Johnson C.A., Adams A.J., Casson E.J. and Brandt J.D. (1993b). Blue-on-yellow perimetry can predict the development of glaucomatous visual field loss. *Arch Ophthalmol* 111:645-650.

Jonas J.B., Müller-Bergh J.A., Schlötzer-Schrehardt U.M. and Naumann G.O.H. (1990). Histomorphometry of the human optic nerve. *Invest Ophthalmol Vis Sci* 31:736-44.

Kahana E., Alter M. and Feldman S. (1976). Optic neuritis in relation to multiple sclerosis. *J Neurol* 213:87-95.

Katz J. and Sommer A. (1986). Asymmetry and variation in the normal hill of vision. *Arch Ophthalmol* 104:65-68.

Katz J. and Sommer A. (1987). A longitudinal study of the age-adjusted variability of automated visual fields. *Arch Ophthalmol* 105:1083-1086.

Katz J. and Sommer A. (1988). Reliability Indexes Of Automated Perimetric Tests. *Arch Ophthalmol* 106:1252-1254.

Katz J. and Sommer A. (1990). Screening for glaucomatous visual field loss. The effect of patient reliability. *Ophthalmology* 97:1032-1037.

Katz J., Sommer A. and Witt K. (1991). Reliability of visual field results over repeated testing. *Ophthalmology* 98:70-75.

Kaufmann H. and Flammer J. (1989). Clinical experience with the Bebié-curve. *Perimetry Update 1988/89.* Proceedings of the VIIIth International Perimetric Society Meeting. Ed: A. Heijl. Amsterdam, Berkeley & Milano. Kugler & Ghedini. pp.235-238.

Kaufmann H., Flammer J. and Rutishauser C. (1990). Evaluation of visual fields by ophthalmologists and by OCTOSMART program. *Ophthalmologica* 201:104-109.

Keele S.W. (1986). Motor control. *Handbook of perception of human performance. Cognitive processes and performance.* Eds: K. R. Boff, L. Kaufmann and J. P. Thomas. Wiley, New York. pp.30-34.

Keltner J.L., Johnson C.A. and Balestrery F.G. (1979). Suprathreshold static perimetry: Initial clinical trials with the fieldmaster automated perimeter. *Arch Ophthalmol* 97:260-272.

Keltner J.L., Johnson C.A., Beck R.W., Cleary P.A. and Spurr J.O. (1993a). Quality control functions of the visual field reading center (VFRC) for the Optic Neuritis Treatment Trial (ONTT). *Controlled Clinical Trials* 14:143-159.

Keltner J.L., Johnson C.A., Spurr J.O. and Beck R.W. (1993b). Baseline visual field profile of optic neuritis. The experience of the optic neuritis treatment trial. *Arch Ophthalmol* 111:231-234.

Keltner J.L. and Johnson C.A. (1994). Visual field reading center (VRFC): methodology of tracking changes in Humphrey Visual Fields over six months of follow-up in the optic neuritis treatment trial (ONTT). *Personal Communication.*

Keltner J.L. and Johnson C.A. (1995). Short-wavelength automated perimetry in neuro-ophthalmological disorders. *Arch Ophthalmol* 113:475-481.

Kinnunen E. (1983). The incidence of optic neuritis and it's prognosis for multiple sclerosis. *Acta Neurol Scand* 68:371-377.

King D., Drance S.M., Douglas G.R. and Wijsman K. (1986). The detection of paracentral scotomas with varying grids in computed perimetry. *Arch Ophthalmol* 104:524-525.

Klewin K.M. and Radius R.L. (1986). Background illumination and automated perimetry. *Arch Ophthalmol* 104:395-397.

Koch P., Roulier A. and Fankhauser F. (1972). Perimetry - the information theoretical basis for its automation. *Vis Res* 12:1619-1630.

Kolb H. (1991). Anatomical pathways for color vision in the human retina. *Vis Neurosci* 7:61-74.

Koskela P.U., Airaksinen P.J. and Tuulonen A. (1990). The effect of jogging on visual field indices. *Acta Ophthalmol* 68:91-93.

Krakau C.E.T. (1985). A statistical trap in the evaluation of visual field decay. *Acta Ophthalmol* 63(suppl 173):19-21.

Krakau C.E.T. (1986). Hazards in the evaluation of visual field decay. *Doc Ophthalmol* 63:239-246.

Krakau C.E.T. (1989). Temporal summation and perimetry. *Ophthalmic Res* 21:49-55.

Kulikowski J.J. and Tolhurst D.J. (1973). Psychophysical evidence for sustained and transient detectors in human vision. *J Physiol* 232:149-162.

Kulze J.C., Stewart W.C. and Sutherland S.E. (1990). Factors associated with a learning effect in glaucoma patients using automated perimetry. *Acta Ophthalmol* 68:681-686.

Lachenmyer B., Kiermeir U. and Kojetinsky S. (1994). Neighbouring points of a normal visual field are not statistically independent. *Invest Ophthalmol Vis Sci* 35:1322.

Lambrou G.N., Schalk P., Rechenmann R.V. and Bronner A. (1987). Computer-assisted visual field assessment: quantification, three- and four-dimensional displays. *Doc Ophthalmol Proc*

Ser 49. Proceedings of the Seventh International Visual Field Symposium. Eds: E. L. Greve and A. Heijl. Dordrecht. Martinus Nijhoff/Dr W. Junk. pp.207-215.

Langerhorst C.T., van den Berg T.J.T.P. and van Spronsen R. (1985). Results Of a Fluctuation Analysis and Defect Volume Program For Automated Static Threshold Perimetry With the Scoperimeter. *Doc Ophthalmol Proc Ser 42.* Proceedings of the Sixth International Visual Field Symposium. Eds: A. Heijl and E. L. Greve. Dordrecht. Dr W. Junk. pp.1-6.

Langerhorst C.T., van den Berg T.J.T.P., Veldman E. and Greve E.L. (1987). Population study of global and local fatigue with prolonged threshold testing in automated perimetry. *Doc Ophthalmol Proc Ser 49.* Proceedings of the Seventh International Visual Field Symposium. Eds: E. L. Greve and A. Heijl. Dordrecht. Martinus Nijhoff/Dr W. Junk. pp.657-662.

Langerhorst C.T. (1988). *Automated perimetry in glaucoma*: Fluctuation behavior and general and local reduction in sensitivity. Kugler & Ghedini. Amsterdam.

Lepore F.E. (1991). The origin of pain in optic neuritis: determinants of pain in 101 eyes with optic neuritis. *Arch Neurol* 48:748-749.

Lewis R.A., Johnson C.A., Keltner J.L. and Labermeier P.K. (1986). Variability of quantitative automated perimetry in normal observers. *Ophthalmology* 93:878-881.

Lindenmuth K.A., Skuta G.L., Rabbani R. and Musch D.C. (1989). Effects of pupillary constriction on automated perimetry in normal eyes. *Ophthalmology* 96:1298-1301.

Lindenmuth K.A., Skuta G.L., Rabbani R., Musch D.C. and Bergstrom T.J. (1990). Effects of pupillary dilation on automated perimetry in normal patients. *Ophthalmology* 97:367-370.

Livingstone M.S. and Hubel D.H. (1987). Psychophysical evidence for separate channels for the perception of form, colour, movement and depth. *J Neurosci* 7:3416-3468.

Livingstone M.S. and Hubel D.H. (1988). Do the relative mapping densities of the magno- and parvocellular systems vary with eccentricity? *J Neurosci* 8:4334-4339.

Lynn J.R. and Tate G.W. (1975). Computer controlled apparatus for automatic visual field examination. *United States Patent.* N°: 3,883,234. May 1975.

Lynn J.R., Batson E.P. and Fellman R.L. (1985). Internal inconsistencies vs Root Mean-Square as measures of the threshold variability. *Doc Ophthalmol Proc Ser 42.* Proceedings of the Sixth International Visual Field Symposium. Eds: A. Heijl and E. L. Greve. Dordrecht. Dr W. Junk. pp.7-15.

Mandava S., Caprioli J. and Zulauf M. (1992). Glaucoma pattern index to quantify glaucomatous visual field loss. *J Glaucoma* 1:178-183.

Mandava S., Zulauf M., Zeyen T. and Caprioli J. (1993). An evaluation of clusters in the glaucomatous visual field. *Am J Ophthalmol* 116:684-691.

Mann C., Orr A. and Rubillowicz M. (1988). Automated Static Perimetry In Chloroquine and Hydroxychloroquine Therapy. *Can J Ophthalmol* 23:93-93.

Marchini G., Pisano F., Bertagnin F., Marraffa M. and Bonomi L. (1991). Perimetric learning effect in glaucoma patients. *Glaucoma*. 13:102-106.

Marra G. and Flammer J. (1991). The learning and fatigue effect in automated perimetry. *Graefe's Arch Clin Exp Ophthalmol* 229:501-504.

Marshall J. (1985). Radiation and the ageing eye. *Ophthal Physiol Opt* 5:241-263.

Martin-Boglind L. (1991). High-pass resolution perimetry in uncomplicated myopia. *Acta Ophthalmol* 69:516-520.

McCluskey D.J., Douglas J.P., O'Connor P.S., Story K., Ivy L.M. and Harvey J.S. (1986). The effect of pilocarpine on the visual field of normals. *Ophthalmology* 93:843-846.

McMillan T.A., Stewart W.C. and Hunt H.H. (1992). Association of reliability with reproducibility of the glaucomatous visual field. *Acta Ophthalmol* 70:665-670.

McNaught A.I., Crabb D.P., Fitzke F.W. and Hitchings R.A. (1995). Modelling series of visual fields to detect progression in normal-tension glaucoma. *Graefe's Arch Clin Exp Ophthalmol* 233:750-755.

Merigan W.H. and Eskin T.A. (1986). Spatio-temporal vision of macaques with severe loss of P-beta retinal ganglion cells. *Vis Res* 26:1751-1761.

Merigan W.H. (1989). Chromatic and achromatic vision of macaques: the role of the P pathway. *J Neurosci* 9:776-783.

Merigan W.H. and Maunsell J.H.R. (1990). Macaque vision after magnocellular lateral geniculate lesions. *Vis Neurosci* 5:347-352.

Merigan W.H., Katz L.M. and Maunsell J.H.R. (1991). The effects of parvocellular lateral geniculate lesions on the acuity and contrast sensitivity of macaque monkeys. *J Neurosci* 11:994-1001.

Messmer C. and Flammer J. (1991). Octopus program G1X. *Ophthalmologica* 203:187-188.

Mikelberg F.S. and Drance S.M. (1984). The mode of progression of visual field defects in glaucoma. *Am J Ophthalmol* 98:443-445.

Mikelberg F.S., Schulzer M., Drance S.M. and Lau X. (1986). The rate of progression of scotomas in glaucoma. *Am J Ophthalmol* 101:1-6.

Mikelberg F.S., Drance S.M., Schulzer M. and Wijsman K. (1987). The effect of miosis on visual field indices. *Doc Ophthalmol Proc Ser 49.* Proceedings of the Seventh International Visual Field Symposium. Eds: E. L. Greve and A. Heijl. Dordrecht. Martinus Nijhoff/Dr W. Junk. pp.645-649.

Miller B.A. and Gelber E.C. (1990). Aphakic Visual-Fields By Automated Perimetry. *Ann Ophthalmol* 22:419-422.

Miller K.N., Shields B. and Ollie A.R. (1989). Automated kinetic perimetry with two peripheral isopters in glaucoma. *Arch Ophthalmol* 107:1316-1320.

Mills R.P. (1985). Quantatative perimetry: Dicon. *Automatic perimetry in glaucoma.* Eds: S. M. Drance and D. Anderson. Grune & Stratton, Orlando. pp.99-112.

Mills R.P., Lau W. and Schulzer M. (1991). Estimating short-term fluctuations without double determinations. Validation of a method. *Perimetry Update 1990/91.* Proceedings of the IXth International Perimetric Society Meeting. Eds: R. P. Mills and A. Heijl. Amsterdam, New York & Milano. Kugler & Ghedini. pp.202-208.

Mills R.P., Barnebey H.S., Migliazzo C.V. and Li Y. (1994). Does saving time using FASTPAC or suprathreshold testing reduce quality of visual fields? *Ophthalmology* 101:1596-1603.

Morgan R.K., Feuer W.J. and Anderson D.R. (1991). Statpac 2 glaucoma change probability. *Arch Ophthalmol* 109:1690-1692.

Morrissey S.P., Miller D.H. and Kendall B.E. (1993). The significance of brain magnetic resonance imaging abnormalities at presentation with clinically isolated syndromes suggestive of mulitple sclerosis. *Brain* 116:135-146.

Morrison J.D. and Jay J.L. (1993). Changes in visual function with normal aging, cataract and intraocular lenses. *Eye* 7:20-25.

Moss I.D., Hudson C., Dengler-Harles M., Wild J.M., Whitaker D.J. and O'Neill E.C. (1992). A 3dB step single crossing algorithm for full threshold automated perimetry. *Invest Ophthalmol Vis Sci* 33:969.

Moss I.D. and Wild J.M. (1994). The influence of induced forward light scatter on the normal blue-on-yellow perimetric profile. *Graefe's Arch Clin Exp Ophthalmol* 232:409-414.

Moss I.D., Wild J.M. and Whitaker D.J. (1995). The Influence Of Age-Related Cataract On Blue-On-Yellow Perimetry. *Invest Ophthalmol Vis Sci* 36:764-773.

Mutlukan E. (1994). The effect of refractive blur on the detection sensitivity to light offsets in the central visual field. *Acta Ophthalmol* 72:189-94.

Nelson-Quigg J.M., Twelker J.D. and Johnson C.A. (1989). Response properties of normal observers and patients during automated perimetry. *Arch Ophthalmol* 107:1612-1615.

Neuhann T. and Greite J.H. (1981). Reliability of visual field examinaation in clinical routine. *Doc Ophthalmol Proc Ser 26.* Proceedings of the Fourth International Visual Field Symposium. Eds: E. L. Greve and G. Verriest. The Hague. Dr W. Junk. pp.55-61.

Norden L.C. (1989). Reliability in perimetry. *J Am Optom Assoc* 60:880-890.

Noureddin B.N., Poinoosawmy D., Fitzke F.W. and Hitchings R.A. (1991). Regression analysis of visual field progression in low tension glaucoma. *Br J Ophthalmol* 75:493-495.

O.N.S.G. (1991). Optic Neuritis Study Group. The clinical profile of optic neuritis: experience of the optic neuritis treatment trial. *Arch Ophthalmol* 109:1673-1678.

O'Brien C. and Schwartz B. (1990). The visual field in chronic open angle glaucoma: the rate of change in different regions of the field. *Eye* 4:557-562.

O'Brien C., Schwartz B., Takamoto T. and Wu D.C. (1991). Intraocular pressure and the rate of visual field loss in chronic open-angle glaucoma. *Am J Ophthalmol* 111:491-500.

O'Brien C. and Schwartz B. (1993). Point by point linear regression analysis of automated visual fields in primary open angle glaucoma. *Perimetry Update 1992/93.* Proceedings of the Xth International Perimetric Society Meeting. Ed: R. P. Mills. Amsterdam & New York. Kugler. pp.149-152.

O'Brien C., Poinoosawmy D., Wu J. and Hitchings R. (1994). Evaluation of the Humphrey FASTPAC threshold program in glaucoma. *Br J Ophthalmol* 78:516-519.

O'Brien C. and Wild J.M. (1995). Automated perimetry in glaucoma - room for improvement? *Br J Ophthalmol* 79:200-201.

Oden N. (1993). Regression analysis of visual field progression in low tension glaucoma. *Br J Ophthalmol* 77:194.

O'Donnell N.P., Birch M.K. and Wishart P.K. (1995). Fastpac error is within the long-term fluctuation of Standard Humphrey threshold visual field testing. *Perimetry Update 1994/95.* Proceedings of the XIth International Perimetric Society Meeting. Eds: R. P. Mills and M. Wall. Amsterdam & New York. Kugler. pp. 231.

Olsson J., Rootzén H. and Heijl A. (1989). Maximum likelihood estimation of the frequency of false positive and false negative answers from the up-ans-down staircases of computerized perimetry. *Perimetry Update 1988/89.* Proceedings of the VIIIth International Perimetric Society Meeting. Ed: A. Heijl. Amsterdam, Berkeley & Milano. Kugler & Ghedini. pp.245-251.

Olsson J., Bengtsson B., Heijl A. and Rootzén H. (1995). Improving estimation of false-positive and false-negative response in computerized perimetry. *Perimetry Update 1994/95.* Proceedings of the XIth International Perimetric Society Meeting. Eds: R. P. Mills and M. Wall. Amsterdam & New York. Kugler. pp. 219.

Paradine C.M. and Rivett B.H.P. (1966). Statistical Methods for Technologists. *Two-factor analysis of variance with replications.* English Universities Press, London. pp.246-248.

Paulsson L. and Sjöstrand J. (1980). Contrast sensitivity in the presence of a glare light. *Invest Opthalmol Vis Sci* 19:401-406.

Pearson P.A., Baldwin L.B. and Smith T.J. (1990). The relationship of mean defect to corrected loss variance in glaucoma and ocular hypertension. *Ophthalmologica* 200:16-21.

Pennebaker G.E., Stewart W.C., Stewart J.A. and Hunt H.H. (1992). The effect of stimulus duration upon the components of fluctuation in static automated perimetry. *Eye* 6:353-355.

Percy A.K., Nobrega F.T. and Kurland L.T. (1972). Optic neuritis and multiple sclerosis: an epidemiologic study. *Arch Ophthalmol* 87:135-139.

Perry V.H., Oehler R. and Cowey A. (1984). Retinal ganglions which project to the dorsal lateral geniculate nucleus in the macaque monkey. *Neuroscience* 12:1101-1123.

Phillips M.L., Foster D.H., Honan W.P., Edgar G.K. and Heron J.R. (1994). Optic neuritis. Differential losses of luminance and chromatic function near a scotoma. *Brain* 117:767-773.

Potts A.M., Hodges D., Shelman C.B., Fritz K.J., Levy N.S. and Mangnall Y. (1972). Morphology of the primate optic nerve II. Total fiber size distribution and fiber density distribution. *Invest Ophthalmol Vis Sci* 11:989-1003.

Rabineau P.A., Gloor B.P. and Tobler H.J. (1985). Fluctuations in threshold and effect of fatigue in automated static perimetry (with the Octopus 201). *Doc Ophthalmol Proc Ser 42.* Proceedings of the Sixth International Visual Field Symposium. Eds: A. Heijl and E. L. Greve. Dordrecht. Dr W. Junk. pp.25-33.

Rains J.D. (1963). Signal luminance and position effects in human reaction time. *Vis Res* 3:239-251.

Rebolleda G., Munoz F.J., Fernandez V.J.M., Pellicer T. and del C.J.M. (1992). Effects of pupillary dilation on automated perimetry in glaucoma patients receiving pilocarpine. *Ophthalmology* 99:418-423.

Reynolds M., Stewart W.C. and Sutherland S. (1990). Factors that influence the prevalence of positive catch trials in glaucoma patients. *Graefe's Arch Clin Exp Ophthalmol* 228:338-341.

Riedel K.G., Gilg T. and Leibhardt E. (1985). Wahrnehmungsstörungen im peripheren gesichtsfeld unter alkoholeinfluß. *Klin Monatsbl Augenheilk* 186:279-283.

Rizzo III J.F. and Lessell S. (1991). Optic neuritis and ischaemic optic neuropathy. Overlapping clinical profiles. *Arch Ophthalmol* 109:1668-1672.

Robinson D.A. (1964). The mechanics of human saccadic eye movement. *J Physiol* 174:245-264.

Rodriguez M., Siva A., Cross S.A., O'Brien P.C. and Kurland L.T. (1995). Optic neuritis: a population-based study in Olmstead County, Minnesota. *Neurology* 45:244-250.

Russell M.H.A., Murray I.J., Metcalfe R.A. and Kulikowski J.J. (1991). The visual defect in multiple sclerosis and optic neuritis. A combined psychophysical and electrophysiological investigation. *Brain* 114:2419-2435.

Rutishauser C., Flammer J. and Haas A. (1989). The distribution of normal values in automated perimetry. *Graefe's Arch Clin Exp Ophthalmol* 227:513-517.

Sample P.A., Esterson F.D., Weinreb R.N. and Boynton R.M. (1988). The aging lens - invivo assessment of light absorption in 84 human eyes. *Invest Ophthalmol Vis Sci* 29:1306-1311.

Sample P.A. and Weinreb R.N. (1992). Progressive color visual field loss in glaucoma. *Invest Ophthalmol Vis Sci* 33:2068-2071.

Sanabria O., Feuer W.J. and Anderson D.R. (1991). Pseudo-loss of fixation in automated perimetry. *Ophthalmology* 98:76-78.

Sanchez R.M., Dunkelberger G.R. and Quigley H.A. (1986). The number and diameter distributions of axons in the monkey optic nerve. *Invest Ophthalmol Vis Sci* 27:1342-1350.

Sandberg-Wolheim M., Bynke H., Cronqvist S., Holtas S., Platz P. and Ryder L.P. (1990). A long-term prospective study of optic neuritis: evaluation of risk factors. *Ann Neurol* 27:386-393.

Saunders R.M. (1975). The critical duration of temporal summation in the human central fovea. *Vis Res* 15:699-703.

Schäfer B., Lachenmayr B., Schaumberger M., Oepke D. and Gleissner M. (1993). Comparison of Fastpac/4-2dB standard strategy of the Humphrey Field Analyzer in normal and glaucomatous eyes. *Invest Ophthalmol Vis Sci* 34:1264.

Schaumberger M., Schafer B. and Lachenmayr B.J. (1995). Glaucomatous Visual-Fields - Fastpac Versus Full Threshold Strategy Of the Humphrey Field Analyzer. *Invest Ophthalmol Vis Sci* 36:1390-1397.

Schiller P.H. and Malpelli J.G. (1977). Properties and tectal projections of monkey ganglion cells. *J Neurophysiol* 40:428-445.

Schultz J.S., Werner E.B., Krupin T., Bishop K.I. and Koelle J. (1987). Intraocular pressure and visual field defects after Argon laser trabeculoplasty in chronic open-anlge glaucoma. *Ophthalmology* 94:553-557.

Schulzer M., Mills R.P., Hopp R.H., Lau W. and Drance S.M. (1990). Estimation of the short-term fluctuation from a single determination of the visual field. *Invest Ophthalmol Vis Sci* 31:730-735.

Schulzer M. (1994). Errors in the diagnosis of visual field progression in normal-tension glaucoma. *Ophthalmology* 101:1589-1594.

Schwartz B. and Nagin P. (1985). Probability maps for evaluating automated visual fields. *Doc Ophthalmol Proc Ser 42.* Proceedings of the Sixth International Visual Field Symposium. Eds: A. Heijl and E. L. Greve. Dordrecht. Dr W. Junk. pp.39-48.

Schwartz B. (1995). Rate of change of visual fields over time in glaucoma: velocity versus acceleration. *Perimetry Update 1994/95.* Proceedings of the XIth International Perimetric Society Meeting. Eds: R. P. Mills and M. Wall. Amsterdam & New York. pp.13-24.

Searle A.E., Wild J.M., Shaw D.E. and O'Neill E.C. (1991). Time-related variation in normal automated static perimetry. *Ophthalmology* 98:701-707.

Shapiro L.R., Johnson C.A. and Kennedy R.L. (1989). KRAKEN. A computer simulation procedure for static, kinetic, suprathreshold static and heuristic perimetry. *Perimetry Update 1988/89.* Proceedings of the VIIIth International Perimetric Society Meeting. Ed: A. Heijl. Amsterdam, Berkeley & Milano. Kugler & Ghedini. pp.431-438.

Shin Y.S., Suzumura H., Furuno F., Harasawa K., Endo N. and Matsuo H. (1991). Classification of glaucomatous visual field defects using the Humprhey Field Analyzer box plots. *Perimetry Update 1990/91.* Proceedings of the IXth International Perimetric Society Meeting. Eds: R. P. Mills and A. Heijl. Amsterdam, New York & Milano. Kugler & Ghedini. pp.235-243.

Silveira L.C.L. and Perry V.H. (1991). The topography of magnocellular projecting ganglion cells (M-ganglion cells) in the primate retina. *Neuroscience* 40:217-237.

Sloan L.L. (1939). Instruments and techniques for the clinical testing of light sense III - an apparatus for studying regional differences in light sense. *Arch Ophthalmol* 22:233-251.

Sommer A., Enger C. and Witt K. (1987). Screening for glaucomatous visual field loss with automated threshold perimetry. *Am J Ophthalmol* 103:681-684.

Sommer A., Katz J., Quigley H.A., Miller N.R., Robin A.L., Richter R.C. and Witt K.A. (1991). Clinically detectable nerve fiber atrophy precedes the onset of glaucomatous field loss. *Arch Ophthalmol* 109:77-83.

Spahr J. (1975). Optimization of the presentation pattern in automated static perimetry. *Vis Res* 15:1275-1281.

Stewart W.C., Shields M.B. and Ollie A.R. (1989). Full threshold versus quantification of defects for visual field testing in glaucoma. *Graefe's Arch Clin Exp Ophthalmol* 227:51-54.

Stewart W.C. and Hunt H.H. (1993). Threshold variation in automated perimetry. *Surv Ophthalmol* 37:353-361.

Stewart W.C., Rogers G.M., Crinkley C.M.C. and Carlson A.N. (1995). Effect of cataract extraction on automated fields in chronic open-angle glaucoma. *Arch Ophthalmol* 113:875-879.

Sturmer J., Gloor B. and Tobler H.J. (1985). The glaucomatous visual-field in detail as revealed by the Octopus F- programs. *Doc Ophthalmol Proc Ser 42.* Proceedings of the Sixth International Visual Field Symposium. Eds: A. Heijl and E. L. Greve. Dordrecht. Dr W. Junk. pp.391-401.

Suzuki Y., Araie M. and Ohashi Y. (1993). Sectorization Of the Central 30-Degrees Visual-Field In Glaucoma. *Ophthalmology* 100:69-75.

Suzumura H., Furuno F. and Matsuo H. (1985). Volume of the 3-Dimensional visual field and its objective evaluation by shape coefficient - normal values by age and abnormal visual field. *Doc Ophthalmol Proc Ser 42.* Proceedings of the Sixth International Visual Field Symposium. Eds: A. Heijl and E. L. Greve. Dordrecht. Dr W. Junk. pp.533-537.

Suzumura H. (1988). Visual fatigue-like effect in glaucomas with repeated threshold measurement. *Acta Soc Ophthalmol Jap* 92:220-224.

Takashima M., Nagata S. and Kani K. (1993). Examination of receptive fields using automated perimeter. *Perimetry Update 1992/93.* Proceedings of the Xth International Perimetric Society Meeting. Ed: R. P. Mills. Amsterdam & New York. Kugler. pp.537-541.

Taylor K.P., McManus P. and Miller D. (1984). Computerized perimeters. *Ann Ophthalmol* 16:915-917.

Thaung J., Beckman C., Abrahamsson M. and Sjöstrand J. (1995). The 'light scattering factor'. Importance of stimulus geometry, contrast definition and adaptation. *Invest Ophthalmol Vis Sci* 36:2313-2317.

Traquair H.M. (1938). *An introduction to clinical perimetry.* London. Henry Klimpton.

Travis D. and Thompson P. (1989). Spatiotemporal contrast sensitivity and colour vision in multiple sclerosis. *Brain* 112:283-303.

Treutwein B. (1995). Adaptive psychophysical procedures. *Vision Res* 35:2503-2522.

Trobe J.D. and Glaserm J.S. (1978). Quantatative perimetry in compressed optic neuropathy and optic neuritis. *Arch Ophthalmol* 96:1210-1216.

Trobe J.D. (1994). High-dose corticosteroid regimen retards development of multiple sclerosis in Optic Neuritis Treatment Trial. *Arch Ophthalmol* 112:35-36.

Trope G.E. and Britton R. (1987). A comparison of Goldmann and Humphrey automated perimetry in patients with glaucoma. *Br J Ophthalmol* 71:489-493.

Tynan P.D. and Sekular R. (1982). Motion processing in peripheral vision: reaction time and perceived velocity. *Vis Res* 22:61-68.

Tyrrell R.A. and Owens D.A. (1988). A rapid technique to assess the resting states of the eyes and other threshold phenomena: The modified binary search (MOBS). *Behaviour Research Methods, Instruments, and Computers* 20:137.

Ulrich J. and Groebke-Lorenz W. (1983). The optic nerve in multiple sclerosis. A morphological study with retrospective clinico-pathological correlations. *Neuro-ophthalmology* 3:149-159.

van den Berg T.J.T.P., van Spronsen R., van Veenendaal W.G. and Bakker D. (1985). Psychophysics Of Intensity Discrimination In Relation to Defect Volume Examination On the Scoperimeter. *Doc Ophthalmol Proc Ser 42.* Proceedings of the Sixth International Visual Field Symposium. Eds: A. Heijl and E. L. Greve. Dordrecht. Dr W. Junk. pp.147-151.

van den Berg T.J.T.P. (1987). Relation between media disturbances and the visual field. *Doc Ophthalmol Proc Ser 49.* Proceedings of the Seventh International Visual Field Symposium. Eds: E. L. Greve and A. Heijl. Dordrecht. Martinus Nijhoff/Dr W. Junk. pp.33-38.

Wall M. (1990). Loss of P retinal ganglion cell function in resolved optic neuritis. *Neurology* 40:649-653.

Wall M., Kardon R. and Moore P. (1993). Effect of stimulus size on test-retest variability. *Perimetry Update 1992/93.* Proceedings of the Xth International Perimetric Society Meeting. Ed: R. P. Mills. Amsterdam & New York. Kugler. pp.371-376.

Weber J. and Dobek K. (1986). What is the most suitable grid for computer perimetry in glaucoma patients? *Ophthalmologica* 192:88-96.

Weber J. and Geiger R. (1989). Grey scale display of perimetric results - the influence of different interpolation procedures. *Perimetry Update 1988/89.* Proceedings of the VIIIth International Perimetric Society. Ed: A. Heijl. Amsterdam, Berkeley & Milano. Kugler & Ghedini. pp.447-454.

Weber J. and Krieglstein G.K. (1989). Graphical analysis of topographical trends (GATT) in automated perimetry. *Int Ophthalmol* 13:351-356.

Weber J. (1990). Eine neue Strategie für die automatisierte statische Perimetrie. *Fortschr Ophthalmol* 87:37-40.

Weber J. and Ulrich H. (1991). A Perimetric Nerve-Fiber Bundle Map. *Int Ophthalmol* 15:193-200.

Weber J. and Diestelhorst M. (1992). Perimetric follow-up in glaucoma with a reduced set of test points. *Ger J Ophthalmol* 1:409-414.

Weber J. and Rau S. (1992). The properties of perimetric thresholds in normal and glaucomatous eyes. *Ger J Ophthalmol* 1:79-85.

Weber J. (1993). Quantification of congruence between the right and left visual fields. *Graefe's Arch Clin Exp Ophthalmol* 231:704-710.

Weber J., Koll W. and Krieglstein G.K. (1993). Intraocular pressure and visual field decay in chronic glaucoma. *Ger J Ophthalmol* 2:165-169.

Weber J. and Baltes J. (1995). Spatial summation in glaucomatous visual fields. *Perimetry Update 1992/93.* Proceedings of the XIth International Perimetric Society Meeting. Eds: R. P. Mills and M. Wall. Amsterdam & New York. Kugler. p.65.

Weber J. and Klimaschka T. (1995). Test time and efficiency of the dynamic strategy in glaucoma perimetry. *Ger J Ophthalmol* 4:25-31.

Webster A.R., Luff A.J., Canning C.R. and Elkington A.R. (1993). The Effect Of Pilocarpine On the Glaucomatous Visual-Field. *Br J Ophthalmol* 77:721-725.

Weinreb R.N. and Perlman J.P. (1986). The effect of refractive correction on automated perimetric thresholds. *Am J Ophthalmol* 101:706-709.

Werner E.B. and Drance S.M. (1977). Early visual field disturbances in glaucoma. *Arch Ophthalmol* 95:1173-1175.

Werner E.B., Adelson A. and Krupin T. (1988a). Effect of patient experience on the results of automated perimetry in clinically stable glaucoma patients. *Ophthalmology*. 95:764-767.

Werner E.B., Bishop K.I., Koelle J., Douglas G.R., LeBlanc R.P., Mills R.P., Schwartz B., Whalen W.R. and Wilensky J.T. (1988b). A comparison of experienced clinical observers and statistical tests in detection of progressive visual field loss in glaucoma using automated perimetry. *Arch Ophthalmol* 106:619-623.

Werner E.B., Petrig B., Krupin T. and Bishop K.I. (1989). Variability of automated visual fields in clinically stable glaucoma patients. *Invest Ophthalmol Vis Sci* 30:1083-1089.

Werner E.B., Krupin T., Adelson A. and Feitl M.E. (1990). Effect of patient experience on the results of automated perimetry in glaucoma suspect patients. *Ophthalmology* 97:44-48.

Whalen W.R. (1985a). Basic Software - Printout results. *Computerized visual fields. What they are and how to use them.* Eds: W. R. Whalen and G. L. Spaeth. Slack, New York. pp.68-70.

Whalen W.R. (1985b). Routine reliability parameters. *Computerized visual fields. What they are and how to use them.* Eds: W. R. Whalen and G. L. Spaeth. Slack, New York. pp.75-78.

Wiesel T.B. and Hubel D.H. (1966). Spatial and chromatic interactions in the lateral geniculate body of the rhesus monkey. *J Neurophysiol* 29:1115-1156.

Wild J.M., Wood J.M., Flanagan J.G., Good P.A. and Crews S.J. (1986). The interpretation of the differential threshold in the central visual field. *Doc Ophthalmol* 62:191-202.

Wild J.M., Wood J.M., Hussey M.K. and Crews S.J. (1987a). The Quantification Of the Visual-Field In Computer-Assisted Threshold Perimetry. *Doc Ophthalmol Proc Ser 49.* Proceedings of the Seventh International Visual Field Symposium. Eds: E. L. Greve and A. Heijl. Dordrecht. Martinus Nijhoff/Dr W. Junk. pp.191-199.

Wild J.M., Wood J.M., Worthington F.M. and Crews S.J. (1987b). Some concepts on the use of three-dimensional isometric plots for the representation of differential sensitivity. *Doc Ophthalmol* 65:423-432.

Wild J.M., Dengler-Harles M., Searle A.E., O'Neill E.C. and Crews S.J. (1989). The influence of the learning effect on automated perimetry in patients with suspected glaucoma. *Acta Ophthalmol* 67:537-545.

Wild J.M., Betts T.A. and Shaw D.E. (1990). The influence of a social dose of alcohol on the central visual field. *Jpn J Ophthalmol* 34:291-297.

Wild J.M., Searle A.E.T., Dengler-Harles M. and O'Neill E.C. (1991). Long-term follow-up of base-line learning and fatigue effects in the automated perimetry of glaucoma and ocular hypertensive patients. *Acta Ophthalmol* 69:210-216.

Wild J.M., Hussey M.K., Flanagan J.G. and Trope G.E. (1993). Pointwise topographical and longitudinal modeling of the visual field in glaucoma. *Invest Ophthalmol Vis Sci* 34:1907-1916.

Wild J.M., Moss I.D., Whitaker D. and Oneill E.C. (1995). The Statistical Interpretation Of Blue-On-Yellow Visual-Field Loss. *Invest Ophthalmol Vis Sci* 36:1398-1410.

Wild J.M., Cubbidge R.P., Pacey I.E. and Robinson R. (1996). Pointwise analysis of short-wavelength automated perimetry thresholds in a normal population. *Invest Ophthalmol Vis Sci* 37:S1087.

Wildberger H. and Robert Y. (1988). Visual fatigue during prolonged visual field testing in optic neuropathies. *Neuro-ophthalmol* 8:167-174.

Wilensky J.T. and Joondeph B.C. (1984). Variation in visual field measurements with an automated perimeter. *Am J Ophthalmol* 97:328-331.

Wilensky J.T., Mermelstein J.R. and Siegel H.G. (1986). The use of different-sized stimuli in automated perimetry. *Am J Ophthalmol* 101:710-713.

Winn B., Whitaker D., Elliott D.B. and Phillips N.J. (1995). Factors affecting light-adapted pupil size in normal human subjects. *Invest Ophthalmol Vis Sci* 35:1132-1137.

Wood J.M., Wild J.M., Good P.A. and Crews S.J. (1986). Stimulus investigative range in the perimetry of retinits pigmentosa : some preliminary findings. *Doc Ophthalmoi* 63:287-302.

Wood J.M., Wild J.M. and Crews S.J. (1987a). Induced intraocular light scatter and the sensitivity gradient of the normal visual field. *Graefe's Arch Clin Exp Ophthalmol* 225:369-373.

Wood J.M., Wild J.M., Hussey M.K. and Crews S.J. (1987b). Serial examination of the normal visual field using Octopus automated projection perimetry: Evidence for a learning effect. *Acta Ophthalmol* 65:326-333.

Wood J.M., Wild J.M., Smerdon D.L. and Crews S.J. (1987c). The Role Of Intraocular Light Scatter In the Attenuation Of the Perimetric Response. *Doc Ophthalmol Proc Ser 49.* Proceedings of the Seventh International Visual Field Symposium. Eds: E. L. Greve and A. Heijl. Dordrecht. Martinus Nijhoff/Dr W. Junk. pp.51-59.

Wood J.M., Wild J.M., Bullimore M.A. and Gilmartin B. (1988). Factors affecting the normal perimetric profile derived by automated static threshold LED perimetry. I. Pupil size. *Ophthalmic Physiol Opt* 8:26-31.

Wood J.M., Wild J.M., Smerdon D.L. and Crews S.J. (1989). Alterations in the shape of the automated perimetric profile arising from cataract. *Graefe's Arch Clin Exp Ophthalmol* 227:157-161.

Wright C.E., Drasdo N.D. and Harding G.H. (1987). Pathology of the optic nerve and visual association areas: information given by the flash and pattern visual evoked potential and the temporal and spatial contrast sensitivity function. *Brain* 110:107-120.

Wu D.C., Schwartz B. and Nagin P. (1987). Trend analyses of automated visual fields. *Doc Ophthalmol Proc Ser 49.* Proceedings of the Seventh International Visual Field Symposium. Eds: E. L. Greve and A. Heijl. Dordrecht. Martinus Nijhoff/Dr W.Junk. pp.175-189.

Young W.O., Stewart W.C., Hunt H. and Crosswell H. (1990). Static threshold variability in the peripheral visual field in normal subjects. *Graefe's Arch Clin Exp Ophthalmol* 228:454-457.

Zalta A.H. (1989). Lens rim artifact in automated threshold perimetry. *Ophthalmology* 96:1302-1311.

Zalta A.H. and Burchfield J.C. (1990). Detecting early glaucomatous field defects with the size I stimulus and Statpac. *Br J Ophthalmol* 74:289-293.

Zeyen T.G. and Caprioli J. (1993). Progression of disc and field damage in early glaucoma. *Arch Ophthalmol* 111:62-65.

Zeyen T.G., Zulauf M. and Caprioli J. (1993). Priority of test locations for automated perimetry in glaucoma. *Ophthalmology* 100:518-522.

Zulauf M., Flammer J. and Signer C. (1986). The influence of alcohol on the outcome of automated static perimetry. *Graefe's Arch Clin Exp Ophthalmol* 224:525-528.

Zulauf M. and Caprioli J. (1991). Fluctuation of the visual field in glaucoma. *Glaucoma Update (Ophthalmic Clinics of North America).* Ed: J. Caprioli. Saunders, Philadelphia. pp.671-697.

Zulauf M., Caprioli J., Hoffman D.C. and Tressler C.S. (1991). Fluctuation of the differential light sensitivity in clinically stable glaucoma patients. *Perimetry Update 1990/91*. Proceedings of the IXth International Perimetric Society Meeting. Eds: R. P. Mills and A. Heijl. Amsterdam, New York & Milano. Kugler & Ghedini. pp.183-188.

Zulauf M., Caprioli J., Boeglin R.J. and Lee M. (1992). Number of stimuli as a reliability parameter in perimetry. *Ger J Ophthalmol* 1:86-90.

Zulauf M. and Caprioli J. (1993). Stimulus size 3 and 5 in perimetry for glaucoma. *Invest Ophthalmol Vis Sci* 34(suppl):1262.

Zulauf M. (1994). Normal visual fields measured with Octopus Program G1. I. Differential light sensitivity at indivisual test locations. *Graefe's Arch Clin Exp Ophthalmol* 232:509-515.

Zulauf M., Fehlmann P. and Flammer J. (1996). Perimetrie mit der normalen Octopus-Strategie und der 'dynamischen' Strategie nach Weber - Erste Ergebniße bezüglich Reproduzierbarkeit der Messungen bei Glaukompatienten. *In Press.*

APPENDIX 1: HFA Tools© manual.

A1.1. Introduction.

HFA Tools© consists of a suite of IBM compatible C programs. Each executable program (.exe) forms an add-on module to the suite. The programs can be broadly classified into five integrated layers which provide data conversion, data manipulation, statistical procedures and data display (Figure A1.1). All command line data in the manual assumes that HFA Tools© is situated in a sub-directory (named 'toolkit') of the root directory.

A1.2. DATA CONVERSION LAYER.

Two data formats may be converted for statistical analysis. The first format is derived directly from diskettes used with the Humphrey Field Analyzer (HFA). The second is derived from the visual fields database of the Optic Neuritis Treatment Trial (ONTT). Two executable programs, HDISK and VPCONV, were developed in order to transfer all data from the HFA and ONTT diskettes to a PC compatible format.

A1.2.1. HDISK.EXE

A1.2.1.1. Overview.

Data saved for use on the HFA is written in proprietary code which cannot be directly read by the PC. HDISK.EXE creates a unique file name for each converted field. The file header information contains the file name, patient name, eye examined, data of birth, date of examination and stimulus parameter details. For the given field examination, the file lists the measured sensitivity at each visual field location and includes both sensitivity values for those locations at which a double determination of sensitivity is made.

A1.2.1.2. Procedure.

⇒ Place the HFA diskette in the A: or B: drive as appropriate.

⇒ From the directory that the output field files are to be stored, run HDISK.EXE with the command line:

C:\toolkit\hdisk

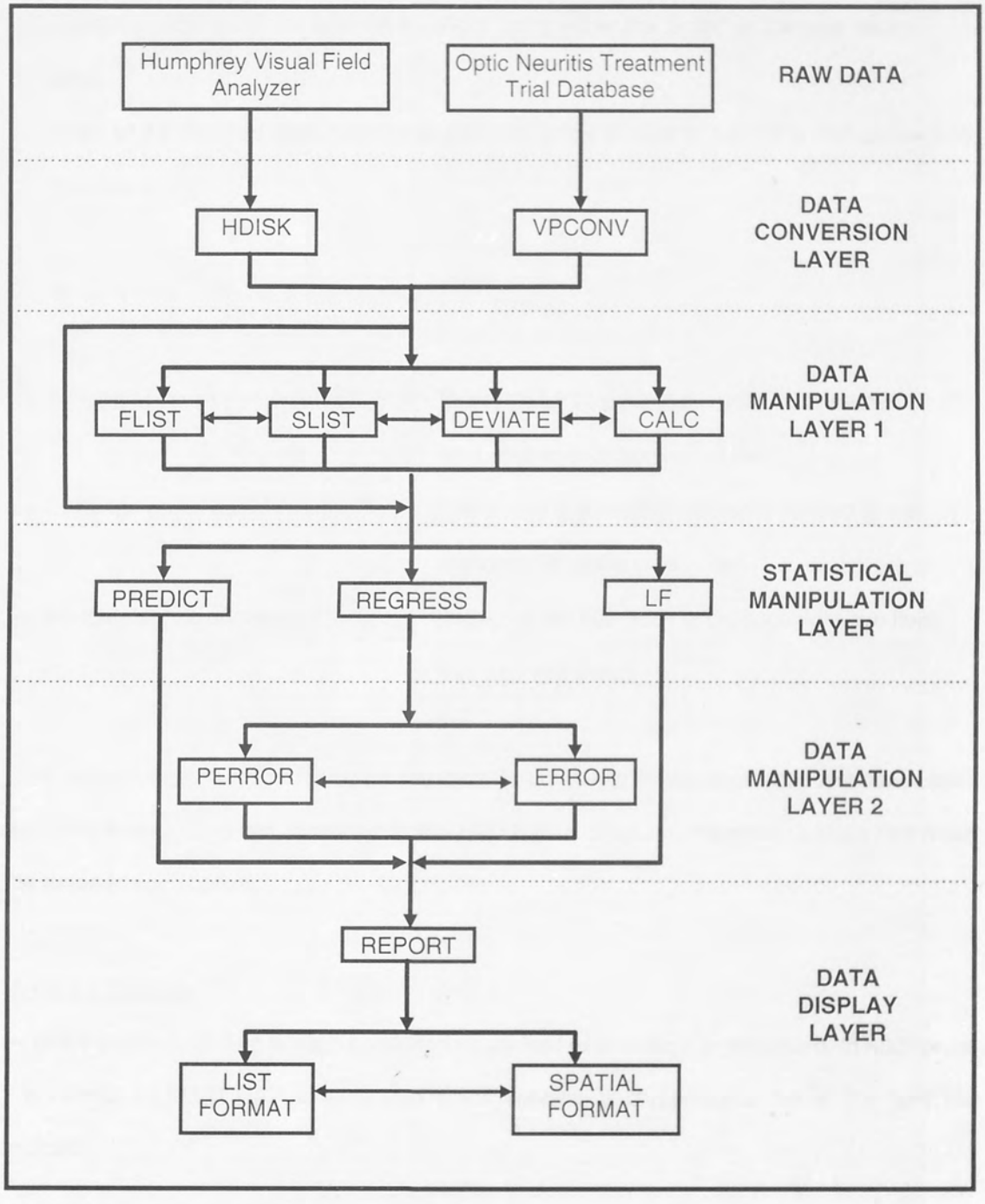

Figure A1.1: Integration of the Toolkit modules.

A list of all the visual field examinations contained on the HFA diskette appears showing the patient name, the eye examined and the program used (eg. 24-2). The command keys to move around the visual field examination list are displayed at the base of the screen.

⇒ Select the required visual field examinations using either the "enter" or carriage return keys.

⇒ When all the required fields have been selected, press escape to begin the field conversion procedure.

Three conversion options are displayed:

⇒ Print list of file names created? Y/N [prints to LPT1 a list of the unique file names attributed to each converted file]

⇒ Generate numerical file names? Y/N [generates a numerical file name instead of the standard file name (see notes)]

⇒ All right, left, no conversion? R/L/N [reflect all left eye fields to produce right eye field files and vice versa]

The 'no conversion' option maintains the data as contained in the original HFA examination. No default responses are contained in the HDISK.EXE program; therefore, a response must be made to each option.

A1.2.1.3. Output:

A field file corresponding to each converted visual field examination is generated. In addition, a file named FILELIST.DAT is generated which contains a chronological list of the field file names.

A1.2.1.4. Notes.

Each visual field examination creates a unique file name for each converted field. The following example illustrates the protocol used to generate each file name:

John Green exam: 24-2 on 7th August 1996

GR130807.JL2

The file name (GR130807) consists of the first two letters of the patient surname, stimulus parameters (1=stimulus colour white; 3=stimulus size III), day of examination (07), month of examination (08). The extension (.JL2) relates to the patients forename initial, the eye examined and a code for the type of examination (24-2 etc.).

A1.2.2. VPCONV.EXE

A1.2.2.1. Overview.

The database of the ONTT is compiled in five comma delimited files containing the outcomes of all visual field examinations of each of the 484 patients enrolled in the trial. VPCONV.EXE was developed to extract each visual field examination of each patient and produce a single field file.

A1.2.2.2. Procedure.

⇒ Place the HFA diskette in the A: or B: drive as appropriate.

⇒ From the directory that the output files are to be stored, run VPCONV.EXE with the command line:

C:\toolkit\vpconv [filename] [number]

where [filename] denotes the file to be converted and [number] denotes the number assigned to the first field file. If no number is entered, the default assigns the first field file as 1.

A1.2.2.3. Output.

VPCONV.EXE produces each visual field examination as a numbered file.

A1.3. DATA MANIPULATION LAYER 1.

The first layer of data manipulation programs is optional and enables data or sections of data within each field file to be prepared for use in the statistical manipulation layer.

A1.3.1. FLIST.EXE

A1.3.1.1. Overview.

FLIST.EXE allows the user to select a custom set of field files for use in the statistical layer.

A1.3.1.2. Procedure.

⇒ From the directory that the output files of HDISK.EXE are stored, run FLIST.EXE with the command line:

C:\toolkit\flist

⇒ From the list of files displayed, select the field files to be included in the FLIST.EXE output file.

⇒ When the 'save files' option is selected, the FLIST.EXE program prompts for a user defined filename for the list of selected files.

A1.3.1.3. Output.

A chronological list of the selected field files with a user defined name.

A1.3.2. SLIST.EXE

A1.3.2.1. Overview.

SLIST.EXE allows the user to select a sub-set of stimulus locations from the program 30-2 or 24-2 format which may be selectively analysed in the statistical manipulation layer and the CALC.EXE program.

A1.3.2.2. Procedure.

⇒ From the directory that the output file is to be stored, run SLIST.EXE with the command line:

C:\toolkit\slist

⇒ Enter the cartesian co-ordinates of the stimulus locations to be included.

The ordinate and abscissa values should be separated by a comma. Each co-ordinate should be entered on a single line. The program prompts for a user defined name for the set of co-ordinates.

A1.3.2.3. Output.

A list of the selected cartesian co-ordinates in a file with a user defined name.

A1.3.3. DEVIATE.EXE

A1.3.3.1. Overview.

DEVIATE.EXE uses the field files created by HDISK.EXE or FLIST.EXE and calculates the total and pattern deviation at each location and produces corresponding total and pattern deviation field files. The header information of the field file is maintained in the total or pattern deviation field file.

A1.3.3.2. Procedure.

Ensure that the files storing data regarding the age related decline in sensitivity are situated in the same directory as the DEVIATE.EXE executable file. The filenames of these files are: AGE50.102, AGE50.302, AGELOSS.DAT, COEFF.102, COEFF.302.

⇒ Run DEVIATE.EXE with the command line:

C:\toolkit\ deviate

DEVIATE.EXE prompts for the following:

⇒ Enter name input filelist:	[list of files to be converted *eg. filelist.dat*]
⇒ Enter flist to create:	[user defined list of converted files]
⇒ Enter source path:	[DOS address where filelist and files to be converted are stored]
⇒ Enter destination path:	[DOS address where converted files are to be stored]

A1.3.3.3. Output.

The output files are stored in the specified directory with unique filenames (see notes).

A1.3.3.4. Notes.

Each total deviation file is stored with the original filename and the extension .td. Similarly, each pattern deviation file is stored with the original filename and the extension . pd.

A1.3.4. CALC.EXE

A1.3.4.1. Overview.

The CALC.EXE program calculates unweighted visual field indices for each field of the specified file list.

A1.3.4.2. Procedure.

Ensure that the AGE50.102, AGE50.302, AGELOSS.DAT, COEFF.102, COEFF.302 files are located in the same directory as the field files.

⇒ From the directory that the HDISK.EXE converted files are stored, run CALC.EXE with the command line:

C:\toolkit\calc

⇒ CALC.EXE prompts for the file list of the visual field examination files for which the visual field indices are to be calculated.

The file list corresponds to filelist.dat for HDISK.EXE converted examinations or a custom file list produced by FLIST.EXE.

⇒ CALC.EXE prompts for a user defined filename in which the results are to be stored.

A1.3.4.3. Output.

The visual field indices calculated are mean sensitivity (MS), mean defect (MD), loss variance (LV), short-term fluctuation (SF), corrected loss variance (CLV), mean deviation (MDV),

pattern standard deviation (PSD) and corrected pattern standard deviation (CPSD). The CALC.EXE output file contains the results of all the field files contained within the specified file list. The indices MD and MDV indices respect the Octopus and Humphrey sign conventions.

A1.4. STATISTICAL MANIPULATION LAYER.

A1.4.1. REGRESS.EXE

A1.4.1.1. Overview.

REGRESS.EXE performs pointwise univariate linear regression at each stimulus location against time to follow-up for the field files contained in a specified file list. The program models the measured sensitivity or the pattern deviation against time to follow-up and may also forecast these values at a specified time period.

A1.4.1.2. Procedure.

Ensure that the AGE50.102, AGE50.302, AGELOSS.DAT, COEFF.102, COEFF.302 files and the graphics file EGAVGA.BGI are located in the same directory as the file list and the field files.

⇒ From the directory that the output files are to be stored, run REGRESS.EXE with the command line:

C:\toolkit\regress

REGRESS.EXE prompts for the following:

⇒ Enter name for log file: [user defined name of list of files that are to be processed]

⇒ Enter prediction file name: [user defined name for the forecast field files]

⇒ Use ordinal time axis? (y/n): [specifies real-time ordinal axis or examination number ordinal axis]

⇒ Perform pattern deviation? (y/n):

If no prediction filename is entered, the REGRESS.EXE program performs univariate linear regression modelling by default.

A1.4.1.3. Output.

An image of the univariate linear regression outcome at each stimulus location is automatically generated on the screen (Figure A1.2). The graphs corresponding to each stimulus location may be scrolled through using the '↑↓' keys. The statistics relating to each individual regression plot are also displayed at the side of the graph. The standard .log file contains the values for the regression statistics corresponding to the modelled sensitivity or pattern deviation values. The .log file with the prediction filename contains the values for the forecast regression statistics. A postscript file (.ps) is generated which contains two spatial displays of the stimulus locations incorporated by the selected program format. The first spatial display identifies the stimulus locations at which the regression coefficient is significantly different from zero and the greytone of the symbol indicates the statistical probability (Figure A1.3); the second spatial display depicts the corresponding data for stimulus locations at which the regression coefficient is significantly different from the normal rate of decline with age.

A1.4.2. PREDICT.EXE

A1.4.2.1. Overview.

PREDICT.EXE performs multivariate linear regression of a series of field files against examination number for a selected file list.

A1.4.2.2. Procedure.

⇒ From the directory that the output files are to be stored, run PREDICT.EXE with the command line:

C:\toolkit\predict

PREDICT.EXE prompts for the following:

⇒ Filename for output data: [user defined name for the output fields]

⇒ Remove blindspots (y/n):

⇒ Filename for point subset?: [s-list filename of stimulus co-ordinates]

⇒ Skip <=0 in r squared calcs: [omit stimulus locations with a measured sensitivity of ≤0dB]

Figure A1.2. (Photograph)

An example of the screen output for a single stimulus location generated by REGRESS.EXE.

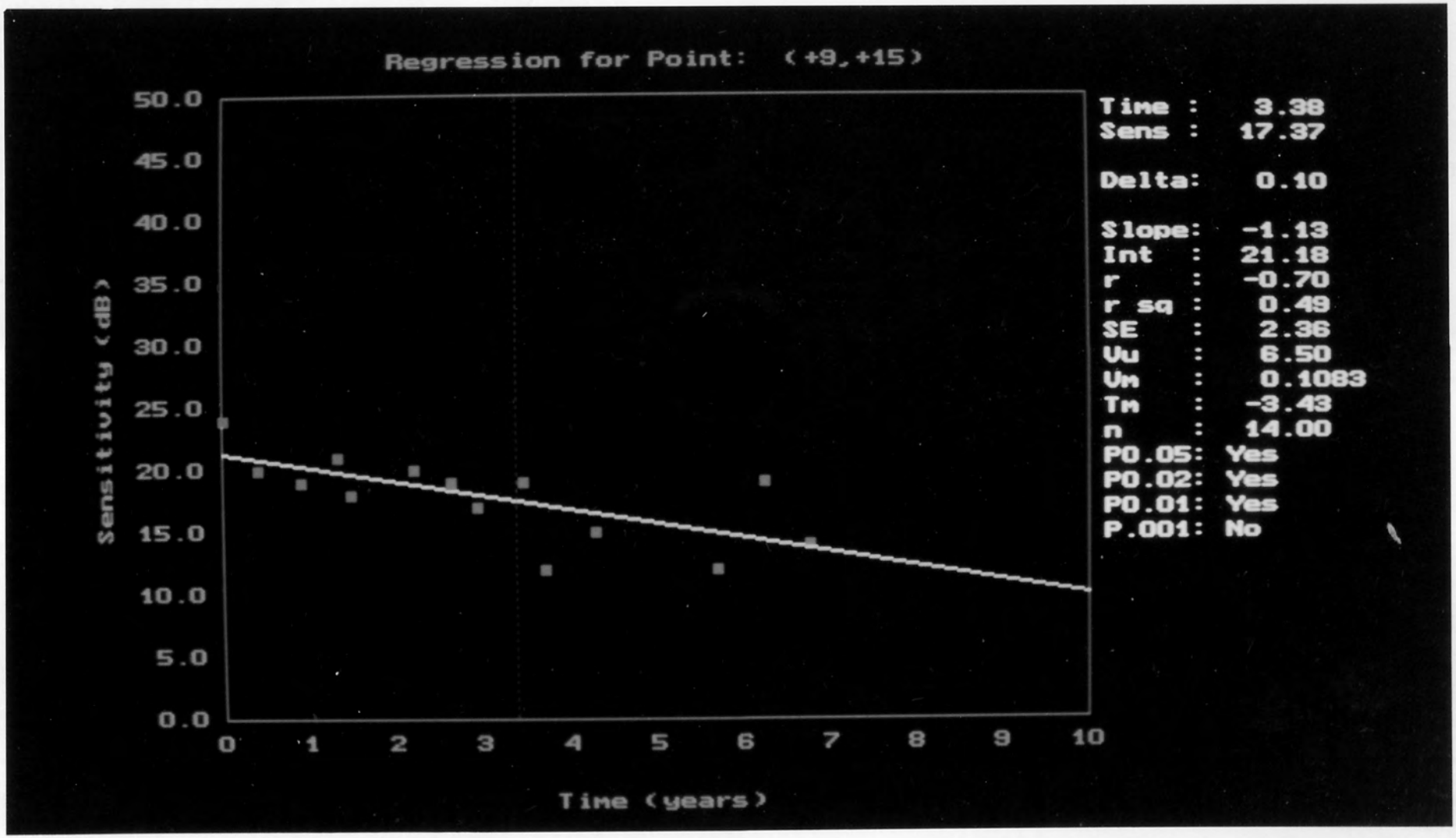
Regression for Point: (+9,+15)
Sensitivity (dB)
50.0
45.0
40.0
35.0
30.0
25.0
20.0
15.0
10.0
5.0
0.0
0
1
2
3
4
5
6
7
8
9
10
Time (years)
Time : 3.38
Sens : 17.37
Delta: 0.10
Slope: -1.13
Int : 21.18
r : -0.70
r sq : 0.49
SE : 2.36
Vu : 6.50
Vm : 0.1083
Tm : -3.43
n : 14.00
P0.05: Yes
P0.02: Yes
P0.01: Yes
P.001: No

Figure A1.3. An example of a probability postscript file generated by REGRESS.EXE for stimulus locations at which the slope of the function is significantly different from zero (T_m).

SPATIAL PRINTOUT OF SIGNIFICANT VALUES OF Tm

[file: photo]

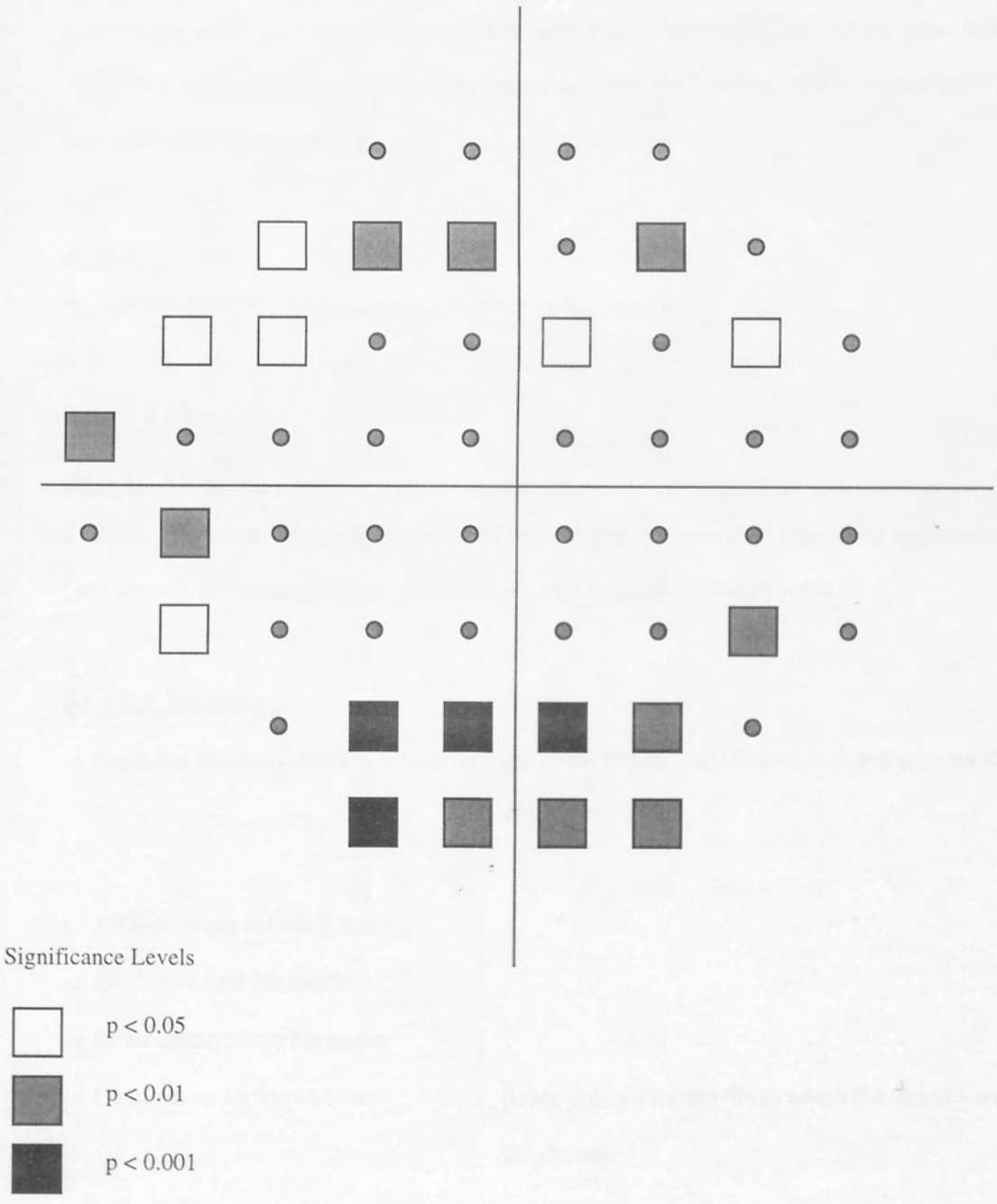

A1.4.2.3. Output.

The .log file contains the list of field files processed and the mean average percentage error (MAPE) between the measured and forecasted fields as a whole. From a single field file, PREDICT.EXE generates a modelled second field (file extension .M02) and a file containing the pointwise percentage error between the modelled and measured sensitivity values (file extension .L02). For each of the next consecutive modelled fields, each modelled field is based upon all the preceding fields in the series. From a minimum of two fields, PREDICT.EXE forecasts a third field (file extension .F03) and a file containing the pointwise percentage error between the forecasted and measured sensitivity values (file extension .E03). For each of the next consecutive forecast fields, the forecast field is based upon all the preceding fields in the series.

A1.4.2.4. Notes.

See PERROR.EXE for the calculation of the percentage error.

A1.4.3. LF.EXE

A1.4.3.1. Overview.

LF.EXE calculates the homogeneous (LF(Ho)), heterogeneous (LF(He)) and aggregate error components of the long-term fluctuation between a specified pair of fields.

A1.4.3.2. Procedure.

⇒ From the directory that the output files are to be stored, run LF.EXE with the command line:

C:\toolkit\lf

LF.EXE prompts for the following:

⇒ Enter first field file name:

⇒ Enter second field file name:

⇒ Enter name for log file: [User defined for the file in which the results are to be stored]

A1.4.3.3. Output.

The log file contains the ANOVA summary table for the global LF values (LF(Ho), LF(He) and the aggregate error) and a spatial printout of the two fields from which the LF components have been calculated.

A1.5. DATA MANIPULATION LAYER 2.

The second layer of data manipulation programs is optional and enables the outcome files of the statistical manipulation layer to undergo further analysis.

A1.5.1. ERROR.EXE

A1.5.1.1. Overview.

The ERROR.EXE module generates global values for the coefficient of determination (R^2), mean average percentage error (MAPE) and mean error (ME) between a forecasted field, generated by the REGRESS.EXE module, and the corresponding measured field.

A1.5.1.2. Procedure.

⇒ From the directory that the output files are to be stored, run ERROR.EXE with the command line:

C:\toolkit\error

ERROR.EXE prompts for the following:

⇒ Enter name of observed field:

⇒ Enter name of predicted field:

⇒ Convert fields to 24-2 (y/n):

⇒ Enter name of subset file:

A1.5.1.3. Output.

The data corresponding to R^2, MAPE and ME are written to the screen.

A1.5.2. PERROR.EXE

A1.5.2.1. Overview.

PERROR.EXE calculates the pointwise percentage error between a forecasted field generated by REGRESS.EXE and its corresponding measured field.

A1.5.2.2. Procedure.

⇒ From the directory that the output files are to be stored, run PERROR.EXE with the command line:

C:\toolkit\perror

PERROR.EXE prompts for the following:

⇒ Measured field name:

⇒ Predicted field name:

⇒ Results field name: [User defined name for the output data]

A1.5.2.3. Output.

A file is generated, with the user defined name, which lists the percentage error between the forecasted and measured sensitivity at each stimulus location.

A1.5.2.4. Notes.

The calculation of the percentage error between the forecasted and measured sensitivity at each stimulus location is performed as follows:

$$\text{Percentage Error} = \frac{|\text{forecasted} - \text{measured}|}{\text{measured}} .100$$

A1.6. DATA DISPLAY LAYER.

A1.6.1. REPORT.EXE

A1.6.1.1. Overview.

REPORT.EXE generates a printout of the sensitivity or percentage error values at each stimulus location for the specified file. REPORT.EXE may be used with any of the files generated by an HFA Tools© module.

A1.6.1.2. Procedure.

⇒ From the directory that the field file is stored, run REPORT.EXE with the command line:

C:\toolkit\report

REPORT.EXE prompts for the following:

⇒ Field file name:

⇒ List or spatial (l/s):

⇒ Filename (ret=printer): [a user defined filename will save the output to file]

A1.6.1.3. Output.

Selection of the 'list' option generates a printout of the header information, stimulus location co-ordinates and their corresponding sensitivities. Selection of the 'spatial' option generates a printout of the header information and a cartesian grid of the sensitivities at each stimulus location.